Universitetet i Stavanger

FACULTY OF SCIENCE AND TECHNOLOGY

MASTER'S THESIS

Study programme/specialisation: MSc. Petroleum Engineering/ Reservoir Engineering	Spring semester, 2018 Open access
Author: Jaldeepsinh Samantsinh Chauhan	…… (signature of author)
Programme coordinator: Prof. Ingebret Fjelde Supervisor(s): Prof. Ingebret Fjelde	
Title of master's thesis: Transport of CO_2 In Porous Media – A Visualisation Study	
Credits: 30 ECTS	
Keywords: CO_2 injection Visualisation Dyes and pH indicator Carbonated water Enhanced oil recovery Porous media CO_2 dissolution	Number of pages: 162 Stavanger, 15th June 2018

TRANSPORT OF CO_2 IN POROUS MEDIA – A VISUALISATION STUDY

Thesis submitted in partial fulfillment of
the requirements for the degree of
master of science in petroleum engineering

by
JALDEEPSINH SAMANTSINH CHAUHAN

DEPARTMENT OF ENERGY RESOURCES
FACULTY OF SCIENCE AND TECHNOLOGY
2018

Abstract

TRANSPORT OF CO_2 IN POROUS MEDIA – A VISUALISATION STUDY

Jaldeepsinh Samantsinh Chauhan

ADVISOR: Prof. Ingebret Fjelde

The increase in global energy demand coupled with a need to stabilize CO_2 emission levels has called for the development of a strategy with the potential to make energy 'greener'. One such strategy is *Carbon Capture Utilisation and Storage (CCUS)*. Since its inception, one focus area for laboratory studies has been the *visualisation* of pore and core scale processes to better understand the underlying mechanisms that govern improved oil recovery and the storage of CO_2. Work done in this thesis forms a step-by-step understanding of the fluid system, porous media, and the effect of cell dimensions on the visualisation process and acts as a pre-study towards the use of a transparent 2-D model to investigate convection during transport of CO_2 in the porous media.

First, a better understanding of the fluid system was addressed by testing the ability of a pH indicator and different dyes to represent water and oil phases respectively. Static experiments were conducted at ambient conditions by using an analog fluid to represent the change in pH due to the dissolution of CO_2 in water. The visualisation was facilitated using an optical method and the results from these experiments reviewed the performance of dyes and indicator in the oil-water system.

Following this, tests were conducted in graded tubes to determine the ability of dyes/indicator to aid visualisation of imbibition under gravity in a diverse porous media constructed using glass beads of different grain size distribution and wettability. The results from initial tube tests demonstrated a rise in the pH due to a reaction of glass beads with the water phase. Glass beads were treated with an acid to limit the increase in pH, but an alteration in surface properties of glass beads was observed as a result of this treatment. Tube tests were also conducted to examine the effect of varying tube diameter on the movement of water phase in the porous media and the quality of visualisation. Results suggested that the shape of water front invading the porous media was a function of tube diameter and a decrease in diameter facilitated better visualisation but imposed limitations on the ease of operation.

In the next step, experiments were conducted in a glass tube under CO_2 injection at 10 bar and 20°C. These tests demonstrated the ability of the pH indicator to help visualise the movement of CO_2 in water and also confirmed a possible alteration in surface properties of glass beads due to the acid treatment.

Polycarbonate cells of varying thickness were prepared, and imbibition tests were carried out to study the effect of varying cell thickness on the shape of water front in the porous media and the quality of visualisation. The results using porous media packing showed coherence with experimental studies in the literature conducted using etched glass micromodels. Effect of the decrease in cell thickness showed consistency with results obtained in the tube tests of varying diameter.

Previous experiments helped study fluid system, porous media, and the effect of varying cell dimension on visualisation. These observations were used to conduct tests in a low-pressure cell made using Polyoxymethylene (POM). CO_2 injection was facilitated at 10 bar and 20°C, and the experiment conducted in POM cell visually demonstrated the ability of CO_2 rich water to improve oil recovery from the porous media after waterflooding. Tests in POM cell established the operational procedure and initial testing of the cell design with the chosen visualisation technique. We welcome further research based on the techniques and the procedures used in this study.

Acknowledgements

The work done in this thesis is an amalgamation of the efforts of many, to whom I express my sincere appreciation.

First and foremost, I wish to thank my supervisor Prof. Ingebret Fjelde for providing me with an opportunity to work on this thesis. He has always been very patient with me and guided me in the right direction for the successful completion of this project. It is a privilege working alongside him, and I look forward to the future.

I wish to thank the University of Stavanger and the beautiful country of Norway for supporting me during my stay.

I must thank Daniel Strand, Elin Austerheim, and Samuel Issac Poudroux from IRIS for their help in preparation of the laboratory setup necessary for the experiments. I would like to give special thanks to Widuramina Amarasinghe for his invaluable help in experimental work done in POM cell.

My friends in Norway and India have always been influential in shaping me as a person I am today. I am grateful for their support and love.

I want to take this opportunity to express my sincerest gratitude to all my teachers for their support in the development of my knowledge and character.

At last, I wish to thank my family that means the world to me. My parents have been with me through thick and thin, and words are not enough to describe my gratitude and love towards them.

Contents

List of Figures

List of Tables

Nomenclature

ϕ	Porosity
λ	Mobility
μ	Viscosity
σ	Interfacial Tension
θ	Contact angle
C_a	Capillary number
cc	Cubic Centimeters
E	Overall Displacement Efficiency
E_D	Microscopic displacement efficiency
E_V	Macroscopic displacement efficiency
K	Absolute Permeability
K_e	Effective Permeability
k_r	Relative Permeability
M_r	Mobility ratio
N_b	Bond number
P_c	Capillary Pressure
S_{oi}	Initial oil saturation
S_{or}	Residual oil saturation
A	Cross-sectional area
CCS	Carbon Capture and Storage
CCUS	Carbon Capture, Utillization and Storage
CW	Carbonated Water
CWI	Carbonated Water Injection
DIW	Deionized Water
EOR	Enhanced Oil Recovery
GCCSI	Global Carbon Capture and Storage Institute
HCPV	Hydrocarbon Pore Volume

IEA	International Energy Agency
IFT	Interfacial Tension
IPCC	Intergovernmental Panel on Climate Change
M	Molarity
N	Normality
NIST	National Institute of Standards and Technology
OOIP	Original Oil in Place
psi	Pounds per Square Inch
PV	Pore Volume
Q	Flow rate
RF	Recovery Factor
Vb	Bulk Volume
Vp	Pore Volume
WF	Waterflooding
wt%	Percentage by Weight

Chapter 1

Introduction

The 2017 World Energy Outlook published by International Energy Agency (WEO-IEA) predicts the energy demand will grow by 30% from 2017 to 2040 (IEA, 2017). Oil demand will keep on rising because of momentum from other sectors and reach 105 mb/d (million barrels per day) by 2040. Use of Natural gas rises by 45% to 2040 and accounts for a quarter of global energy demand, becoming the second largest fuel in the global energy mix after oil.

According to U.S Department of Energy (U.S DoE), 86% of world primary energy use is supplied by fossil fuels (Grubb, 2009.). The U.S DoE predicts that in 2030, fossil fuels will account for the same share of world's energy and will continue to dominate throughout the 21^{st} century. Estimates by the Intergovernmental Panel on Climate Change (IPCC) indicate that significant reductions from current CO_2 emission levels will be required by 2050 if we are to stabilize atmospheric concentrations of CO_2 (IPCC, 2007).

With the increase in global energy demand, various strategies are being considered which meet energy demand and simultaneously reduce CO_2 emissions. One of these strategies is CO_2 capture and its injection in oil reservoir; this can lead to storage of CO_2 in the formation and improve the oil recovery. The technology is referred to as Carbon Capture Utilisation and Storage (CCUS) (Sohrabi et al., 2011). Storage of captured CO_2 in geologic formations is one of the major mitigation strategies, as it can store large volumes of CO_2 over long periods of time. Types of geologic formations for Carbon Capture and Storage (CCS) include unmineable coal beds, deep saline aquifers (those containing non-potable water) and mature or abandoned oil and gas fields (Sohrabi et al., 2011).

Out of various options we have at present, oil and gas reservoirs make a fitting choice because (Sohrabi et al., 2011):

1. Geology of oil and gas reservoirs is well known for long-term storage and reduces the uncertainty of CO_2 migration.
2. CO_2 injection can improve oil recovery, which can generate more revenue and help offset a part of the cost associated with CCUS.

Extensive studies have been conducted to demonstrate the use of CO_2 for increased oil recovery and its simultaneous storage in the reservoir. Majority of these studies share a common goal: to understand CO_2 interactions with oil-water system and minerals in the reservoir rock. Numerous visualisation techniques like Positron Emission Tomography (PET) and X-ray Computed Tomography (CT) have allowed high-resolution imaging of

the core and pore-scale processes. Micromodels have also been used to facilitate the study of the oil-water system in pores. Several studies have been conducted where visualisation is facilitated using optical methods such as pH indicators, tracers, and projection methods like Mach-Zehnder Interferometry.

In this thesis, we limit ourselves to use of an optical method for visualisation of processes involving CO_2 injection. Work done in this thesis is to assist an ongoing project at International Research Institute of Stavanger (IRIS) which aims at the investigation of convection during CO_2 transport in porous media using a high-pressure 2-D cell. Before conducting tests in the high-pressure cell, a study of different variables in the system needs to be performed. Some of these variables are fluids selection, porous media, cell dimensions (thickness and width) and operational limitations. In this thesis, a step by step testing of different variables affecting the visualisation process is performed.

The primary objectives of this thesis are to:

1. Study the *fluid system*: Identify pH indicators and dyes to represent water and oil phases respectively. Emphasis is laid on the selection of dyes and indicators which are soluble only in the phase they represent, i.e., the oil-soluble dye does not interact with water phase and vice-a-versa.
2. Study the *porous media*: Conduct tests in graded tubes (called 'tube tests' in this thesis) to study the ability of dyes to represent oil and water phases in the porous media. Tests are conducted by making the porous media more diverse through alteration of the grain size and mixing hydrophilic and hydrophobic grains to provide uneven wettability distribution. Effect of altering the porous media on water invasion and oil recovery is studied. The effect of varying the internal diameter of the tube on the movement and shape of the invading water front is also investigated.
3. Conduct tests in larger tubes at low-pressure *CO_2 injection*: CO_2 injection at 10 bar is carried out with the oil-water system in diverse porous media and results are compared with tube tests. The ability of pH indicator to facilitate visualisation of CO_2 dissolution in water and oil is also examined.
4. Study the effect of varying *cell dimension*: Polycarbonate cells of varying thicknesses are prepared to study the shape of invading water front as a function of cell dimensions. Quality of visualisation and the operational ease due to variation in cell thickness is analysed.
5. Conduct tests in a *Polyoxymethylene (POM) cell*: Tests are conducted in the POM cell using the observations made while studying different variables in the tests mentioned above. POM cell tests will form a basis for conducting further work at high pressure and temperature.

Following the introduction, the thesis has been organized in the following manner:

Chapter-2 (Fundamentals of Oil Recovery):

This chapter discusses basic concepts used for qualitative and quantitative analysis of different recovery mechanisms. We conclude the chapter by introducing imbibition principles which will help interpret results in this thesis.

Chapter-3 (CO_2 as a Displacing Fluid for EOR):

This chapter introduces the use of CO_2 as an injection fluid. We conclude the chapter by looking into visualisation studies conducted in the field of CO_2 storage and recovery.

Chapter-4 (Experimental Procedures and Materials Used):

This chapter provides information on materials used in the experimental work and procedures for different experiments which will help achieve the objectives of this thesis.

Chapter-5 (Results and Discussion):

This chapter discusses observations made during the experimental work conducted in this thesis. Conclusions drawn from these experiments are also discussed.

Chapter-6 (Summary and proposed future work):

In this chapter, we review the conclusions drawn from this study and recommend ideas for future work.

Chapter 2

Fundamentals of Oil Recovery

2.1 Oil Recovery Mechanisms

Oil recovery mechanisms have been traditionally classified into three stages: primary, secondary and tertiary (Green & Willhite, 1998). Primary recovery results from the use of natural energy present in the reservoir as the main source of energy for displacement of oil to producing wells. On an average, primary oil recoveries range between 5 and 20% of the original oil-in-place (OOIP) (Stalkup, 1984).

Secondary recovery processes are usually implemented after primary production declines (Green & Willhite, 1998). Traditional secondary recovery processes are water flooding and gas injection; the term secondary recovery is now almost synonymous with water flooding. Improvement in oil recovery after implementation of secondary recovery processes is usually in the range of 20 to 40% OOIP (Stalkup, 1984). Studies in North Sea reservoirs have reported a slightly higher recovery in the range of 35 to 40% of OOIP after implementation of secondary recovery processes (Tzimas, Georgakaki, Cortes, & Peteves, 2005).

Tertiary recovery is the third stage of production that is obtained after implementing secondary recovery process (Green & Willhite, 1998). Tertiary processes use miscible gases, chemicals, and thermal energy to displace additional oil after secondary recovery processes become uneconomical. In some situations, the so-called tertiary recovery methods might act as secondary recovery operations. Because of such situations, tertiary recovery can also be defined as Enhanced Oil Recovery (EOR).

A classification of EOR methods by Van Poollen has the following three categories (Van Poollen, 1980):

1. Thermal methods, which include steam stimulation (also known as huff and puff), steam flood (including hot water injection), and in situ combustion.
2. Chemical methods, which include surfactant-polymer injection, polymer flooding, and caustic flooding.
3. Miscible displacement methods, which include injection of hydrocarbon gas, inert gas and CO_2 injection under high pressure.

In the next sections of this chapter, parameters in reservoir technology relevant for this thesis are introduced.

2.2 Recovery Efficiency

Oil recovery efficiency is a product of microscopic and macroscopic displacement efficiency (Green & Willhite, 1998). Microscopic displacement efficiency is a measure of the effectiveness of the injected fluid to mobilize oil from pore space. It is reflected in the value of residual oil saturation, in regions contacted by displacing fluid (Green & Willhite, 1998). Equation 2.1 represents microscopic displacement efficiency.

$$E_D = \frac{S_{oi} - S_{or}}{S_{oi}} \tag{2.1}$$

Where,
S_{oi}: Initial Oil saturation
S_{or}: Residual Oil Saturation

Factors affecting microscopic displacement efficiency are saturation history of the rock-fluid system, rock pore geometry and structure, reservoir pressure and temperature, oil composition, dead-end pore volume, and fluid phase behaviour and properties (Sehbi, Frailey, & Lawal, 2001).

Macroscopic displacement efficiency is the effectiveness of displacing fluids to contact volume of the reservoir (Green & Willhite, 1998). It represents how effectively the injected fluid sweeps out the reservoir, areally and vertically. Factors affecting macroscopic displacement efficiency are well pattern, reservoir heterogeneities and the differences in fluid properties of the displacing and reservoir fluid (Sehbi et al., 2001).

Overall displacement efficiency (E) is a product of microscopic and macroscopic displacement efficiencies as shown in equation 2.2 (Green & Willhite, 1998):

$$E = E_D.E_V \tag{2.2}$$

Where,
E : Overall displacement efficiency
E_D: Microscopic displacement efficiency
E_V: Macroscopic/Volumetric displacement efficiency

The choice of EOR fluid should be such that it controls the mobility ratio (EOR fluid/reservoir fluid), density differences, interfacial tension (IFT) and viscosity ratios to improve the recovery factor.

2.3 Porosity

Porosity is influential in determining the oil storage capacity of a reservoir and is defined as the ratio of pore volume (void space, V_p) to bulk volume (V_b).

$$\phi = \frac{V_p}{V_b} \tag{2.3}$$

Porosity values in sandstones generally are in the range of 10 to 40% (Conybeare, 1967) and in carbonates, it is in range of 5 to 25% (Keelan, 1982). Total porosity includes all pores; interconnected and isolated. Effective porosity excludes isolated pores and volume occupied by clay-bound water (Schlumberger, 2018a). Porosity is affected by parameters like grain size, packing, sorting, grain shape and amount of intergranular matrix and cement (Pettijohn, 1975).

2.4 Permeability

Permeability is the capacity of rocks to transmit fluids through a porous medium. Darcy (D) is the standard unit of permeability. Permeability is affected by factors such as pore geometry, porosity, bedding and confining pressure (Zolotukhin & Ursin, 2000). Types of permeability are:

1. Absolute permeability:
   Absolute permeability (K) is defined as permeability of rock in presence of single fluid. Henry Darcy gave a fundamental relationship for determining permeability (Darcy, 1856). Darcys Law is given by:

$$Q = -\frac{KA}{\mu}.\frac{\Delta p}{L} \tag{2.4}$$

   Where,
   Q: Flow rate
   μ: Viscosity of the fluid at experiment conditions
   A: Cross-sectional area
   L: The length of the sample
   Δp: Pressure drop across the core sample

2. Effective and relative permeability:
   Presence of two or more fluids in the reservoir affects flow properties of each fluid (Zolotukhin & Ursin, 2000). The permeability of reservoir rock to one fluid in the presence of other is called effective permeability to that fluid. Depending on the relative saturation of each fluid phase, their effective permeabilities are given by the equation 2.5:

$$K_{e,i} = -\frac{q_i \mu_i}{A}.\frac{L}{\Delta p}, i = o, w, g \tag{2.5}$$

   o, w, g = oil, water and gas respectively.

   The ratio of effective permeability (at given saturation) to absolute permeability gives relative permeability (k_r) (see equation 2.6). Pore geometry, saturation history, rock type, formation wettability and reservoir temperature and pressure affect relative permeability (Guo, Ma, Li, Hao, & Wang, 2012).

$$k_{r,i} = \frac{K_{e,i}}{K}, i = o, w, g \tag{2.6}$$

2.5 Interfacial Tension

Interfacial tension (σ) exists between the molecules of two fluids in contact with each other. IFT represents the amount of energy that keeps the two fluids apart. Due to the presence of immiscible phases in reservoirs, surface energy related to fluid interfaces influences fluid saturations, displacement of phases and fluid distribution (Green & Willhite, 1998).

Depending on the amount of cohesive forces between their molecules, two fluids can have different IFTs. The lower the IFT between the fluids, easier it is to achieve miscibility (Zolotukhin & Ursin, 2000).

2.6 Wettability

Fluid-solid interface also affects the fluid distribution in the porous media. Wettability is the tendency of one fluid to adhere to a solid surface in the presence of another (Green & Willhite, 1998). The fluid phase which is more strongly attracted to the solid is known as the wetting phase. Reservoir rocks can be water-wet, oil-wet, intermediate wet or mixed wet.

Intermediate wettability is a result of both the fluids wetting the solid, but one is slightly more attracted than another. Mixed wettability varies from one point to another due to heterogeneity in chemical composition of exposed rock (solid surface) (Green & Willhite, 1998). Fig. 2.1 shows water drop in contact with a homogenous rock surface in the presence of oil phase.

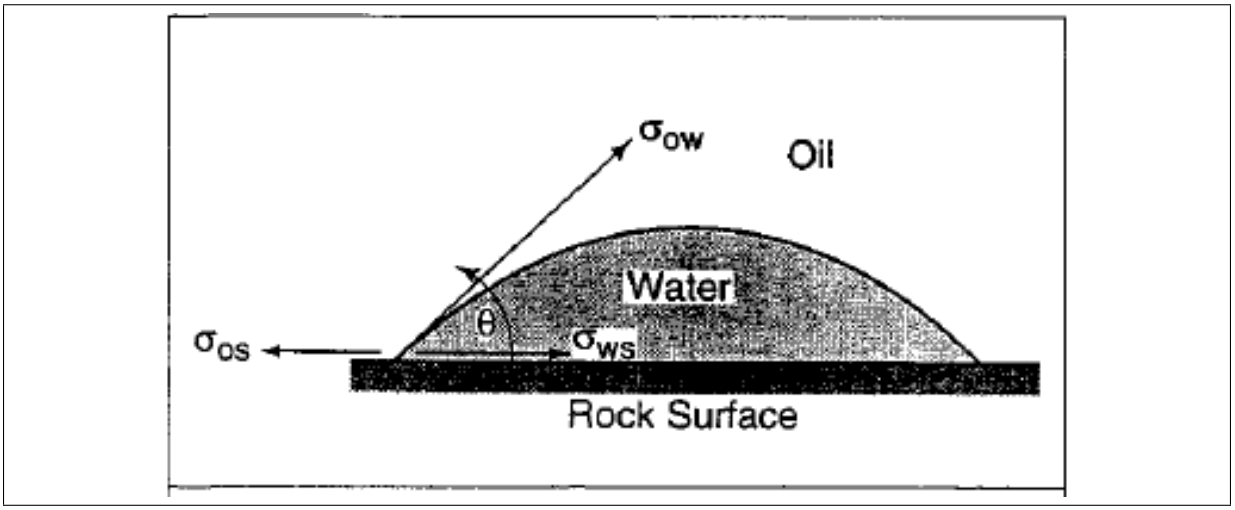

Figure 2.1: Interfacial forces at an interface between two immiscible fluids and a solid (Green & Willhite, 1998).

Using force balance in fig. 2.1,

$$\sigma_{os} - \sigma_{ws} = \sigma_{ow} \cos\theta \tag{2.7}$$

Where,
σ_{os}: IFT between solid and oil.
σ_{ws}: IFT between solid and water.
σ_{ow}: IFT between oil and water.
θ: Contact angle measured through the water phase.
Contact angle can be a good representative of wettability. If $\theta < 90°$, solid surface is water wet. If $\theta > 90°$, solid surface is oil wet. For $\theta \approx 90°$, the surface is intermediate wet.

2.7 Capillary Number and Bond Number

Capillary number represents the ratio of viscous forces to capillary forces in the flow through a capillary (Green & Willhite, 1998). Capillary number is given by:

$$C_a = \frac{u.\mu_w}{\sigma_{ow}} \tag{2.8}$$

Where,
u: Mean velocity of the water phase.
μ_w: Viscosity of the water phase.
σ_{ow}: IFT between oil and water phase.

Bond number represents the ratio of gravity to capillary forces in the flow through a capillary (Sajadian & Tehrani, 1998). Bond number is given as:

$$N_b = \frac{\Delta\rho_{ow}.g.K}{\sigma_{ow}} \tag{2.9}$$

Where,
$\Delta\rho_{ow}$: Difference in density between oil and water phase.
g: Acceleration due to gravity.
K: Absolute permeability.
σ_{ow}: IFT between oil and water phase.

2.8 Capillary Pressure

Capillary pressure is defined as the difference in pressure between two immiscible fluid phases due to interfacial tension between these phases (Green & Willhite, 1998).

$$P_c = P_{nw} - P_w \tag{2.10}$$

Where,
P_{nw}: Pressure in the non-wetting phase
P_w: Pressure in the wetting phase.
As seen from equation 2.10, larger pressure exists in the non-wetting phase.

$$P_c = \frac{2\sigma_{ow}\cos\theta}{r} \tag{2.11}$$

The capillary pressure depends on IFT between the fluids, contact angle (θ) and the size of capillary (Green & Willhite, 1998). P_c may be positive or negative. The sign pf P_c expresses the phase with lower pressure and the one that preferentially wets the capillary.

2.9 Mobility

Mobility of a fluid phase (λ_i), is given by (Green & Willhite, 1998):

$$\lambda_i = \frac{k_{r,i}}{\mu_i}, i = o, w, g \tag{2.12}$$

Where,
$k_{r,i}$: Relative permeability of the fluid.
μ: Viscosity of the fluid.

In displacement processes it is more useful to use Mobility ratio, M_r:

$$M_r = \frac{\lambda_D}{\lambda_d} = \frac{\frac{k_{r,D}}{\mu_D}}{\frac{k_{r,d}}{\mu_d}} \tag{2.13}$$

Where,
D= displacing fluid.
d= displaced fluid.

Mobility ratio affects both areal and vertical sweep efficiency and the stability of the displacement process. At higher M_r (M_r >1), the displacement front becomes unstable and the sweep efficiency decreases (Green & Willhite, 1998). A low mobility ratio is desired (M_r <1) for higher recovery and stable displacement front.

2.10 Miscibility

Injected CO_2 may become miscible or remain immiscible with oil, depending on reservoir temperature, pressure and oil properties (Verma, 2015). A miscible CO_2-EOR process generally achieves higher recovery as compared to immiscible process.

1. Miscible mode: At constant temperature and composition, the lowest pressure at which dynamic miscibility can be achieved is known as minimum miscibility pressure (MMP). At minimum miscibility pressure, the interfacial tension is zero, and no interface exists between the fluids (Schlumberger, 2018b).

   Researchers have also defined MMP as the pressure at which more than 80 percent of oil-in-place (OIP) is recovered at CO_2 breakthrough (Holm & Josendal, 1974). Oil recovery of at least 90% at 1.2 Hydrocarbon pore volume (HCPV) of CO_2 injected is often used as a rule of thumb for estimating MMP (see fig.2.2).

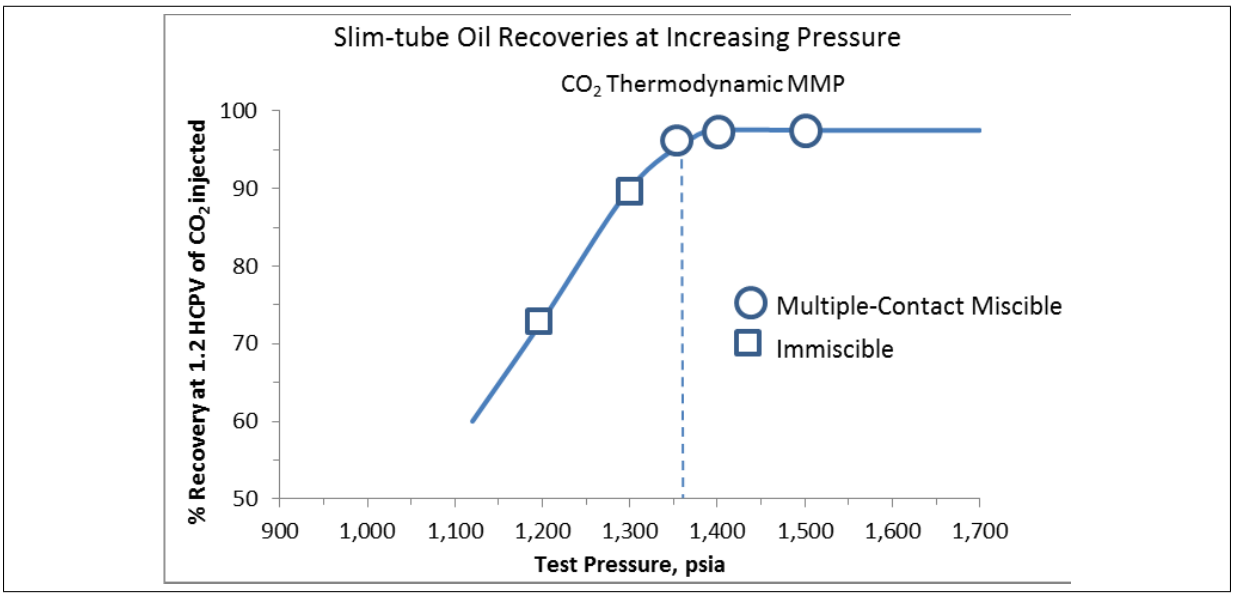

Figure 2.2: Slim tube oil recoveries at increasing pressures for fixed oil composition and temperatures (Yellig & Metcalfe, 1980).

Hydrocarbon miscible mechanisms can be divided into three types (Verma, 2015):

(a) First Contact: Solvents of this type mix with reservoir oil in all proportions and the mixture remains in one phase (Verma, 2015). Solvents like CO_2 are not first contact miscible, but they develop miscibility on multiple contacts known as dynamic miscibility, which leads to improved oil recovery.

(b) Vaporizing Gas Drive: Achieves dynamic miscibility by in-situ vaporisation of intermediate molecular-weight hydrocarbons from reservoir oil into the injected gas or CO_2 (Verma, 2015).

(c) Condensing Gas Drive: Achieves multiple-contact miscibility by in-situ transfer of intermediate molecular-weight hydrocarbons from injected gas to the oil phase (Verma, 2015).

2. Immiscible mode: CO_2 will not form a single phase with oil if reservoir oil composition is not favourable or the reservoir pressure is below MMP, and will not be miscible. However, dissolution of CO_2 in oil causes oil swelling and reduction in viscosity which helps improve sweep efficiency and oil recovery (D. Martin & Taber, 1992).

2.11 Physical Properties of CO_2

To understand how CO_2 behaves in the reservoir, it is essential to understand its physical properties and how they change with temperature and pressure. Fig.2.3 shows phase diagram for CO_2 with varying temperature and pressures. CO_2 has a triple point at 5.11 bar and -56.6°C. It is the point where all three phases (gas, liquid and solid) can exist simultaneously in equilibrium. Solid-Gas phase line is called sublimation line. Above Critical point at 73.9 bar and 31.1°C, CO_2 is in supercritical stage with some characteristics of gas and some of liquid (GCCSI, 2018).

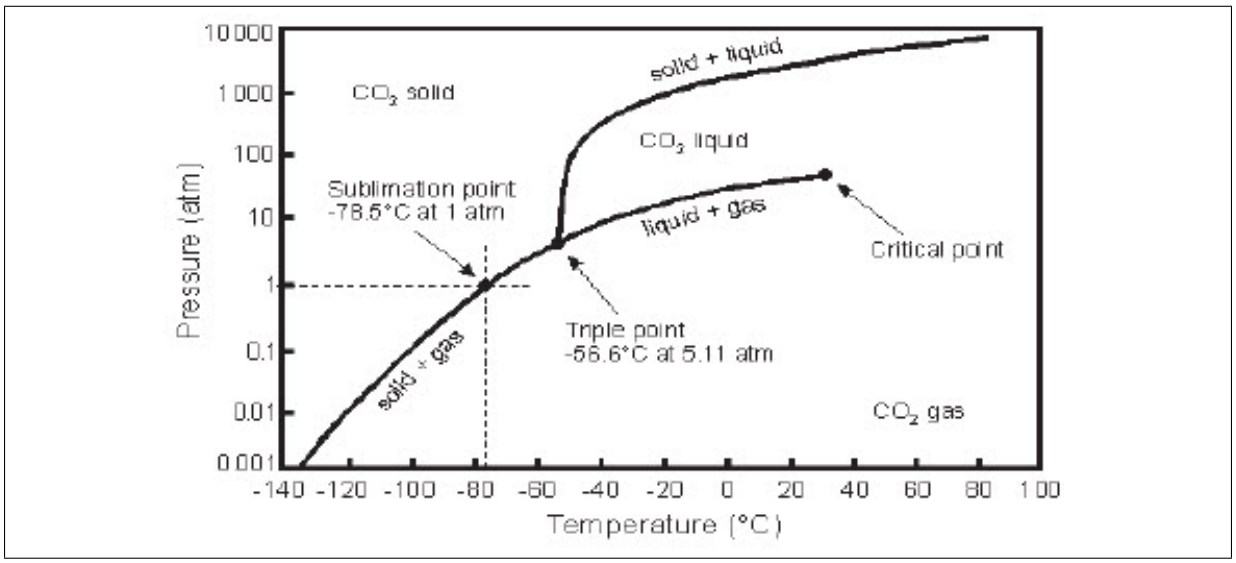

Figure 2.3: Phase diagram of CO_2 (GCCSI, 2018).

Density and Viscosity variation of CO_2 with Temperature and Pressure:
A rapid change in density (fig.2.4) and viscosity (fig.2.5) of CO_2 can be observed as CO_2 goes from gas to liquid and to supercritical phase.

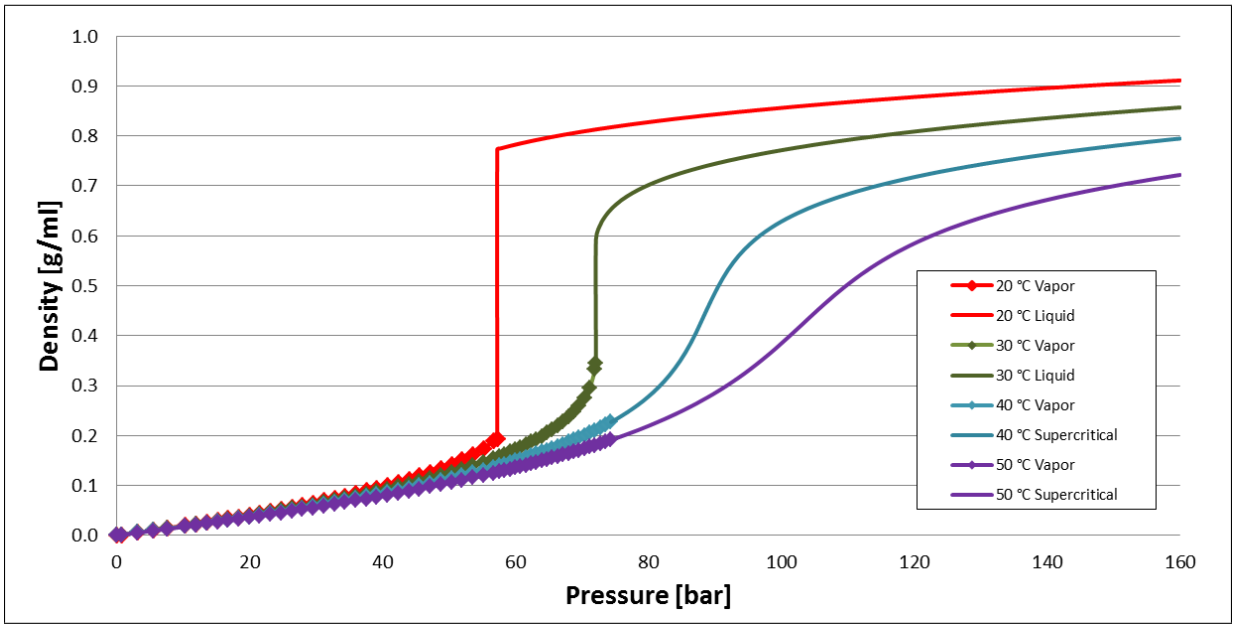

Figure 2.4: Density variation of CO_2 (NIST, 2013).

CO_2 is in supercritical stage at higher than critical temperatures and pressures and forms a phase whose density is close to that of liquid even though its viscosity remains quite low (Verma, 2015). Solubility of CO_2 in water is quite high compared to the solubility of nitrogen or hydrocarbon gases. At conditions like North Sea oil reservoirs, CO_2-to-water ratio would be around 30 Sm^3/m^3 (Sohrabi et al., 2011).

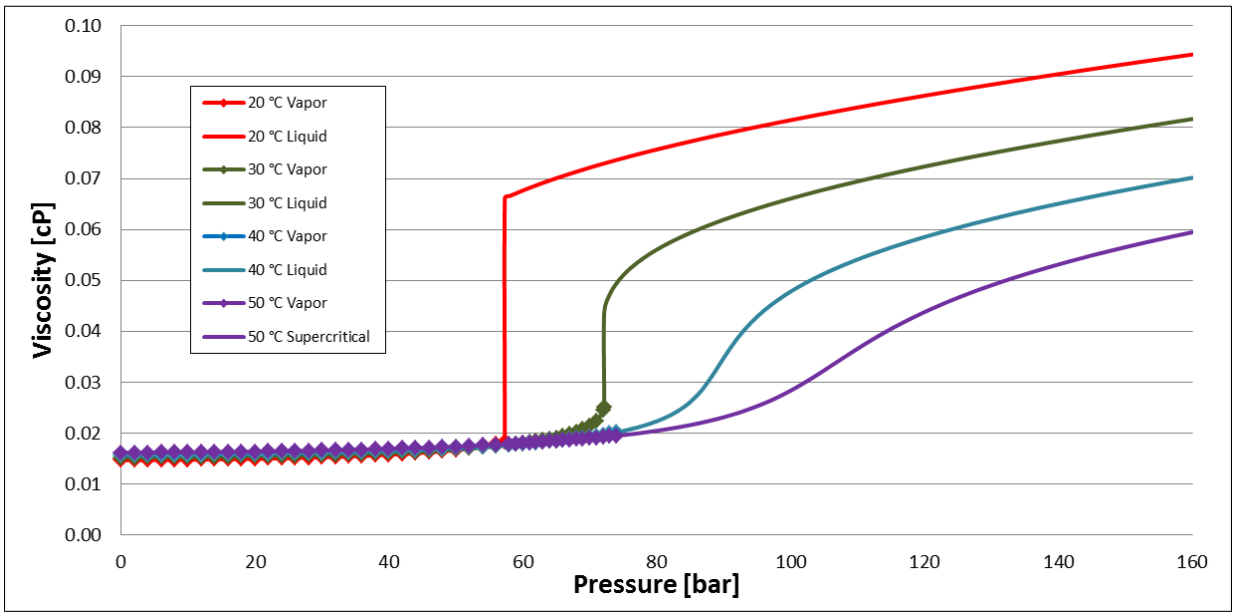

Figure 2.5: Viscosity variation of CO_2 (NIST, 2013).

Fig.2.6 shows solubility of CO_2 in water as a function of temperature and pressure.

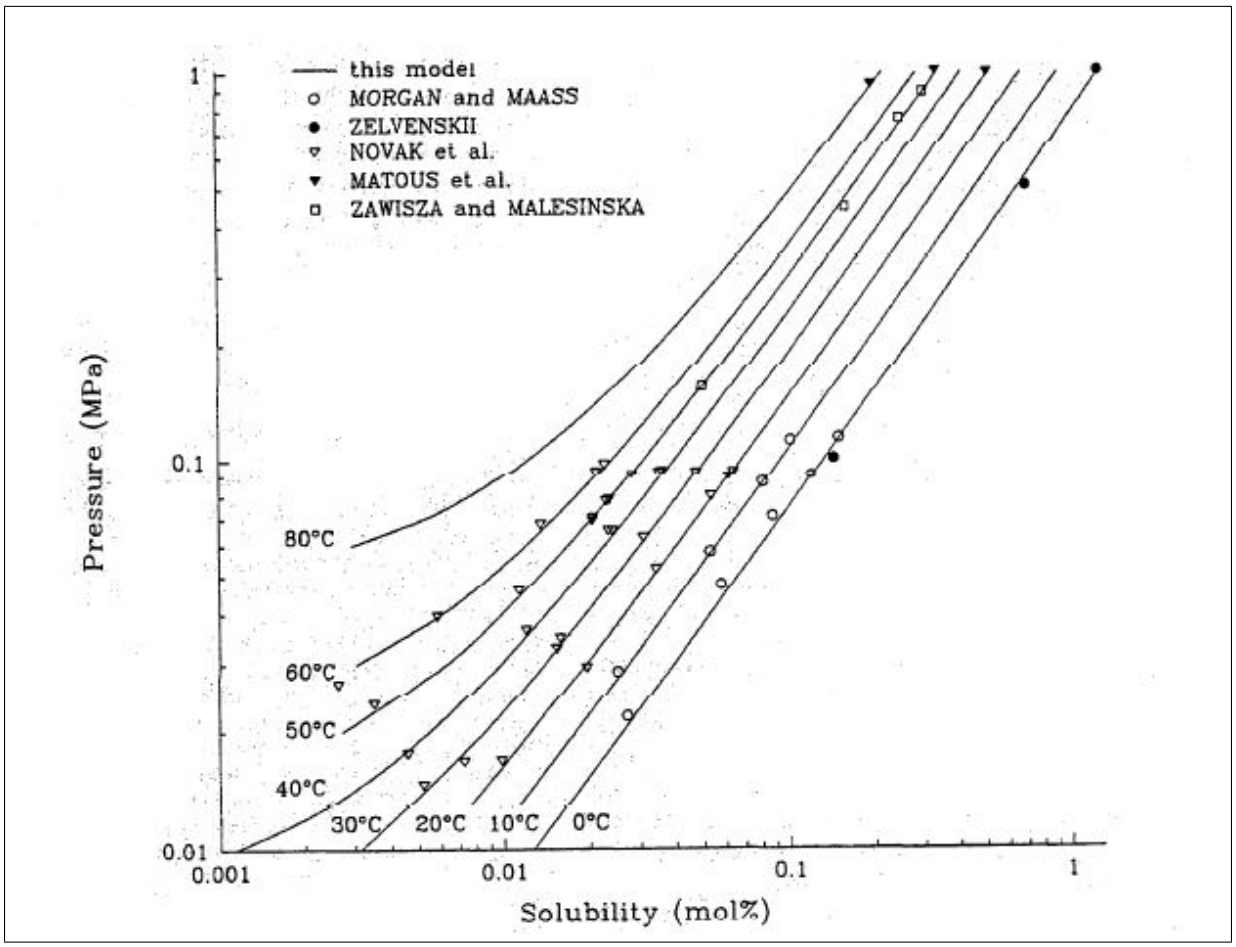

Figure 2.6: Solubility of CO_2 in water as a function of pressure and temperature (Carroll et al., 1991).

2.12 Reaction with minerals

Sandstone reservoir rocks, in general, contain siliceous materials, various carbonates, and clays (Sayegh, Krause, Girard, & DeBree, 1990). Calcium carbonates are predominant, although iron and magnesium carbonates are also common. Different rocks contain different proportions of these minerals, and they react differently to the varied environment caused by CO_2 injection.

The ability of CO_2 injection to improve oil recovery depends on rock type, type of fluids being injected, injection rates and reservoir conditions (Sayegh et al., 1990). At temperatures encountered in oil reservoirs, silica is inert to carbonated water and CO_2 because the quartz-rich sandstone dissolves in the presence of a strong acid like hydrofluoric acid. However siliceous minerals like iron chlorite become unstable in an acidic environment and become water soluble (Sayegh et al., 1990).

Castor et al. (1981) mentioned that alkaline materials (pH>9) readily react with silica (Castor, Somerton, & Kelly, 1981) and Stone et al. (1986) proved that at higher temperatures (steamflood), silica reacts with water to form H_4SiO_4, a soluble silicic acid (Stone, Boon, & Bird, 1986).

The following reactions occur during the dissolution of CO_2 in water:

$$H_2O + CO_2 \rightleftharpoons H_2CO_3 \tag{2.14}$$

$$H_2CO_3 \rightleftharpoons H^+ + HCO_3^- \tag{2.15}$$

$$HCO_3^- \rightleftharpoons H^+ + CO_3^{2-} \tag{2.16}$$

Calcium and Magnesium carbonates readily react with carbonated brines and water-soluble bicarbonates are formed by (Przybylinski, 1987); (Kapelke & Caballero, 1984):

$$H_2O + CO_2 + CaCO_3 \rightarrow Ca(HCO_3)_2 \tag{2.17}$$

$$H_2O + CO_2 + MgCO_3 \rightarrow Mg(HCO_3)_2 \tag{2.18}$$

$$H_2O + CO_2 + FeCO_3 \rightarrow Fe(HCO_3)_2 \tag{2.19}$$

In sandstone reservoirs, carbonate mineral acts as a cementing agent for sand and clay particles (Stone et al., 1986). In cases like that, these particles are released due to the dissolution of cement. They move in the flow path and can accumulate in pore throat and consequently reduce permeability (Sayegh et al., 1990).

Ross et al. (1982) and Bathurst (1972) mentioned that an increase in solubility of calcite is caused by (1) An increase in pressure at constant CO_2 concentration and temperature.(2) An increase in temperature at constant CO_2 partial pressure and (3) Up to a certain extent, the amount of CO_2 dissolved in brine (Ross, Todd, Tweedie, & Will, 1982); (Bathurst, 1972).

Therefore, calcium can precipitate (as $CaCO_3$) with a decrease in pressure by the following reaction (Bathurst, 1972).

$$Ca^{2+} + CO_3^{2-} \rightleftharpoons CaCO_3 \tag{2.20}$$

$$Ca^{2+} + 2\,HCO_3^- \rightleftharpoons CaCO_3 + H_2O + CO_2 \tag{2.21}$$

Formation of an insoluble scale of $CaCO_3$ can lead to a reduction in matrix permeability. This can be a problem at wellbores where large pressure drop occurs, and scale can be formed (Sayegh et al., 1990).

2.13 Drainage and Imbibition

There are two different types of displacement mechanisms in porous media, depending on the wetting properties of the fluids (Lenormand & Zarcone, 1984).

1. Drainage: The displacement of wetting fluid by non-wetting fluid.
2. Imbibition: The displacement of non-wetting fluid by wetting fluid.

Typically, a slow drainage process is characterized when capillary pressure is equal to or higher than threshold pressure of the pore[1], causing the non-wetting fluid to invade the pores (Lenormand, Zarcone, & Sarr, 1983).

It has been determined that wetting and non-wetting fluid can simultaneously flow in the same pore throat. Non-wetting fluid takes the bulk of the throat and wetting fluid remaining in corners of the cross-section and walls of the throat. This is illustrated in fig.2.7.

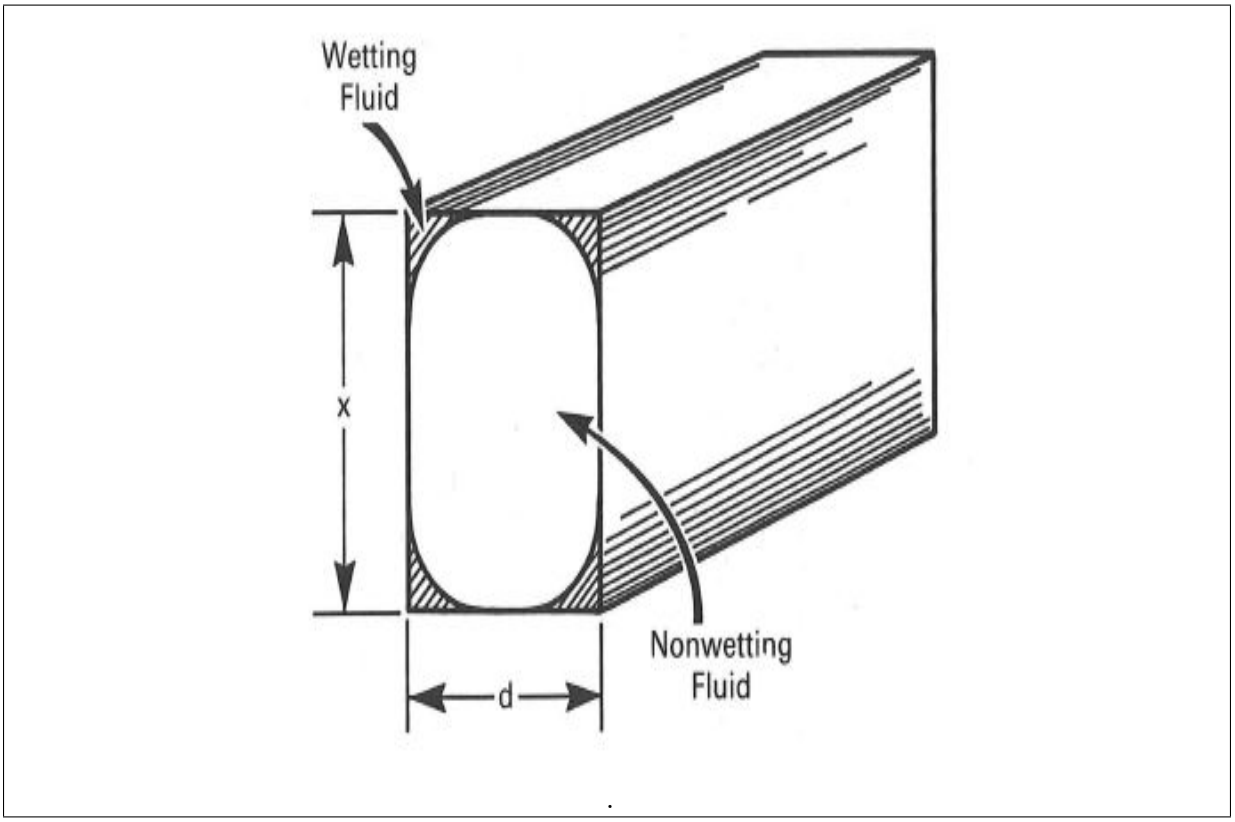

Figure 2.7: Movement of fluids in a pore throat. Used from (Lenormand & Zarcone, 1984)

Lenormand et al. studied imbibition as a superposition of three mechanisms (Lenormand & Zarcone, 1984):

1. Meniscus Displacement: It refers to the displacement of the interface between the fluids. They studied four different types of meniscus displacement and resulting pressure needed for each mechanism. Following are the four mechanisms proposed (as shown in fig.2.8):

[1]Threshold pressure is the capillary pressure in the narrowest part of the pore which must be overcome to invade the pore.

(a) *Piston-type motion*: The meniscus front is inside the throat and displacement of non-wetting fluid occurs when the pressure becomes smaller than capillary pressure in the throat.

(b) *Snap-off*: This occurs only in a throat. When the capillary pressure reaches critical capillary pressure, then interface collapses and wetting fluid occupies the throat forcing non-wetting fluid into the pores.

(c) *In type Imbibition- I1*: Fluid displacement in pores during imbibition is called In-type imbibition (Lenormand et al., 1983). I1 type imbibition occurs when only one throat surrounding the pore is filled with non-wetting fluid.

(d) *In type imbibition- I2*: In this type of imbibition, before wetting the pore with wetting phase, two of the neighbouring throats are filled with non-wetting phase fluid.

Other configurations with 3 or 4 throats filled with non-wetting fluid are very stable, and only "snap-off" mechanism is responsible for displacement (Lenormand & Zarcone, 1984).

2. Flow of non-wetting phase: This refers to the flow of non-wetting fluid displaced by the meniscus. Non-wetting fluid only flows in the bulk of pore throats and not on the walls. Flow can occur only if a continuous path of throats and intersections filled with non-wetting phase exists between the displaced meniscus and network exit. If continuity does not exist, then the non-wetting fluid gets trapped, and meniscus cannot move.

3. Flow of wetting phase: This refers to the flow of wetting fluid from network entry to the meniscus. Lenormand proposed a model to calculate the capillary numbers related to flow of wetting phase along the corners and along the roughness of the porous media. They came up with a characteristic capillary number for each kind of flow in pores.

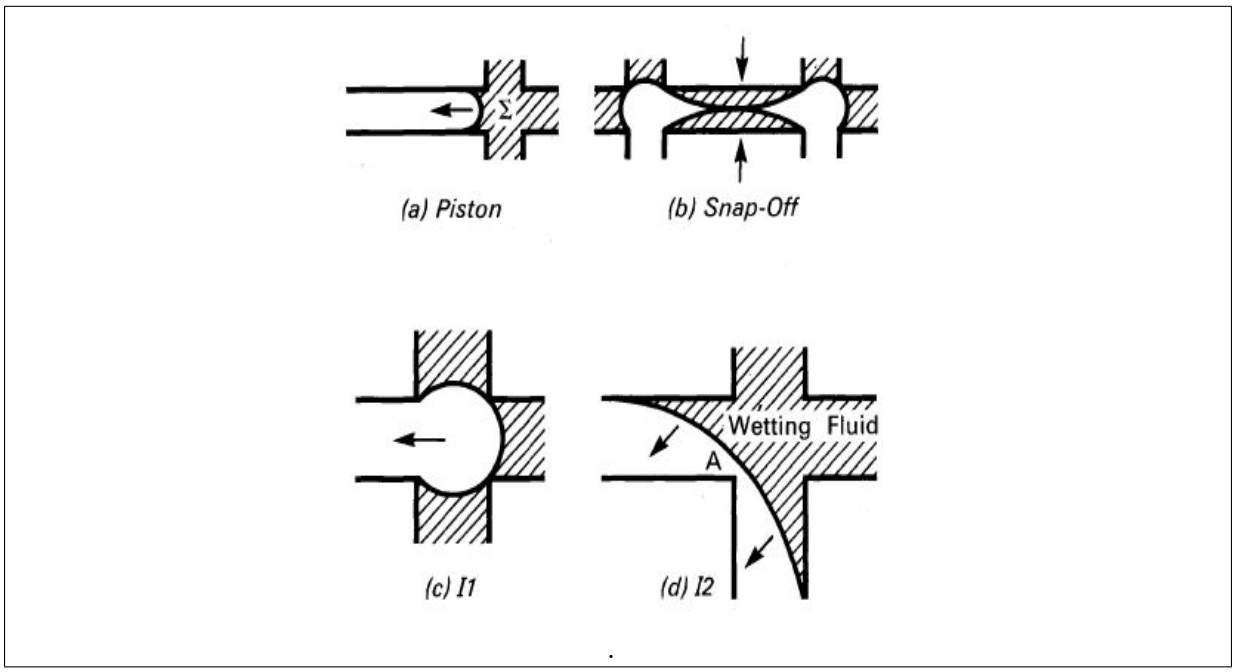

Figure 2.8: Different mechanisms of meniscus displacement. Modified from (Lenormand & Zarcone, 1984)

Chapter 3

CO_2 as a Displacing Fluid for EOR

Visualisation of CO_2 in the fluid system and porous media is the primary focus of this thesis. To understand the visualisation of CO_2 dissolution in water and subsequent movement of carbonated water in the porous media, literature study on the use of CO_2 and carbonated water as a displacing fluid is presented in this chapter. We end this chapter by presenting a summary of experiments done in the field of CO_2 and carbonated water visualisation.

3.1 CO_2 as an Injection Fluid

CO_2 EOR flooding has the potential to recover 15-25% of Original Oil in Place (OOIP) by improving the life of reservoir nearing depletion after secondary recovery, by 15 to 20 years (Grigg & Schechter, 1997). Various CO_2 processes have been studied for use in laboratory analysis and field implementation, such as a) Continuous CO_2 injection; b) Injection of CO_2 gas or liquid slug followed by continuous water injection; c) Injection of CO_2-water mixture; d) Huff and Puff processes; e) CO_2 gas or liquid slug followed by Water Alternating Gas (WAG). (Shi & Kantzas, 2008).

Benefits of using CO_2 for injection are (Espie, 2005):

1. Miscibility with oil is achieved at a lower pressure than other hydrocarbon gases.
2. Fewer problems due to gas override, because of its high density at reservoir conditions.
3. Hydrocarbon gases produced can be used for sales or other purposes.

Various sources of CO_2 include:

1. Natural sources of CO_2, e.g. Permian basin in USA or Hungary.
2. CO_2 produced from a combustion process.
3. CO_2 separated during manufacture of ammonia and hydrogen.

Coal-fired power plants and other large point sources of CO_2 are good candidates for CO_2 capture. Capturing CO_2 from these sources is very expensive and in addition to that very low pressure of flue gas (1 atm) and its low CO_2 content (10-15%) makes it more expensive to capture CO_2 and compress it for use. CO_2 injection projects in many oil

reservoirs are uneconomical due to high costs associated with the large volumes of CO_2 needed for injection (Sohrabi et al., 2011).

3.1.1 CO_2 EOR in the North Sea

Currently, the average recovery factor from Norwegian oil fields is 46% and Norwegian Petroleum Directorate (NPD) reports that many reservoirs in the area have temperature and pressure suitable for CO_2-EOR (Pham & Halland, 2017).

Advantages of using CO_2 as injection fluid in North sea are (Akervoll & Bergmo, 2010):

1. Many North Sea oil compositions are miscible with CO_2 at reservoir temperature and pressure, this will enable target residual oil after waterflooding.
2. Density of CO_2 at reservoir conditions is less than injected water in most cases, which will help improve sweep efficiency.

Simulation study proved that oil recovery by miscible CO_2 injection on NCS could recover approximately 63% OOIP, compared to approximately 43% OOIP by Waterflooding (WF) (Lindeberg & Holt, 1994).

The largest CO_2 injection in a pure CCS project is applied on Norwegian Continental shelf (NCS) in the Sleipner field (GCCSI, 2016). The CCS project on Sleipner is considered one of the global pioneers of CO_2 capture and storage. Captured CO_2 is injected into a sandstone reservoir, and over 17 million tonnes of CO_2 has been injected since the project commenced (1996). CO_2 injection in offshore field operations faces challenges such as (Gozalpour, Ren, & Tohidi, 2005):

- Cost of acquiring CO_2.
- Insufficient reservoir characterisation.
- Increase in corrosions in wells, flowlines and facilities.
- Scaling and asphaltene deposition due to alteration of equilibrium between components in reservoir fluids, upon introduction of CO_2.
- Well distances in offshore Norway are often around 1 km. As well distance increases, the segregation of CO_2 at the top of reservoir and water at the bottom of the reservoir will reduce sweep efficiency (Akervoll & Bergmo, 2010).

The number of successful CO_2 EOR projects on field scale is limited. Some of them are Weyburn-Midale project (Preston et al., 2005), Rangely Weber Unit (National Energy Technology Laboratory, 2018), Daqing and Liaohe (Global CCS Institute, 2010) and Salt Creek (zeroco2.no website, 2018).

3.2 Carbonated Water as an Injection Fluid

Conventional CO_2 injection faces many challenges. An alternate strategy is to use Carbonated Water (CW), i.e. use of CO_2 dissolved in water for storage and recovery improvement. Carbonated water overcomes some challenges faced by conventional CO_2 injection in the following ways:

1. Carbonated Water Injection (CWI) requires less CO_2 compared to conventional CO_2 injection. CO_2 needed for carbonation of water can be obtained from low-cost sources like nearby oil and gas fields (e.g., CO_2 separated from natural or associated gas), downstream activities (refineries or petrochemical plants) or other industrial sources (Verma, 2015). High CO_2 concentration in these sources and high pressure makes CO_2 capture and transport less expensive compared to obtaining CO_2 from flue gas.

2. CW is denser than native brine (Hebach, Oberhof, & Dahmen, 2004); this reduces the risk of buoyancy-driven leakage from the geologic formation and presents us with an alternative for CO_2 storage. Mobility contrast between CW-Oil system is less than the CO_2-Oil system; this limits fingering in the reservoir during CWI and provides better sweep efficiency, leading to more even distribution and delivery of CO_2 in the reservoir (Sohrabi et al., 2011).

   Due to CO_2 dissolution in oil, the oil viscosity is reduced, and this makes the mobility ratio more favourable. The oil volume expands and increases the relative permeability to oil. Miller and Jones showed that volume of a 17° API oil expanded by 20% when saturated with CO_2 at 138 bar and 60°C. They also showed viscosity reduction of 10° API oil from 7000 cP to 100 cP at 60°C when saturated with CO_2 (Miller & Jones, 1981).

3. During CWI, CO_2 stored in the rock is retained through solubility mechanism which is one of the safest mechanisms for geologic storage. CO_2 Storage through solubility mechanism is more advantageous than storage by conventional CO_2 injection where CO_2 remains as free gas pushing against the caprock for thousands of years with higher risk for leakage (Sohrabi et al., 2011).

4. Can be implemented in fields with limited modifications of waterflooding (WF) facilities.

5. Suitable for environments with limited CO_2 supply.

6. Development of the transition zone is not a requirement for Carbonated Waterflooding (CWF) since mass transfer dominates CO_2 moving from water to oil phase. Minimum Miscibility Pressure does not dictate displacement efficiency.

Various factors like carbonation level of the injected water, pressure, temperature and reactivity of crude oil influence CWI performance (J. Martin, 1951). Yang et al. showed that water oil IFT reduced up to 20% due to CO_2 dissolution in water (Yang, Tontiwachwuthikul, & Gu, 2005).

3.3 Laboratory Scale Studies on the Use of Carbonated Water

1. In late 1940's sand pack experiments conducted by Monteclaire Research proved that using CW after water flooding could reduce residual oil saturation further by 15% Pore volume (PV) (Lake, Carey, Pope, & Sepehrnoori, 1984).
2. Improvement in recovery factor by 15-25% was reported by Johnson et al. using CWF in sand packs at 24°C and 52 bar carbonation pressure (Johnson, Macfarlane, Breston, & Neil, 1952).
3. Martin reported a 12% increment in oil recovery using CW. He also concluded that water with reduced carbonation led to less improvement in oil recovery compared to fully CO_2 saturated water (J. Martin, 1951).
4. In 1960's, Holm conducted experiments in which he injected CW as a slug followed by chase water at 24°C and 76 bar using oils with viscosities 0.8 cP, 5 cP, 90 cP. Improvements in recovery factor (compared to WF) were reported to be 5%, 23% and 69% respectively (Holm, 1963).
5. In 1970's, Institut Francais du Petrole (IFP) reported oil recovery improvements of 13.9% PV from CW injection conducted in core flooding experiments using Bati Raman oil and Dodan gas (CO_2 concentration around 88%) (Khatib, Earlougher, & Kantar, 1981).
6. Mayer et al. conducted two sets of core flooding experiments in 1981 and 1985, where they reported improvement in oil recovery from 13% PV to 21.5% PV for samples used in 1981 (oil viscosity of 475 cP at 52°C) and an average oil recovery improvement of 19.4% with samples used in 1985 (oil viscosity of 406 cP at 52°C) (Mayer, Earlougher Sr, Spivak, & Costa, 1988).
7. Sohrabi et al. (2009) used micromodels to investigate CWF at pressure of 138 bar and temperature of 38°C. The oil recovery increase of 8.8% HCPV was reported for light oil (0.8 cP at 38°C) and recovery increase of 23.8% HCPV was reported for viscous oil (16.5 cP at 38°C) case (Sohrabi, Riazi, Jamiolahmady, Ireland, & Brown, 2009).
8. Dong et al. performed experiments using sand packs with Deionised (DI) water and dead oil from the Gulf of Mexico. At flowrates of 2PV/D (Darcy velocity close to 1ft/D), recovery factor improved by 6% PV (using CW as secondary flooding) and 9% (using CW as tertiary flooding) (Dong, Dindoruk, Ishizawa, & Lewis, 2011).
9. Recently, Sohrabi et al. (2015) conducted a series of CWI experiments at 172 bar and 38°C with "live" crude oil (containing dissolved gas). They observed the formation of a new phase within oil during carbonated water injection. They concluded that even small saturation of a new phase could considerably reduce the mobility of CW, which in turn reduces water production and improves oil recovery (Sohrabi, Emadi, Farzaneh, & Ireland, 2015).

3.4 Field Scale Studies on the Use of Carbonated Water

Carbonated water flooding has been implemented at full field scale from as early as 1950's. It was called K&S project and was located 10-miles north of Bartlesville, Oklahoma. It was reported that CWF produced 37% more oil than WF (Hickok & Ramsay Jr, 1962).

Scott and Forrester (1965) reported another field application of CWF in the Domes Unit, 15-miles west of Bartlesville. Approximately $1/3^{rd}$ PV of equivalent CW was injected and chased by plain water. Slug injection of CW gave an increment in oil recovery of about 9% PV (Scott & Forrester, 1965).

3.5 Visualisation Techniques

Miscible and immiscible displacement processes have received much attention at pore scale. Several techniques have been implemented to visualise CO_2 and carbonated water injection in porous media. Some of these are:

1. Use of X-ray CT and PET for high resolution visualisation of fluid flow in porous media.
2. Materials like glass, acrylic and polycarbonates have been widely used to create micromodels to help study micro displacement. Micromodels help to observe and investigate the motion of fluids and menisci, in terms of microgeometry and physical characteristics of liquids, gases and solids present (Sajadian & Tehrani, 1998).
3. Optical methods based on the use of projection methods like *Mach-Zehnder Interferometry* are also common. Various dyes and indicators have been used to trace fluid movement in porous media and provide a better understanding of fluid flow during CO_2 injection process.

Micromodel studies can help understand the microscopic and macroscopic behaviour of displacement processes and help model flow mechanisms on larger scales. Micromodels can be used to study complex interaction between effects of viscous, capillary and gravity forces with pore geometry and topology.

Micromodels can be used to observe effects of change in pore geometry, density difference, wettability, initial saturation and a combination of variables like capillary number (C_a) and bond number (N_b). Although it has been difficult to isolate individual variables, an interrelationship between them has been illustrated by various studies. Various studies conducted using 2-D models and micromodels for visualisation of fluids and recovery processes in porous media are mentioned below:

- Micromodel studies began as early as in 1952 when Chatenever and Calhoun studied two-phase flow in porous media (Chatenever & Calhoun Jr, 1952). Kimber and Caudle studied the distribution of gas and oil, before and after two-phase flow by use of photographic enlarger. This study helped considerably improve visibility at a microscopic level and overall model view (Kimbler & Caudle, 1957).
- McKellar and Wardlaw introduced the use of mirror glass, with silver and copper bonded to the glass. This technique helped develop a wide variety of patterns including repetitive designs. It also facilitated the development of heterogeneous models with irregular patterns. They conducted air-water displacements and

mercury porosimetry to examine effects of wettability, heterogeneity and network topology in various network types (McKellar & Wardlaw, 1982).

- Chatzis and Dullien presented a critical analysis of "Pore doublet model" for interpretation of trapping of one phase by another during displacement. Their studies in micromodels showed that imbibition is strongly linked to the flow of wetting phase as bulk fluid films which result in snap-off of the non-wetting phase at pore constrictions (Chatzis & Dullien, 1983).
- Sajadian and Tehrani used homogenous and heterogeneous network micromodels to study gravity drainage at 35 bar (Sajadian & Tehrani, 1998). Dastyari et al. used 2-D glass etched micromodels with and without fractures to compare free and forced gravity drainage (Dastyari, Bashukooh, Shariatpanahi, Haghighi, & Sahimi, 2005).
- Hatiboglu and Babadagli used 2-D models to study co- and counter-current type transfer between matrix and fracture due to diffusion (Hatiboglu & Babadagli, 2005). Sohrabi et al. have studied carbonated water injection in glass micromodels using n-decane, dead oil and live oil (Sohrabi et al., 2015). Riazi et al. used glass micromodels to study mechanisms involved in CO_2 injection and storage (Riazi, Sohrabi, Bernstone, Jamiolahmady, & Ireland, 2011).
- Hele-Shaw cell has widely been used in visualisation experiments. Hele-Shaw cell consists of two flat plates (at least one of them is transparent) parallel to each other, sealed on the edges and separated by a spacer. Table 3.1 shows some of the studies conducted in CO_2-water system. In this thesis, polycarbonate was used to prepare cells of varying thickness, and glass beads represented the porous media in the cell.

Several studies have been conducted using pH indicators for visualisation of CO_2 and water system (Emami-Meybodi, Hassanzadeh, Green, & Ennis-King, 2015). Some of these studies use surrogate/analog fluids as a representative of one of the phases. In this thesis, we have used dyes and pH indicator to colour oil and water phases respectively. Dyes and indicators were used to observe the movement of fluids in porous media and visualise various phenomena that occur during CO_2 injection.

Author	Setup used	Fluids[1]	Visualisation technique used
(Kneafsey & Pruess, 2010)	Hele-Shaw cell	CO_2- water	pH indicator in water
(Backhaus, Turitsyn, & Ecke, 2011)	Hele-Shaw cell	Water- PG	PG used as analog fluid
(Kneafsey & Pruess, 2011)	Hele-Shaw and bead pack	CO_2- water	pH sensitive dye in water
(MacMinn, Neufeld, Hesse, & Huppert, 2012)	Bead pack	MEG- water	MEG as a surrogate fluid
(Soroush et al., 2012)	Hele-Shaw cell	Water- brine	Dyed brine as a surrogate fluid
(Faisal, Chevalier, & Sassi, 2013)	Hele-Shaw cell	CO_2- water	pH indicator in water
(Agartan et al., 2015)	Bead pack	Water- PG	Dyed water phase. PG as a surrogate fluid

Table 3.1: Visualisation studies conducted in CO_2 – water system

Some limitations in visualisation studies mentioned above are:

1. Etched glass micromodels have been used to study fluid system where heterogeneity provided by etched pores is limited. Use of glass beads opposed to etched glass provides more complex pore distribution.
2. Micromodel studies are limited to visualising processes at a microscopic scale and are usually narrowed to a small section of pores.
3. pH indicators used in these studies are not exclusively water soluble.

[1]PG stands for Propylene glycol and MEG stands for Monoethylene glycol

4. One of the phases (Oil, water or CO_2) has to be digitally coloured to distinguish from other fluids in porous media.

Work done in this thesis aims to overcome these limitations by:

1. Using glass beads to represent complex porous media. Glass beads of varied size distribution and mixed wettability were used.
2. Polycarbonate cells of height 13.8 cm were prepared to visualise fluid system in pores. Size of the cell represents a bigger scale opposed to microscopic visualisation.
3. Dyes were used to represent the oil phase, and pH indicator was used in the water phase to visualise the dissolution of CO_2 as a change in colour from blue to yellow.

Chapter 4

Experimental Procedures and Materials Used

Experimental procedures and materials used in this thesis are presented in this chapter. This chapter is divided into six sections, and an outline of various sections is given below:

1. First, we begin by looking at different chemicals used in this thesis. Following that is a list of porous media types used in the experiments.
2. In the next section, an experimental procedure for preparation and testing of various dyes and pH indicator is presented. Dyes and indicator are used to aid visualisation of the oil and water phases.
3. After indicator testing, a procedure for conducting tests in graded tubes is presented. Indicator solutions selected in the previous step are tested in an oil-water system in porous media. Tests are conducted by making porous media diverse, and effects of varying internal diameter of the tube are also studied.
4. In the next section, a procedure for experiments conducted in a larger tube at low-pressure CO_2 injection (10 bar) is presented. These tests are conducted to study the capacity of CO_2 rich water to mobilise oil from porous media and simultaneously visualise the movement of water phase into the porous media (imbibition).
5. After tests in larger tubes, a procedure for preparation and testing in polycarbonate cells of varying thickness is presented. These tests help understand the effect of varying cell thickness on the water phase movement in porous media and limitations posed in the visualisation of tests.
6. Finally, a procedure to conduct experiments in Polyoxymethylene (POM) cell is presented. These experiments are used as baseline tests for future work at realistic reservoir conditions in a cell of similar design.

Experimental conditions: Experiments involving CO_2 injection were carried out at a pressure of 10 bar and room temperature (20°C). Glass beads were used as porous media and visualisation was performed using an optical method. In this case, using a Nikon D5200 camera.

Fig.4.1 shows the contribution of experiments outlined above in achieving the primary objectives of this thesis.

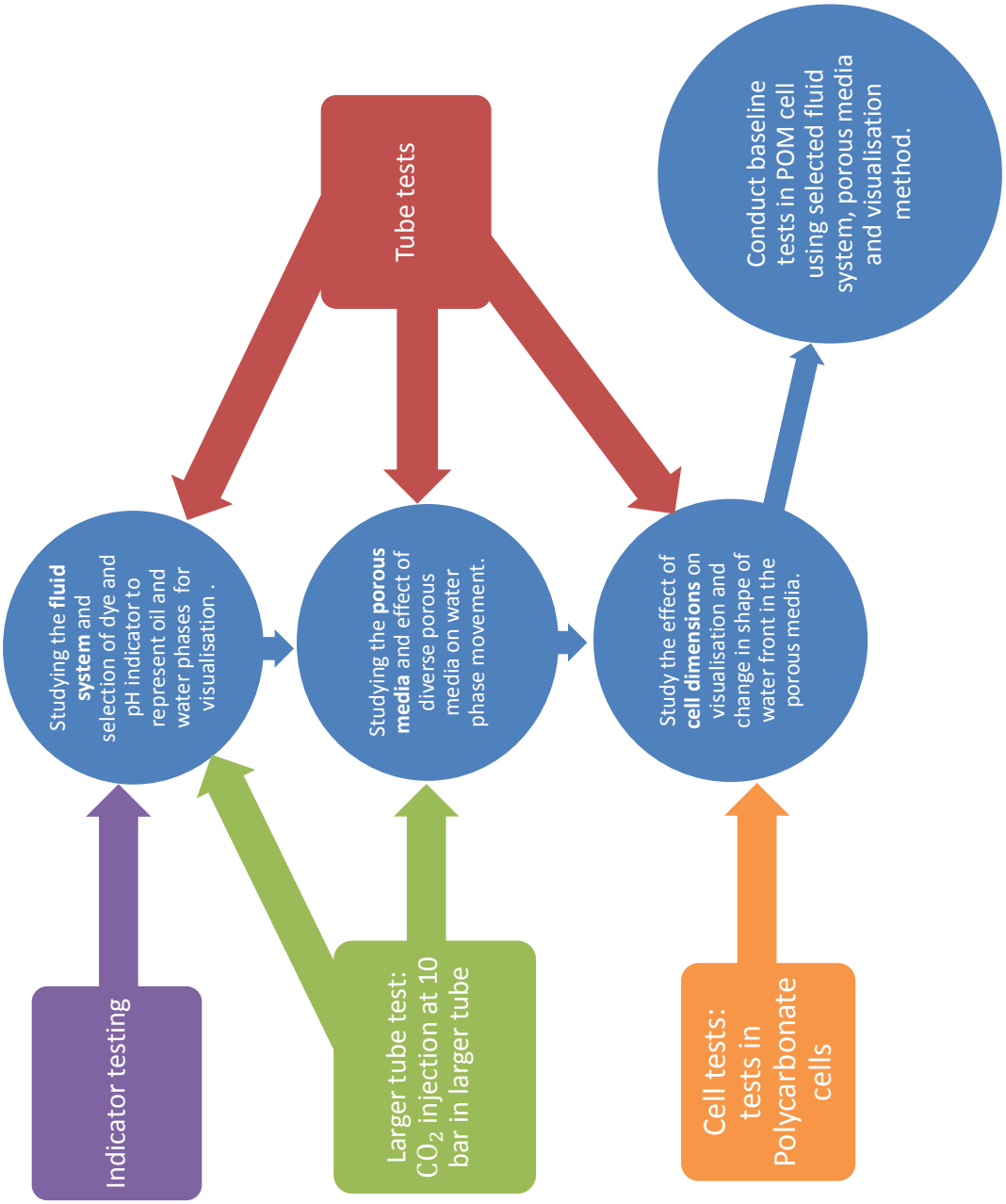

Figure 4.1: A chart showing the interrelationship between experiments to achieve the objectives of this thesis.

4.1 Materials Used

4.1.1 Chemicals Used

Presented in table 4.1 are chemicals used in the experimental work conducted in this thesis.

Chemical Name	Chemical Formula	Grade	Purity	Supplier
Sudan Blue II	$C_{22}H_{26}N_2O_2$	R &D use	98%	Sigma-Aldrich
Sudan II	$C_{18}H_{16}N_2O$	R &D use	pure	Acros Organics
Sudan III	$C_{22}H_{16}N_4O$	R &D use	pure	Alfa Aesar
Bromothymol Blue	$C_{27}H_{28}Br_2O_5S$	R &D use	pure	Alfa Aesar
Methanol	CH_3OH	Lab use only	98.5%	VWR chemicals
Hydrochloric Acid	HCl	For analysis	37%	Merck
n-Decane	$C_{10}H_{22}$	For synthesis	94%	Merck
Sodium Hydroxide	NaOH	For analysis	99%	Merck
Acrifix 2R 0190[1]	$C_5H_8O_2$	For sealing	60-100%	Evonik

Table 4.1: Chemicals used.

Sudan blue II is an oil-soluble dye that comes under the family of sudan blue dyes. Sudan II and Sudan III are oil-soluble dyes that come under the family of sudan red dyes. These dyes are used in the experiments for visualisation of the oil phase.

Bromothymol blue is a water soluble pH indicator. The reason for selection of Bromothymol blue is its change in colour over a pH range from 6.0 (yellow) to 7.6 (blue), which makes it a good indicator of dissolved CO_2 and other weak acidic solutions. It is used for visualisation of the water phase and CO_2 dissolved in the water phase. In the pH range of 7 to 7.6, it shows a greenish blue colour.

4.1.2 Porous media

Presented in table 4.2 are types of porous media (glass beads) used in this thesis. Porous media of type A and type B were supplied by Preciball, and porous media of type C and type D were supplied by Sigmund Lindner (SiLibeads). Porous media of given sizes were selected to compare results with ongoing projects at IRIS.

Porous media label	Wetting type	Size (μm)	Composition
Type A	Water wet	150	72% SiO_2, 13% Na_2O, 9% CaO, 4% MgO and 2% further
Type B	Water wet	90-150	72% SiO_2, 13% Na_2O, 9% CaO, 4% MgO and 2% further
Type C	Water wet	70-110	72.3% SiO_2, 13.3% Na_2O, 8.9% CaO, 4% MgO and 1.5% further
Type D	Hydrophobic[2]	70-110	72.3% SiO_2, 13.3% Na_2O, 8.9% CaO, 4% MgO and 1.5% further

Table 4.2: Types of porous media used.

Size distribution of porous media type C and type D is given in appendix C on page 143.

[1] Acrifix is a commercial name for the sealing glue. It is a solution of an acrylic polymer in Methyl Methacrylate.

[2] Made hydrophobic by coating with n-Octyltriethoxysilane (done by the supplier).

4.2 Indicator Testing

Indicator testing involves examination of different indicator solutions to observe their behaviour in an oil-water system. The first part of the procedure details the preparation of indicator solutions and the second part covers testing of these indicator solutions in an oil-water system. Experiments performed in this section are referred to as 'Indicator tests'.

4.2.1 Description

Objective

These experiments aim to test different dyes and indicator solutions to select the best candidates to be used in the visualisation of oil and water phases.

The experiments are divided into following three parts:

1. In the first part, one phase (e.g. oil) is dyed and tested with another un-dyed phase (e.g. water) in a 10 mL graded tube to determine the stability[3] of a dye in the presence of another. 0.1 M HCl was added to mimic the change in pH due to CO_2 dissolution in water. The observations on (oil/water) phase behaviour with a change in pH are made.
2. Following this, both oil and water phases are dyed and taken together in a tube to study their stability in the presence of one another. Observations are made in case of movement of dye from one phase to another upon addition of acid (0.1 M HCl).
3. In the last part, observations are made on the stability of water phase indicator solution in the presence of stock tank oil from North Sea reservoir. The properties of stock tank oil are given in table 4.3.

Chemical property	Value (at 20°C)
Viscosity	66.36 cP
Density	0.8620 g/cc

Table 4.3: Stock tank oil properties.

Materials Used

The following materials are used in the Indicator testing experiments:

- Water phase (De-ionised water).
- Oil phase (n-Decane and crude oil).
- 10 mL syringe (to add water and oil phase to the tube).
- Chemicals and dyes (HCl, NaOH, Sudan II/III, Sudan blue II and Bromothymol blue).
- Test tubes, graded 10 mL.
- Volumetric flask (250 mL).

[3]In this thesis, stability means the ability of dye to retain colour over time.

- Volumetric flask (50 mL).
- Weight scale.
- Magnetic stirrer.
- Camera.

4.2.2 Procedures

4.2.2.1 Preparation of chemical solutions

0.01N NaOH

Add 0.2 g of NaOH to 250 mL DI water, and dilute up to 500 mL with DI water. Mix the solution on a magnetic stirrer for 1 hour.

0.1M HCl

Fill a volumetric flask about 125 mL with DI water. Use a pipette of suitable size and transfer 2.1 mL of HCl into the volumetric flask. Use a magnetic stirrer for even mixing. Fill the flask up to 250 mL mark with DI water and mix on a magnetic stirrer for 1 hour. *Note:* - Never add water to concentrated acid.

Bromothymol blue indicator solution

Preparing 0.04 wt% aqueous bromothymol blue solution: Dissolve 0.1 g (gram) Bromothymol blue powder in 16 mL 0.01N NaOH, and dilute with de-ionised (DI) water until the total weight of the solution is 250 g. Mix the solution on a magnetic stirrer for 1 hour. This pH indicator solution will be further diluted to be used as water phase in the experiments.

Dyes in n-decane

Preparing 0.04 wt% oleic sudan blue/red solution: Dissolve 0.02 g of sudan blue II/sudan II/sudan III in 20 mL n-decane. Add more n-decane until the total weight of the solution is 50 g. Mix the solution on a magnetic stirrer for 1 hour. Use syringe filter of 0.45 microns to remove any precipitation in the solution.

4.2.2.2 Testing of Indicator solutions in an oil-water system

Label	Water phase	Oil phase
Indicator test I	DI water	n-decane
Indicator test II	DI water / dyed water	Sudan blue II (0.04wt% in n-decane)
Indicator test III	DI water / dyed water	Sudan II (0.04wt% in n-decane)
Indicator test IV	DI water / dyed water	Sudan III (0.04wt% in n-decane)
Indicator test V	Dyed water solution	stock tank oil

Table 4.4: Indicator testing experiments.

Table 4.4 shows different experiments conducted using indicator solutions.

Indicator test I: Testing bromothymol blue indicator in an oil-water system

- Add 5 mL DI water and 5 mL n-decane in a test tube graded 10 mL.
- Add 0.5 mL of bromothymol blue indicator solution to the test tube and observe the movement of the indicator solution and change in colour.
- Add drop by drop 0.01 N NaOH and observe the change in colour of water phase due to the change in pH.
- Add drop by drop 0.1 M HCl into the test tube to observe the change in water/oil system. Note the change in colour upon addition of acid and notice the stability of indicator solution, i.e. if indicator solution is losing colour over time due to a reaction with the oil phase.

Indicator test I - IV: Testing sudan blue/red in an oil-water system

Dyed water phase in these experiments was: 4.5 mL DI water+ 0.5 mL bromothymol blue indicator solution. That is 0.004 wt% bromothymol blue in DI water.

- Add 5 mL DI water and 5 mL dyed n-decane (0.04 wt% sudan blue II/sudan II/sudan III in n-Decane) in a test tube.
- Add 2-3 drops of 0.1 M HCl into the test tube to observe the changes in the oil phase.
- For experiments involving both oil and water phases to be dyed: Add 5 mL dyed water phase and 5 mL dyed oil phase in a test tube of 10 mL grading. Add 2-3 drops of 0.1 M HCl using a pipette into the test tube and observe changes in the system.

Indicator test V: Testing of the dyed water phase in the presence of crude oil

- Add 3 mL of stock tank oil and 6 mL dyed water phase to a test tube. Allow them to separate.
- Add 2-3 drops of 0.1 M HCl into the test tube to observe changes in the system.
- Observe the tube for 24 hours and note any changes in the colour of the indicator solution in water over time due to a reaction with the oil.

4.2.2.3 Procedure for pH measurement

- 'PHM 92 Lab pH meter' manufactured by 'Radiometer' is used for measuring pH of the water phase.
- Ensure that the pH meter is calibrated in the range of pH measurement to be performed (e.g. 4-7 or 7-10).
- Dip the electrode in the solution to be measured, and allow the reading to stabilise.
- Once stable, note the reading on pH meter. Clean the electrode using DI water before next measurement.

Note: pH measurements can vary with an error of $\pm$ 0.05. Variation in pH measurements is a result of a variety of factors like minor variations in room temperature, variations in temperature of the sample, cleanliness of glassware used and variation in the calibration of the pH meter.

4.3 Tube tests with porous media

These experiments involve studying the oil-water system in a porous media. Oil mobilisation from pores by water phase under gravity is observed in graded tubes of 10 mL. Oil recovery and movement of water phase into the porous media were studied. Experiments conducted in this section are referred to as 'Tube tests'.

4.3.1 Description

Objective

In Indicator tests (section 4.2), we examined the stability of dyes and indicator solution. This experiment aims to study the ability of dyes and indicator solution to represent oil and water phases in the porous media. 0.1 M HCl is added to mimic the change in pH due to the dissolution of CO_2 in water and represent the transport of CO_2 in the system.

Label	Porous media	Tube dia.	Water phase	Oil phase
TT I	Type A	12.5 mm	DI water	Sudan blue II (0.04wt% in n-decane)
TT II	Type A	12.5 mm	Dyed water	n-decane (un-dyed)
TT III	Type A	12.5 mm	Dyed water	Sudan II (0.04wt% in n-decane)
TT IV	Type A	12.5 mm	Dyed water	Sudan III (0.04wt% in n-decane)
TT V	Type C	12.5 mm	Dyed water	Sudan II (0.04wt% in n-decane)
TT VI	Acid-washed type C	12.5 mm	Dyed water	Sudan II (0.04wt% in n-decane)
TT VII	Type D	12.5 mm	Dyed water	Sudan II (0.04wt% in n-decane)
TT VIII	Acid-washed type D	12.5 mm	Dyed water	Sudan II (0.04wt% in n-decane)
TT IX	Mix (Type C+ Type D)	12.5 mm	Dyed water	Sudan II (0.04wt% in n-decane)
TT X	Acid-washed Mix	12.5 mm	Dyed water	Sudan II (0.04wt% in n-decane)
TT XI	Type C	7.85 mm	Dyed water	Sudan II (0.04wt% in n-decane)
TT XII	Type C	5.55 mm	Dyed water	Sudan II (0.04wt% in n-decane)
TT XIII	Type C	3.75 mm	Dyed water	Sudan II (0.04wt% in n-decane)

Table 4.5: List of tube tests.

Table 4.5 gives information about tube tests conducted in this thesis. Label 'TT' refers to 'tube test'. Dyed water phase was 4.5 mL DI water+ 0.5 mL bromothymol blue indicator solution.

The experiments are divided into following three parts:

1. Tests in porous media type A (TT I-IV): Experiments conducted in this part used porous media without varying the particle size or the nature of porous media (acid-washing or mix of hydrophilic and hydrophobic). These tests laid a basic understanding of imbibition process visualisation and movement of the water phase in porous media to displace the oil. At the end of this test, a dye which best-represented the oil phase in porous was chosen for further experiments.
2. Tests in porous media type C/D (TT V-X): These experiments were conducted by making the porous media more varied by altering the size distribution of glass beads and changing the wettability by mixing hydrophobic and hydrophilic glass beads. Oil recovery with the variation in porous media was studied, and fluid movement was correlated with studies in the literature.

3. Tube tests by varying the internal diameter of the tubes (TT XI- XIII): In this part, experiments with the oil-water system in porous media type C were performed by varying the internal diameter of the tube. These tests helped study the effect of the decrease in tube diameter on the shape of water front in porous media and formed a basis for determining the cell thickness to be used in cell tests in section 5.4 on page 96.

Materials Used

The following materials are used in tube tests:

- Water phase (DI water dyed and un-dyed).
- Oil phase (n-necane-dyed and un-dyed).
- 0.1 M HCl.
- 10 mL syringe (to add water and oil phase to the tube).
- Test tubes graded 10 mL.
- Porous media (Type A/ C/ D).
- Camera.

4.3.2 Procedure

4.3.2.1 Tube tests in porous media type A: Tube test I - IV

Experiments were carried out at room temperature (20°C) and atmospheric pressure. Four experiments conducted in glass beads of type A include:

1. Undyed water phase and oil dyed with sudan blue II in porous media.
2. Water phase dyed with bromothymol blue and undyed oil in porous media.
3. Water phase dyed with bromothymol blue and oil dyed with sudan II in porous media.
4. Water phase dyed with bromothymol blue and oil dyed with sudan III in porous media.

A simplified procedure for four experiments conducted in porous media type A is given below:

- Add 3 mL oil phase to the test tube. Add porous media to the tube and notice time taken by glass beads to settle under gravity.
- Once the glass beads have settled at the bottom of test tube notice the interface between glass beads and the free oil phase. Document the settling of glass beads and check the visibility of the interface.
- Add water phase to the test tube, begin with few droplets and then increase to few mL (not more than 5 mL). Notice the movement of water phase through the oil phase and in the porous media. Check if water and oil phases can be distinguished in the porous media.
- Add 3-4 drops of 0.1 M HCl to the tube and note changes in the system in the presence of an acidic water phase.

4.3.2.2 Tube tests in porous media type C/D: Tube test V- X

Glass beads of type C and D (different size distribution, refer tab. 4.2 on page 25) are used in the following experiments to make porous media more varied. A variation in wettability of porous media is achieved by mixing glass beads of type C (hydrophilic) and type D (hydrophobic).

While conducting tube test with dyed water phase and undyed oil phase (subsection 5.2.1.2 on page 56), it was observed that the addition of glass beads to water phase caused the pH of water phase to rise from 7.67 to 9.68. To solve this issue, a procedure to treat glass beads using hydrochloric acid is presented below. In this thesis, glass beads treated with hydrochloric acid are referred to as 'acid-washed glass beads'.

4.3.2.3 Preparation of acid-washed glass beads

It is believed that CaO in the glass beads reacts with water to increase the pH.

During preparation of glass beads; heating of $CaCO_3$ leads to:

$$CaCO_3 \longrightarrow CaO + CO_2 \tag{4.1}$$

$$CaCO_3 + 2HCl \longrightarrow Ca^{2+} + 2Cl^- + H_2CO_3 \tag{4.2}$$

We aim to treat $CaCO_3$ present in the glass beads by an reaction with HCl, as per equation 4.2.
Molar mass of $CaCO_3$= 100.0869 g/mol and molar mass of HCl= 36.46 g/mol.

Assuming the glass beads contain 25% $CaCO_3$ during preparation, i.e. 25 g of $CaCO_3$/ 100 g glass beads. Using equation 4.2,

Number of moles of $CaCO_3$ = Given mass/ Molar mass = 25/100.0869 = 0.2497 moles.

Number of moles of HCl required = (moles of $CaCO_3$)*(stoichiometric ratio between HCl and $CaCO_3$ = (0.2497)*(2) = 0.4995 moles.

Concentration of HCl required = Number of moles/ Volume of HCl = 0.4995/ 0.5 = 0.9991 mol/L.

In this glass beads cleaning procedure, amount of acid used is roughly 5 times (weightwise) the amount of glass beads.

The procedure for preparation of acid-washed glass beads is given below:

- Take 100 g glass beads of type C or type D in a beaker. The acid added will be 5 times the amount (weightwise) of glass beads, i.e. 500 g.
- Slowly add 0.99 M HCl to the beaker. Observe if there is any reaction of acid and glass beads to release heat or gases.
- Add in total 500 g of 0.99 M HCl to 100 g glass beads and mix on a magnetic stirrer for 4 hours.
- Using a sieve, drain out the acid to separate the glass beads from the liquid.
- Wash the glass beads thoroughly with DI water to remove any acid covering the surface of glass beads.
- After washing glass beads with DI water, dry them in an oven at 50 °C for 24 hours. This gives enough time for water present between the beads to evaporate.

- After 24 hours, take glass beads out of the oven and allow them to cool down to room temperature. Upon cooling down, add 5 wt% acid-washed glass beads to the water and measure pH.
- If measured pH is still above 8.5 follow the above procedure and allow glass beads to mix with acid for a longer time. Alternatively, the concentration of acid used to treat glass beads can be increased by estimating more $CaCO_3$ in the calculations.

Preparation of 0.99 M HCl

Fill a volumetric flask about 350 mL with DI water. Use a measuring cylinder to transfer 82.7 mL of HCl into the volumetric flask. Use a magnetic stirrer for even mixing. Fill the flask up to 500 mL mark with DI water and mix the solution on a magnetic stirrer for 1 hour.

After acid-washing the glass beads, the pH of water phase with the addition of glass beads (5 wt% to water phase) was measured again, and results are mentioned in subsection 5.2.2 on page 64.

Six experiments conducted in glass beads of type C/D are:

1. Oil-water system in porous media type C (refer tab. 4.2 on page 25).
2. Oil-water system in acid-washed porous media type C.
3. Oil-water system in porous media type D.
4. Oil-water system in acid-washed porous media type D.
5. Oil-water system in a mix of porous media type C+ type D (50 wt% each).
6. Oil-water system in a mix of acid-washed porous media type C+ acid-washed porous media type D (50 wt% each).

For the preparation of a mix of porous media of type C+ type D: Take 25 gm each of type C and type D porous media in a beaker and mix them thoroughly. Fill them in a tube and use a vortex mixer (as shown in fig. 4.2 on the following page) for even mixing of the glass beads.

For the preparation of a mix of acid-washed porous media of type C+ type D: Take 25 gm each of acid-washed type C and acid-washed type D porous media in a beaker and follow similar procedure as mentioned in the paragraph above.

A simplified procedure for six experiments in glass beads type C/D is given below:

- Add 3 mL oil phase to the test tube. Add porous media (of the type depending on the experiment) to the tube till the level reaches approximately halfway on the tube. For better packing place the test tube in an ultrasonic bath for 10 minutes.
- Once the glass beads have settled at the bottom of test tube notice the interface between glass beads and the free oil phase. Document the settling of glass beads and check the visibility of the interface.
- Add water to the test tube, begin with few droplets and then increase to few mL. Notice the movement of the water phase in the porous media.
- Add 3-4 drops of 0.1 M HCl to the tube and note changes in the system in the presence of the acidic water phase.

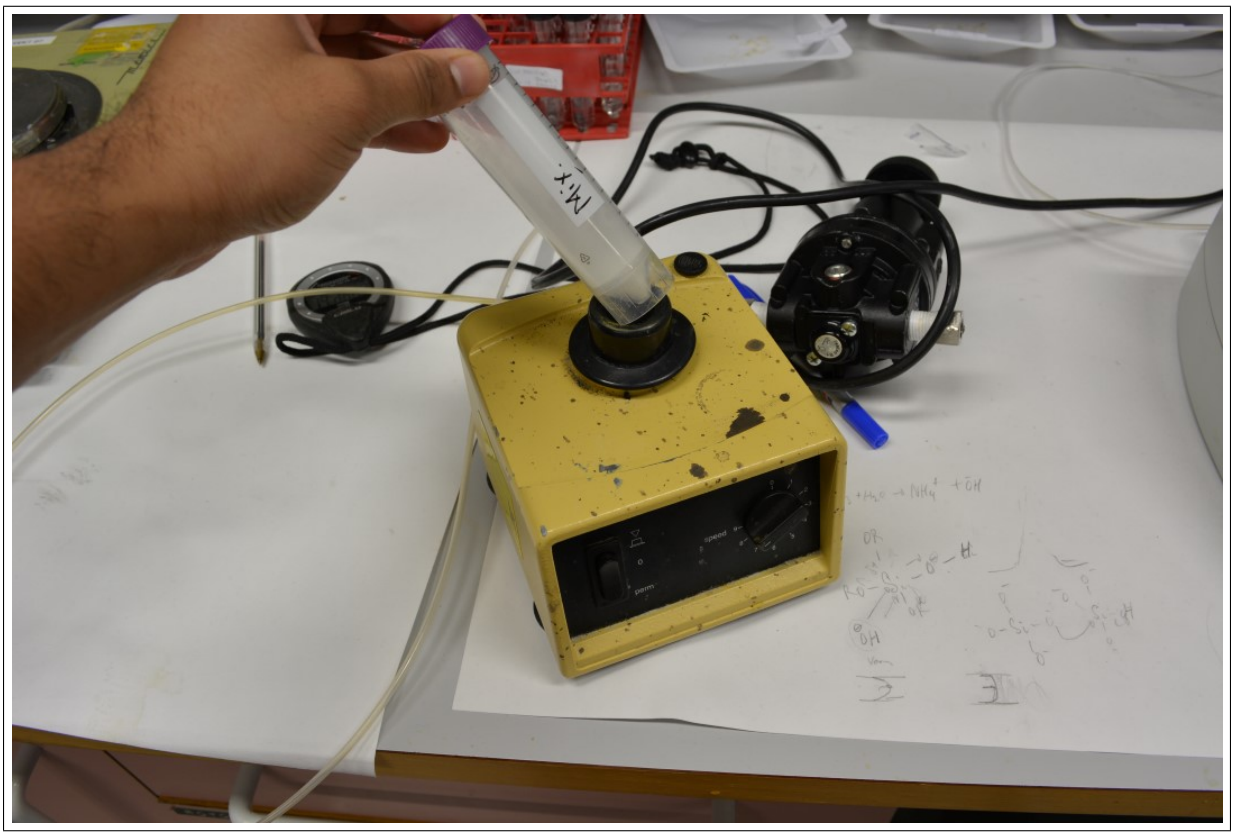

Figure 4.2: Vortex mixer for proper mixing of porous media.

4.3.2.4 Tube tests by varying diameter of the tube: Tube test XI - XIII

The diameter of tubes used in previous tests was 12.5 mm. In this test, tubes of varying diameter are used to study oil-water system in porous media. Glass beads of type C are used, and the addition of 0.1 M HCl mimics the change in pH due to the dissolution of CO_2 in the water phase.

Three experiments were conducted in tubes of internal diameter: 7.85 mm, 5.55 mm and 3.75 mm. A simplified procedure for these experiments is mentioned below:

- Add oil phase to the test tube till the height of oil column is approximately $1/3^{rd}$ total height of the tube (since tubes are of varying diameter a fixed quantity of oil phase will give a different height of oil column in each tube). Add porous media to the tube till the level reaches approximately halfway on the tube. For better packing place the test tube in an ultrasonic bath for 10 minutes.
- Once the glass beads have settled at the bottom of test tube notice if there is excess oil column on top of glass beads, remove it carefully using a syringe.
- Add water to the test tube, begin with few droplets and then increase to few mL. Notice the shape of the water front in the porous media.
- Add 3-4 drops of 0.1 M HCl to the tube and note changes in system in the presence of acidic water phase.

4.4 Tests in a larger tube with CO_2 injection at low pressure (10 bar)

CO_2 injection at 10 bar is carried out in these experiments in a larger tube. Maximum allowable working pressure for this tube is 40 bar, but for these experiments, the operating conditions are limited to a pressure of 10 bar and room temperature (20°C). Fig. 4.3 on page 36 shows larger tube used in these experiments (diameter = 11 mm). Experiments performed in this section are referred to as 'test in larger tube' or 'larger tube test'.

4.4.1 Description

Objective

Studies in literature have shown that CO_2 concentration in water at 10 bar and 20°C is 0.5 mol% (1.21 wt%) (fig. 2.6 on page 12). Tests in a larger tube with CO_2 injection at 10 bar can confirm if the amount of CO_2 dissolved under these conditions is sufficient to change the pH of water phase (seen as a change in colour from blue to yellow) or not. Movement of CO_2 enriched water phase through porous media is also studied in these tests.

Observations are made on CO_2 movement in the water phase, change in oil phase viscosity, CO_2 front type, the effect of CO_2 rich water phase in pores and oil recovery by varying the porous media.

Table 4.6 shows experiments conducted in larger tube. 'LT' refers to 'Larger tube'.

Label	Water phase	Oil phase	Porous media
LT I	Dyed water	–	–
LT II	Dyed water	Dyed oil	–
LT III	Dyed water	–	Type C
LT IV	–	Dyed oil	Type C
LT V	Dyed water	Dyed oil	Type C
LT VI	Dyed water	Dyed oil	Acid-washed type C
LT VII	Dyed water	Dyed oil	Type D
LT VIII	Dyed water	Dyed oil	Acid-washed type D
LT IX	Dyed water	Dyed oil	Mix (type C+type D)
LT X	Dyed water	Dyed oil	Acid-washed mix

Table 4.6: Experiments conducted in the larger tubes.

These experiments are divided into the following five parts:

1. LT I : The first part is to inject CO_2 with only water phase present in the tube.
2. LT II: In the second part, CO_2 is injected into the tube with a small layer of oil on top of the water phase. This test is used to study the effect of the oil layer on CO_2 movement in the water phase.

3. LT III: The third part is to observe the movement of CO_2 with water phase present in porous media.
4. LT IV: The fourth part is to study the injection of CO_2 with oil phase present in porous media. This test is used to study if CO_2 dissolution leads to visible swelling of oil.
5. LT V- X: In the last part, we study the capacity of CO_2 rich water to mobilise oil from porous media and compare it with tube tests conducted in porous media of type C/D (Sub-subsection 4.3.2.2 on page 31).

Materials Used

Following is the list of materials used in the larger tube tests:

- Dyed water phase (10 mL bromothymol blue indicator solution+ 90 mL DI water).
- Dyed oil Phase (n-decane dyed with 0.04 wt% sudan II).
- Gas phase: CO_2 (99 % pure).
- Larger tubes.
- 30 mL syringe (to add water and oil phase to the tube).
- Piston cell for CO_2 injection.
- Pump to inject CO_2 into the tube.
- Backpressure regulator set at 10 bar.
- Manometer (to measure the pressure during CO_2 injection).
- Porous media (Type C and D).
- Camera.

Fig. 4.4 on the following page shows a schematic of the experimental setup under injection conditions of the experiment. Fig. 4.5 on page 37 shows schematic of experimental setup at the end of an experiment when the tube is depressurised and cleaned for the next experiment.

A piston cell is used to facilitate CO_2 injection in the tube. It is essential to use O-rings in the piston cell which can withstand CO_2 injection. The piston cell is checked at regular intervals to ensure the integrity of the O-rings. A back-pressure regulator is used in the system as a safety mechanism in case the pressure in tube rises above experimental conditions. Nitrogen (N_2) is filled at 10 bar on the gas side of the back-pressure regulator.

It is important that inlet valve to the tube be opened very slowly during the injection process so that the liquid level is not vigorously disturbed and the system is pressurised gradually. In case there is a leak in the system, it can be fixed quickly if the tube is slowly pressurised.

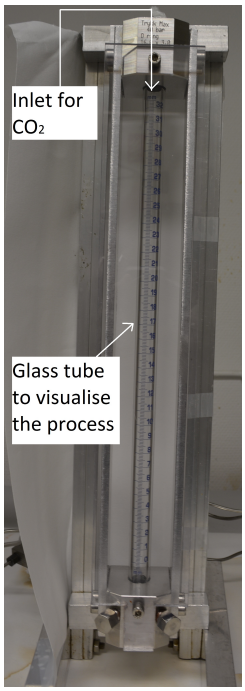

Figure 4.3: The larger tube used for experiments with CO_2 injection at 10 bar.

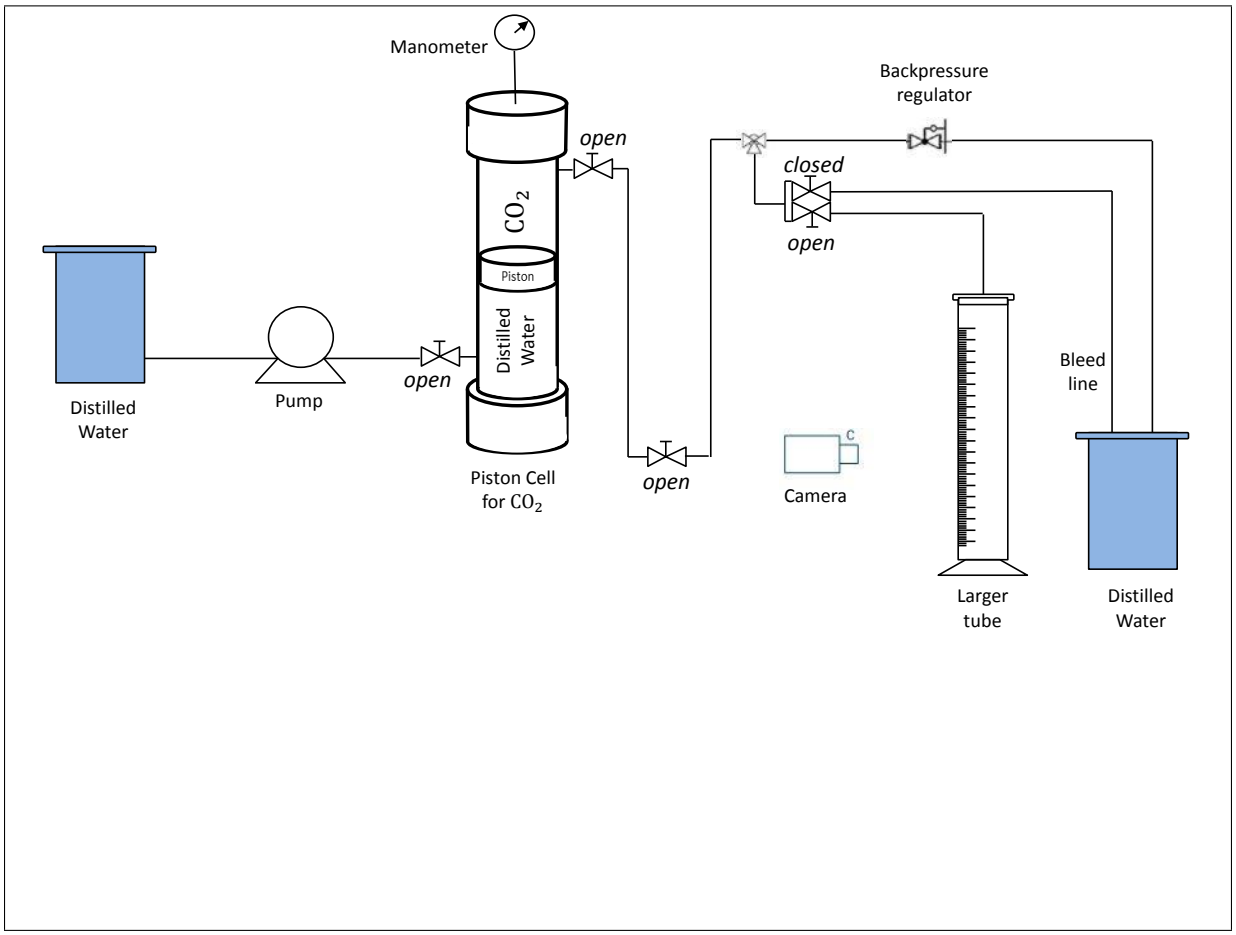

Figure 4.4: Larger tube test: Schematic of the experimental setup during injection.

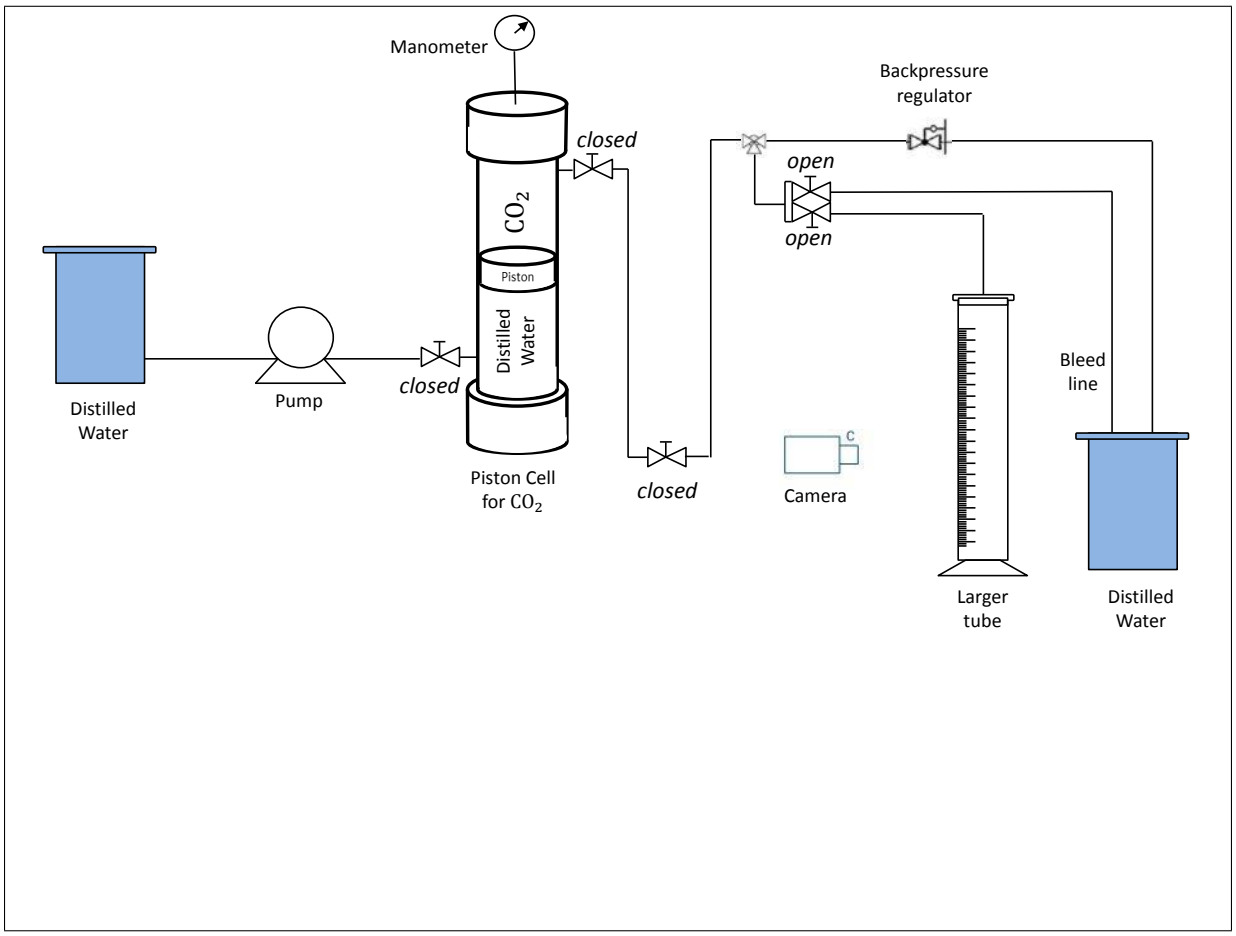

Figure 4.5: Larger tube test: Schematic of the experimental setup during pressure bleed-off in the tube.

4.4.2 Procedures

Ensure that glass tube is cleaned adequately before each experiment. Following is the procedure for different parts of the experiment:

4.4.2.1 LT I: CO_2 injection with only water phase in the tube

- Use a syringe to inject the water phase till half the height in the tube.
- Slowly open the inlet valve to the tube and start CO_2 injection from the piston cell. Use the pump to maintain a constant pressure of 10 bar during the experiment.
- Observe the shape of the CO_2 front moving into the water phase and note the change in colour of the water phase.
- Note the time taken by CO_2 to reach the bottom of the tube. Document the change in colour using a camera.
- Carefully depressurise the system upon completion of experiment and clean the tube for use in the next test.

4.4.2.2 LT II: CO_2 injection with a layer of oil on top of the water phase in the tube

- Use a syringe to inject water phase till half the height in the tube.
- Inject oil phase in the tube to make a small layer of oil on top of the water phase.

- Slowly open the inlet valve to the tube and start CO_2 injection from the piston cell. Use the pump to maintain a constant pressure of 10 bar during the experiment.
- Observe the movement of CO_2 and time taken to reach the bottom of the tube as compared to the case above.
- Carefully depressurise the system upon completion of experiment and clean the tube for use in the next test.

4.4.2.3 LT III: CO_2 injection with water present in the porous media

- Inject water phase into the tube till $1/3^{rd}$ the height of the tube.
- Add porous media (type C) to the tube till the interface between glass beads and the free water phase is at half the height in the tube. Dismount the tube from the support and place in an ultrasonic bath for 10 minutes to provide better packing of the porous media.
- Carefully remove excess water phase from the tube to leave a column of 1 cm above the boundary of glass beads-free water phase.
- Slowly open the inlet valve to the tube and start CO_2 injection from the piston cell. Use the pump to maintain a constant pressure of 10 bar during the experiment.
- Observe the movement of CO_2 rich water phase in the porous media.
- Carefully depressurise the system upon completion of experiment and clean the tube for use in the next test.

4.4.2.4 LT IV: CO_2 injection with oil present in the porous media

- Inject oil phase into the tube till $1/3^{rd}$ the height of the tube.
- Add porous media (type C) to the tube till the interface between glass beads and free oil phase is at half the height in the tube. Dismount the tube from the support and place in an ultrasonic bath for 10 minutes.
- Carefully remove excess oil phase from the tube to leave a column of 0.5-1 cm above the boundary of glass beads-free oil phase.
- Slowly open the inlet valve to the tube and start CO_2 injection from the piston cell. Use the pump to maintain a constant pressure of 10 bar during the experiment.
- Observe if there is any movement of CO_2 in the free oil phase or porous media. Look for possible swelling due to the dissolution of CO_2 in oil.
- Carefully depressurise the system upon completion of experiment and clean the tube for use in the next test.

4.4.2.5 LT V- X: CO_2 injection with oil-water system in the porous media

Similar to tube tests conducted with glass beads of type C/D (Sub-subsection 4.3.2.2 on page 31), experiments in the larger tube under CO_2 injection will be conducted to make observations on oil recovery and movement of CO_2 rich water phase in varied porous media. Given below is a simplified procedure for six experiments conducted by varying the porous media:

- Inject oil phase into the tube till $1/3^{rd}$ the height of the tube.
- Add porous media to the tube till the interface between glass beads and free oil phase is at half the height in the tube. Place the tube in an ultrasonic bath for 10 minutes.

- Once the glass beads have settled, notice the level of the free oil phase. In case of excess oil, carefully remove oil to leave a column of 1-1.5 cm above the boundary of glass beads-free oil phase.
- Using a syringe, slowly add water phase to the tube.
- After addition of water phase slowly open the inlet valve to the tube and start CO_2 injection from the piston cell. Use the pump to maintain a constant pressure of 10 bar during the experiment.
- Observe the changes in the level of oil in the tube and CO_2 movement in the porous media. Note the change in colour of water phase.
- Carefully depressurise the system upon completion of experiment and clean the tube for use in the next test.

4.4.2.6 Procedure for cleaning of the tube after the experiment

- Carefully depressurise the tube and disconnect the inlet tubing.
- Use DI water to flush out glass beads and liquids from the tube.
- After all the liquids and porous media are removed from the tube, use methanol to remove oil phase and remaining glass beads from the walls of the tube.
- Use DI water again to clean the cell from glass beads followed by second use of methanol.
- Set the tube under a fume hood and allow methanol to evaporate. Purge the tube with N_2 and initiate next experiment.

Note: Use of ultrasonic bath provided better packing of glass beads. This can be observed in table A.3 on page 140 as significant variation in porosity when no ultrasonic bath was used compared to lower and small range of porosity values when using an ultrasonic bath.

4.5 Tests in polycarbonate cells

Polycarbonate cells of varying thickness are prepared, and an oil-water system is tested in these cells. Addition of 0.1 M HCl is used to represent CO_2 dissolution in water. Imbibition under gravity facilitates oil mobilisation from porous media. The experiments conducted in this section are referred to as 'Cell test' in this thesis.

4.5.1 Description

Objective

Researchers have widely studied visualisation of imbibition process in porous media. Some limitations of these studies are:

- Use of etched micromodels where the sizes of pore throat and pores are known.
- Visualisation on a microscopic scale is limited to a small section of the porous media.
- Use of digital tools to distinguish oil and water phases in pores.

In these experiments, we aim to overcome these limitations by studying imbibition process in complex porous media (glass beads) packed in a polycarbonate cell of height 13.8 cm with dyed oil and water phases to provide a better visualisation of phase movement in the porous media.

Polycarbonate plates are cut to required dimensions and glued together to form the cells. Cells are tested by varying the thickness from 3, 5 and 8 mm. Imbibition under gravity is studied to understand the motion of fluids, and the shape of water front in the porous media represents a characteristic of the displacement process.

Table 4.7 presents a list of experiments done in polycarbonate cells. 'CT' refers to 'Cell test'.

Label	Water phase	Oil phase	Cell thickness	Porous media
CT I	Dyed water	Dyed oil	3 mm	Type B
CT II	Dyed water	Dyed oil	5 mm	Type B
CT III	Dyed water	Dyed oil	8 mm	Type B
CT IV	Dyed water	Dyed oil	3 mm	Type C
CT V	Dyed water	Dyed oil	5 mm	Type C
CT VI	Dyed water	Dyed oil	8 mm	Type C

Table 4.7: Experiments conducted in polycarbonate cells.

Following experiments are conducted in this section:

1. CI I-III: Test starts with a cell thickness of 3 mm, and later the thickness is varied to 5 mm and 8 mm. Varying thickness is used to determine which thickness gives best ability to visualise the motion of fluids. The smaller the thickness of the cell, the closer it is to a 2-D model. The effect of cell thickness on the shape of invading water front is also studied.
2. CT IV- VI: The effect of a minor variation in the pore size on the front pattern development and ability to visualise the motion of fluids in porous media is studied.

Materials Used

The following materials are used in the cell tests:

- Dyed water phase (10 mL bromothymol blue indicator solution+ 90 mL DI water).
- Dyed oil phase (n-decane-dyed with 0.04 wt% Sudan II).
- 0.1 M HCl.
- 30 mL syringe (to add water and oil phase to the cell).
- Methanol (for cleaning).
- Polycarbonate sheet (to be cut into required dimensions and glued together to form cells).
- Acrifix 2R 0190 (Sealing glue for polycarbonate sheets).
- Porous media (Type B/C).
- Camera.

4.5.2 Procedures

4.5.2.1 Preparation of polycarbonate cells

Cell dimensions: Width: 6.9 cm, Height (2*W): 13.8 cm, Thickness: Varying from 3 mm, 5 mm and 8 mm. Please refer to fig. 4.6 on page 43 during preparation procedure.

- Cut polycarbonate plate to final width and height to form two faces of the cell.
- Place the two faces of the cell (represented by side A and side B in fig. 4.6) on top of each other with a spacer in between.
- Use the same polycarbonate material as a spacer. A spacer of given thickness (3 mm, 5 mm or 8 mm) is glued between the faces (represented by blue in fig.4.6). The width of a spacer used is 5 mm.
- For the bottom of the cell, cut a polycarbonate sheet of width (6.9 cm) and varying thickness as shown in bottom view of fig.4.6.
- Once the sides of the cell are glued, leave it to dry and set.
- The inner volume of the cell can be calculated depending on the thickness of spacer (3, 5 or 8 mm), height (13.8 cm) and width[4] (5.9 cm) of the cell.

4.5.2.2 Cell tests with varying thickness of cells and porous media type B/C.

The experiments are carried out at atmospheric pressure and room temperature (20°C). Use of an ultrasonic bath provides better packing of porous media into the cell.

Porous media: Cell tests are conducted using two types of porous media (type B and type C). It was observed from tube tests and tests in larger tubes that acid treatment of glass beads was a possible cause for alteration in properties of glass beads, which in turn affect the movement of the water phase in the porous media. Hence in this experiment, porous media of type C and type B are used. First set of tests are conducted in glass beads type B. Following that, similar experiments are carried out with glass beads type C to observe the effect of small variation in grain size on the front pattern development.

[4]Width decreased by 1 cm due to the use 5 mm wide spacer on both sides of the cell.

A simplified procedure for experiments conducted in polycarbonate cells is given below:

- Use a syringe to inject the oil phase into the cell.
- Fill glass beads into the cell till the glass beads-oil interface is at half the height of the cell.
- Transfer the cell to an ultrasonic bath (as shown in fig.4.7) for 10 minutes. Use of ultrasonic bath releases air trapped in the pores and provides better packing of glass beads.
- Upon settlement of glass beads, add water phase to the cell. Start with few droplets and increase to few mL gradually.
- Record the movement of the water phase in porous media using a camera.
- Add 3-4 drops of 0.1 M HCl to the cell and observe the effect on oil mobilisation due to invasion of low pH water in the porous media.

4.5.2.3 Cleaning procedure for polycarbonate cells

- Inject DI water to remove the glass beads from the cell. A small diameter tubing made from Polyetheretherketone (PEEK) is used in this case.
- Once the majority of glass beads are removed by injecting DI water, place the polycarbonate cell in an ultrasonic bath for 10 minutes. Use of the ultrasonic bath helps remove oil and glass beads stuck on the face of the cell.
- Use methanol to clean the cell thoroughly to get rid of all the oil phase present in the cell from the experiment.
- Place the cell under a fume hood and let methanol evaporate. Check for any visible glass beads on the surface of the cell and use more methanol to clean the cell if needed.

Note: Do not use toluene to remove oil from the cell. Toluene reacts severely with polycarbonate and may render the cell useless for further experiments.

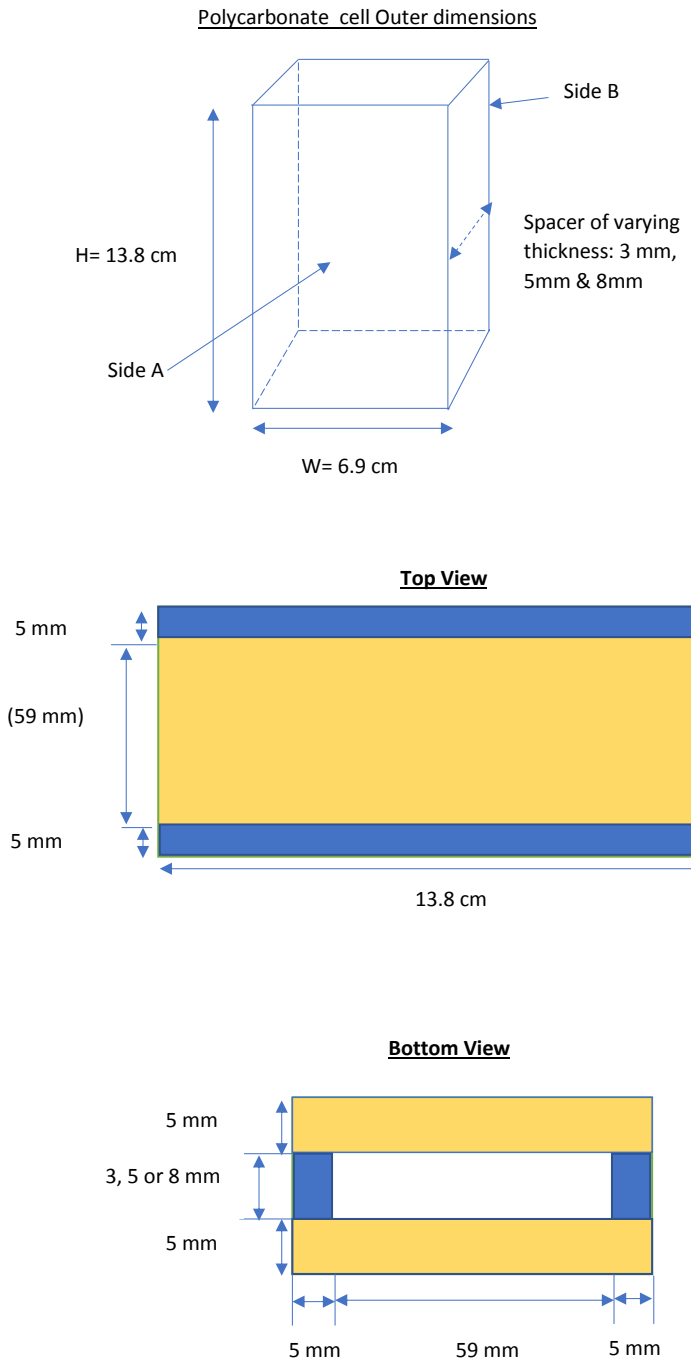

Figure 4.6: Dimensions of polycarbonate cells from different viewpoints.

Figure 4.7: Polycarbonate cell in an ultrasonic bath.

4.6 Tests in POM cell with CO_2 injection at low pressure (10 bar)

Experiments conducted in the previous sections helped to study the fluid systems, porous media, and visualisation method. In these experiments, we inject CO_2 in a 2-D cell made of Polyoxymethylene (POM). POM cell has a maximum allowable working pressure of 20 bar, although the tests in POM cell are conducted at 10 bar to maintain consistency in procedure with other experiments and compare results. The tests conducted in POM cell are used to study the effectiveness of selected visualisation technique, develop systematic procedures and test them to have baseline results before conducting experiments in a high-pressure cell. Experiments conducted in this section will be referred to as 'POM cell tests' in this thesis.

Label	Water phase	Oil phase	Porous media
POM cell test I	Dyed water	–	–
POM cell test II	Dyed water	Dyed oil	–
POM cell test III	Dyed water	Dyed oil	Type C

Table 4.8: Experiments conducted in the POM cell.

4.6.1 Description

Objective

Table 4.8 gives a list of experiments conducted in the POM cell. These experiments, combined with results from experiments conducted in previous four sections in this chapter will form the baseline for further work on the cell. Tests in the POM cell are divided into following three parts:

1. The first test is to visualise CO_2 injection with only water phase present in the cell.
2. The second test is to visualise CO_2 injection with a small layer of oil on top of the water phase. The effect of the oil layer on the dissolution of CO_2 is studied.
3. In the last part of testing, injection of CO_2 with an oil-water system in the porous media is studied.

Materials Used

The following materials are used in POM cell tests:

- Dyed water phase (100 mL bromothymol blue indicator solution + 900 mL DI water). 2-3 drops of NaOH were added to adjust the pH in the range of 8.0–8.1 (a higher range is selected due to drop in pH over time when stored in piston cell as opposed to diluted every time for an experiment).
- Dyed oil phase (n-decane-dyed with 0.04 wt% sudan II).
- POM cell.
- Piston cell for CO_2/N_2/water phase injection.
- Pump to inject CO_2 to the POM cell.

- Backpressure regulator set at 10 bar.
- Manometer (to measure pressure during CO_2 injection).
- Porous media (Type C).
- Camera.

Fig.4.8 shows an outlook of the cell assembly. The minimum thickness of the cell is 5 mm and tests can be conducted by varying the thickness. In the reported experiments, a thickness of 5 mm was selected. This is done to allow light to pass through the porous media to facilitate visualisation process and simultaneously assist in homogeneous packing of porous media. A back pressure regulator is installed to avoid high-pressure development in the cell, and specially designed glass filter modules are installed to prevent any glass beads from being removed if a flooding test is conducted.

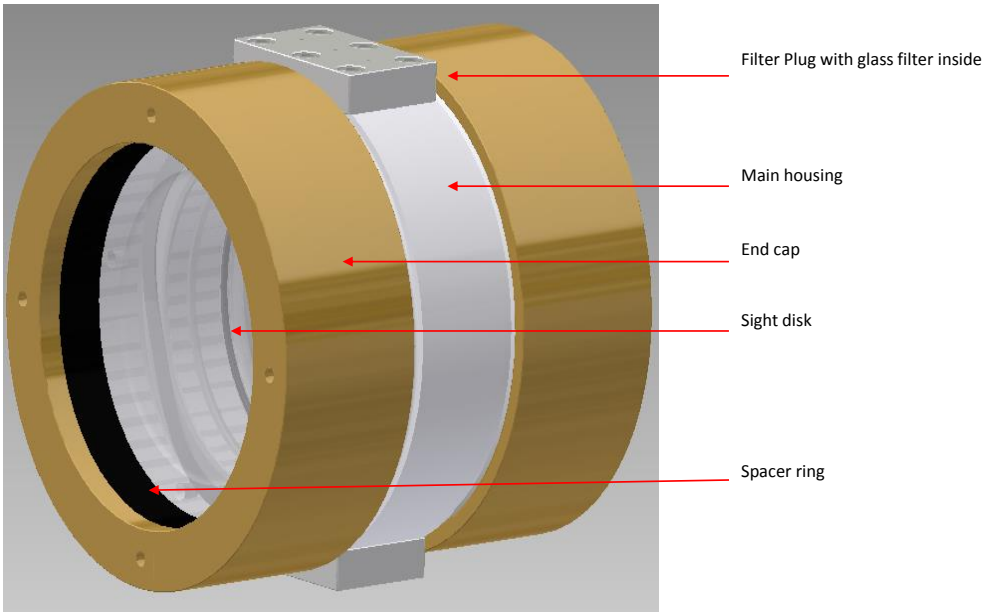

Figure 4.8: Visualisation of the POM cell assembly.

On top and bottom of the cell are filter modules with a provision for glass filter inside. For our set of experiments, we did not use glass filter on top of the cell for ease of filling the cell with fluids and porous media. As seen from fig.4.9, there are three entry points in the filter module. On the inlet filter module, each entry point is used for following purposes:

- One to inject the water phase and CO_2 into the cell (see fig.4.10).
- The second one to connect the back pressure regulator to the cell. N_2 is used on the gas side of the back pressure regulator which has a set pressure of 10 bar.
- The third inlet point is used to inject oil, glass beads, and to release air during the injection of the water phase in the cell. During CO_2 injection, this inlet point is closed until the experiment ends and the cell is depressurised.

Figure 4.9: Filter module used in the POM cell.

Diameter of the cell: 170 mm, width of the spacer: 5 mm.

Fig. 4.10 on the next page shows a schematic of the experimental setup used in this experiment. Experimental setup and testing procedures for POM cell were developed by Widuramina Amarasinghe[5]. Work done in this thesis includes minor variations in the established procedures.

4.6.2 Procedures

4.6.2.1 POM cell test I: CO_2 injection with only water phase in the cell

This experiment aims to observe the movement pattern of CO_2 in the water phase under low pressure (10 bar) injection.

- Before an experiment begins, it is important to flush the lines with N_2 to ensure that lines are clean of CO_2 and no mixing of CO_2 and water occurs in the line during injection. For this, open valves V5, V8, V9, V10, V11 and V12 to ensure proper flushing of N_2 through the system.
- Once the system is purged with N_2, close valves V5, V8, V9, V10 and V12 (leave V11 open). Open valves V1, V2, V3 and V4 and start water injection into the cell at low flow rate till the water level reaches half the height of the cell.
- Upon completion of water injection into the cell. Close valves V1, V2, V3, V4 and V11.

[5]Widuramina is a PhD candidate at IRIS.

- Open valves V5, V6, V10. Start the pump and note when the pressure in pump reaches 10 bar. Very slowly open valve V11 and then V7 to avoid turbulence on the CO_2-water interface. Set the pump at "constant pressure delivery" mode at 10 bar.
- Observe the movement of CO_2 in the water phase and obtain pictures using a camera.

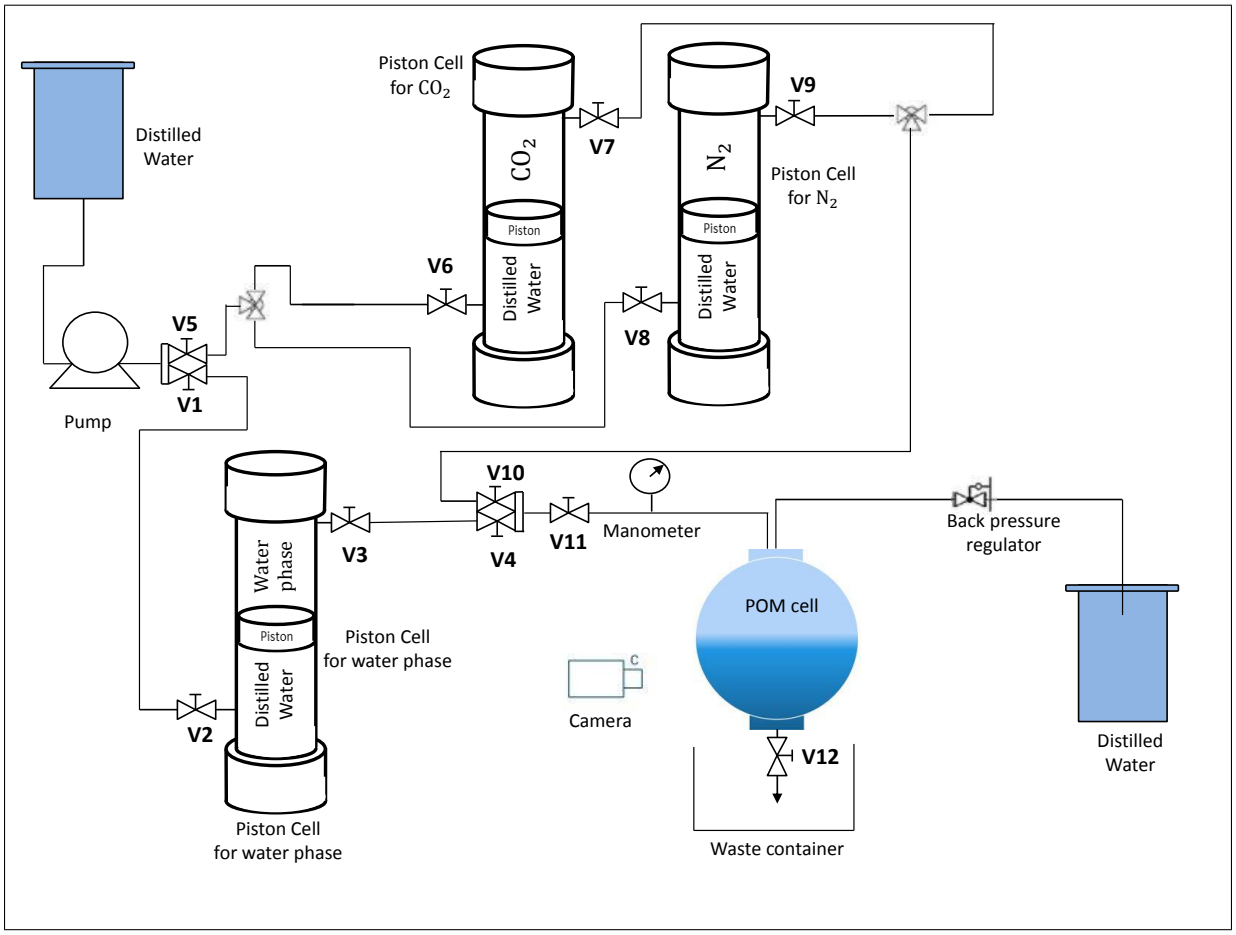

Figure 4.10: POM cell test: Schematic of the experimental setup.

4.6.2.2 POM cell test II: CO_2 injection with oil on top of water phase in cell

The aim of this experiment is to observe the movement of CO_2 in the presence of an oil layer on top of the water phase.

- Clean the POM cell (see sub-subsection 4.6.2.4) and flush the lines with N_2 (see sub-subsection 4.6.2.1) to ensure they are clean.
- Once the system is purged with N_2 close valves V5, V8, V9, V10 and V12 (leave V11 open). Open valves V1, V2, V3, V4, V11 and start water injection into the cell at low flow rate till the water level reaches half the height of the cell.
- Upon completion of water injection into the cell. Close valves V1, V2, V3, V4 and V11.
- Using a syringe of suitable size inject oil phase from one of the entry points in the filter module on the top of the POM cell. Maintain a small layer (<1 cm) of oil on top of the water phase.
- Open valves V5, V6, V10. Start the pump and note when the pressure in pump reaches 10 bar. Very slowly open valves V11 and then V7 to avoid turbulence on the oil-water interface. Set the pump at "constant pressure delivery" mode at 10

bar.
- Observe the movement of CO_2 in the water phase and obtain pictures using a camera.

4.6.2.3 POM cell test III: CO_2 injection with the oil-water system in porous media

The aim of this experiment is to study imbibition under low-pressure CO_2 injection. Visualisation of water invasion in porous media and resulting oil mobilisation is studied. The impact of carbonated water on oil recovery is also investigated.

- Clean the POM cell (see sub-subsection 4.6.2.4) and flush the lines with N_2 (see sub-subsection 4.6.2.1) to ensure they are clean. Once the system is purged with N_2 close valves V5, V8, V9, V10, V11 and V12.
- Using a syringe of suitable size inject oil phase from one of the entry points in the filter module on the top of the POM cell.
- Using a syringe, fill glass beads into the cell till the level of glass beads-oil interface reaches half the height of the cell. If there is excess oil layer (greater than 8 mm) on top of glass beads level, remove it carefully.
- Open valves V1, V2, V3, V4, V11 and start water injection into the cell at a low flow rate.
- Upon completion of water injection to the cell. Close valves V1, V2, V3, V4 and V11.
- Open valves V5, V6, V10. Start the pump and note when the pressure in pump reaches 10 bar. Very slowly open valves V11 and then V7 to avoid turbulence on the oil-water interface. Set the pump at "constant pressure delivery" mode at 10 bar.
- Observe the movement of CO_2 rich water in porous media and obtain pictures using a camera.

4.6.2.4 Cleaning procedure for the POM cell

This part describes cleaning procedure for the POM cell upon completion of a test.

- Upon completion of an experiment, stop the pump and open V12 slowly to remove fluids from the cell. Opening V12 also releases the pressure from the cell.
- Once the cell is depressurised, disconnect the lines and remove the top and bottom filter modules from the cell.
- Clean the cell using DI water. If oil or glass beads are used then clean the cell in cycle DI water- methanol - DI water, to get rid of all oil and glass beads from the cell.
- Allow the cell to dry and clean the filter modules in cycle DI water- methanol- DI water.
- Insert the filter modules in the cell and connect the lines to the filter module on the top of the cell. Purge the lines and system with N_2 before beginning a new test.

Note: If tests are conducted using crude oil then do not use toluene to clean the cell. Toluene reacts severely with Polyoxymethylene. This rection may render cell not suitable for further testing.

Chapter 5

Results and Discussion

5.1 Indicator Testing

Indicator testing was conducted to test the ability of different dyes and indicator solutions to represent oil and water phases in visualisation experiments. Emphasis was laid on:

1. Dyes and pH indicator solutions which were soluble only in the phase they represented, e.g. oil-soluble dye is not affected by a change in pH of the water phase, and water-soluble pH indicator does not react with components present in the oil phase.
2. Addition of 0.1 M HCl to mimic the change in pH due to dissolution of CO_2 in the water phase.

One water-soluble pH indicator and three oil-soluble dyes were tested.

5.1.1 Indicator test I: Testing bromothymol blue indicator in an oil-water system

The aim of this experiment was to test the effect of the addition of bromothymol blue indicator solution in an oil-water system and further demonstrate the influence of a change in pH on the oil-water system.

5.1.1.1 Indicator test I: Bromothymol Blue

Upon mixing oil and water phases in the tube. A distinct line separated both the phases at 5 mL mark in the test tube (marked by an arrow in fig. 5.1a on the following page). Indicator solution stayed in the water phase, and no movement towards oil phase was observed. After complete dissolution, a greenish blue colour in water phase was observed which indicated that pH was in the range of 7.0 – 7.6 (fig. 5.2a).
0.01 N NaOH was added to bring the water phase towards a basic solution. A change in colour of water phase from greenish blue to blue was observed. This change in colour was in line with the nature of bromothymol blue as an indicator in basic solution (fig. 5.2b). HCl (0.1 M) was then added to the tube. The colour of water phase solution changed from blue to yellow. Bromothymol blue acted as an indicator in acidic solutions by exhibiting yellow colour (Fig. 5.2c). The pH Indicator was water soluble and did not lose

colour in the presence of an oil phase.

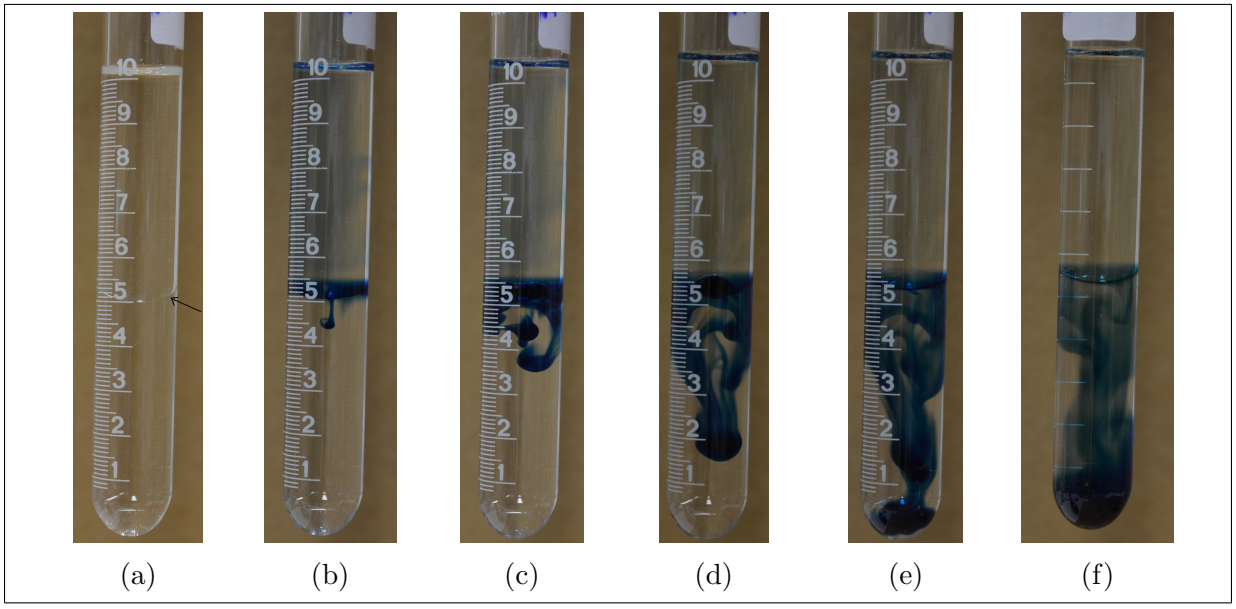

(a) (b) (c) (d) (e) (f)

Figure 5.1: Movement of bromothymol blue indicator in water: pH indicator solution stayed in the water phase and was not soluble in the oil phase.

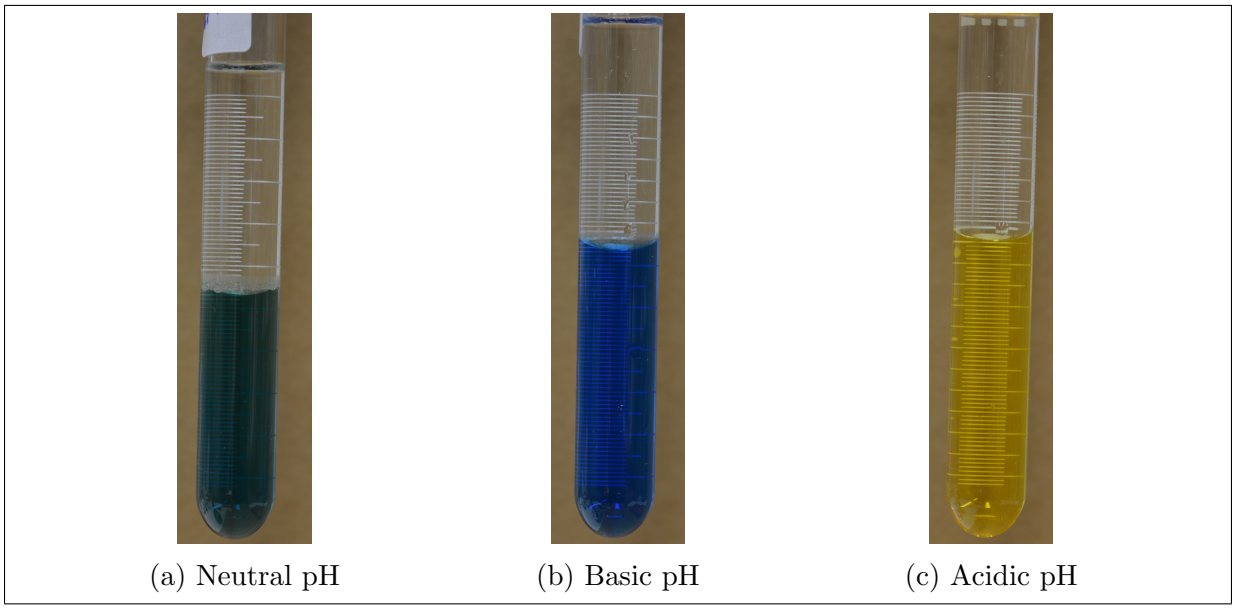

(a) Neutral pH (b) Basic pH (c) Acidic pH

Figure 5.2: Bromothymol blue indicator changed colour with the change in pH.

5.1.2 Testing sudan blue/red in an oil-water system

Sudan blue II, sudan II and sudan III are oil-soluble dyes. These experiments aimed at testing the stability of oil-soluble dyes in the presence of the water phase and record changes due to change in pH upon addition of acid.

5.1.2.1 Indicator testing II - Sudan Blue II

A distinct line separated the oil and water phases at 3 mL mark in the test tube. Sudan blue II stayed in the oil phase, and no movement towards the water phase was observed.

HCl (0.1 M) was added to the tube, the oil dye was stable in the presence of an acidic water phase (this step was testing oil phase in undyed water, fig. 5.3a).
In the next step, both dyed oil and dyed water phase were added to the test tube (as shown in fig.5.3b). Oil and water phases were distinguished mildly by a change in colour near 5 mL mark.

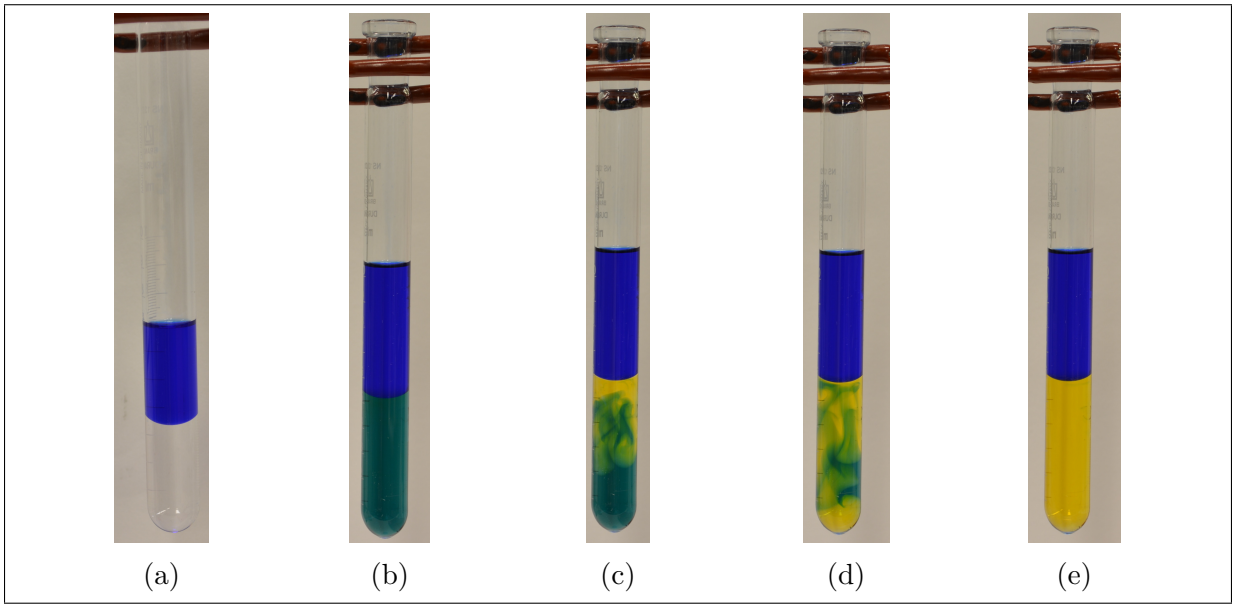

(a) (b) (c) (d) (e)

Figure 5.3: Indicator test II: Sudan blue II was only soluble in the oil phase, and a change in pH did not affect the stability of dye.

No change in colour of oil dye occurred on the addition of acid (fig.5.3e) and the colour of the water phase changed from greenish blue to yellow. It was observed that HCl stayed in the water phase by noticing an increase in the level of oil-water interface.
3 more drops of HCl were added to the test tube, no change in the colour of oil phase was observed as HCl dissolved in the water phase.

5.1.2.2 Indicator testing III - Sudan II

A distinct line separated both the phases at 5 mL mark in the test tube. Sudan II stayed in the oil phase, and no movement towards water phase was observed. HCl was added to the tube, and the oil dye was stable in the presence of acidic water solution (this step was testing oil phase in the undyed water phase, fig.5.4a).
In the next step, 5 mL of both dyed oil and water phase were added to the test tube. A distinct line separated both the phases at 5 mL mark (as shown in fig.5.4b).
HCl was added to test tube to notice any change in the colour of the oil phase dye upon addition of acid. No such change occurred on the addition of acid (fig.5.4e).
It was observed that HCl stayed in the water phase (by noticing the increase in the level of transition line) and the the colour of the water phase changed from greenish blue to yellow.

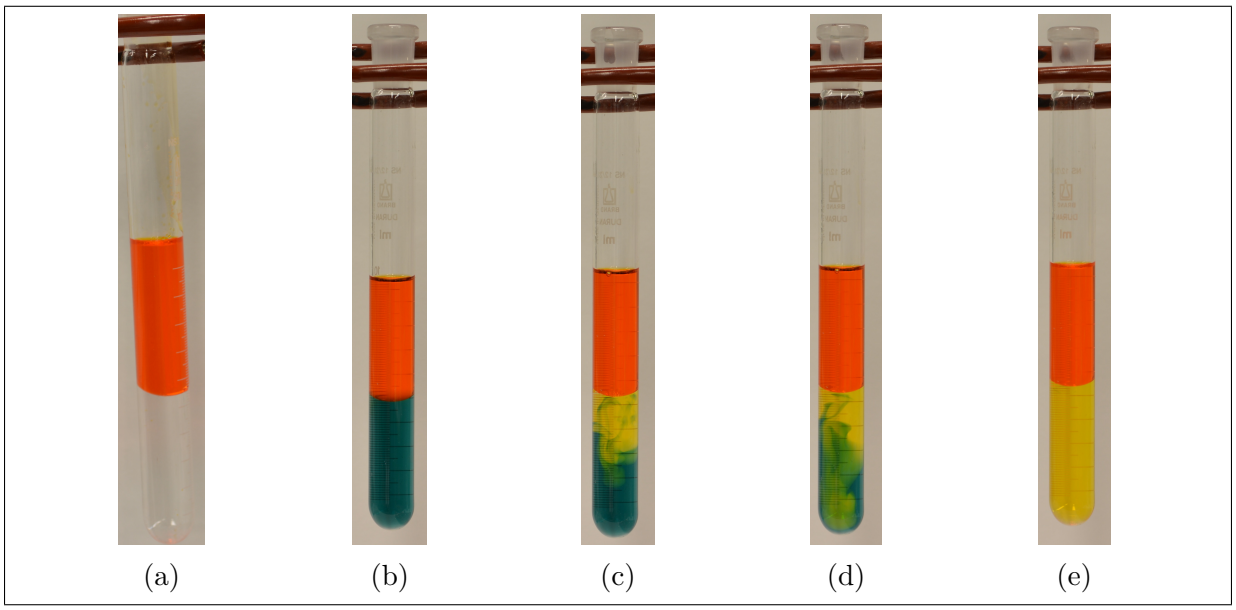

(a) (b) (c) (d) (e)

Figure 5.4: Indicator test III: Sudan II, an oil-soluble dye was not affected by a change in pH of the water phase and showed stability in the oil phase.

5.1.2.3 Indicator testing IV - Sudan III

A distinct oil-water interface was observed at 5 mL mark in the tube. Sudan III stayed in the oil phase, and no movement towards water phase was observed. HCl was added to the tube, and the oil dye was stable upon addition of acid (this step was testing oil phase in the undyed water phase, fig.5.5a).
In the next step, 5 mL of both dyed oil and water phases were taken in a test tube. Both oil and water phases were distinguished at 5 mL mark (as shown in fig.5.5b).
HCl was added to test tube to observe any change in the colour of the oil phase dye upon addition of acid. No such change was observed upon addition of acid (fig.5.5e). The colour of water phase changed from greenish blue to yellow upon addition of acid. It was observed that HCl stayed in the water phase.

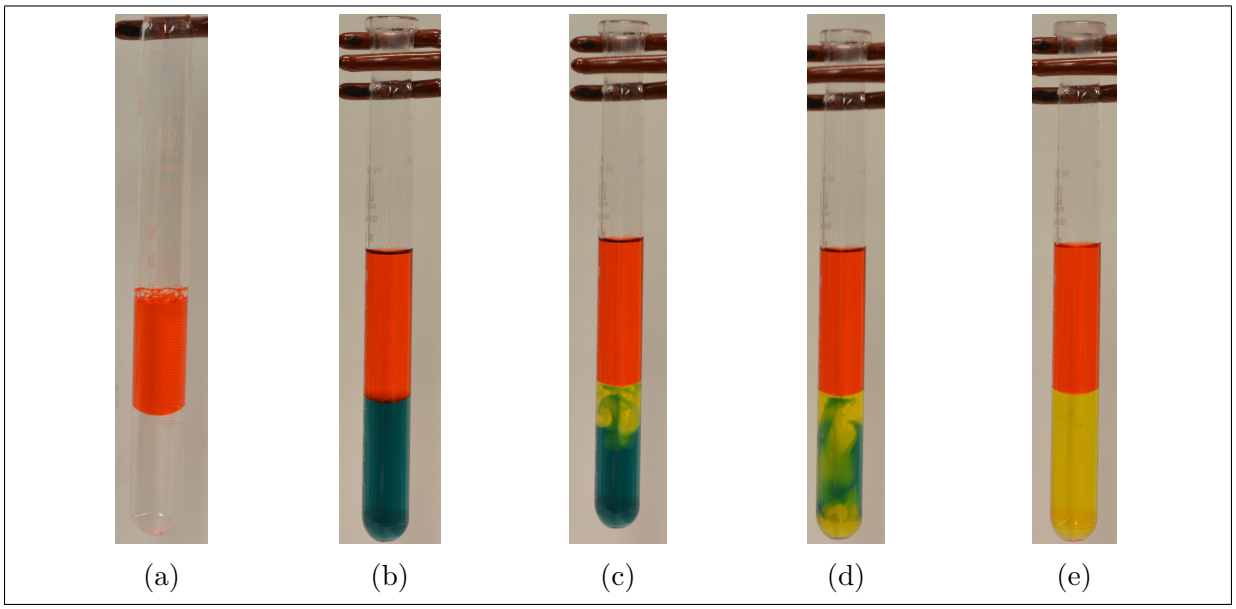

(a) (b) (c) (d) (e)

Figure 5.5: Indicator test IV: Sudan III, an oil-soluble dye was not affected by a change in pH of the water phase and was only soluble in the oil phase.

5.1.3 Indicator testing V - Crude oil system

Upon addition of oil and water phases to the tube, a distinct line separated both the phases at 6 mL mark (seen in fig.5.6a).

The reaction of HCl and water phase caused the pH of water phase to drop below 6 and the colour of the water phase changed from blue to yellow (fig. 5.6b). Oil-water system was left overnight, and it was observed that aqueous indicator phase reacted with crude oil and the colour of the water phase faded with time, as seen from fig.5.6b to fig. 5.6e.

(a) t=0 (b) t=3 min (c) t=275 min (d) t=530 min (e) t=1440 min

Figure 5.6: Indicator test V: The colour of the water phase faded as pH indicator reacted with crude oil.

5.1.4 Conclusions: Indicator testing

Label	Phases in the tube	Distinction of phases	Stability of indicator tested
Indicator test I	DI water / n-decane (un-dyed)	Good	Good
Indicator test II	DI water and dyed water / dyed oil	Intermediate	Good
Indicator test III	DI water and dyed water / dyed oil	Good	Good
Indicator test IV	DI water and dyed water / dyed oil	Good	Good
Indicator test V	Dyed water/ stock tank oil	Good	Poor

Table 5.1: Overview of results: Indicator testing

An overview of results is presented in table 5.1 where the stability and distinction of phases are graded on the scale: good, intermediate and poor.

Bromothymol blue was stable in the presence of undyed and dyed n-decane and upon addition of acidic and basic solutions; exhibited a change in colour according to its nature. The distinction of phases using bromothymol blue and sudan blue II was intermediate due to similar colour of both solutions.

In the test involving crude oil, bromothymol blue was not stable and lost its colour due to a reaction with components in crude oil.

Oil soluble dyes sudan blue II, sudan II and sudan III, showed no solubility in the water phase and did not lose colour due to the decrease in pH.

5.2 Tube tests with porous media

In tube tests, indicator solutions and the dyes studied in previous experiments (sec.5.1) were used to represent the oil and water phases. Visualisation of the water phase movement in porous media and subsequent oil mobilisation was facilitated. The term 'high pH water' used in the observations, refers to water phase which has not reacted with of 0.1 M HCl.

5.2.1 Tube tests in porous media type A

5.2.1.1 Tube test I - Sudan Blue II

Oil phase was taken in a tube, and glass beads were added to keep the oil-glass beads (O-GB) interface at 3 mL mark. The settling time for glass beads was 2 minutes. Upon settlement, a clear interface between glass beads and free oil phase was observed at 3 mL mark (as seen in fig. 5.7b).

Upon settlement of glass beads, DI water was added to the tube. A distinct water-glass beads interface (W-GB) and water-oil interface (W-O) was observed (as in fig. 5.7c). Water phase began invading the porous media and as a result oil trapped in the porous media was mobilised. Oil released from porous media collected at W-GB interface and when the size of a droplet was large enough to overcome capillary forces it moved out of pore space towards the free oil phase on top of the tube.

Water phase invaded the porous media from the sides (walls) of the tube and towards the bottom of the tube, gradually moving towards the center. This movement can be observed in fig. 5.7e and fig. 5.7f as marked by arrows.

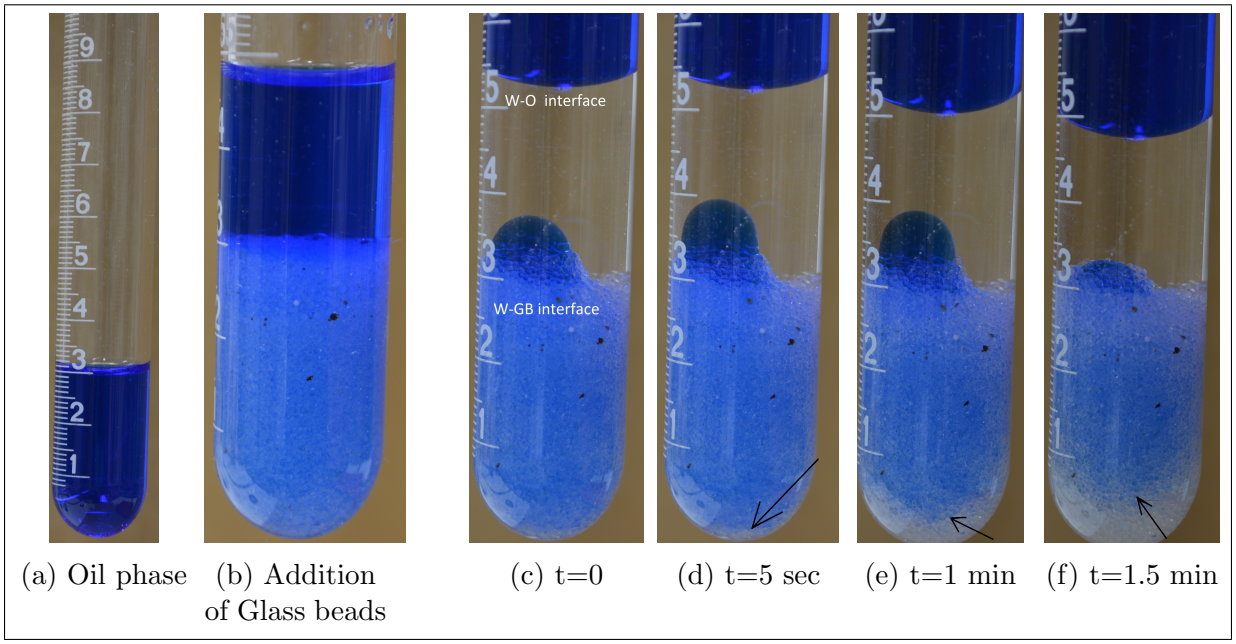

(a) Oil phase (b) Addition of Glass beads (c) t=0 (d) t=5 sec (e) t=1 min (f) t=1.5 min

Figure 5.7: Tube test I: Mobilisation of oil from porous media and movement of water along the sides of the tube.

The water phase moved quickly along the sides of the tube towards the bottom and began displacing oil from the lower section of porous media as seen in fig.5.7d. Movement of the the water phase in porous media was also noticed by a drop in the W-O interface.

At this scale and conditions, the process was quite fast in the beginning and slowed down till it became difficult to observe quick changes. The time taken to reach this stage was approximately 12 minutes. No visible change in oil recovery was observed upon addition of acid (fig. 5.8e). As a deviation from procedure a of total 1 mL of HCl was added to the system, but no change in the colour of oil phase was observed (as seen in fig. 5.8f).

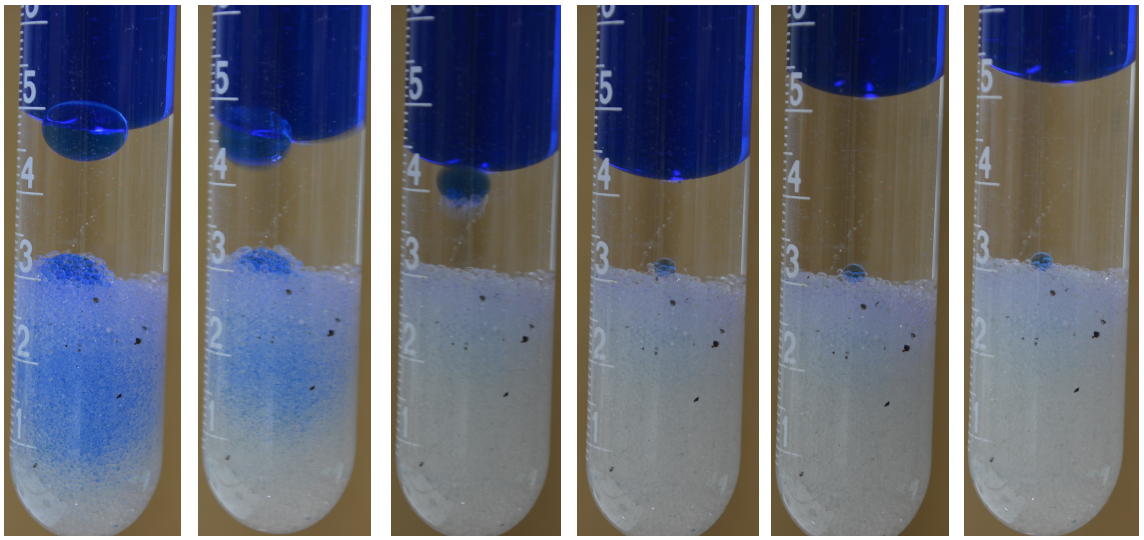

(a) t=2 min (b) t=3 min (c) t=4.5 min (d) t=12 min (e) t=14 min (f) t=16 min

Figure 5.8: Tube test I: Acid did not react with oil to change its colour.

5.2.1.2 Tube test II - Bromothymol Blue

Oil phase was taken in a tube, and glass beads were added to the tube until oil-glass beads (O-GB) interface reached 3 mL mark. The settling time for glass beads was 2 minutes, similar to observation in tube test I. Upon settlement, a distinct interface at 3 mL mark was observed between glass beads and free oil phase (fig.5.9b). The water solution was then added to the system and a distinct water-glass beads interface (W-GB) and water-oil interface (W-O) was observed (fig.5.9c).

Upon addition of water, oil trapped in the porous media was mobilised. Visualisation of oil recovery from porous media was not clear as in tube test I due to the dark colour of water phase. Oil droplet escaping the glass beads was faintly noticed (marked by an arrow in fig.5.9d). The oil recovery process slowed down after 10 minutes.

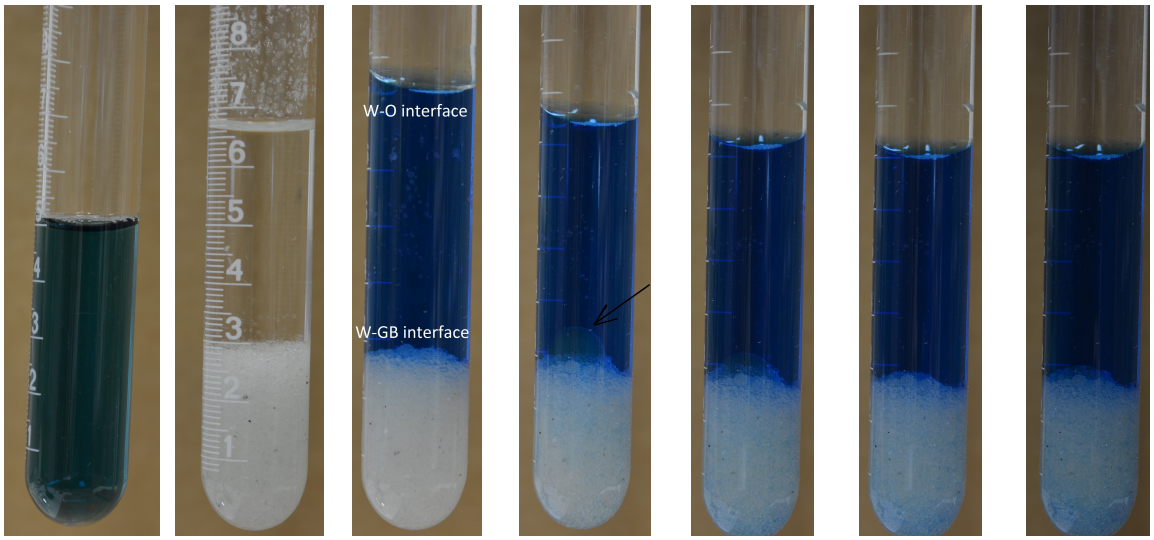

(a) Water phase (b) Porous media (c) t=0 (d) t=1 min (e) t=2 min (f) t=2.5 min (g) t=3 min

Figure 5.9: Tube test II: Movement of water in porous media was similar to observation in tube test I.

The path of the water phase movement in glass beads was not clearly visible as in tube test I, but it was inferred to be similar to tube test I because the blue colour of the water phase intensified in the porous media (seen from fig.5.9e to fig. 5.10b as gradual change in colour of porous media).

HCl was added and the colour of water phase changed from blue to yellow indicating a drop in pH below 6. This change is observed from fig.5.10c to fig.5.10f.

Slow movement of acidic water phase into the porous media was observed (marked by arrows in fig.5.10f and fig.5.10g).

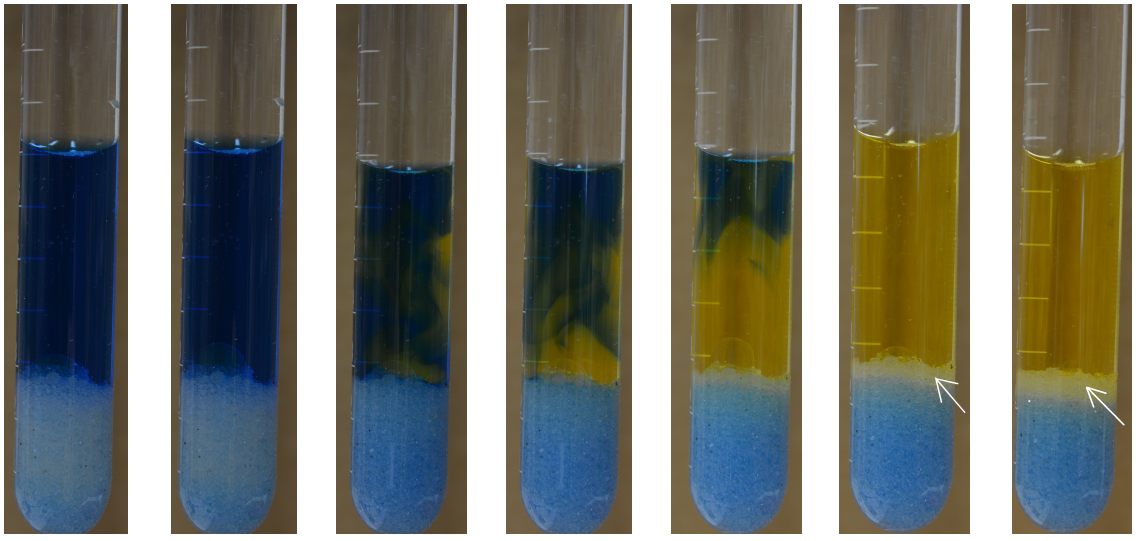

(a) 4.5 min (b) t=6 min (c) t=10 min (d) t=10.5 min (e) t=11 min (f) t=20 min (g) t=70 min

Figure 5.10: Tube test II: Change in colour of water phase upon addition of 0.1 M HCl. A slow movement of low pH water in porous media was observed.

5.2.1.3 Tube test III - Sudan II

Oil phase was taken in a tube, and glass beads were added until the oil-glass beads (O-GB) interface reached 3 mL mark. Settlement time for glass beads was 3 minutes. Upon settlement of glass beads, a faint interface between glass beads and free oil phase was observed, as indicated by the green box in fig.5.11b. A distinct water-glass beads interface (W-GB) and water-oil interface (W-O) was observed on adding water solution to the tube (fig.5.11c).

The oil trapped in the porous media mobilised upon addition of water. Visualisation of oil mobilisation from porous media was better compared to tube test II (Sub-subsection 5.2.1.2) as oil was seen escaping the porous media as dark droplets (marked by an arrow in fig.5.11c). The oil recovery process slowed down after 11 minutes.

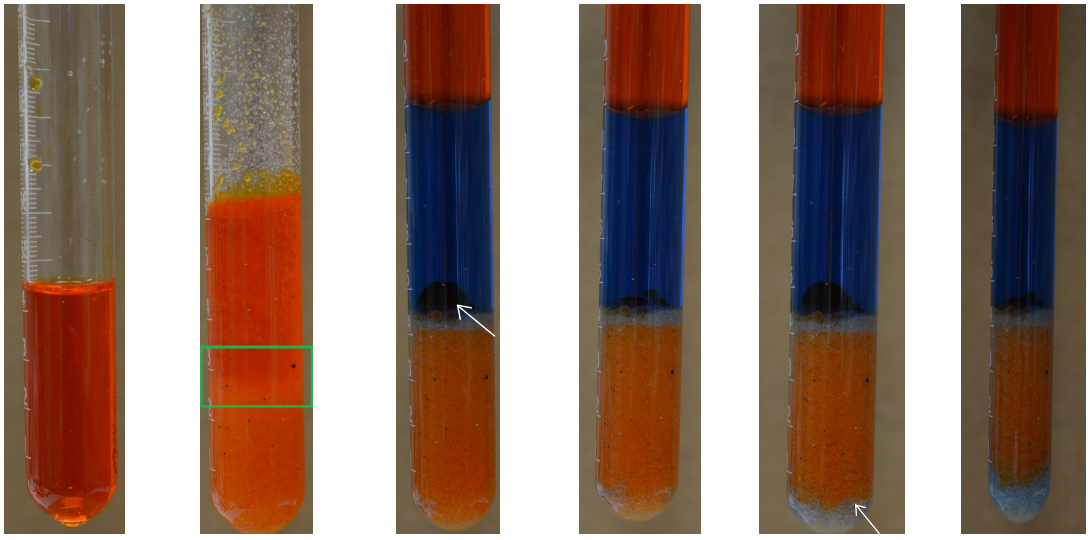

(a) Oil phase (b) Porous media (c) t=0 (d) t=10 sec (e) t=1 min (f) 1.5 min

Figure 5.11: Tube test III: Mobilisation of oil from porous media as dark droplets at water-glass beads interface.

It was possible to visualise the movement of water phase along the sides of the tube and towards the bottom (marked by arrows in fig.5.11e, fig.5.12a and fig.5.12c). The movement of the water phase in glass beads was observed as blue colour of the water phase intensified and colour in porous media changed from orange to blue (fig.5.11, fig.5.12 and fig.5.13).

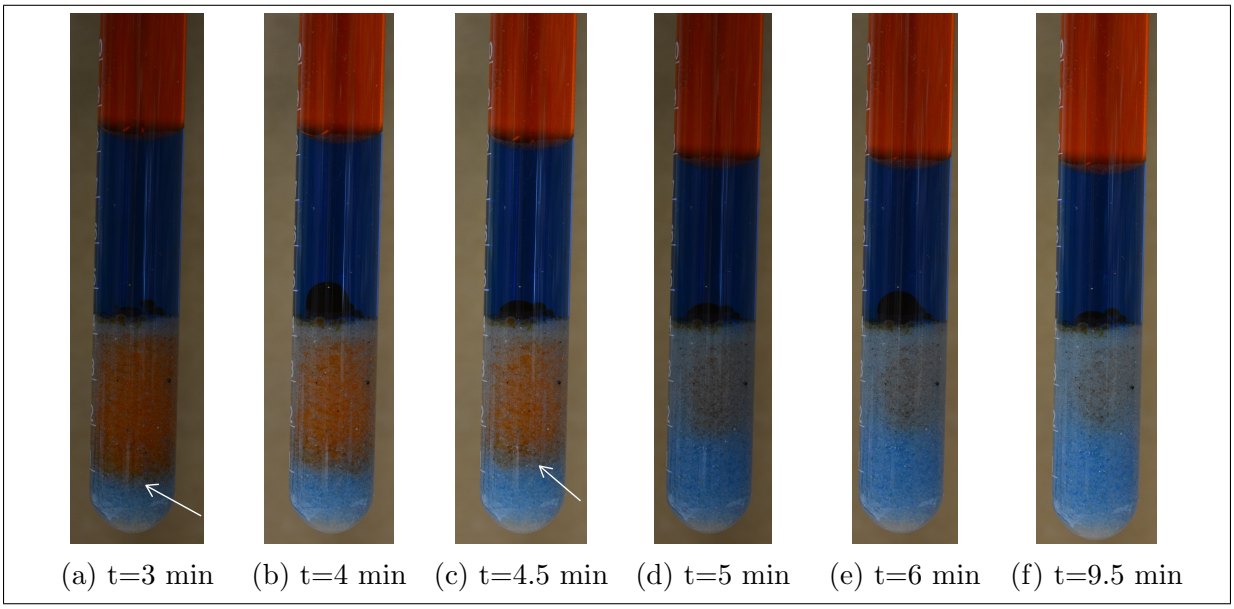

(a) t=3 min (b) t=4 min (c) t=4.5 min (d) t=5 min (e) t=6 min (f) t=9.5 min

Figure 5.12: Tube test III: Invasion of water in porous media was similar to tube test I and II.

As HCl was added to the tube, the colour of water phase changed to yellow indicating a drop in pH below 6 as the water phase changed from basic to acidic solution. No significant change in oil recovery occurred upon addition of acid (fig.5.13a to fig.5.13f).

Similar to tube test II, some movement of low pH water in porous media was observed (marked by an arrow in fig.5.13e).

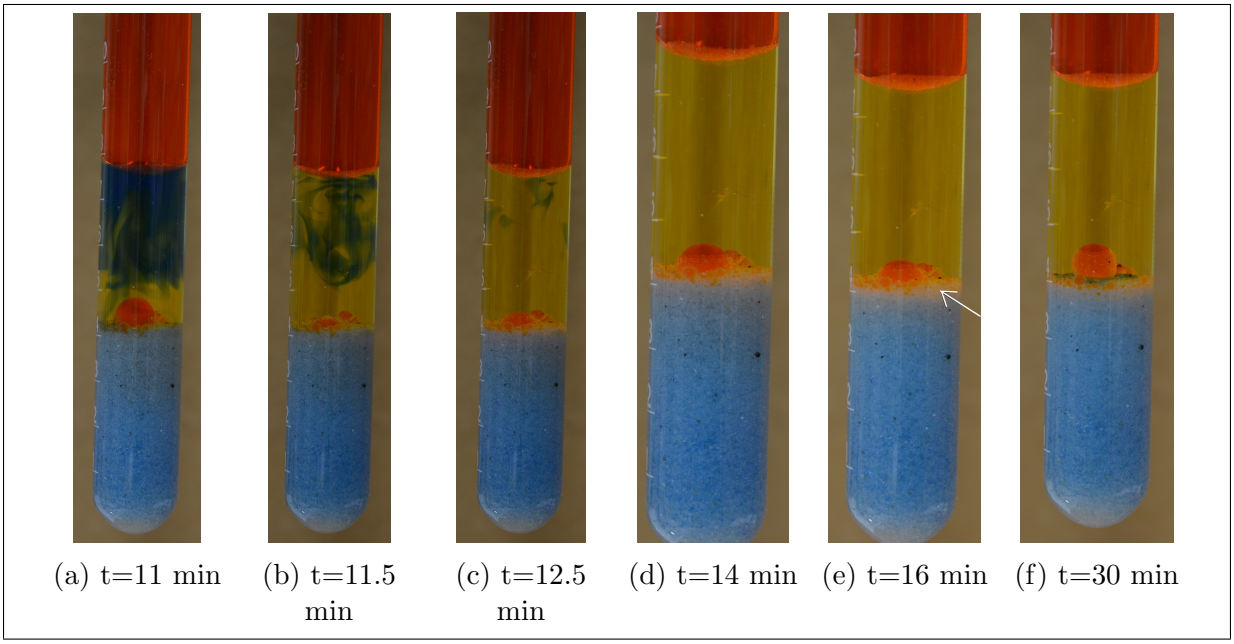

(a) t=11 min (b) t=11.5 min (c) t=12.5 min (d) t=14 min (e) t=16 min (f) t=30 min

Figure 5.13: Tube test III: Addition of HCl to the tube.

5.2.1.4 Tube test IV- Sudan III

Settlement time for glass beads was 2 minutes, and upon settlement of glass beads, a faint interface between glass beads and free oil phase was observed at 4 mL mark (as indicated by the box in fig.5.14b). The water solution was then added to the system and distinct water-glass beads interface (W-GB) and water-oil interface (W-O) was observed (marked by boxes in fig.5.14d).

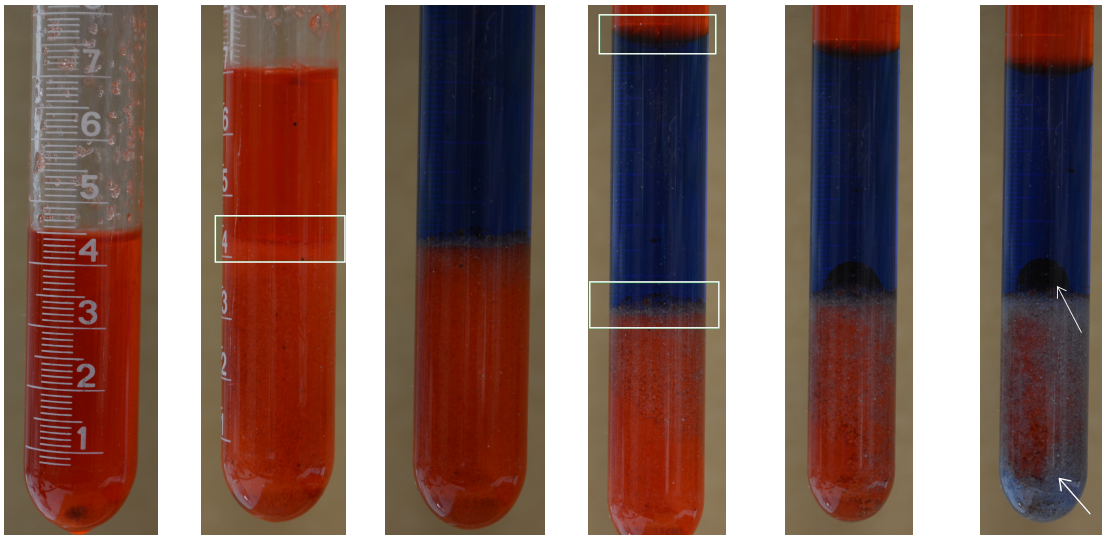

(a) Oil phase (b) Porous media (c) t=0 (d) t=1 min (e) t=2 min (f) t=3 min

Figure 5.14: Tube test IV: Addition of the water solution and the beginning of oil mobilisation from porous media.

Oil trapped in the porous media was mobilised upon addition of water, similar to tube test III, i.e. a dark oil droplet was observed at W-GB interface (white arrow in fig. 5.14f). Visualisation of test IV was poor as compared to test III because of some visible precipitation in oil phase before the experiment started and due to the darker shade of oil phase in test IV.

Majority of porous media was invaded by water phase and oil recovery was a slow process after 10 minutes. The movement of the water phase in porous media was similar to tube test III, i.e. water phase moved along the sides of the tube and then towards the bottom. It has been marked by arrows in fig. 5.14f, fig.5.15c and fig.5.15f.

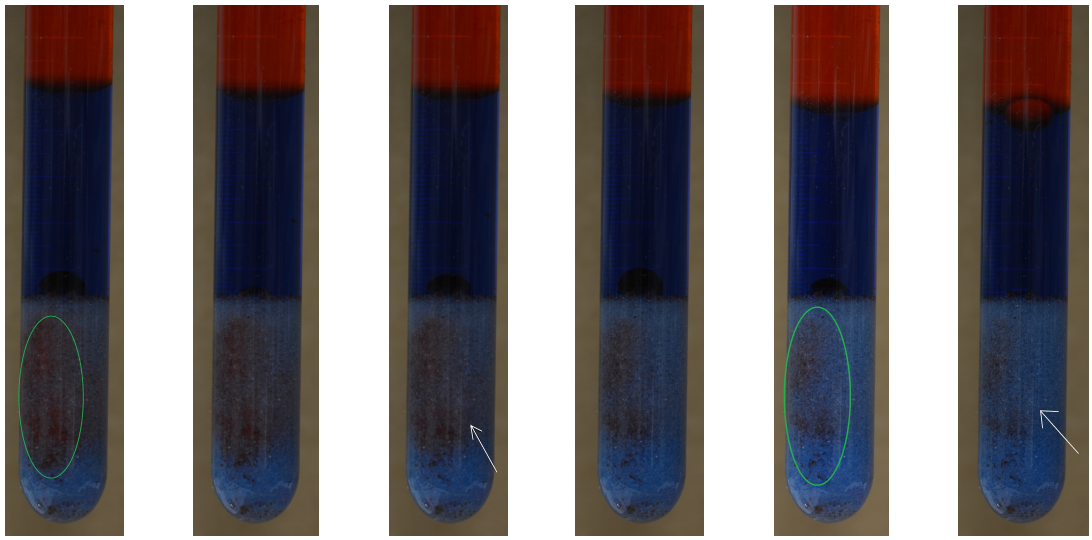

(a) t=4 min (b) t=4.5 min (c) t=5 min (d) t=6 min (e) t=6.5 min (f) t=7 min

Figure 5.15: Tube test IV: Water invasion was along the side walls of the tube as in tube test III, but the path of water movement was different (from back-right of the tube to front-left).

Movement of the water phase in porous media was observed to be from the back of the tube towards front. Water phase movement was observed as oil in porous media (represented by orange) decreased gradually on the left side of the tube (marked green in fig.5.15a and fig.5.15e).

HCl was added, and the colour of the water phase changed to yellow indicating a drop in pH below 6 (from fig.5.16c to fig.5.16f). No significant improvement in oil recovery was observed upon addition of acid. A limited movement of low pH water in pores was observed (marked by an arrow in fig.5.16f).

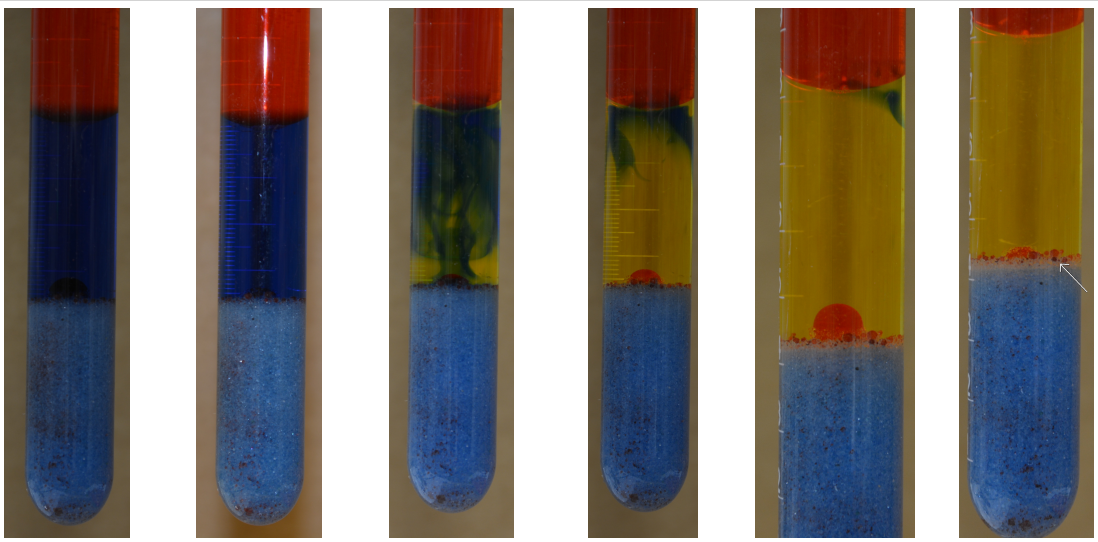

(a) t=8 min (b) t=9 minutes (c) t=11 min (d) t=12 min (e) t=14 min (f) t=30 min

Figure 5.16: Tube test IV: Addition of HCl to tube showed a similar effect as in tube test III, no increment in recovery was observed.

5.2.1.5 Conclusions: Tube tests in porous media type A

Table 5.2 gives an overview of observations from tube test I-IV. T_s and T_m are settlement time for glass beads and time until water phase invades majority of the porous media and oil recovery slows down, respectively. Accuracy in recovery calculations: 10 % recovery$\approx$ 0.2 mL oil recovered. The quality of contrast between both the phases is graded on the scale: good, intermediate and poor.

Label	pH of water solution	T_s	T_m	Recovery (%)	Movement of water	Visualisation contrast
TT I	7.0	2 min	12 min	77	Walls of tube	Good
TT II	7.58	2 min	10 min	77	Walls of tube	Poor
TT III	7.62	3 min	11 min	88	Walls of tube	Good
TT IV	7.63	2 min	10 min	86	Walls of tube	Intermediate

Table 5.2: Tube test I-IV: Overview of observations.

Following conclusions are drawn from these tests:

1. Bromothymol blue successfully represented a change in pH due to the addition of 0.1 M HCl, by showing a change in colour to yellow.
2. Of the three oil dyes tested, sudan II was selected to represent oil phase in further experiments because:
   (a) The colour of the oil phase while using sudan blue II was similar to the water phase. Due to the difficulty in distinguishing between both the phases in the porous media sudan blue II was not used.
   (b) Preparation of oil phase using sudan III showed minor precipitation. Syringe filter was used to remove the precipitates, but not entirely. Oil phase also showed a darker colour in porous media which did not contrast well in visualisation and studying images after experimentation (seen in TT IV).
   (c) Limitations posed by sudan blue II and sudan III coupled with more quantity of sudan II available for experimentation made sudan II a suitable choice to represent oil phase in further experiments.
3. The movement of water phase in the porous media followed a similar path in all the four tests, entrance into pores from side walls of the tube towards the bottom. The following are the reasons for this behaviour:
   (a) Imbibition under gravity conditions leads to a very low capillary number of the displacing phase and the effects of invasion percolation are encountered in this situation. Calculations based on this theory are performed in cell test experiments (Section 5.4).
   (b) The grain size was not well distributed as porous media of diameter 150 μm was used instead of varied grain size. This caused the water phase to percolate through the porous media rather than invade as piston-type displacement. The settlement time for glass beads was in the range of 2-3 minutes. Therefore, air entrapment in the porous media might be a possible reason for the unsteady movement of the water front. An ultrasonic bath was used in further tests to provide better packing of porous media.
   (c) The glass tube used was preferentially water wet and offered low resistance compared to the oil-filled porous media; therefore water phase chose to move

in paths of lower resistance.

4. Imbibition under these conditions was a speedy process as the majority of porous media was invaded in 10-12 minutes.
5. Addition of HCl did not improve the oil recovery from pores. We can infer that HCl can be used only to mimic a change in pH during CO_2 injection and not the improvement in recovery.
6. Upon adding water solution to the tube, the colour of water changed from greenish blue to blue (seen in fig.5.9a and fig. 5.9c on page 57). The change in colour indicated a change in pH of the water phase due to a reaction with glass beads. This effect was studied in subsection 5.2.2.
7. Recovery factors calculations for all four tests are explained in Appendix A.1 on page 135. Recovery factors indicate the porous media used was water wet.

Note: All recovery factors calculated in this thesis are expressed as % of Pore Volume (PV).

5.2.2 Effect of glass beads on pH of water phase

In the tube test II, it was observed that addition of glass beads to water phase caused the colour of the water to change from greenish blue to blue (seen in fig.5.9a and fig. 5.9c on page 57). One explanation of this phenomena was the rise in pH due to the reaction between glass beads and the water phase. Based on the composition of glass beads given in table 4.2 it was believed that CaO in glass beads reacted with water to cause the increase in pH.

To verify this explanation, pH of the water phase was measured before and after the addition of glass beads. Upon addition of glass beads, pH of the water phase increased from 7.67 to more than 9.65 (refer table 5.3).

Glass beads were treated with acid to negate the rise in pH. The pH of the water phase was measured after acid-washing, and it was observed that acid-washing the glass beads limited the rise in pH. Results of pH measurements before and after the acid-washing are given in table 5.3.

Sample type	pH
Water solution	7.67
Glass beads type A	9.78
Glass beads type B	9.83
Glass beads type C	9.68
Acid washed glass beads (type C)	7.95
Glass beads type D	9.8
Acid washed glass beads (type D)	7.37
Mix[1]	9.73
Mix (Acid washed)	7.78

Table 5.3: pH variation upon addition of different types of glass beads.

[1]The mix of glass beads (acid washed and non-acid washed) is 50 wt% type C + 50 wt% type D.

5.2.3 Tube tests in porous media of type C/D

Glass beads in the size range of 70-110 μm were used to conduct six experiments in this phase of tube tests. These experiments were performed to understand imbibition process with low pH water (to mimic CO_2 rich water) as displacing fluid. HCl was added 1-2 minutes after adding the water solution to the tube. These experiments were analogous to experiments conducted in a larger tube under low-pressure CO_2 injection. Hence, a time delay of 2 minutes was accounted to mimic necessary valve operations and pump settings to be done before CO_2 injection commenced.

5.2.3.1 Tube test V: Oil-water system in porous media type C

Use of the ultrasonic bath provided better packing of porous media in the tube. The water phase was then added to the tube, and imbibition process commenced. Movement of water in porous media was piston-like in the beginning and later switched to faster advancement along the walls.

HCl was added to the tube after 2 minutes. The dissolution of acid in water phase was quick, and colour of water phase changed from blue to yellow (fig.5.17d). Movement of low pH water in porous media was also piston-like, and a shade of blue was observed in the porous media at invading water front (marked by an arrow in fig.5.17f).

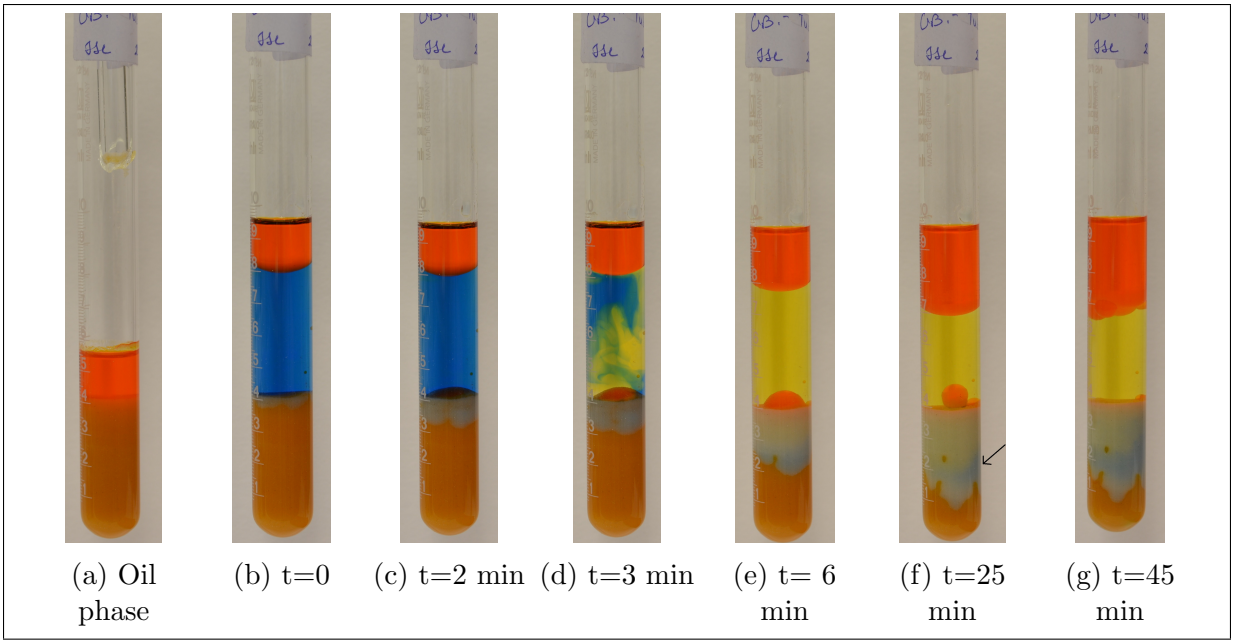

(a) Oil phase (b) t=0 (c) t=2 min (d) t=3 min (e) t= 6 min (f) t=25 min (g) t=45 min

Figure 5.17: Tube test V: Oil recovery by low pH water (yellow) was a slow process compared to tube test I - IV

The blue shade was due to the water phase that invaded the porous media before addition of acid. Another possible reason was the rise in pH due to the reaction of the water phase and porous media, causing the water phase to appear blue during visualisation. After 25 minutes, imbibition was a very slow process and minimal increment in oil production was noticed (as seen in fig.5.17f and fig.5.17g).

One possible reason for no further increment in recovery could be snap-off in pore throats. For imbibition to occur, movement of non-wetting phase is required (see section 2.13).

If non-wetting phase ceases to move then meniscus (at wetting and non-wetting phase interface) cannot move further and the imbibition process stops.

5.2.3.2 Tube test VI: Oil-water system in acid-washed porous media type C

Similar to tube test V, the use of an ultrasonic bath provided better packing of the porous media.

Upon addition of the water phase to the tube, the imbibition process commenced. The movement of water in porous media was slower compared to tube test V. Upon addition of HCl to the tube, the dissolution of acid in the water phase was quick, and the colour of the water phase changed from blue to yellow indicating that pH dropped below 6 (fig.5.18b).

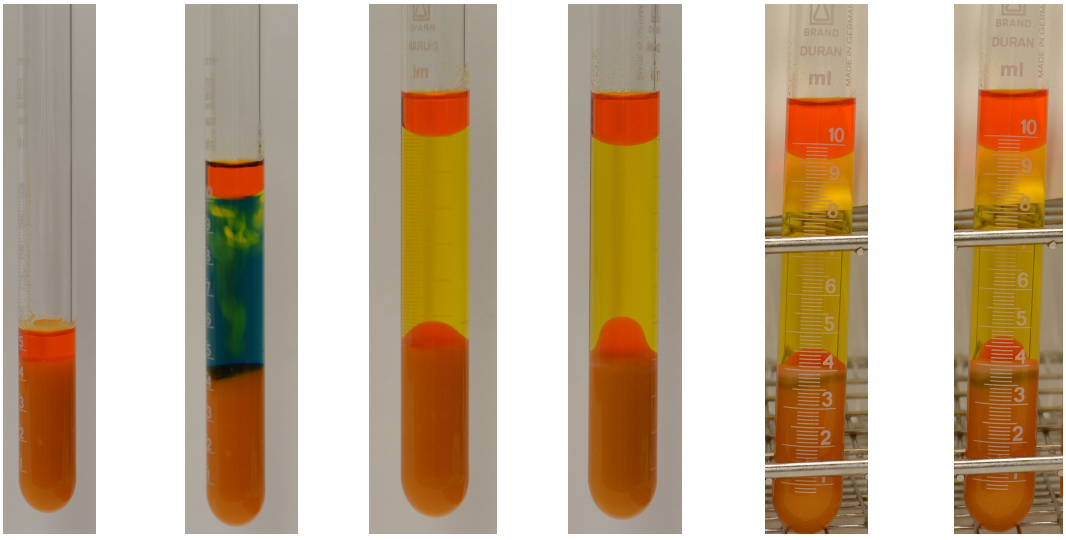

(a) Oil phase (b) t=2 min (c) t=9 min (d) t=16 min (e) t=30 min (f) t=45 min

Figure 5.18: Tube test VI: Movement of water in porous media was piston-like, but lower oil recovery was obtained in this test compared to tube test V.

The movement of low pH water was piston like (fig.5.18e), and over the same timescale of the experiment as tube test V, less oil recovery was observed. Table 5.4 shows recovery factors for tube test V and tube test VI. Appendix A.1 shows recovery factor calculations in tube tests.

During the acid treatment of glass beads, the reaction of acid and glass beads was believed to cause changes on the surface of glass beads. One such change might be to make the surface of glass beads rough. Before acid treatment, the roughness of glass beads was minimal ($< 0.02\mu m$). The change in roughness affects the movement of water phase in the porous media.

Test label	Recovery (%)
Tube test V	71
Tube test VI	22

Table 5.4: Comparison between oil recovery in tube test V and tube test VI.

Note: Accuracy of recovery: 10 % recovery $\approx$ 0.2 mL oil recovered.

5.2.3.3 Tube test VII: Oil-water system in porous media type D

Similar to tube test V and VI, the use of an ultrasonic bath provided better packing of the porous media. The movement of the water phase in porous media was limited compared to tube test V. HCl was added to the tube, and quick dissolution in the water phase was observed as the colour of water phase changed from blue to yellow (fig.5.19b).

The porous media used in this test was hydrophobic. Hence, a negligible amount of oil was recovered from pores. The experiment continued for 180 minutes, but the recovery factor calculations were done at t= 45 minutes. Minor recovery observed in this test is attributed to the presence of impurities in the glass beads during the manufacturing process or handling and transfer of glass beads. The presence of these impurities results in glass beads not being completely hydrophobic.

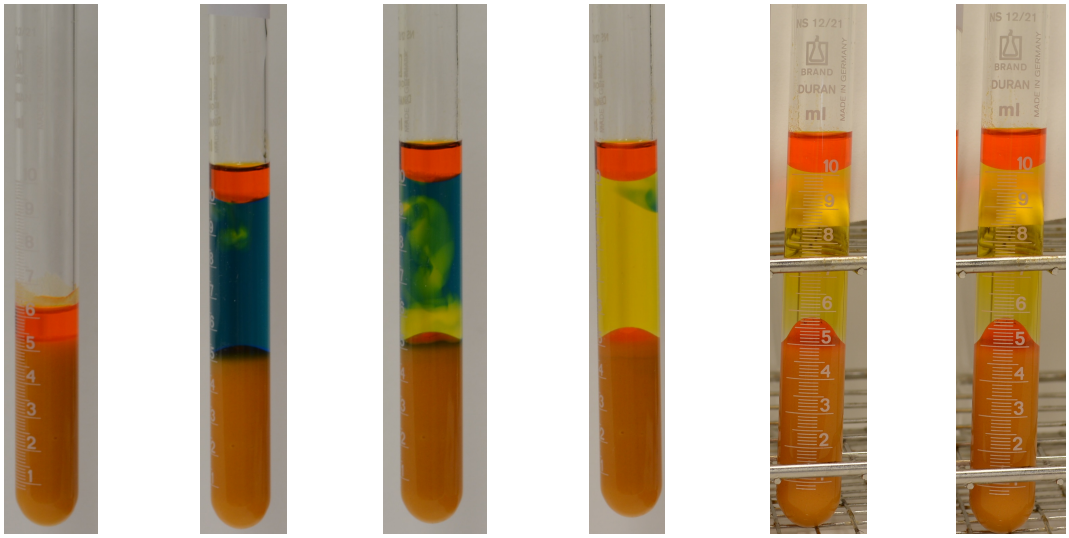

(a) Oil phase (b) t=2 min (c) t=3 min (d) t=15 min (e) t=45 min (f) t=180 min

Figure 5.19: Tube test VII: Oil recovery from porous media was negligible due to the hydrophobicity of porous media.

5.2.3.4 Tube test VIII: Oil-water system in acid-washed porous media type D

The use of an ultrasonic bath provided better packing of the porous media. When the water phase was added to the tube (fig.5.20b), it did not show any movement in the porous media. After 2 minutes, HCl was added to the tube and the colour of water phase changed from blue to yellow due to the dissolution of acid (fig.5.20c).

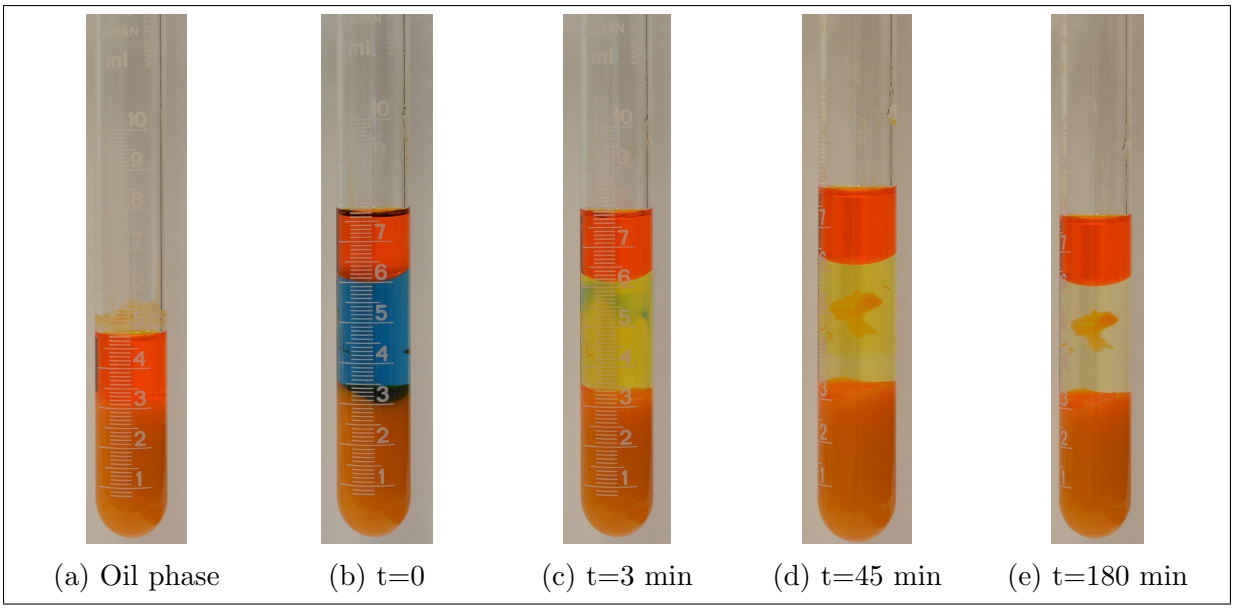

(a) Oil phase (b) t=0 (c) t=3 min (d) t=45 min (e) t=180 min

Figure 5.20: Tube test VIII: No oil was mobilised from porous media when using acid washed hydrophobic glass beads.

The water phase did not show any movement in acid-washed glass beads type D as opposed to in glass beads type D. Comparing fig.5.19e and fig.5.20d it was observed that oil was mobilised from the porous media type D, but no oil mobilisation took place when the same porous media was acid-washed. The experiment continued for 180 minutes, but the recovery factor calculations were done at t= 45 minutes.

Test label	Recovery (%)
Tube test VII	5
Tube test VIII	0

Table 5.5: Comparison between oil recovery in tube test VII and tube test VIII.

Table 5.5 compares oil recovery in tube test VII to that in tube test VIII. Acid-washing removed the impurities present in porous media type D and is believed to cause changes in the surface properties (e.g. roughness) of glass beads.

Note: Accuracy of recovery: 10 % recovery $\approx$ 0.2 mL oil recovered.

5.2.3.5 Tube test IX: Oil-water system in mix porous media (type C+ type D)

In this experiment, porous media of type C and type D were mixed (50 wt% each) and used as porous media. The mixing of glass beads provided uneven wettability distribution to the porous media.

Upon addition of the water phase to the tube (fig.5.21b), piston type movement of the water phase in the porous media was observed. After 2 minutes, HCl was added to the tube, and the colour of water phase changed from blue to yellow. The movement of low pH water in porous media was also observed to be piston-like (seen in fig.5.21d to fig.5.21h).

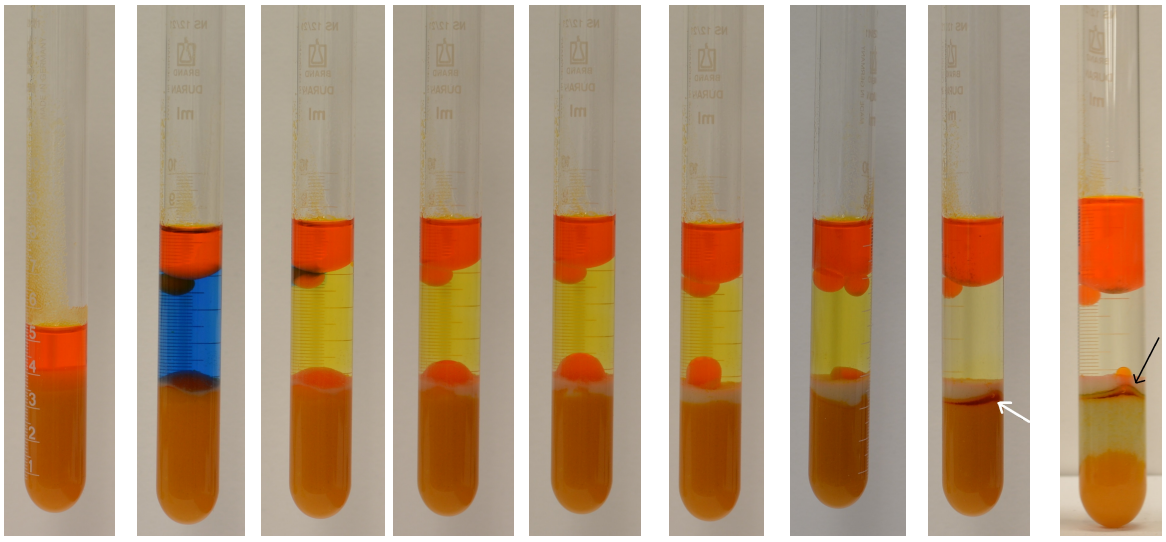

(a) Oil phase (b) t=1 min (c) t=4 min (d) t=21 min (e) t=26 min (f) t=30 min (g) t=32 min (h) t=38 min (i) t=50 min

Figure 5.21: Tube test IX: Piston like movement of the water phase in porous media and formation of oil bank in pores due to snap-off.

A small layer of oil was observed in porous media (marked by an arrow in fig.5.21h). The formation of oil bank in the porous media was a result of snap-off in pores already swept by water phase. As the oil phase became discontinuous in pores already swept by water, it could not move further up and accumulated in porous media to form a small oil bank. As time progressed, the oil bank grew in size, and due to the difference in density of water and oil phases, oil from the bank began to escape from the porous media and into the free oil phase on top of the tube (marked by an arrow in fig.5.21i).

5.2.3.6 Tube test X: Oil-water system in mix-acid washed porous media (type C+ type D)

In this experiment, acid-washed porous media of type C and type D were mixed (50 wt% each) and used as porous media. The use of an ultrasonic bath provided better packing of the porous media.

On adding the water phase imbibition began with piston type movement of the water phase in porous media (fig.5.22c). The addition of HCl to the tube changed the colour of the water phase changed from blue to yellow. The movement of low pH water in porous media was not piston-like, and oil was observed to leave the pores near the walls of the tube rather than the center of the tube (seen in fig.5.22d).

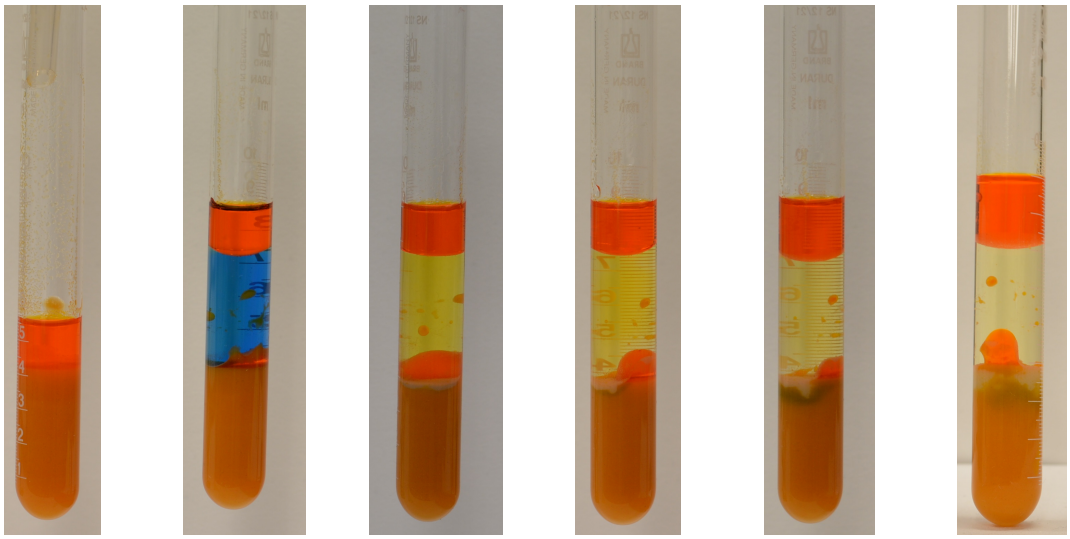

(a) Oil phase (b) t=1 min (c) t=10 min (d) t=20 min (e) t=35 min (f) t=45 min

Figure 5.22: Tube X: Acid-washed porous media showed lower oil recovery compared to non-acid washed porous media of the same type.

Test label	Recovery (%)
Tube test IX	53
Tube test X	24

Table 5.6: Comparison between oil recovery in tube test IX and tube test X.

In table 5.6 the oil recovery in tube test IX is compared to that in tube test X. Recovery in acid-washed porous media was less compared to recovery in same porous media when not acid-washed. One reason for this might be the alteration in roughness of glass beads, causing the water phase to move slower in porous media.

Note: Accuracy of recovery: 10 % recovery $\approx$ 0.2 mL oil recovered.

5.2.3.7 Conclusion: Tube tests in porous media type C/D

Table 5.7 gives an overview of observations from tube test I- X. Accuracy of recovery calculations was: 10 % recovery ≈ 0.2 mL oil recovered.

Label	pH of water solution	Porous media type	Movement of water	Recovery (%)
TT I- IV	7.58 – 7	Type A	Along the walls	77 – 88
TT V	7.66	Type C	Piston-like + along the walls	71
TT VI	7.65	Acid-washed type C	Piston-like	22
TT VII	7.65	Type D	Along the walls	5
TT VIII	7.68	Acid-washed type D	No movement observed	0
TT IX	7.7	Mix (type C+type D)	Piston-like	53
TT X	7.65	Acid-washed mix	Piston-like	24

Table 5.7: Tube tests I-X: Overview of observations.

To account for variation in porous media, the porous media used were of varying size distribution (70-110 μm), acid-washed and a mix of hydrophilic (type C) and hydrophobic (type D) glass beads. The following conclusions were drawn from these tests:

1. Addition of glass beads to water phase caused the pH to rise from 7.67 to more than 9.65. Acid-washing the glass beads limited this rise in pH.
2. A piston-like movement of the water phase in porous media was observed, opposed to along the side walls of the tube (as observed in tube tests in porous media type A). Possible reasons for this type of displacement are (Geistlinger & Mohammadian, 2015):
   (a) Wettability: When comparing tube test III with tube test V, only grain size in porous media changed. Both the porous media were water-wet and similar rise pH was observed upon reaction with the water phase. Hence it can be inferred that wettability change was not the factor for the difference in displacement pattern.
   (b) Flow rate: All tests in this section were performed at the water phase movement under gravity and in tubes of the same diameter. No pump or additional force was used to drive the imbibition process. Hence, the flow rate was not a factor for change in displacement pattern.
   (c) Pore throat geometry and pore network topology: Size distribution of glass beads was changed from 150 μm in tube test I-IV to 70-110 μm in tube test V-X. A variation in the grain size of porous media led to change in the size of pores and pore throats. In tube tests I-IV, settlement of glass beads was gravity-driven. The use of an ultrasonic bath in tube tests V- X provided a better packing compared to gravity settlement. These changes in the type of glass beads size and packing were factors for the difference in displacement pattern.
3. Lenormand et al. studied the change in shape of water front during an imbibition process. Our results are in line with their findings in glass micromodels. In small pores, imbibition occurs as successive I2 jumps (imbibition I2 type) to fill the network line after line and as a result "Frontal Drive" with a very flat front can be observed (Lenormand & Zarcone, 1984), which was noticed as piston-like displacement in our case.

4. The mobilisation of oil from porous media was a slower process in tube tests V-X compared to tube tests I-IV. The slow mobilisation of oil from pores is attributed to displacement pattern of the water phase. Movement by precursor thin film flow (as in tube test I- IV) is always faster compared to bulk advance due to piston-like displacement (Geistlinger & Mohammadian, 2015). Hence, our experiments visually confirm results from theory.

5. In tube test V (fig. 5.17g on page 65) it was observed that after 25 minutes, oil recovery was a slow process and negligible increment in oil recovery was noted. The limited increment in oil recovery can be explained using imbibition theory that a discontinuity of oil phase occurs in the areas swept by water, which ceases the movement of oil phase from pores towards the free oil phase on top. If there is no movement of non-wetting phase, then meniscus stops to move, and imbibition process stops.

6. The development of an oil bank in porous media was observed in tube test IX (fig. 5.21h on page 69). The reason for this was the snap-off in pores above the oil bank. Snap-off led to discontinuity of oil phase and restricted the upwards movement of the oil phase. As a result, oil accumulated in the porous media.

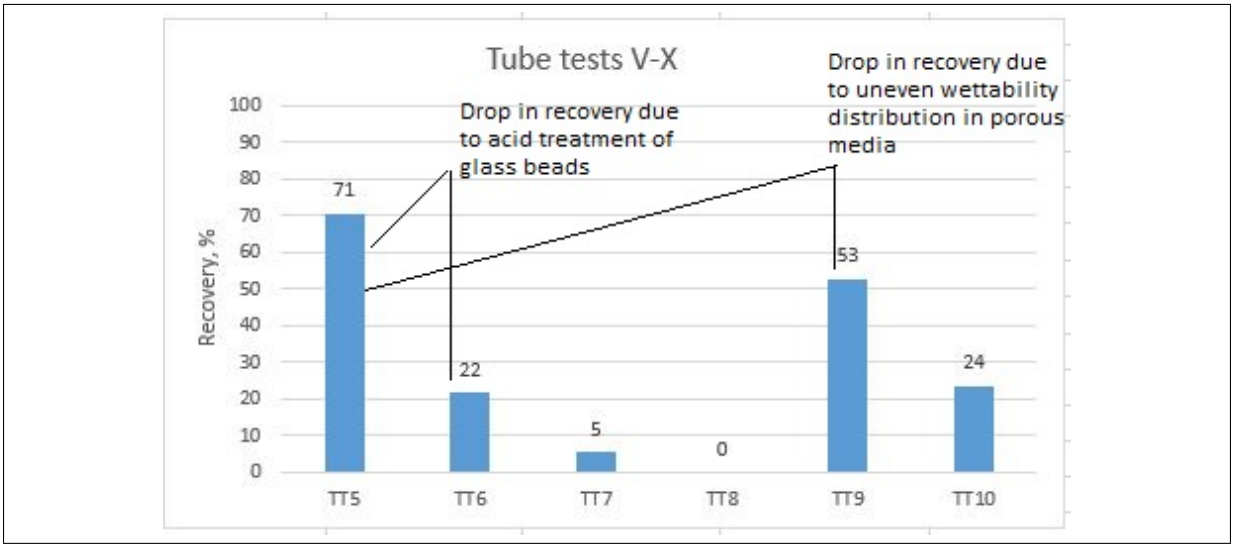

Figure 5.23: Recovery from tube tests in porous media type C/D.

7. Fig. 5.23 shows recovery for tube tests V-X. From the chart, it can be inferred that acid treatment of glass beads caused oil recovery to be lower in tube test VI compared to tube test V. Recovery calculations in these experiments are also a function of time. Acid treatment of glass beads is believed to change the roughness of porous media and cause slower movement of the water phase, which can delay the oil recovery. Another reason for low oil recovery might be the ability of glass beads to adsorb oil phase after acid treatment, but more study needs to be done to understand this phenomenon.

8. It is observed from the data that recovery using glass beads of mixed type (tube test IX) is lower than recovery factor using only water wet glass beads (tube test V). Mixing the glass beads of type C and D in tube test IX caused uneven wettability distribution and introduced hydrophobicity in porous media, which prevented the water from recovering oil in pores surrounded by hydrophobic glass beads.

5.2.4 Tube tests by varying diameter of tube

Three experiments were conducted in this part of tube tests. Tubes of varying internal diameter were used to study:

1. The packing of porous media and visualisation of the oil-water system.
2. The shape of water front in the porous media.
3. Oil recovery mechanism.

Conducting tests in tubes of varying diameter will provide a basis for designing polycarbonate cells and insight into procedure development.

5.2.4.1 Tube test XI: test in tube of internal diameter 7.85 mm

The filling of the porous media did not pose any difficulty, and the use of an ultrasonic bath provided better packing of the porous media. The water solution was then injected into the tube, and oil mobilisation from porous media began. The movement of water in porous media was piston-like. Oil trapped in the porous media behind left behind the invading water front was observed (in fig.5.24c). HCl was added to the tube and the colour of water phase changed to yellow as the pH dropped below 6.

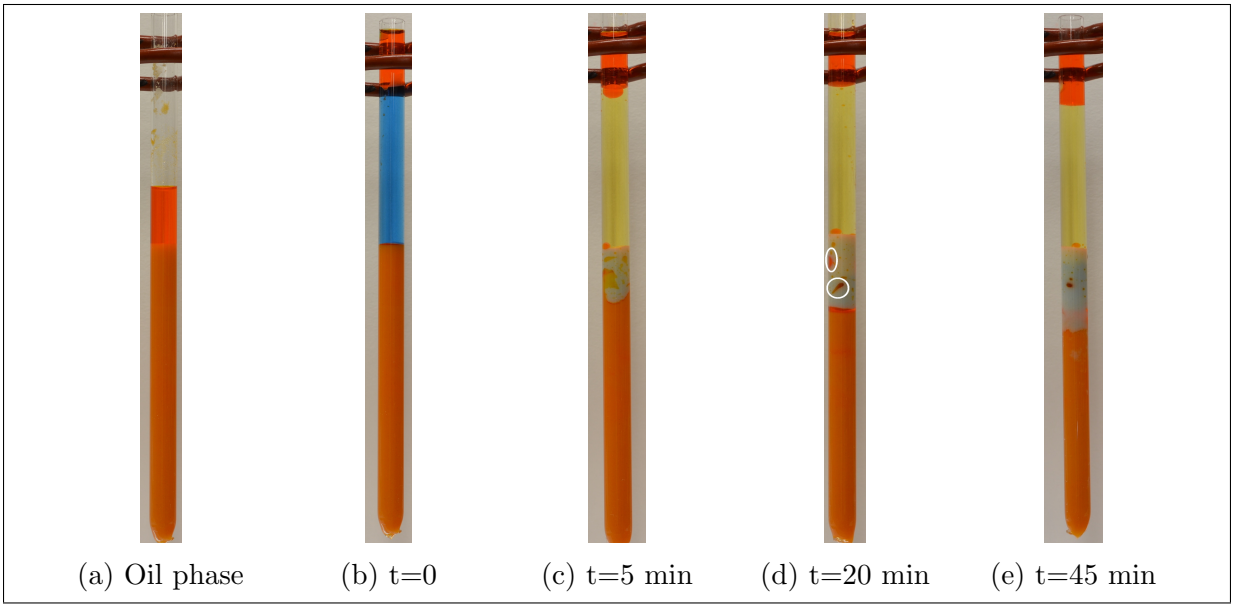

(a) Oil phase (b) t=0 (c) t=5 min (d) t=20 min (e) t=45 min

Figure 5.24: Tube test XI (d=7.85 mm): Movement of water in porous media was piston-like and oil left behind the high pH water front was partially recovered by low pH water.

Movement of low pH water in pores was a slow process. As low pH water invaded the porous media, a fraction of the trapped oil was mobilised (marked by circles in fig.5.24d). After 25 minutes, the movement of low pH water in pores was a slow process, and the experiment was stopped after 45 minutes. The oil recovery at the end of the experiment was 26% (recovery calculations for tube test XI-XIII are explained in appendix A.2 on page 138).

Note: Accuracy in recovery calculations : 10% recovery = 4.3 mm height of oil column in the tube.

5.2.4.2 Tube test XII: test in tube of internal diameter 5.55 mm

The filling of porous media in the tube was more difficult compared to tube test XI, and use of an ultrasonic bath provided proper packing of glass beads in the pores. The movement of the water phase in porous media was piston-like near the entrance of porous media (seen in fig.5.25b to fig.5.25d). After 2 minutes, HCl was added to the tube and the colour of water phase changed to yellow as the pH dropped below 6.

After 5 minutes, the water phase began to move along the side walls of the tube (fig.5.25e) and the front movement was no longer piston-like. The movement of water in the porous media was a crossover between piston-type displacement and movement along side walls of the tube. The rise of oil droplets from the porous media to free oil phase on top of the tube was a slow process due to the resistance offered by a low diameter of the tube (fig.5.25d shows oil drop slowly rising in the tube).

As the low pH water invaded the porous media, oil trapped in porous media behind high pH water front (blue) front was partially recovered. Recovery of trapped oil was visualised as a decrease in the oil volume in porous media, marked by a circle in fig.5.25f. The movement of the water phase in the porous media was quick compared to tube test XI, and recovery of oil was calculated to be 81%.

Note:Accuracy in recovery calculations: 10% recovery = 4.3 mm height of oil column in the tube.

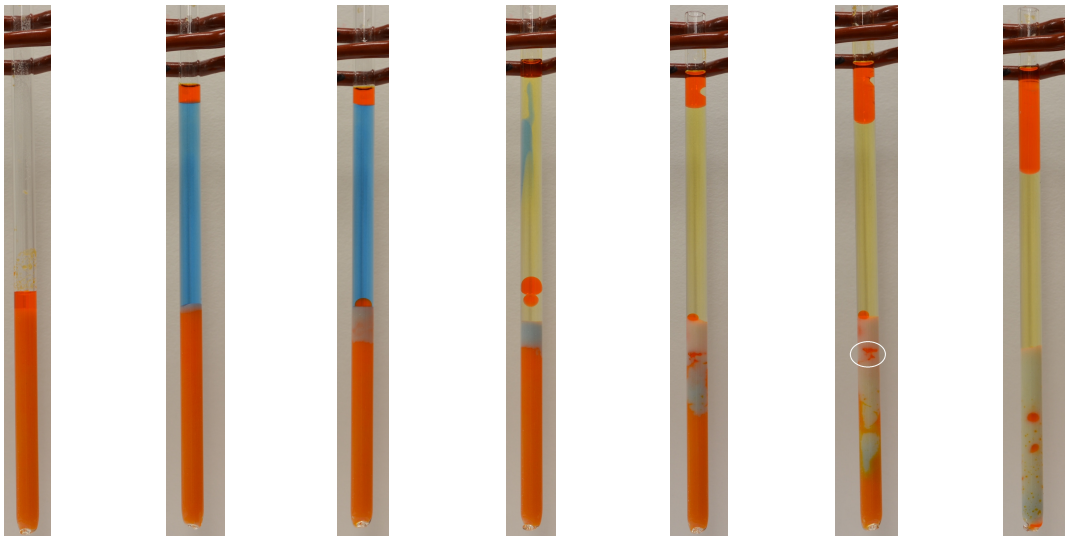

(a) Oil phase (b) t=0 (c) t=1.5 min (d) t=3 min (e) t=10 min (f) t=30 min (g) t=45 min

Figure 5.25: Tube test XII (d=5.55 mm): Movement of water in porous media was a crossover between piston-like and movement along the side walls of the tube. The mobilisation of oil from porous media was a fast process compared to tube test XI.

5.2.4.3 Tube test XIII: test in tube of internal diameter 3.75 mm

The filling of porous media in the tube was challenging compared to tube test XI and XII. The reason being; as glass beads were added to the tube, the air in the tube could not be displaced due to the small diameter of the tube. A layer of air trapped between glass beads and oil phase is seen in fig.5.26a (marked by an arrow). The use of an ultrasonic bath helped proper packing of the glass beads. Upon addition of water solution in the tube, oil was mobilised from the porous media. Due to the low diameter of the tube, oil droplets rising from the porous media faced significant resistance as they moved towards the free oil phase on top (as seen in fig.5.26b). The formation of an oil bank in porous media was observed (marked by arrows in fig.5.26c and fig.5.26d). The oil bank grew bigger and eventually escaped from porous media (marked by an arrow in fig.5.26e).

The addition of HCl lowered the pH, and the colour of water phase changed to yellow. There was a limited movement of water in porous media due to the formation of oil bank. The invasion of water in the porous media was a slow process, and the movement of an oil droplet rising from porous media towards free oil phase on top of the tube was hindered by the low diameter of the tube. Oil recovery was calculated to be 18%.

Note: Accuracy in recovery calculations: 10% recovery = 3.3 mm height of oil column in the tube.

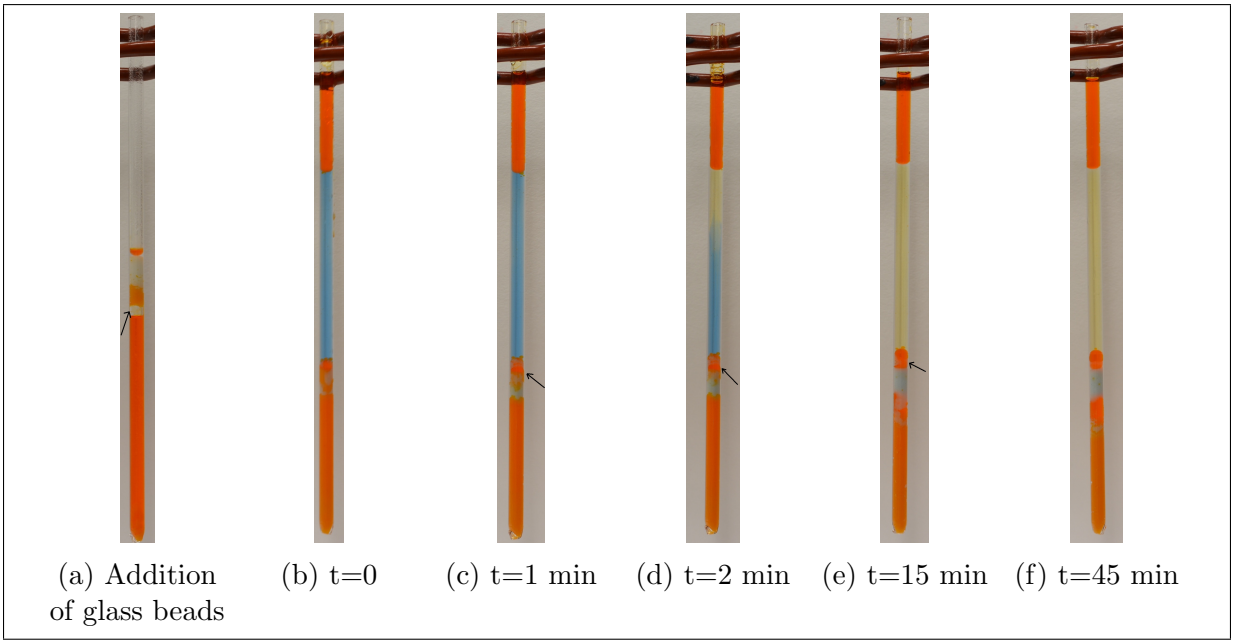

(a) Addition of glass beads (b) t=0 (c) t=1 min (d) t=2 min (e) t=15 min (f) t=45 min

Figure 5.26: Tube test XIII (d=3.75 mm): Low diameter of the tube posed difficulty in packing the porous media. Rising oil droplets in tube faced resistance due to the small diameter of the tube.

5.2.4.4 Conclusions: Tube test by varying the diameter of the tube

Table 5.8 gives an overview of observations in tube test XI-XIII. Operational difficulty means the difficulty in filling the porous media and cleaning the tube at the end of the experiment. It is graded as negligible, intermediate and challenging.

Label	pH of water solution	Tube diameter	Movement of water	Operational difficulty
TT XI	7.66	7.85 mm	Piston-like	Negligible
TT XII	7.68	5.55 mm	Piston-like + along the walls	Intermediate
TT XIII	7.65	3.75 mm	Piston-like	Challenging

Table 5.8: Tube text XI- XIII: Overview of observations.

The following were the conclusions drawn from these tests:

1. As the diameter of tube decreased it was more challenging to fill the porous media in the tube due to less space left for air to escape during packing. The use of an ultrasonic bath provided better packing in each case. This test was a base study for cell tests (Section 5.4).
2. As the diameter of tube decreased, the oil droplets escaping porous media faced more resistance while rising through the tube to reach the free oil phase on top.
3. The movement of water front in the tube of diameter 7.85 mm showed piston-like advancement similar to tube test V where the diameter of the tube was 12.5 mm.
4. In tube test XII, where the diameter of the tube was 5.55 mm shape of water front was piston-like close to entrance of pores and switched to percolation process (movement along the side walls of the tube) downstream of the water-glass beads interface.
5. Due to the small internal diameter of the tube in test XIII, the oil escaping the porous media could not move towards the free oil phase on top of the tube. Further testing in cells will provide more information about the water front movement.

5.3 Tests in a larger tube with CO_2 injection at low pressure (10 bar)

In these experiments, CO_2 injection was carried out at 10 bar and the movement of CO_2 in the water phase was studied. Experiments were also conducted on the oil-water system in varying porous media. *Note*: The term 'high pH water' used in this section refers to water phase which has not reacted with CO_2.

5.3.1 Larger tube test I: CO_2 injection with water phase in the tube

Upon initiation of CO_2 injection in the tube, a reaction of CO_2 and water stuck on walls of the tube (during water solution injection) instantly formed low pH water which was observed as a thin yellow layer on top of the water phase in the tube (marked by an arrow in fig.5.27b.

Fig.5.27c and fig.5.27d show zoomed in view of the tube where CO_2 moved along the centre of the tube. The colour of the water phase changed to yellow as CO_2 reacted with the water phase and formed carbonated water. Due to the presence of a pH indicator in water phase, a change in colour to yellow indicated the drop in pH below 6. Higher density of carbonated water compared to the water phase, led to downwards movement of carbonated water in the tube. Studies in the literature have stated carbonated water being denser than native brine (Hebach et al., 2004); this test provided visualisation of that fact.

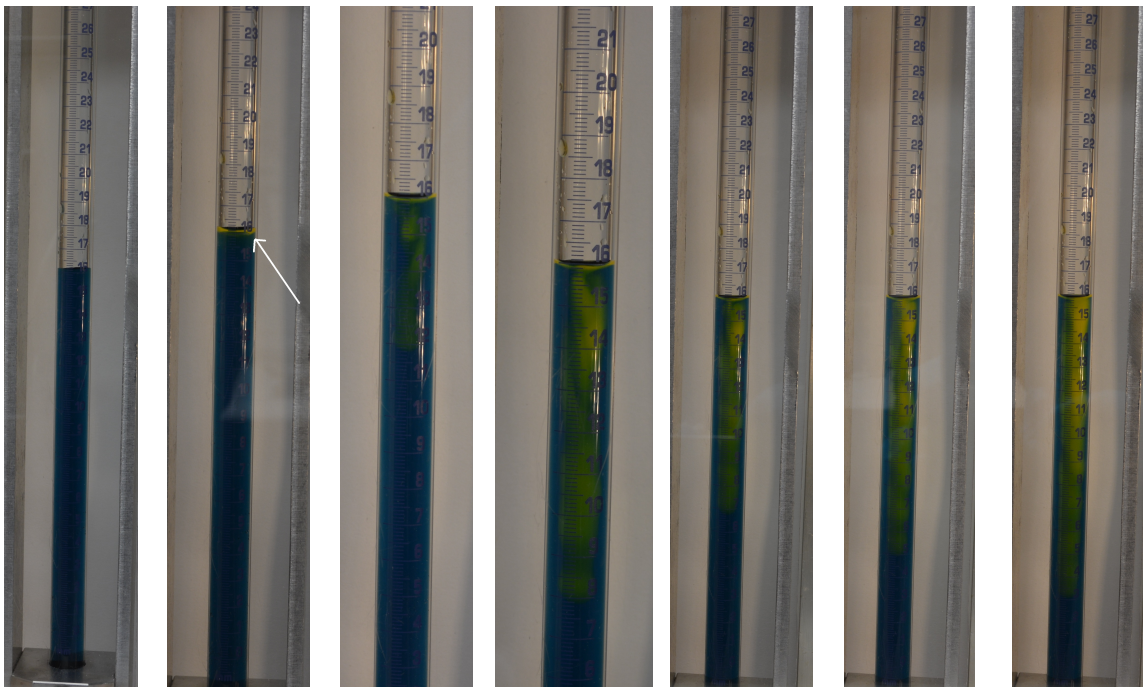

(a) Water phase (b) t=30 sec (c) t=3 min (d) t=3.5 min (e) t=4 min (f) t=4.5 min (g) t=5 min

Figure 5.27: Larger tube test I: CO_2 injection caused an immediate change in colour of water phase from blue to yellow. Movement of CO_2 along the centre of the tube was observed.

Movement of CO_2 in the water phase was a fast process under conditions of this experiment. As seen in fig.5.28b, CO_2 front reached the bottom of the tube 6 minutes after injection started. Movement of the CO_2 front as a finger can be attributed to the difference in viscosities of CO_2 and the water phase.

A study by Carroll et al. (1991) showed the concentration of CO_2 in water at 10 bar injection pressure was 1.21 wt%. This test provided visualisation of the carbonated water formation at a low CO_2 concentration in water.

Once CO_2 front reached the bottom of the tube, it began moving upwards in sort of 'convective' manner and reacted with the remaining high pH water (seen as blue in fig. 5.28c to fig. 5.28f). The time taken by CO_2 to react with all the water phase present in the tube was 11 minutes.

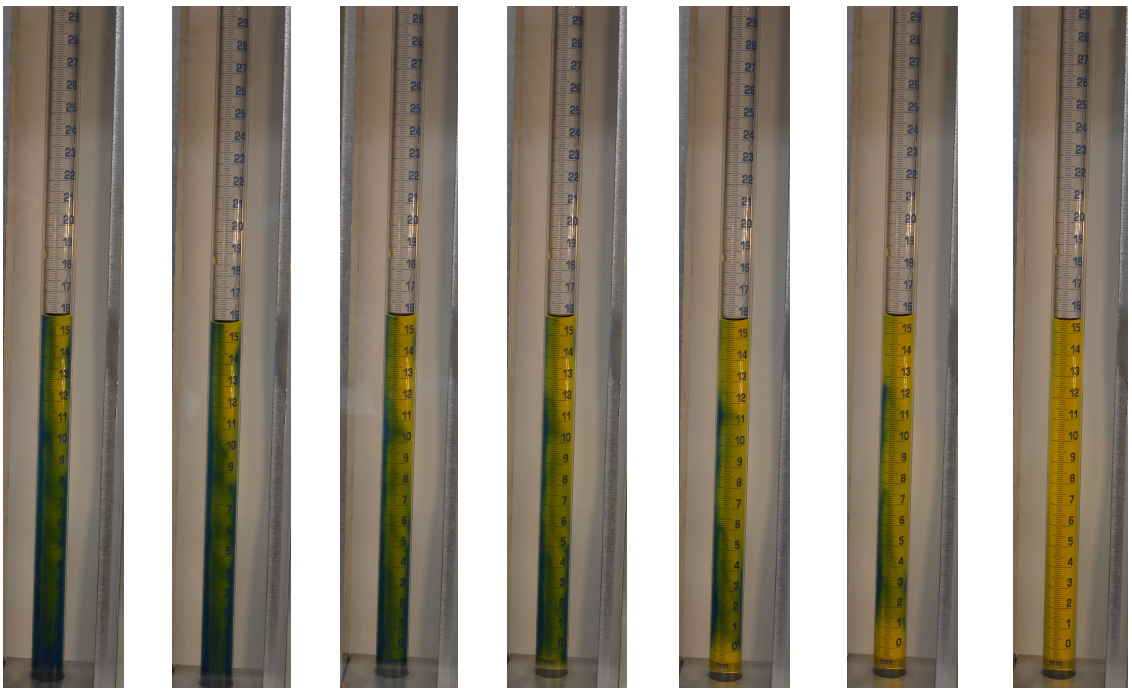

(a) t=5.5 min (b) t=6 min (c) t=7 min (d) t=8 min (e) t=9 min (f) t=10 min (g) t=11 min

Figure 5.28: Larger tube test I: CO_2 reached the bottom of the tube in 6 minutes and moved upwards reacting with high pH water (blue) in the tube.

5.3.2 Larger tube test II: CO_2 injection with a layer of oil on top of the water phase in the tube

This experiment was conducted to observe the effect of an oil layer on the movement of CO_2 in the tube and compare the results from larger tube test I. Similar to larger tube test I, CO_2 reacted immediately with water phase stuck on the walls on the tube and caused a small layer of low pH water (yellow) on top of the water phase (as seen in fig.5.29b).

Presence of the oil phase delayed the movement of CO_2 as it had to pass through the oil phase first before entering the water phase. Fig.5.29c shows the beginning of CO_2 movement in the tube, the colour of water phase changed to yellow upon dissolution of CO_2 indicating a drop in pH below 6.

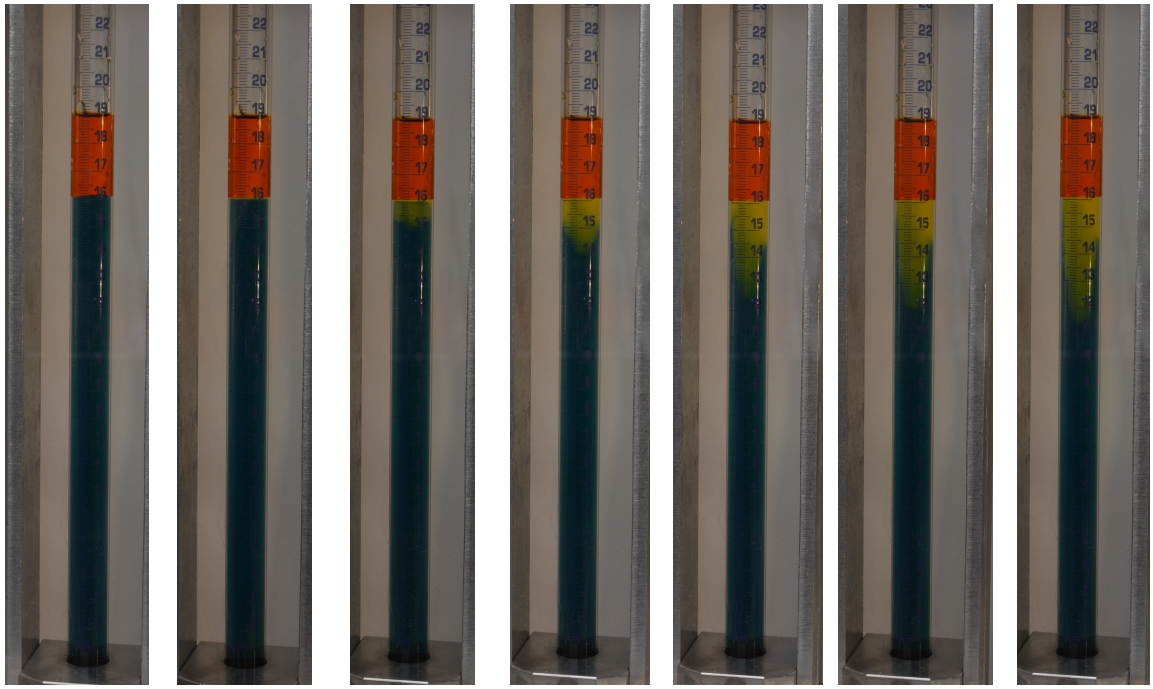

(a) t=0 (b) t=1 min (c) t=3 min (d) t=6 min (e) t=8 min (f) t=10 min (g) t=12 min

Figure 5.29: Larger tube test II: The presence of an oil phase delayed the reaction of CO_2 and water.

As seen in fig.5.30e, CO_2 reached the bottom of the tube in 25 minutes after the start of injection. The shape of the CO_2 front was observed as a finger, similar to the larger tube test I. In this case, the quantity of high pH water (blue) left behind the front was low compared to the previous test (compared in fig.5.28b and fig.5.30d). This was due to the presence of an oil layer on top which delayed movement of CO_2 into the water phase. The delay resulted in the better mixing of CO_2 already present in the water phase.

The time taken for the reaction of CO_2 with all the water phase in the tube was 29 minutes, this was nearly thrice the time it took in larger tube test I.

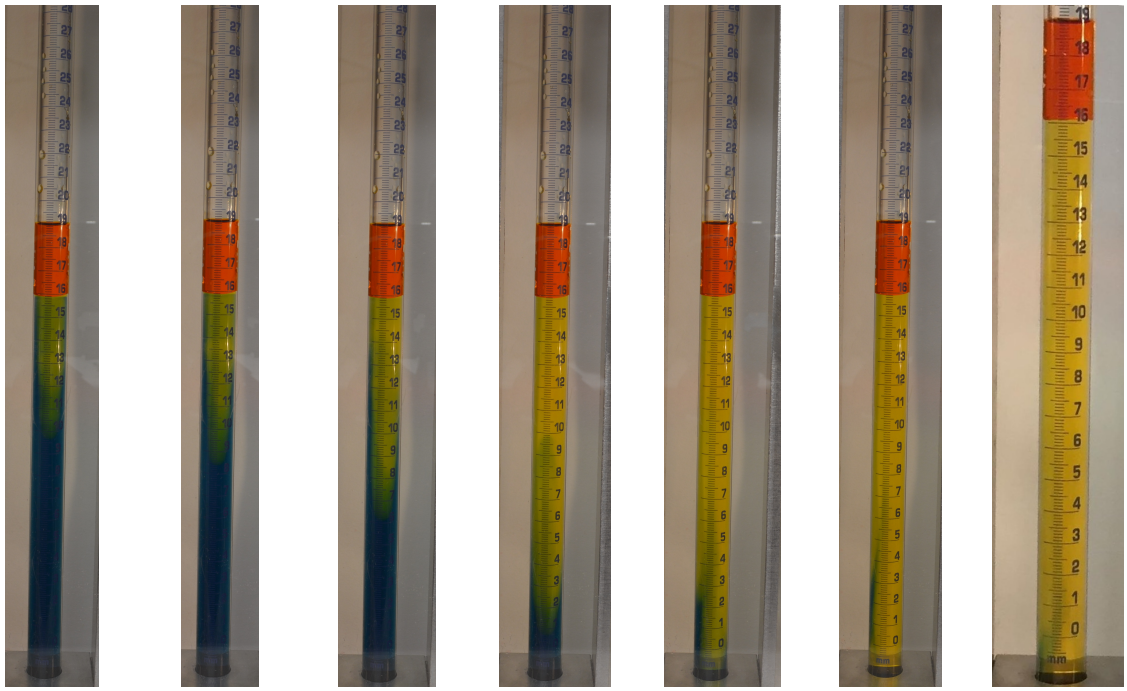

(a) t=14 min (b) t=17 min (c) t=20 min (d) t=23 min (e) t=25 min (f) t=28 min (g) t=29 min

Figure 5.30: Larger tube test II: Less unreacted water phase (blue) was left behind the advancing CO_2 front compared to larger tube test I.

5.3.3 Larger tube test III: CO_2 injection with water present in the porous media

This experiment was conducted to visualise the movement of CO_2 in water-filled porous media. A small amount of water phase was left on top of the glass beads to observe the movement of CO_2 before entering the porous media (fig.5.31b).

CO_2 dissolved completely in the free water phase (in 3 minutes) before moving towards porous media (see fig.5.31d to fig.5.31g). CO_2 movement in the porous media was observed as the colour in porous media changed from blue to white (marked by an arrow in fig.5.31g).

The movement of carbonated water in porous media was a slow process. The experiment continued over the course of 48 hours, and CO_2 rich water invaded less than half the height of porous media. The movement of carbonated water in pores was piston-like as seen in fig.5.32a to fig.5.32g.

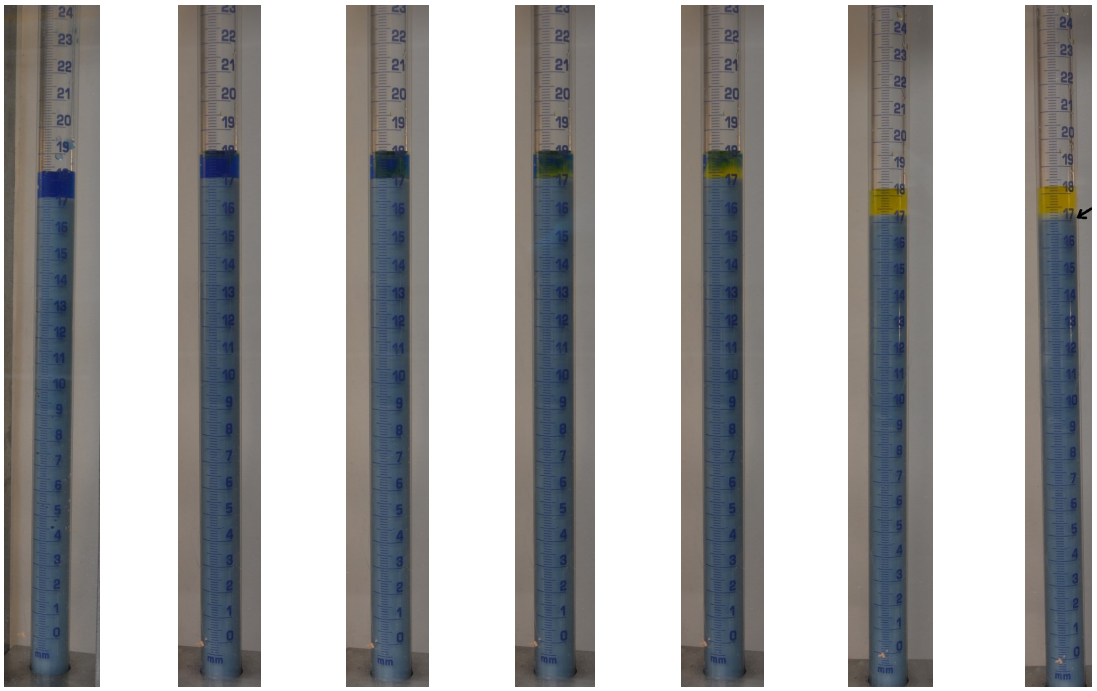

(a) Water phase (b) t=0 (c) t=1 min (d) t=1.5 min (e) t=2 min (f) t=3 min (g) t=20 min

Figure 5.31: Larger tube test III: CO_2 dissolved in the free water phase before moving into the porous media.

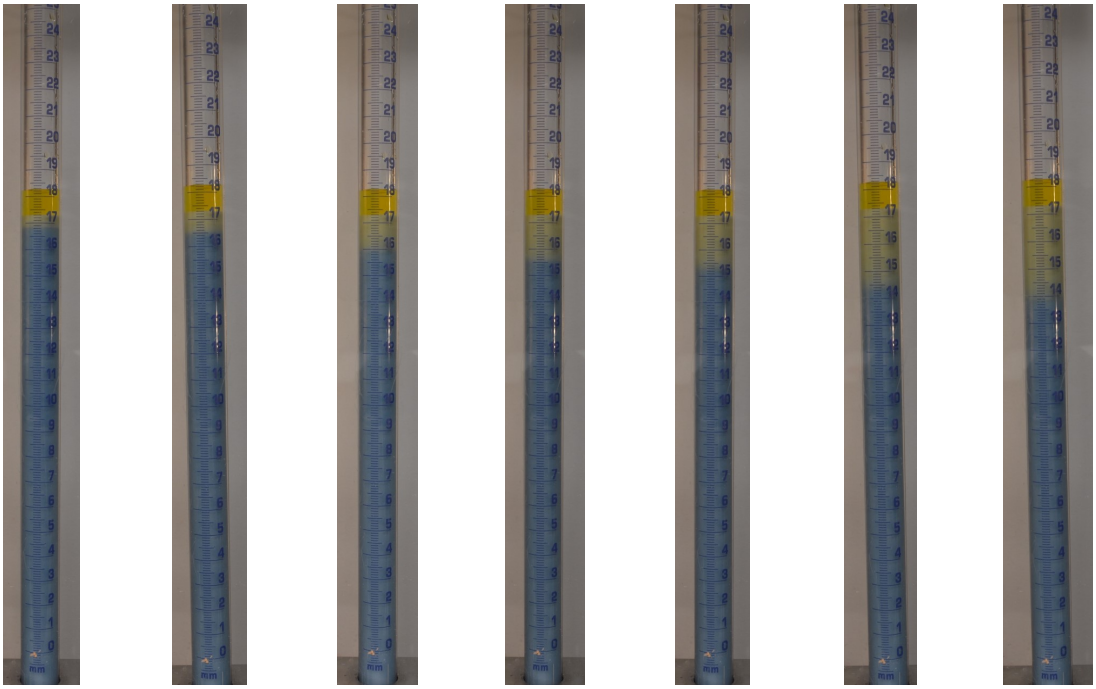

(a) t=1 hour (b) t=2.5 hours (c) t=6.5 hours (d) t=10.5 hours (e) t=12.5 hours (f) t=30.5 hours (g) t=40.5 hours

Figure 5.32: Larger tube test III: Movement of carbonated water in the porous media was a slow piston-like process.

5.3.4 Larger tube test IV: CO_2 injection with oil present in the porous media

This experiment was conducted to observe change in properties of oil phase due to the dissolution of CO_2 and determine the possibility to visualise the movement of CO_2 in the oil phase. Inlet valve to the tube was opened slowly, and CO_2 injection initiated at 10 bar. A small column of oil phase was left on top of glass beads to observe movement in oil level due to the dissolution of CO_2. No visible movement due to CO_2 injection was observed in free oil phase or in the porous media (fig.5.33).

The total time of the experiment was 60 minutes (since initiating CO_2 injection). CO_2 injection at a pressure of 10 bar and 20°C was not enough to visualise any change in properties of oil (e.g.viscosity).

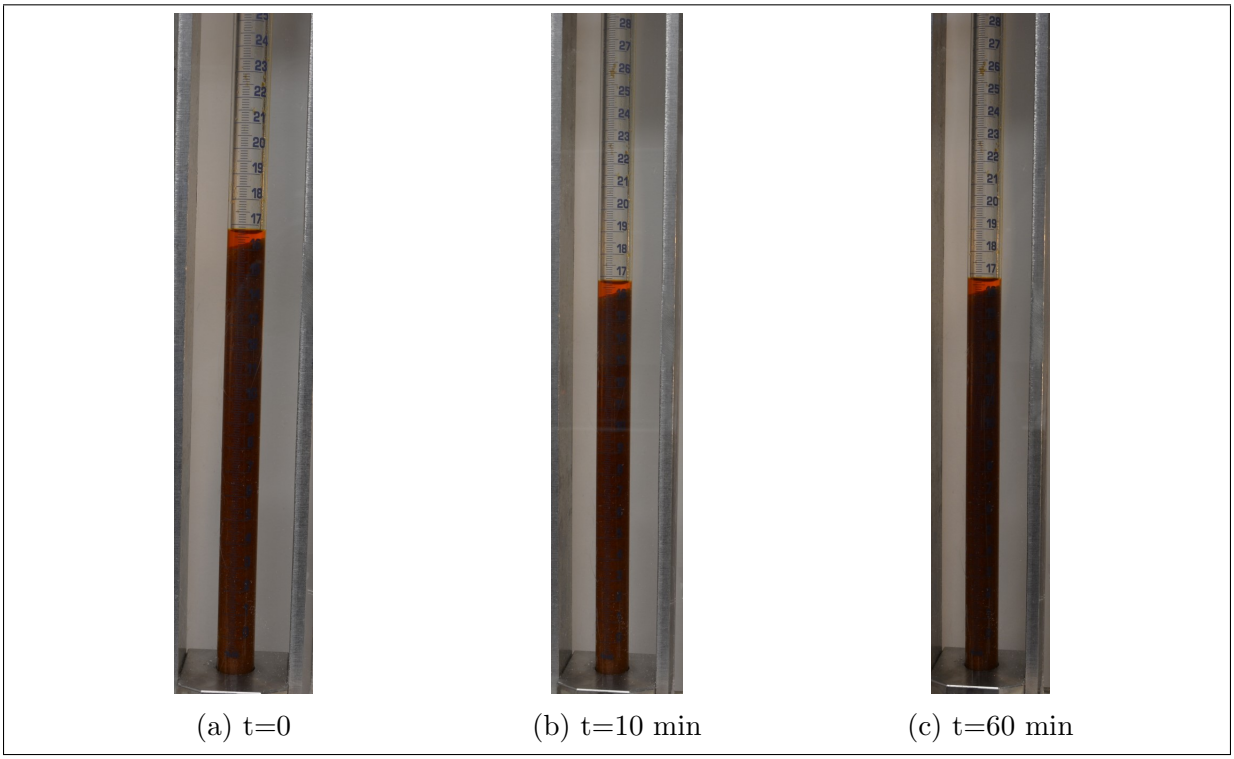

(a) t=0 (b) t=10 min (c) t=60 min

Figure 5.33: Larger tube test IV: CO_2 injection with oil present in the porous media did not show any movement in the oil phase.

5.3.5 Larger tube test V: CO_2 injection with oil-water system in glass beads type C

The aim of the following tests in this section was to study the capacity of CO_2 rich water to mobilise oil from pores and understand imbibition process at constant pressure CO_2 injection. The results are compared with tube tests in porous media type C/D.

The height of tube was much higher compared to the ultrasonic bath, and only 25% of the tube was immersed in the bath. It provided better packing compared to not using an ultrasonic bath.

The oil phase was mobilised from the porous media upon addition of the water solution to the tube. While conducting tube tests a delay of 2 minutes was introduced before addition of HCl to the water phase, this was to account for valve operations and pump settings in this test. It took 1 minute for valve operations before CO_2 injection was initiated in the tube. On starting CO_2 injection, CO_2 moved through oil phase and into the water phase to form carbonated water, causing the pH of the water phase to drop below 6 (fig.5.34d).

An interplay of following factors guided the dissolution CO_2 in the water phase:

1. As the water phase invaded the porous media, oil recovered from porous media accumulated at free oil column on top of the tube. As the free oil column grew in size; the movement of CO_2 in water phase was delayed as CO_2 had to pass through more volume of oil before reaching the water phase. This delayed movement led to a slower conversion of water phase to carbonated water.

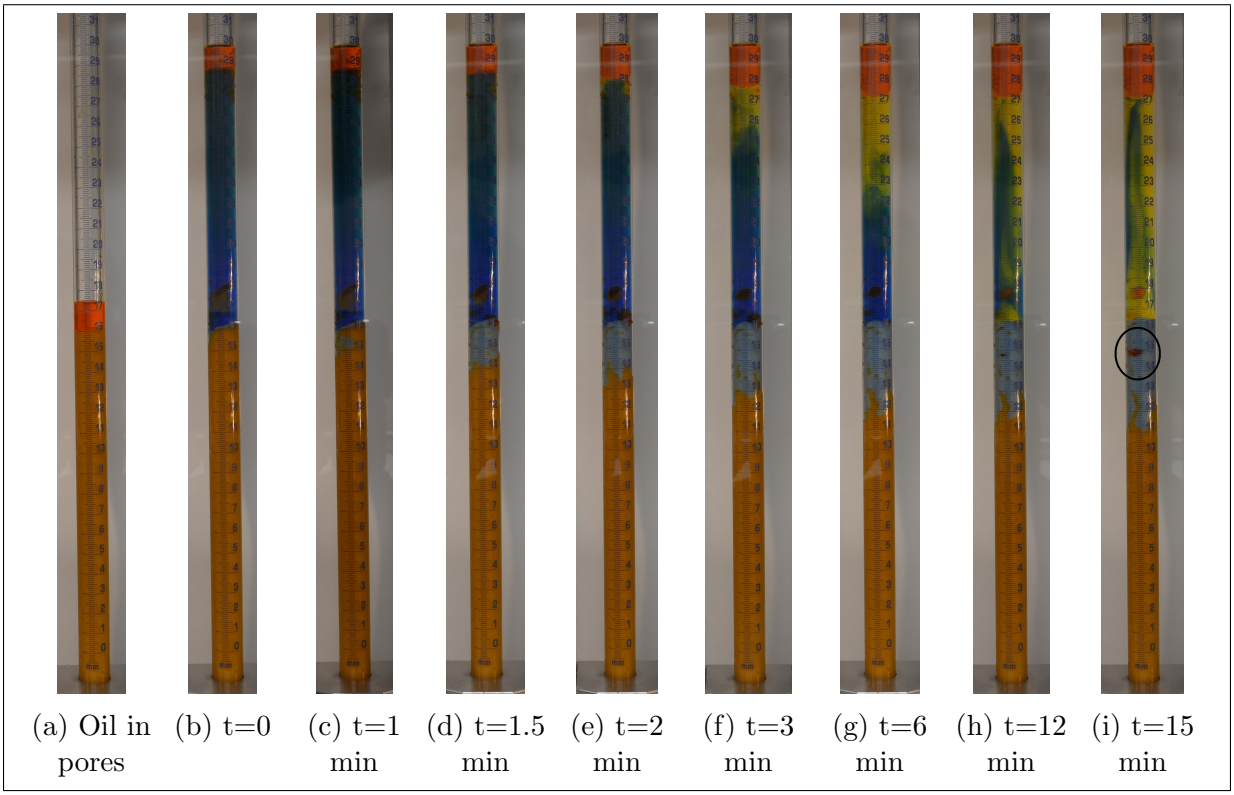

(a) Oil in pores (b) t=0 (c) t=1 min (d) t=1.5 min (e) t=2 min (f) t=3 min (g) t=6 min (h) t=12 min (i) t=15 min

Figure 5.34: Larger tube test V: Movement of CO_2 in water phase was an interplay of two factors.

2. The oil phase escaping the porous media moved as rising oil droplets in the tube. As an oil drop escaped from the porous media and moved through the water phase

into the free oil column on top, turbulence caused by its movement through the water phase provided mixing of CO_2 and the water phase. This process accelerated the formation of carbonated water. The disturbance caused by rising oil droplets was the reason a finger like CO_2 front was not observed in the center of the tube (fig.5.34h and fig.5.34i).

Seen in fig.5.34i (marked by a black circle), was the beginning of oil bank formation in porous media. It took 17 minutes for complete dissolution of CO_2 in the water phase. The oil bank grew as more oil was recovered from the porous media (in fig.5.35). The reason for the growth of oil bank was snap-off of the oil phase in porous media (above the oil bank) already swept by water. As a result of snap-off, the oil phase became discontinuous and could not flow out of the porous media.

The movement of the water front in the porous media was not piston-like and showed an uneven advancement (as marked by an arrow in fig.5.35e). The movement of carbonated water in porous media was piston-like (marked by arrows in fig.5.35f and fig.5.35i) because carbonated water invaded the porous media already swept by high pH water phase.

Appendix A.3 on page 139 explains the recovery calculation procedure for larger tube tests. The recovery factor for this test was 46%.

Note: Accuracy of recovery calculations: 10% recovery ≈ 7 mm height of oil column in the tube.

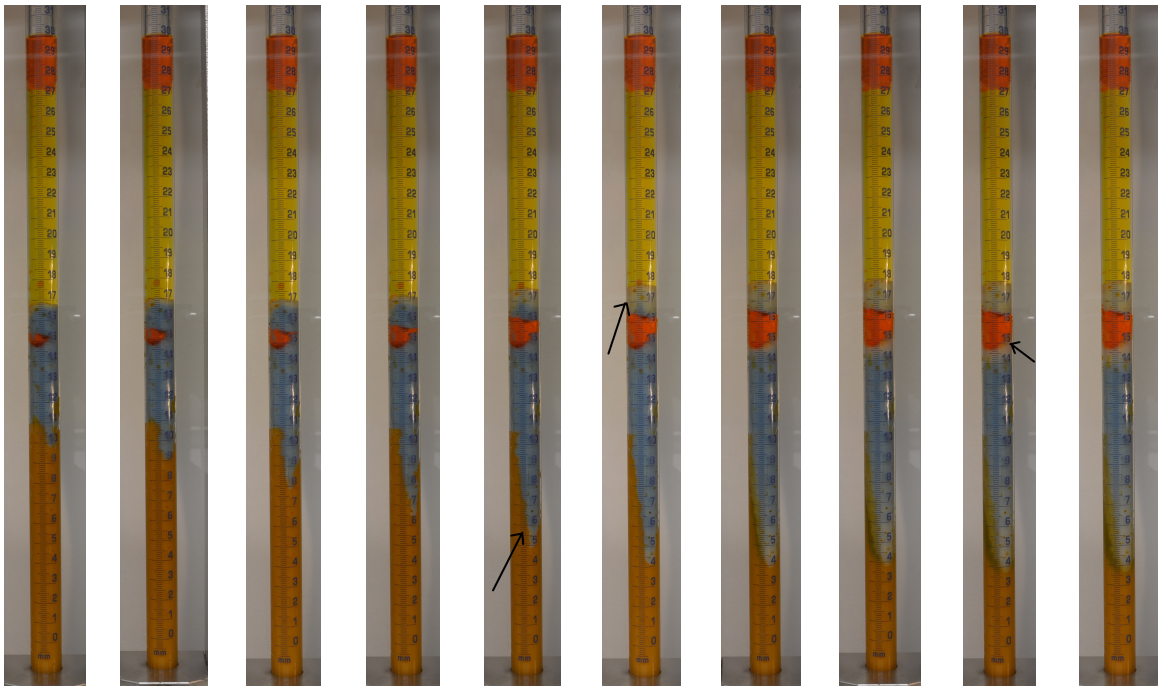

(a) t=19 min (b) t=21 min (c) t=24 min (d) t=27 min (e) t=45 min (f) t=56 min (g) t=387 min (h) t=768 min (i) t=1073 min (j) t=1302 min

Figure 5.35: Larger tube test V: Oil phase discontinuity in pores already swept by the water phase caused a formation of oil bank inside the porous media.

5.3.6 Larger tube test VI: CO_2 injection with oil-water system in acid washed glass beads type C

The oil phase was mobilised from the porous media upon addition of the water solution to the tube. CO_2 moved through the oil phase and into the water phase to form carbonated water and lower the pH of the water phase below 6 (fig. 5.36c). Oil escaping the porous media accelerated the dissolution of CO_2 in the water phase. The time required for complete dissolution of CO_2 into water phase was 18 minutes.

The height of the larger tube prevented it from being completely immersed in the ultrasonic bath, which might have caused the porous media on the bottom to be more densely packed compared to that on the top. As a result, the movement of water in porous media was not piston-like (seen from fig.5.36c and fig.5.36d), as it moved along the sides of the tube and then swept the pores sideways (as seen in fig.5.36e to fig.5.36i). The oil recovered from the porous media moved towards the free oil column on top of the tube. This oil column was seen growing in size from fig.5.36b to fig.5.36i.

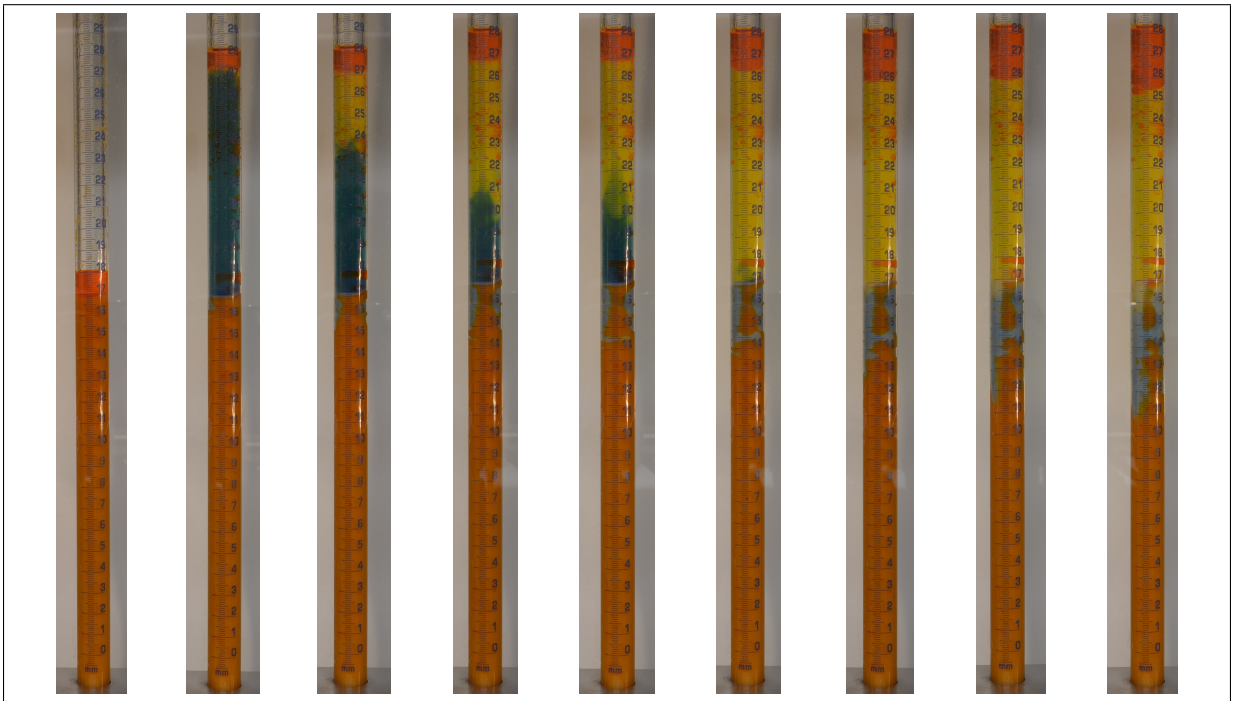

(a) Oil phase (b) t=1 min (c) t=6 min (d) t=12 min (e) t=14min (f) t=18 min (g) t=25 min (h) t=30 min (i) t=42 min

Figure 5.36: Larger tube test VI: Dissolution of CO_2 into the water phase and movement of water phase in the porous media.

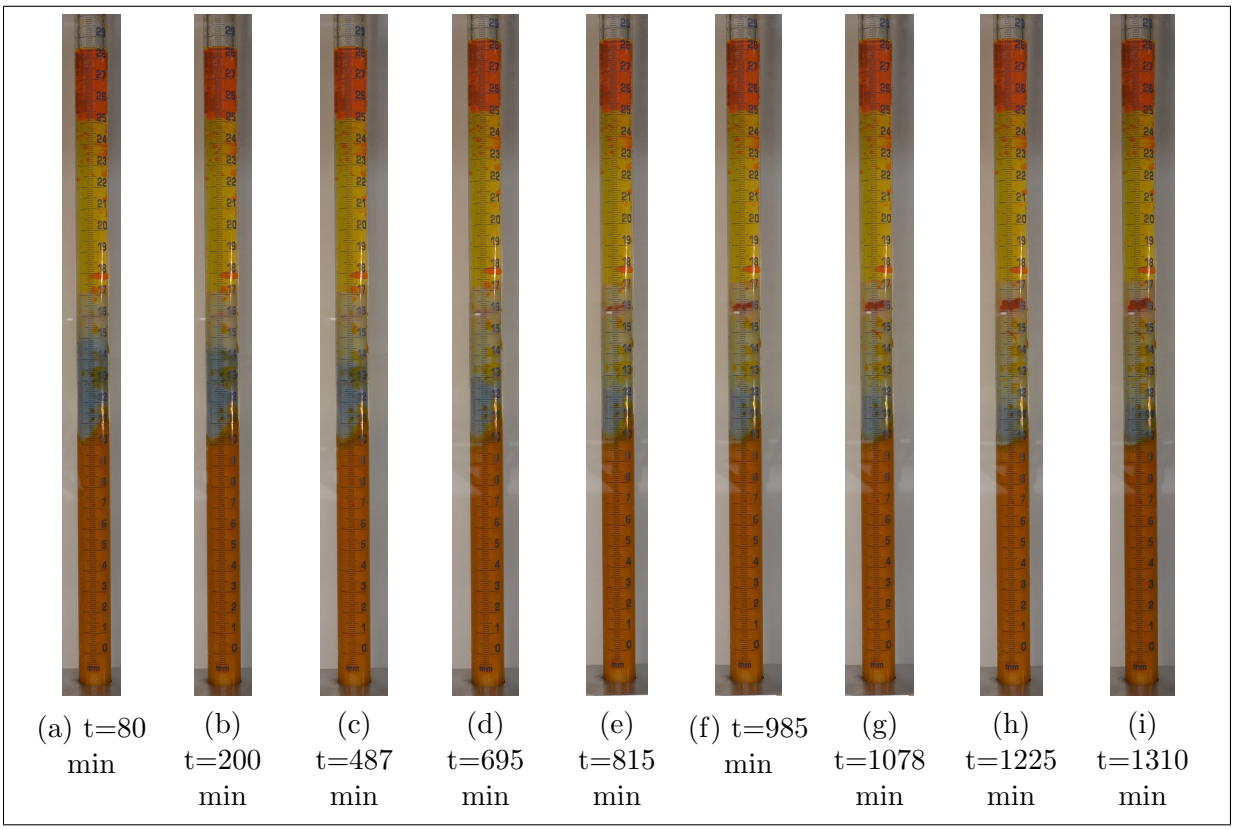

(a) t=80 min (b) t=200 min (c) t=487 min (d) t=695 min (e) t=815 min (f) t=985 min (g) t=1078 min (h) t=1225 min (i) t=1310 min

Figure 5.37: Larger tube test VI: Movement of carbonated water in the porous media and the accumulation of an oil bank in the porous media.

Similar to larger tube test V, the movement of carbonated water in porous media was piston-like. Recovery in this test was estimated to be 28%. Table 5.9 compares the recovery in larger tube test V and VI. Similar to the trend observed during tube tests in glass beads type C and acid-washed glass beads type C (refer to table 5.4 on page 66), recovery in acid-washed glass beads during CO_2 injection was lower compared to non-acid washed glass beads. A possible reason for this is the alteration in surface properties of glass beads (e.g. roughness) during the acid treatment which affects the movement of the water phase in the porous media.

Test label	Recovery (%)
Larger tube test V	46
Larger tube test VI	28

Table 5.9: Comparison between oil recovery in larger tube test V and VI.

Note: Accuracy in recovery calculations: 10% recovery $\approx$ 7 mm height of oil column in the tube.

5.3.7 Larger tube test VII: CO_2 injection with oil-water system in glass beads type D

Upon addition of the water solution to the tube, it began to move along the sides walls of the tube. This is a similar effect as observed in tube test VII (Sub-subsection 5.2.3.3 on page 67). The primary reason for this type of movement was impurities present in the glass beads which result in glass beads not being completely hydrophobic. Hydrophobic glass beads provide resistance to movement of water in the porous media. However, the walls of the tube are water-wet and offer lower resistance. Water movement along the walls of the tube was responsible for oil recovery from pores (seen as droplets escaping porous media in fig.5.38d and fig.5.38f).

When CO_2 injection started, a reaction between CO_2 and water phase led to the formation of carbonated water which appeared yellow in the tube (fig.5.38e).

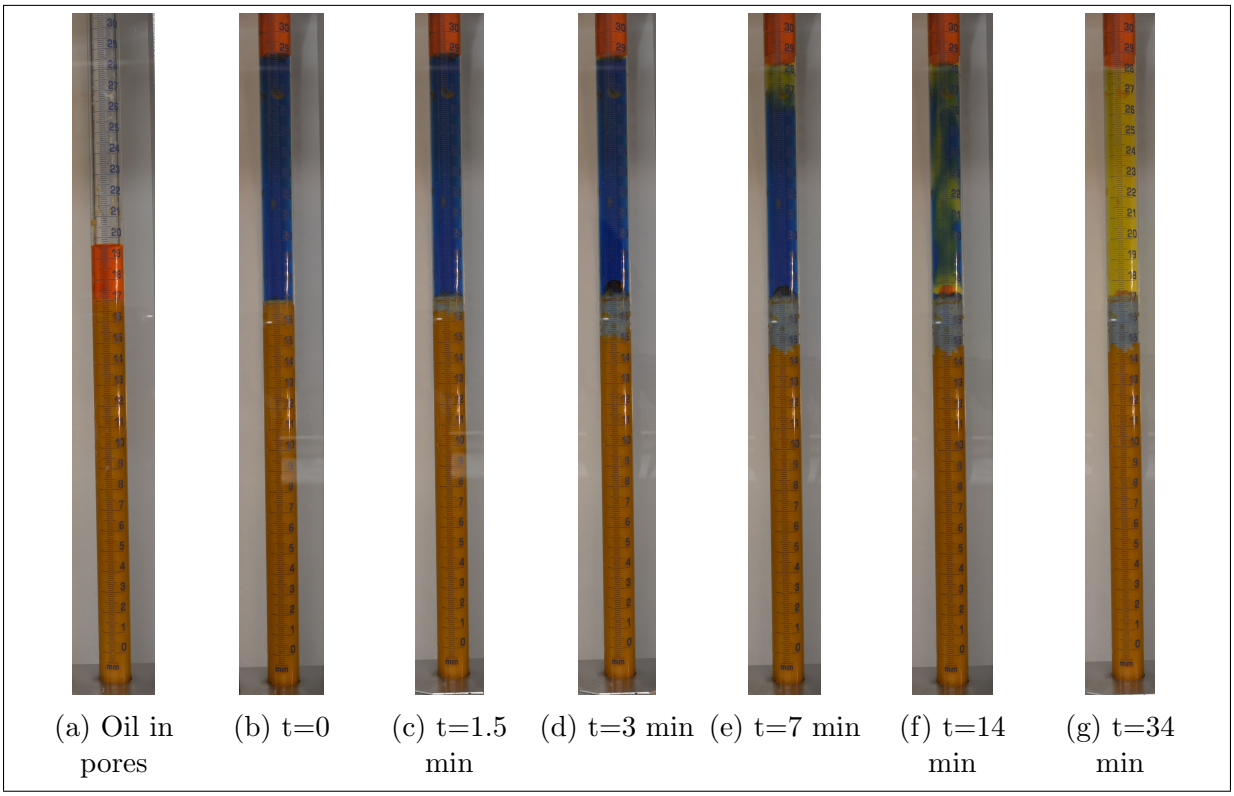

(a) Oil in pores (b) t=0 (c) t=1.5 min (d) t=3 min (e) t=7 min (f) t=14 min (g) t=34 min

Figure 5.38: Larger tube test VII: Movement of water along the walls of the tube due to the low resistance offered by water wet walls of tube compared to hydrophobic porous media.

The time required for complete dissolution of CO_2 into the water phase was 23 minutes. The reason for delayed dissolution compared to previous two tests was because water phase had already invaded majority of porous media (relative to total porous media invaded during the test) before CO_2 injection began. As a result, CO_2 dissolution was not accelerated by mixing caused due to oil droplets moving from porous media to free oil phase on top of the tube.

Movement of carbonated water into the porous media was piston-like (marked by arrows in fig.5.39b and fig.5.39f) and was observed as high pH water (blue) reacted with CO_2 to form carbonated water (seen as decreasing blue shade in pores in fig.5.39). Recovery in this test was calculated to be 7%.

Note: Accuracy in recovery calculations: 10% recovery ≈ 7 mm height of oil column in the tube.

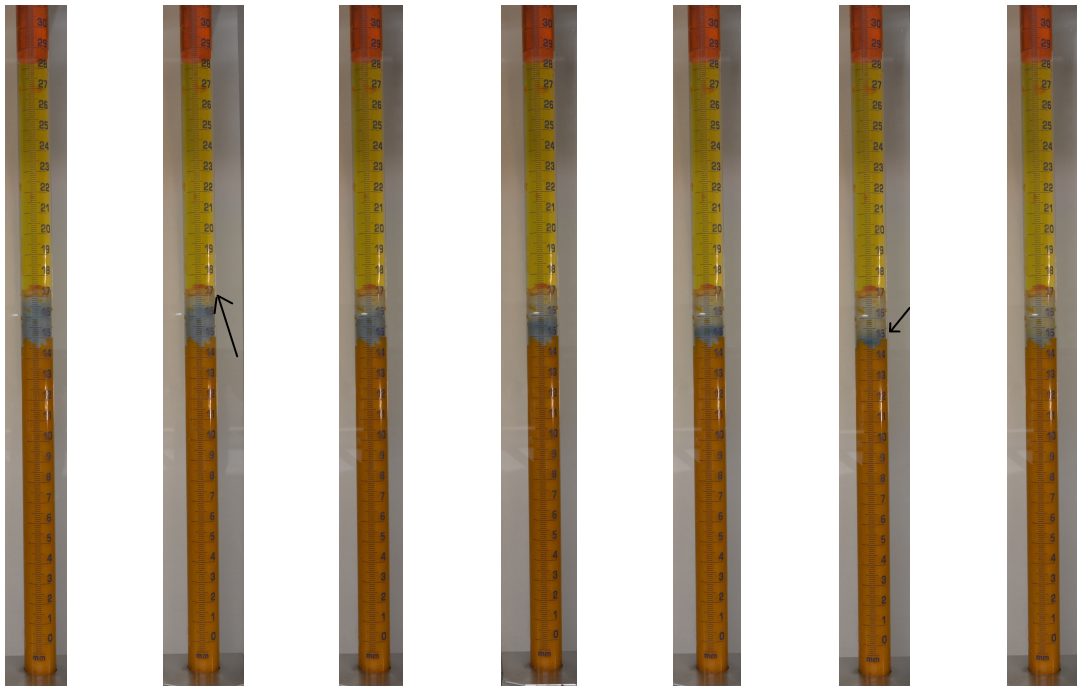

(a) t=160 min (b) t=300 min (c) t=515 min (d) t=665 min (e) t=890 min (f) t=1265 min (g) t=1310 min

Figure 5.39: Larger tube test VII: Movement of carbonated water in the porous media.

5.3.8 Larger tube test VIII: CO_2 injection with oil-water system in acid washed glass beads type D

Upon addition of water solution to the tube, no movement of the water phase was observed in the porous media. This result was similar to observation in tube test with acid-washed glass beads type D. CO_2 moved through the oil phase to react with water phase and form carbonated water (fig.5.40e). Total time required for complete dissolution of CO_2 in water was 25 minutes.

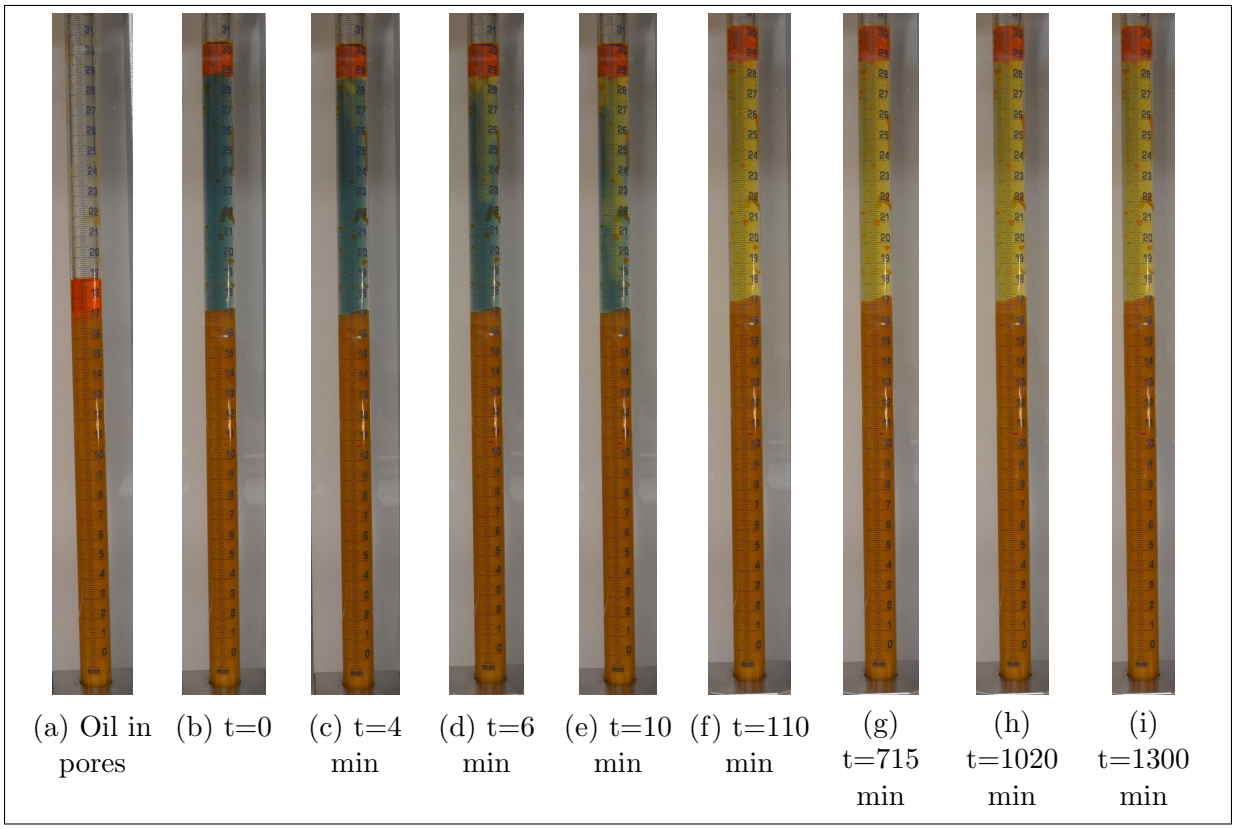

(a) Oil in pores (b) t=0 (c) t=4 min (d) t=6 min (e) t=10 min (f) t=110 min (g) t=715 min (h) t=1020 min (i) t=1300 min

Figure 5.40: Larger tube test VIII: No movement of water in the porous media was observed.

Oil recovery in this test was 0. Table 5.10 compares the oil recovery between larger tube tests VII and VIII. This trend was similar to what was observed in case of tube tests (refer to table 5.5 on page 68).

Test label	Recovery (%)
Larger tube test VII	7
Larger tube test VIII	0

Table 5.10: Comparison between oil recovery in larger tube test VII and VIII.

Note: Accuracy in recovery calculations: 10% recovery $\approx$ 7 mm height of oil column in the tube.

5.3.9 Larger tube test IX: CO_2 injection with oil-water system in mix glass beads (type C+ type D)

Oil was mobilised from the porous media upon addition of water solution to the tube. The dissolution of CO_2 in the water phase was accelerated by oil escaping the porous media towards free oil phase (fig. 5.41e). The time required for complete dissolution of CO_2 into water phase was 19 minutes.

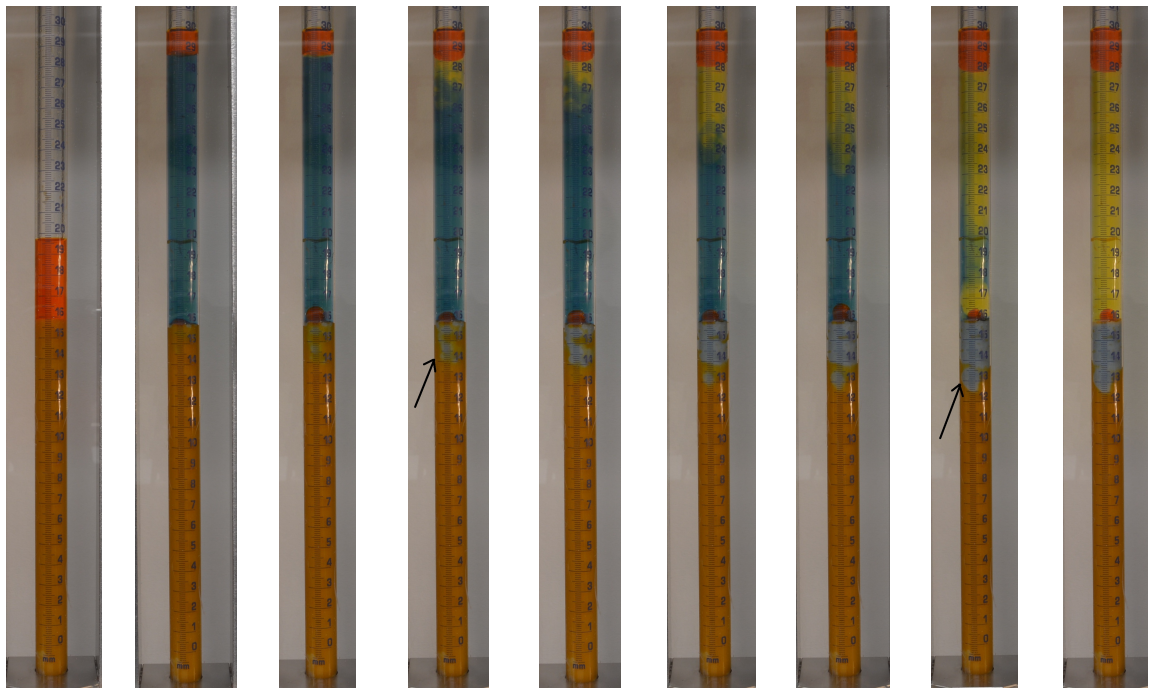

(a) Oil in pores (b) t=0 (c) t=1 min (d) t=2 min (e) t=3 min (f) t=5 min (g) t=6 min (h) t=12 min (i) t=35 min

Figure 5.41: Larger tube test IX: Oil recovery from porous media accelerated the dissolution of CO_2 in water.

Water phase movement into the porous media was not piston-like and fingerlike advancement was observed (marked by arrows in fig.5.41d and fig.5.41h). Oil recovery was noticed by the growth in oil column from fig.5.41b to fig.5.42j.

After complete dissolution of CO_2 in water, the movement of carbonated water in the porous media was piston-like. Oil recovery in this test was 18%.

Note: Accuracy in recovery calculations: 10% recovery $\approx$ 7 mm height of oil column in the tube.

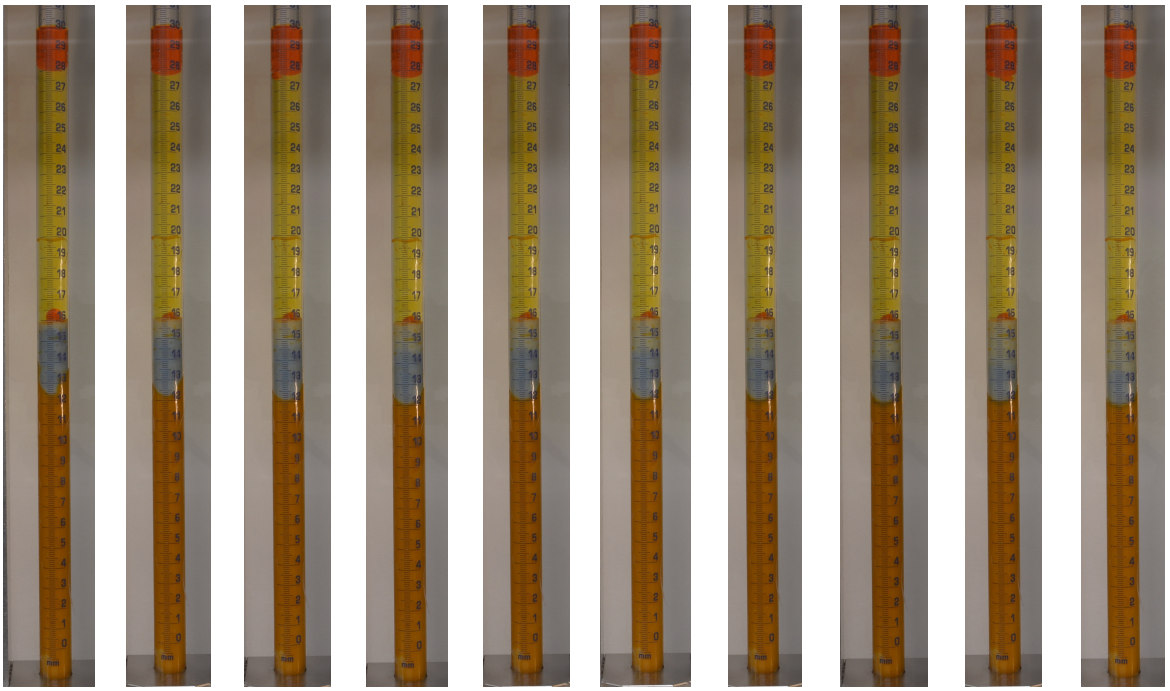

(a) t= 74 min | (b) t=233 min | (c) t=323 min | (d) t=423 min | (e) t=523 min | (f) t=723 min | (g) t=923 min | (h) t=1023 min | (i) t=1173 min | (j) t=1305 min

Figure 5.42: Larger tube test IX: Movement of carbonated water in the porous media.

5.3.10 Larger tube test X: CO_2 injection with oil-water system in mix acid-washed glass beads (type C+ type D)

On adding the water solution to the tube, 2-3 droplets of oil were mobilised from pores (limited movement of water in the porous media can be seen when images are zoomed in fig.5.43). A change in colour of the water phase from blue to yellow indicated the formation of carbonated water due to the dissolution of CO_2 (fig.5.43d). The time required for complete dissolution of CO_2 into water phase was 22 minutes.

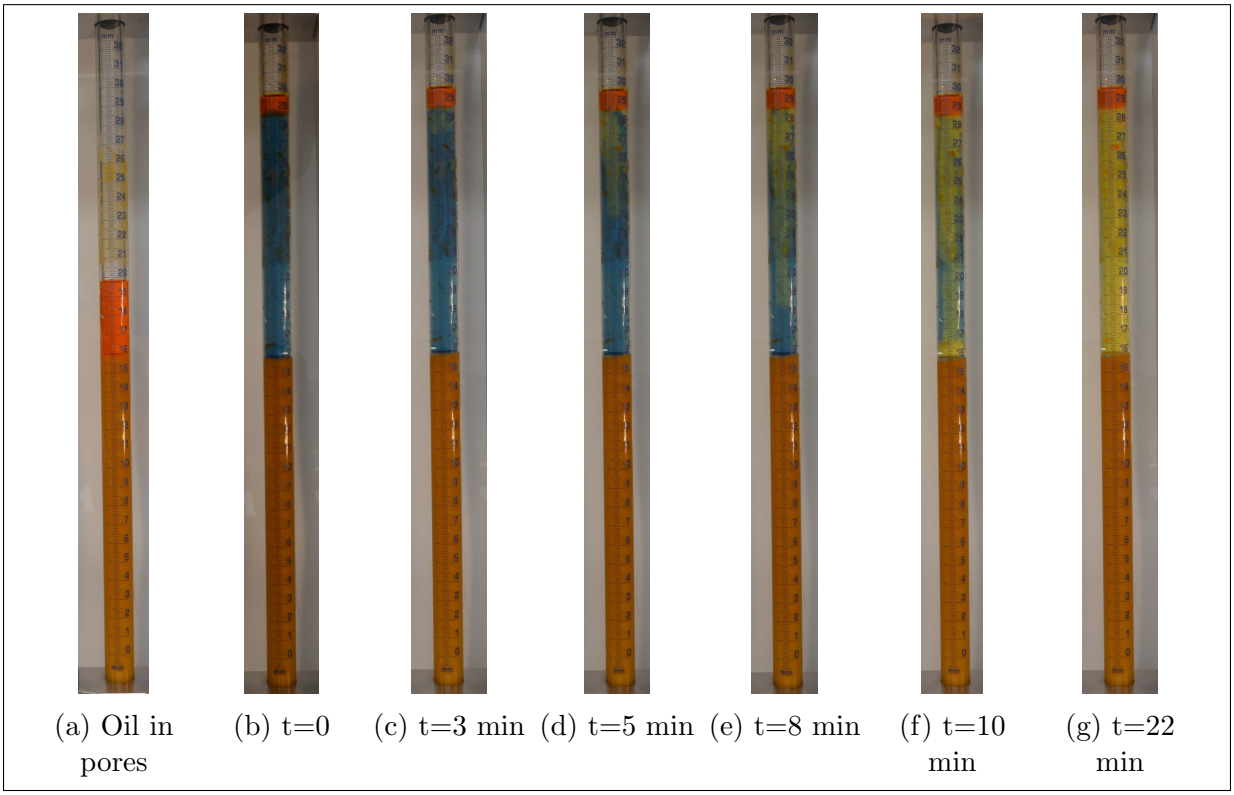

(a) Oil in pores (b) t=0 (c) t=3 min (d) t=5 min (e) t=8 min (f) t=10 min (g) t=22 min

Figure 5.43: Larger tube test X: Dissolution of CO_2 in the water phase.

As seen from the fig.5.44, there was no movement of carbonated water in the porous media. Over the complete course of the test, no additional oil was recovered from the porous media. Oil recovery in this test was 3%. Table 5.11 on the following page compares recovery between larger tube test IX and X. This recovery trend was similar to what was observed in tube test IX and X (refer to table 5.6 on page 70).

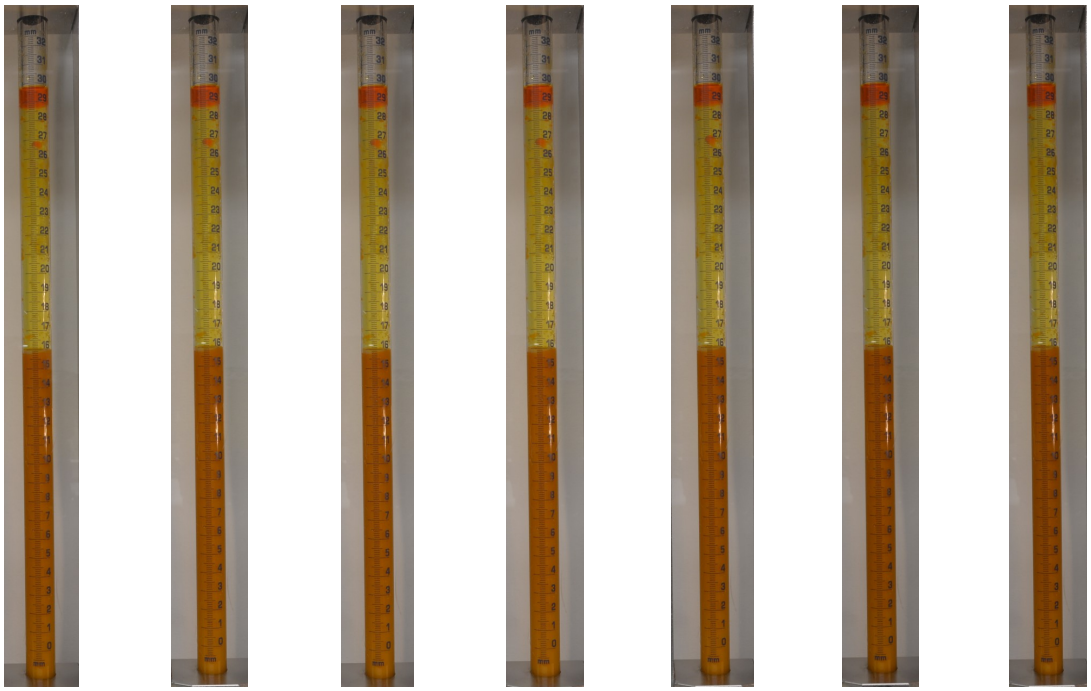

(a) t=30 min (b) t=70 min (c) t=175 min (d) t=340 min (e) t=715 min (f) t=1020 min (g) t=1305 min

Figure 5.44: Larger tube test X: No movement of carbonated water in the porous media was observed.

Test label	Recovery (%)
Larger tube test IX	18
Larger tube test X	3

Table 5.11: Comparison between oil recovery in larger tube test IX and X.

Note: Accuracy in recovery calculations: 10% recovery $\approx$ 7 mm height of oil column in the tube.

5.3.11 Conclusions: Tests with CO_2 injection at 10 bar in larger tube

Low pressure CO_2 injection tests were conducted in a glass tube with the aim of visualising movement of CO_2 in water phase and CO_2 rich water in the porous media of varying types. Oil recovery was estimated and compared with tube tests in porous media type C/D (Sub-subsection 5.2.3.7 on page 71). The following conclusions were drawn from this test:

Label	Time to reach bottom of the tube	Total time to react with water
LT I	6 min	11 min
LT II	25 min	29 min

Table 5.12: Larger tube test I & II: Overview of observations.

1. The presence of an oil column on top of the water phase delayed the dissolution of CO_2 in water, this was observed by comparing the time taken to react with all the water present in the tube in both tests (table 5.12). The delayed dissolution of CO_2 provided better mixing of CO_2 and water phase which is observed in LT II as a small difference in time taken by CO_2 to reach the bottom and to react with all the water phase in the tube.

Label	Movement of CO_2 in liquid	Movement of CO_2 in porous media
LT III	Dissolution in 3 minutes.	Slow, piston-like.
LT IV	No movement visualised	No movement visualised

Table 5.13: Larger tube test III & IV: Overview of observations.

2. Movement of CO_2 in water-filled porous media was a slow piston-like process. From LT IV it is inferred that experimental conditions of 10 bar and 20°C are not sufficient to visualise a change in properties of the oil phase (e.g. viscosity) due to the dissolution of CO_2.

Label	pH of water solution	Porous media	Movement of water phase	Recovery (%)	CO_2 dissolution time
LT V	7.7	Type C	Uneven, non-piston like	46	17 min
LT VI	7.65	Acid-washed type C	Non-piston like	28	18 min
LT VII	7.66	Type D	Walls of tube	7	23 min
LT VIII	7.66	Acid-washed type D	No movement	0	25 min
LT IX	7.65	Mix (type C+type D)	Non-piston like	18	19 min
LT X	7.65	Acid-washed mix	Limited movement	3	22 min

Table 5.14: Larger tube test V-X: Overview of observations.

3. Unlike tube tests V-X, the shape of the water front (before CO_2 injection started) in porous media was inconsistent in all the tests. Piston-like movement was not observed, and the reason for that is believed to be the packing of porous media in the tube. Even though an ultrasonic bath was used, the size of the tube was much larger than what could be immersed in the bath; this led to some loosely packed porous media on the top.
4. The time taken for complete dissolution of CO_2 in the water phase decreased as oil recovery increased. This was due to the accelerated mixing provided by oil droplets

leaving porous media and moving towards the free oil phase on top of the tube. Time taken for complete dissolution in LT VII was an exception as the majority of oil was recovered before CO_2 injection began.

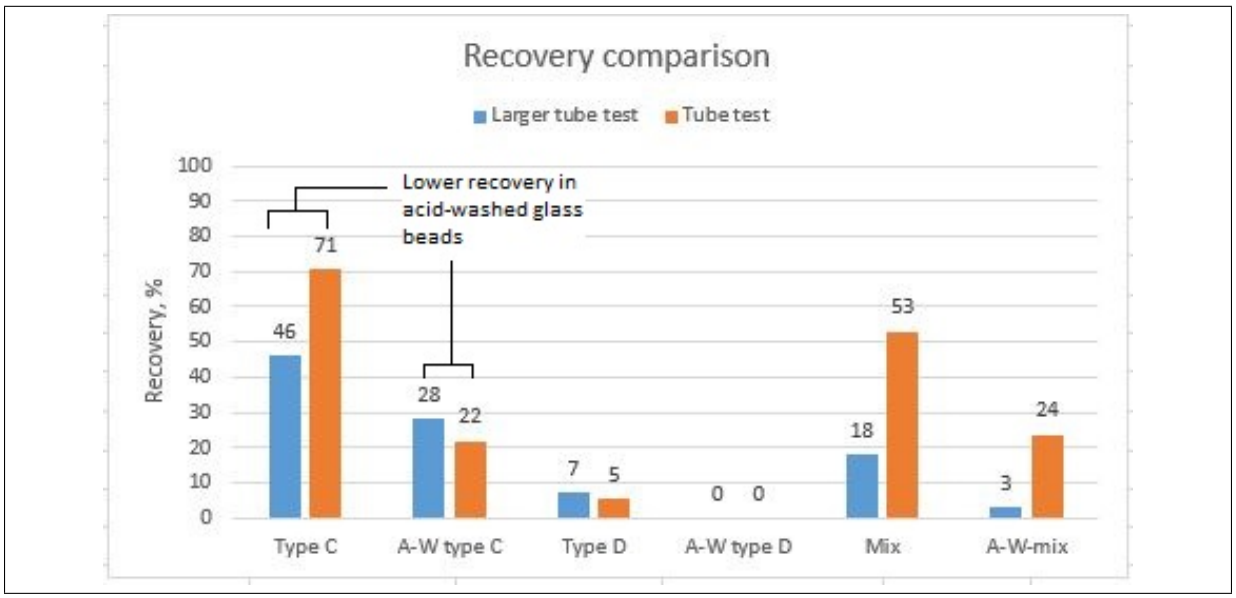

Figure 5.45: Recovery from larger tube tests in porous media type C/D.

Note: Accuracy in recovery calculations for larger tube test: 10% recovery ≈ 7 mm height of oil column in the tube, and for tube tests : 10% recovery ≈ 0.2 mL oil recovered.

5. Fig.5.45 compares the oil recovery with varying porous media types for larger tube tests V-X and tube tests V-X. Similar recovery trend was obtained in tests with and without CO_2 injection when porous media of type C was acid-washed. A decrease in oil recovery is believed to be due to possible alteration in surface properties of glass beads during acid treatment.

6. Mixing glass beads of type C (hydrophilic) and type D (hydrophobic) in LT IX led to decrease in recovery compared to LT V where only type C (hydrophilic) glass beads were used. This was due to porous media becoming partially hydrophobic as a result of mixing. A similar trend was observed in tube test IX ('Mix') and tube test V ('type C').

7. It can be inferred from the different experiments conducted in tubes and a larger tube with CO_2 injection that acid-washing is a possible cause for alteration in surface properties of glass beads (e.g. change in roughness, adsorbtion of oil phase during the tests) and affects the movement of the water phase in porous media.

5.4 Tests in polycarbonate cells

This experiment aimed at studying the effect of varying cell thickness on the front pattern and time taken by water to sweep the porous media filled with oil. 0.1 M HCl was added to mimic pH change due to dissolution of CO_2 in water.

The shape and progress of the front were characteristic of the displacement process. Results from these tests are compared with results obtained in tube test of varying diameter (Subsection 5.2.4 on page 73).

5.4.1 Cell test I: Polycarbonate cell with 3 mm thickness and porous media type B

The use of an ultrasonic bath provided efficient packing of glass beads, and upon settlement of glass beads, a distinct oil-glass beads (O-GB) interface was observed (marked by box in fig.5.46a). The water phase was slowly injected into the cell to avoid disturbance on the glass beads layer (can result in a forced injection of water phase into the porous media) and allow the water phase to move under gravity (fig.5.46b). Water phase started to move instantaneously into the porous media (fig.5.46b) and displacement of oil began. The difference in density of oil and water phases was the primary mechanism of oil recovery.

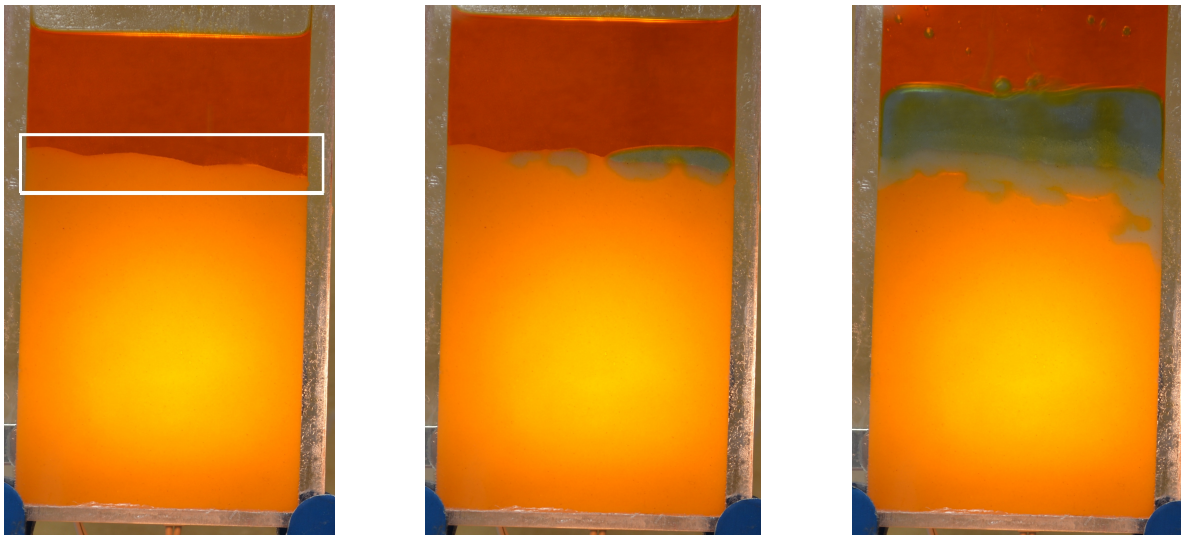

(a) Porous media (b) t=3 sec (c) t=10 sec

Figure 5.46: Cell test I: A distinct oil-glass beads interface was observed after the settlement of glass beads. Immediate movement of water phase into porous media was observed.

Formation of minor finger-like pattern was seen as water phase invaded the porous media (fig.5.47a and fig.5.47b). A possible reason for this was the resistance offered by upwards movement of the oil phase, escaping the porous media and moving towards the free oil phase on top of the cell. As the water phase invaded more section of the porous media, the shape of water front became piston-like (fig.5.47c). The displacement of oil was a quick process (based on the height of cell invaded by water), and upwards movement in the form of oil droplets was clearly observed (fig.5.47).

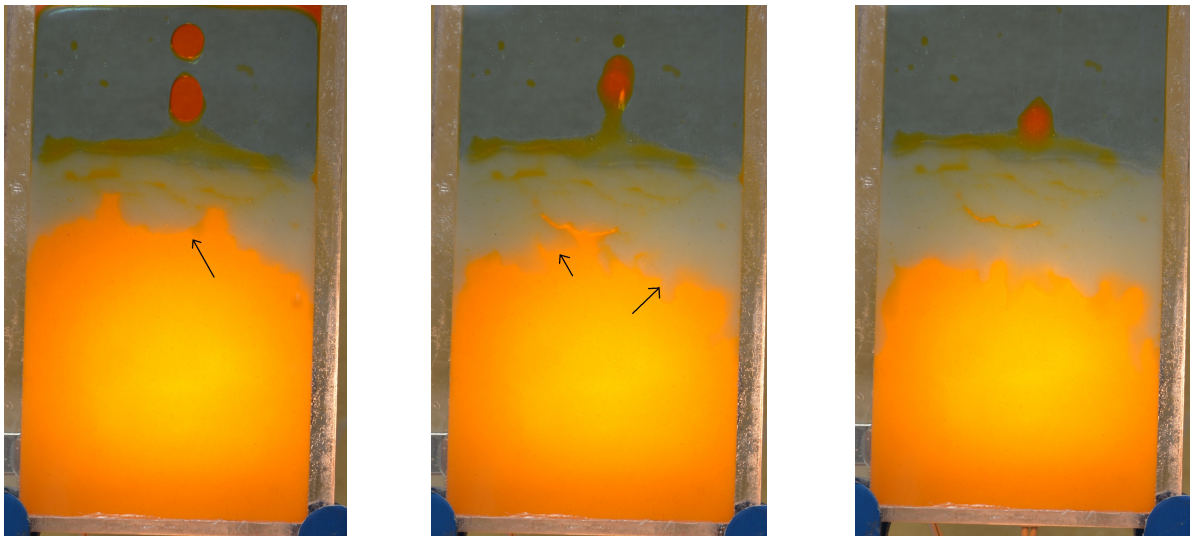

(a) t=1 min (b) t=2 min (c) t=3 min

Figure 5.47: Cell test I: The movement of water phase was piston-like in the porous media.

After 5 minutes, the water phase started to move along the boundaries of the cell (seen in fig.5.48a). Similar to tube test XII (Sub-subsection 5.2.4.2), the movement of the water phase in the porous media was a crossover between piston-like displacement and movement along the edges of the cell. As a result of more even sweep in the beginning, the time taken by water phase to reach the bottom of the cell was 16 minutes (fig.5.48c).

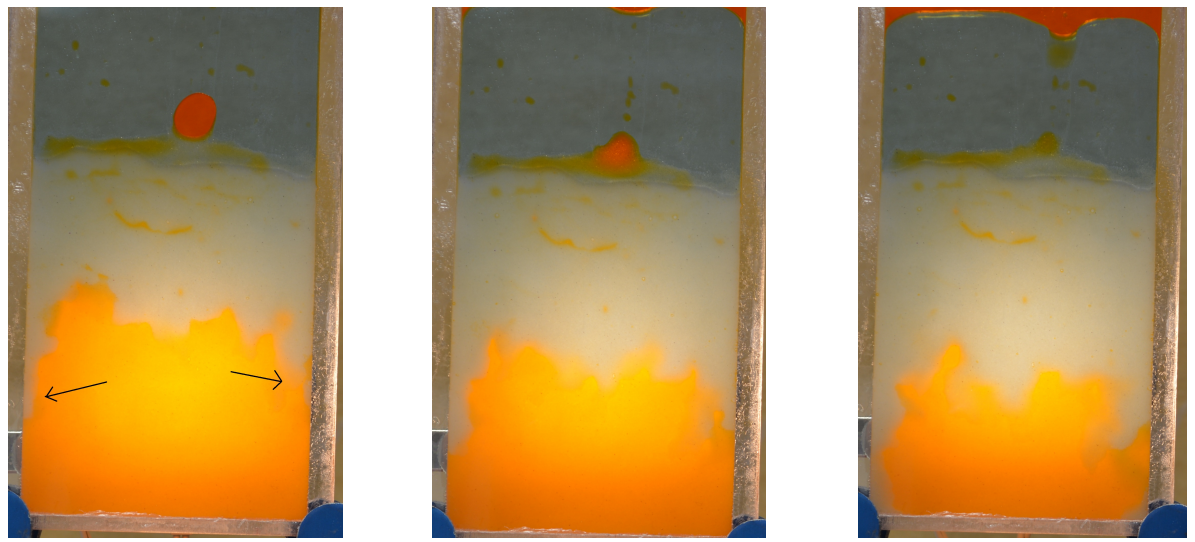

(a) t=6 min (b) t=10 min (c) t=16 min

Figure 5.48: Cell test I: Movement of water phase along the boundaries of the cell.

HCl was added to the cell, and the resulting change in pH caused the colour of the water phase to change from blue to yellow (fig.5.49b). The change in the pH of water phase was a faster process compared to CO_2 injection in the larger tube tests because HCl was insoluble in the oil phase and passed through it to mix with the water phase. Once the water phase reached the bottom of the cell, it moved along the boundary at the bottom of the cell (fig.5.49b and fig.5.49c) and surrounded a part of porous media filled with oil (marked by circles in fig.5.49c).

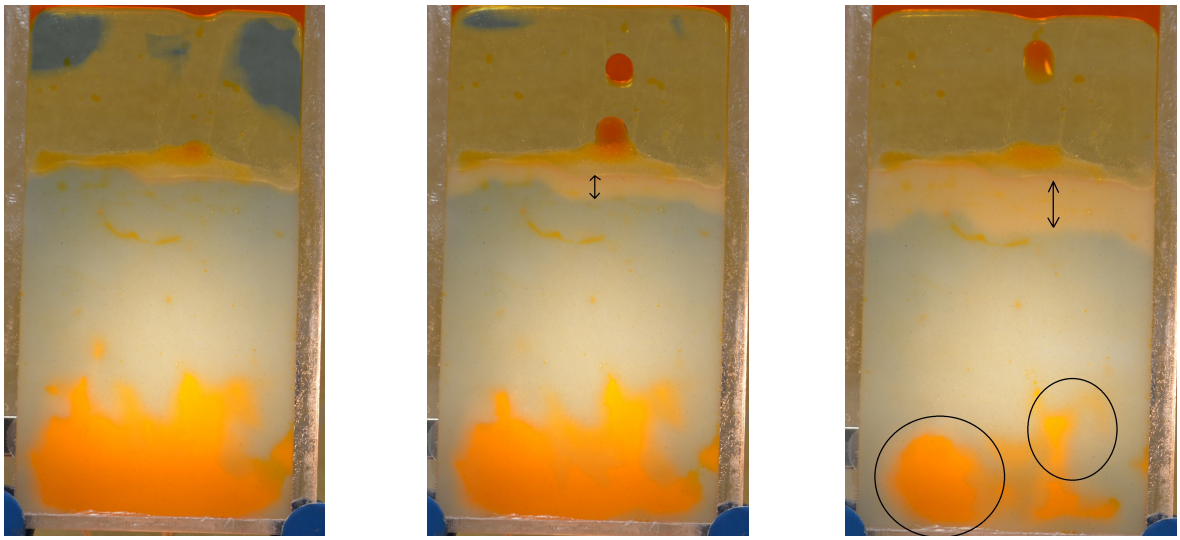

(a) t=23 min (b) t=25 min (c) t=27 min

Figure 5.49: Cell test I: Addition of acid lowered the pH of the water phase and colour changed from blue to yellow.

Oil recovery from the part of porous media surrounded by water phase (fig.5.49c) was a slow process as it took approximately 15 minutes (t=42 -27=15 minutes) to recover a small volume of oil, compared to the amount of oil recovered until t=27 min. The movement of the low pH water (yellow) in the porous media was observed on camera as a change in colour of the porous media from blue to white (fig.5.49 and fig.5.50). At the end of the test, oil trapped in porous media was observed (marked by circles in fig.5.50c).

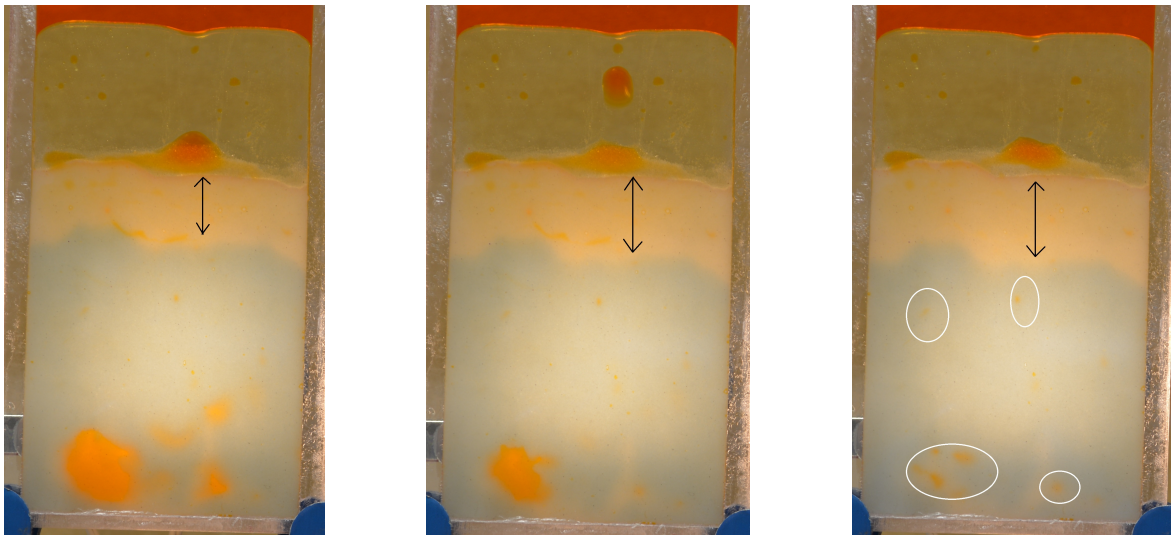

(a) t=32 min (b) t= 37 min (c) t=42 min

Figure 5.50: Cell test I: Oil trapped in the porous media at the end of the test.

5.4.2 Cell test II: Polycarbonate cell with 5 mm thickness and porous media type B

Note: Cell test II was conducted first, and the methodology for placement of light source was still being worked. For this reason a light source is visible behind the cell in fig.5.51 and fig.5.52.

A clear oil-glass beads (O-GB) interface was observed upon settlement of glass beads in the ultrasonic bath (marked by box fig.5.51a). Upon addition, the water phase started to move instantaneously into the porous media mobilising oil from the porous media (fig. 5.51b).

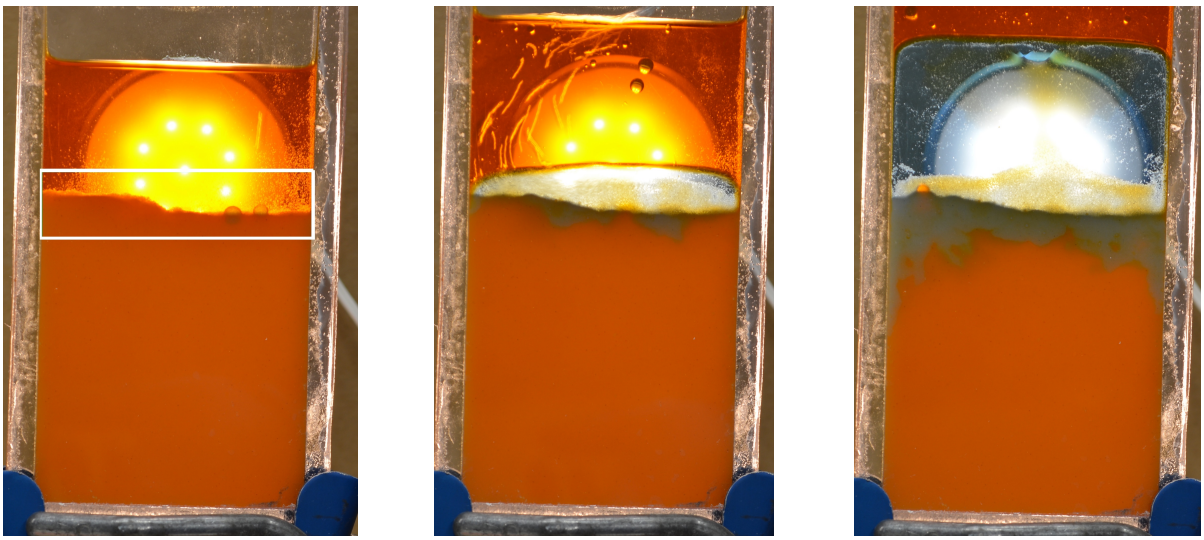

(a) Porous media (b) t=3 sec (c) t=30 sec

Figure 5.51: Cell test II: Water phase began invading the porous media immediately after being added to the cell.

The water phase moved along the boundaries of the cell as marked by arrows in fig.5.52a. This effect was similar to observations made by researchers at University of Alberta (Hatiboglu & Babadagli, 2005). One possible reason for the development of fluid front along the sides of the cell was the lower resistance existing on the boundaries as compared to the center, based on pressure distribution in the cell. A similar effect was also observed by Dastyari et al. (2005) in their work on etched micromodels. A detailed discussion based on this phenomena is presented later in this thesis (Subsection 5.4.4). The movement of water phase was characterised by the development of small fingers as shown in fig.5.52b.

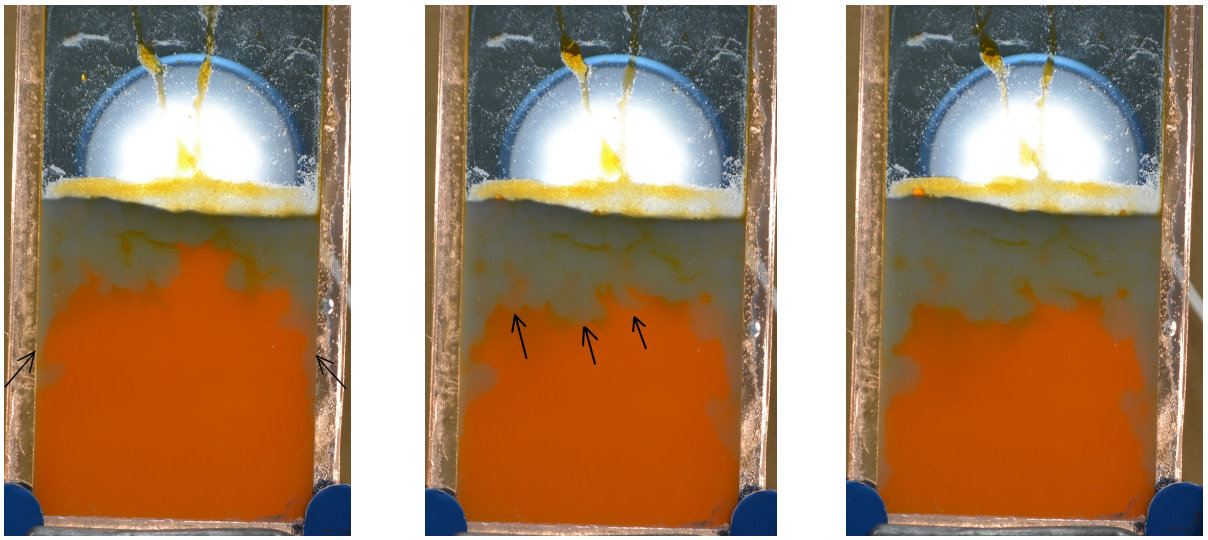

(a) t=1 min (b) t=2 min (c) t=4 min

Figure 5.52: Cell test II: Movement of the water phase was along the edges of the cell.

The time taken to reach the bottom of the cell was 5 minutes (seen in fig.5.53a). Once the water front reached the bottom of the cell, it moved along the bottom boundary of the cell; this effect was similar to what was observed in cell test I. The water phase can be seen moving along the bottom boundary of the cell as marked by arrows in fig.5.53c and fig.5.54.

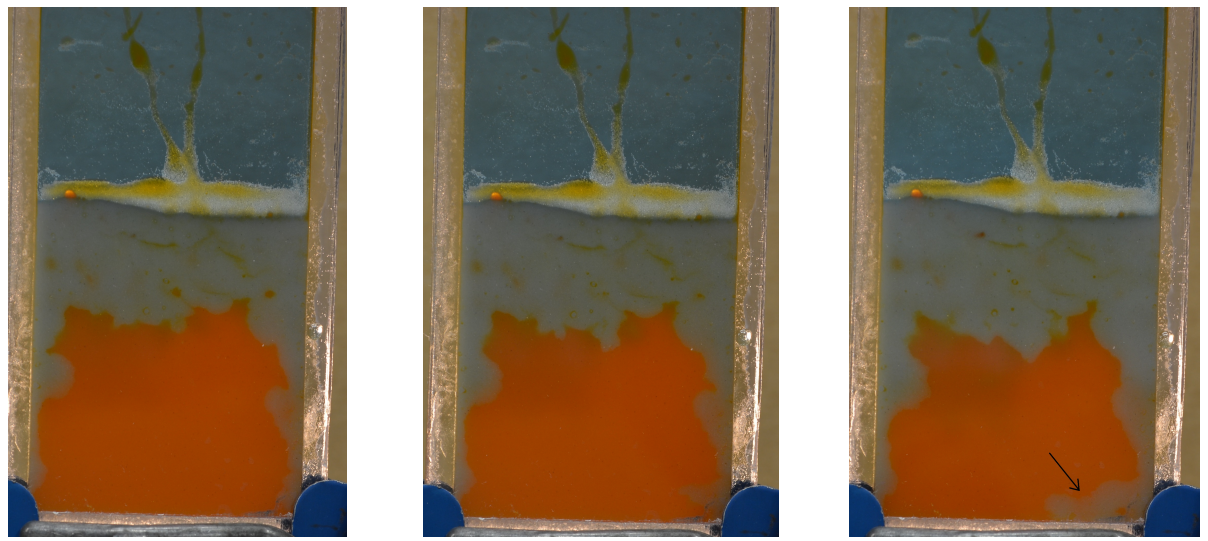

(a) t=5 min (b) t=6 min (c) t=9 min

Figure 5.53: Cell test II: Upon reaching the bottom of the cell, water front begins to move along the bottom boundary of the cell.

Oil mobilisation was a slow process once the water phase covered the bottom boundary of the cell, surrounding a portion of oil-filled porous media. Unswept oil in the porous media was displaced slowly by gravity forces, seen as reducing oil region in fig.5.54, fig.5.55 and fig.5.56. During the introduction of the water solution in the cell, there was a creation of flow channel on cell walls which provided a path for upwards oil movement (marked by arrows in fig.5.54a).

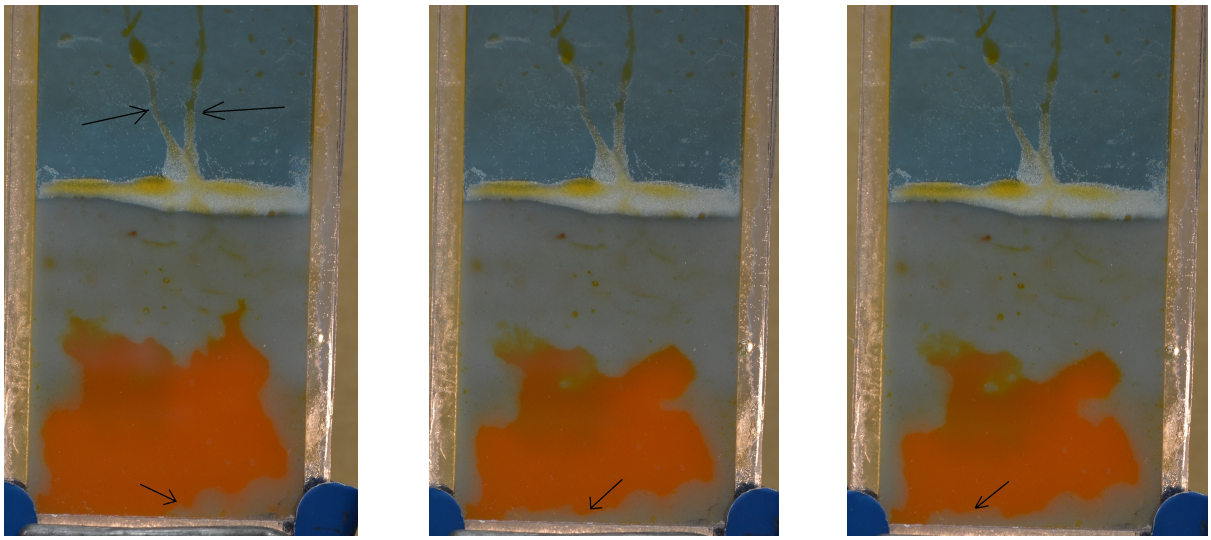

(a) t=11 min (b) t=16 min (c) t=18 min

Figure 5.54: Cell test II: Water phase moving along the bottom boundary of the cell.

Similar to cell test I, the addition of HCl caused a quick change in pH of the water phase as the colour changed from blue to yellow (fig.5.55c).

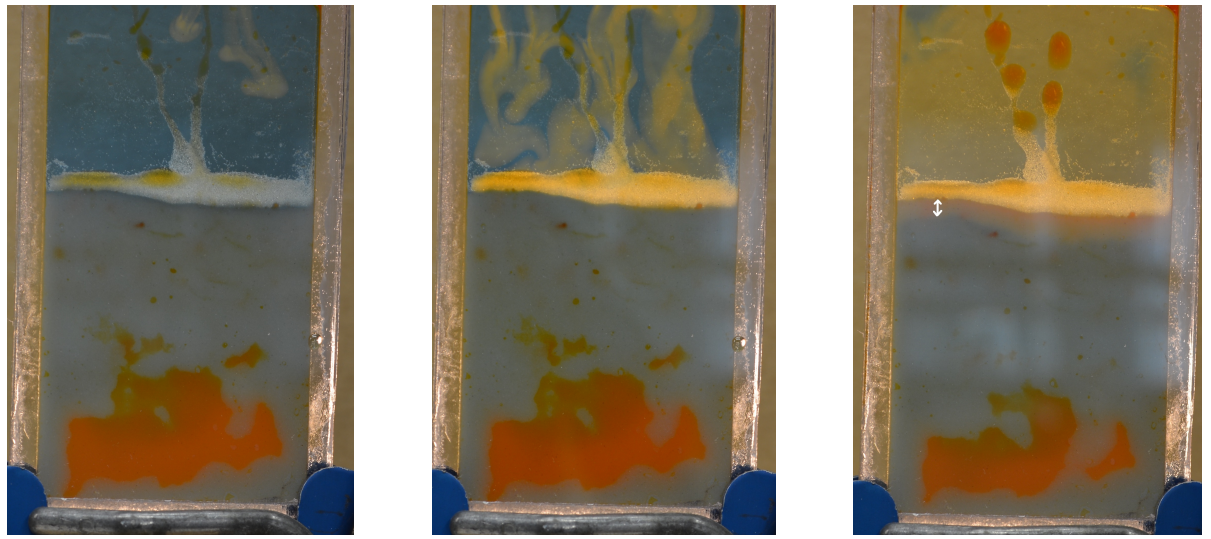

(a) t=26 min (b) t=27 min (c) t=33 min

Figure 5.55: Cell test II: Addition of HCl to the cell changes the colour of water phase from blue to yellow.

The movement of the low pH water (yellow) in porous media was a very slow process. This can be seen marked by double-ended arrows in fig.5.55c and fig.5.56. Oil trapped in porous media upon complete invasion of water phase was observed (marked by circles in fig.5.56c).

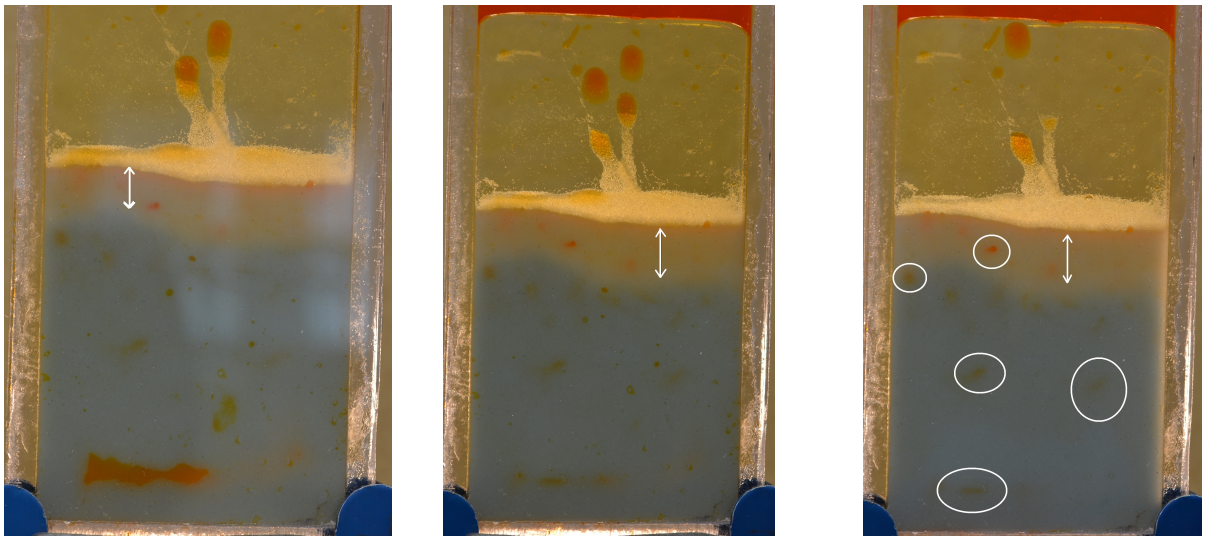

(a) t=49 min (b) t=55 min (c) t= 70 minutes

Figure 5.56: Cell test II: Oil trapped in porous media after water phase invasion is seen marked by circles.

5.4.3 Cell test III: Polycarbonate cell with 8 mm thickness and porous media type B

The use of an ultrasonic bath provided better packing of glass beads, and upon settlement, a clear oil-glass beads (O-GB) interface was observed (marked by box fig.5.57a). The water phase was injected slowly and continuously into the cell (fig.5.57b). Unlike cell test I and II, the water phase movement in the porous media was not instantaneous.

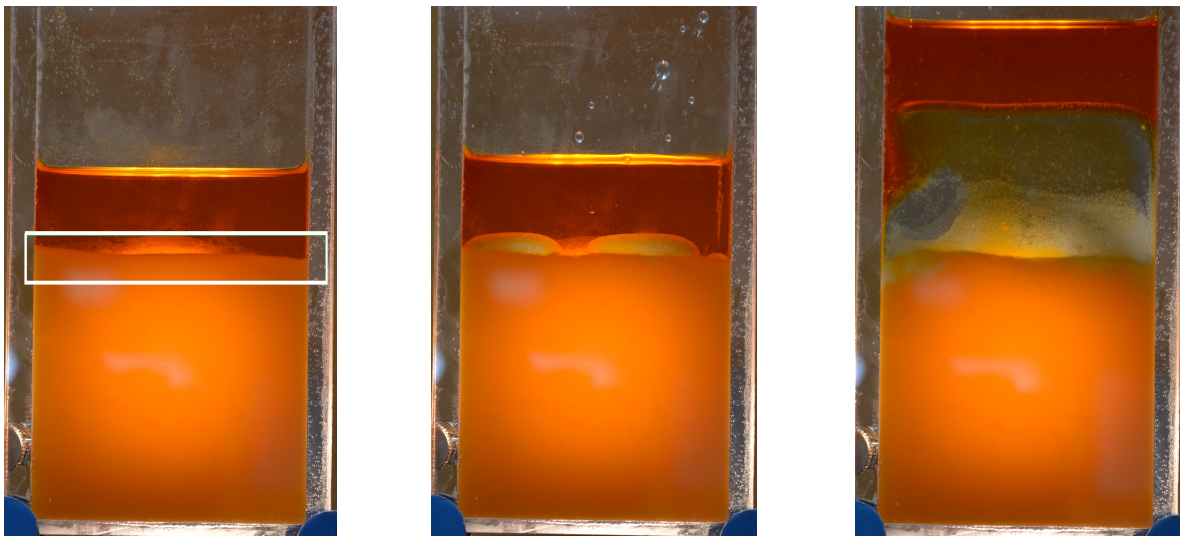

(a) Porous media (b) t=3 sec (c) t=10 sec

Figure 5.57: Cell test III: Movement of water phase into the porous media was not instantneous.

The water phase began moving along the side edges of the cell as shown by arrows in fig.5.58b. Compared to cell test II, the movement along the sides of the cell was more pronounced in this test. The advancement of the water front was also characterised by small fingers as seen in fig.5.58c.

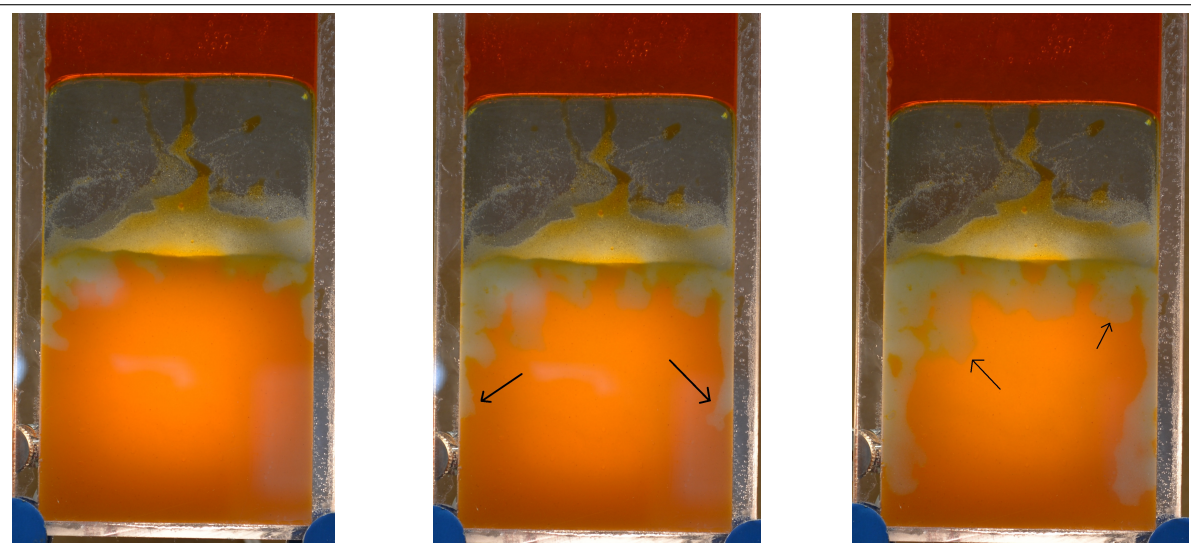

(a) t=2 min (b) t=7 min (c) t=10 min

Figure 5.58: Cell test III: Movement of the water phase along the side edges of the cell was observed.

The time taken by the water phase to reach the bottom of the cell was 15 minutes, which was thrice the amount of time it took for a similar result in cell test II. Once the water phase reached the bottom of the cell, it moved along the bottom cell boundary (marked by arrows in fig.5.59b, fig.5.59c and fig.5.60a), this movement was similar to observation in cell test II.

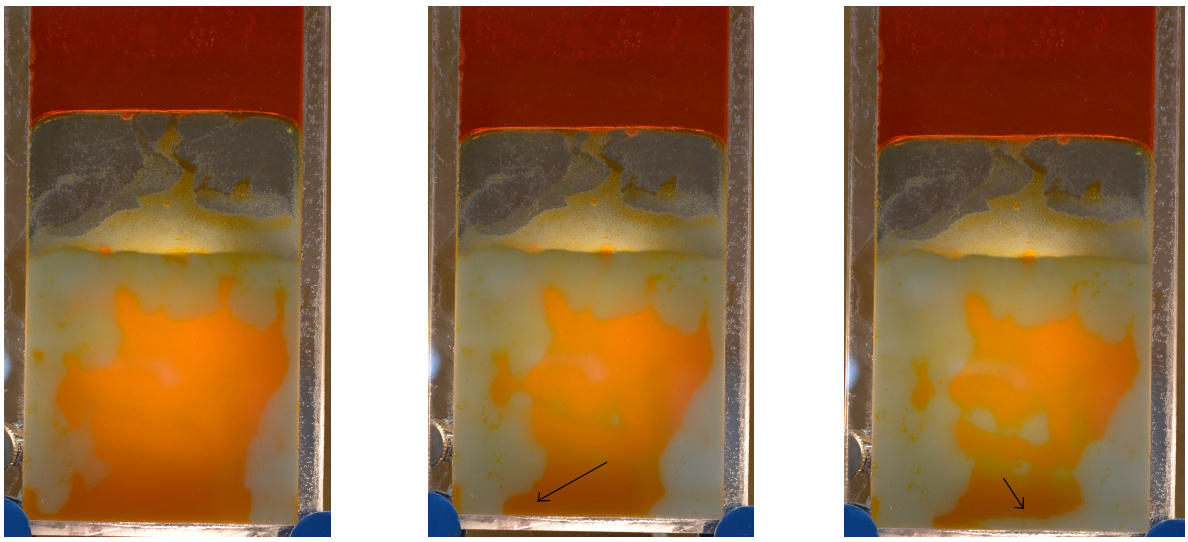

(a) t=15 min (b) t=22 min (c) t=30 min

Figure 5.59: Cell test III: The movement of water phase along the bottom boundary of the cell was observed.

Oil mobilisation from porous media was a very slow process after the water front covered the bottom boundary of the cell. Unswept oil in the porous media surrounded by the water phase was displaced slowly, seen as reducing oil region in fig.5.60 and fig.5.61. HCl was added to the cell, and due to the change in pH, the colour of water changed from blue to yellow. The visualisation of change in colour of water phase was poor.

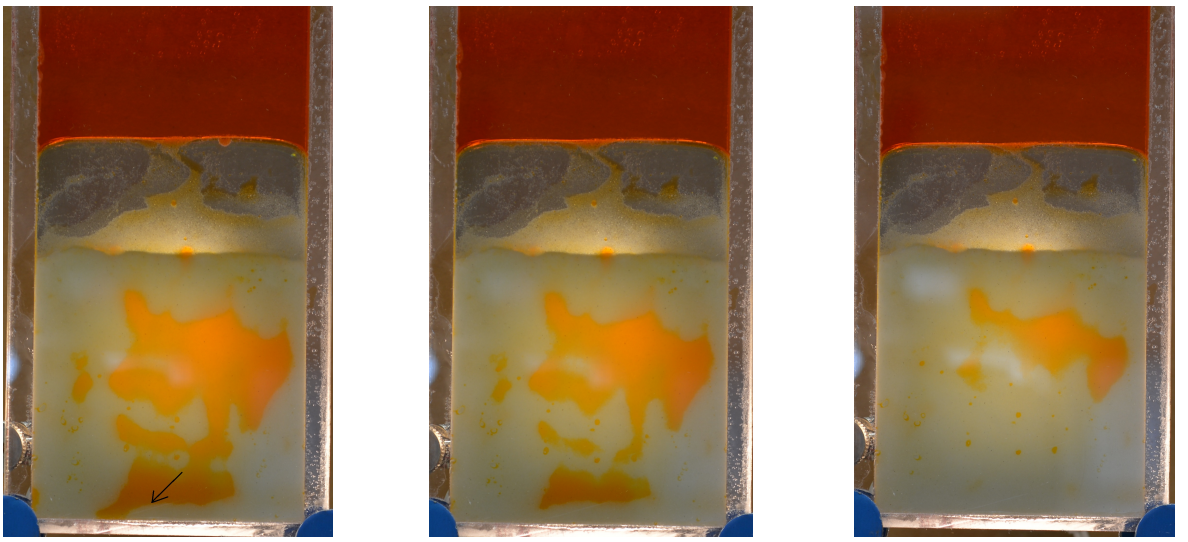

(a) t= 33 min (b) t=36 min (c) t=44 min

Figure 5.60: Cell test III: Visualisation of the change in pH of water phase upon addition of HCl was poor.

The movement of low pH water (yellow) in the porous media was a very slow process and could not be observed very clearly on camera in this case. Upon complete water phase movement into the porous media, oil trapped in the porous media at the end of the test was observed (marked by circles in fig.5.61c).

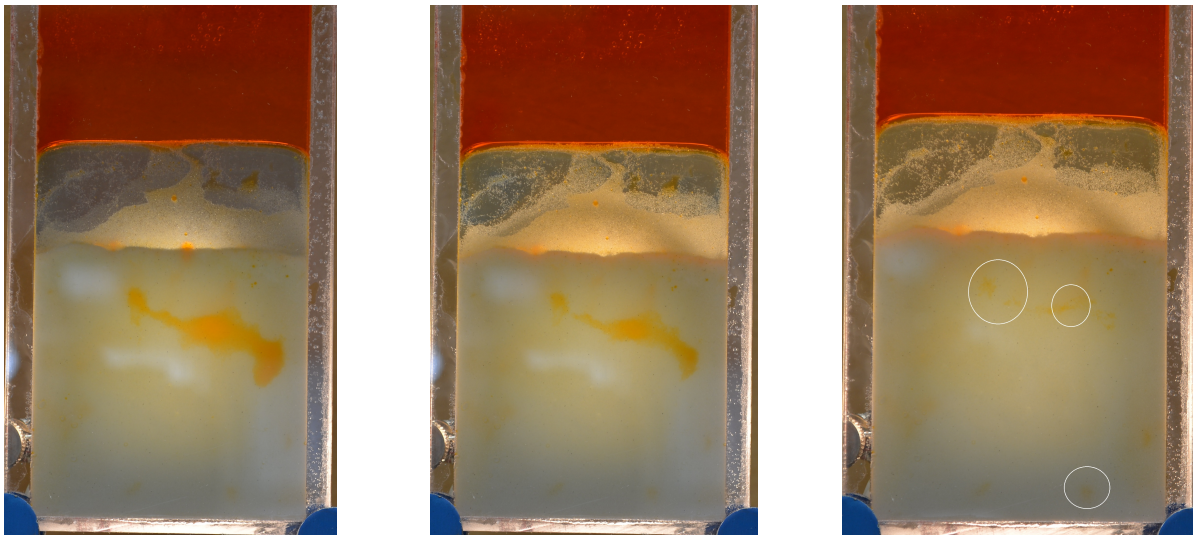

(a) t=51 (b) t=55 min (c) t=62 min

Figure 5.61: Cell test III: Oil trapped in the porous media at the end of the test.

5.4.4 Conclusions: Cell tests with varying thickness in porous media type B

The objective of these tests was to visualise imbibition process in polycarbonate cell of varying thickness and to correlate the observations made on the shape of invading front with studies done in literature using glass micromodels.

Label	Cell thickness	Cell volume	Shape of water front	T_b	Visualisation
CT I	3 mm	24.4 cc	Piston-like+ limited movement on the sides	16 min	Good
CT II	5 mm	40.7 cc	Piston-like+ along the side edges	5 min	Good
CT III	8 mm	65.1 cc	Percolation type	15 min	Poor

Table 5.15: Cell tests (CT) I-III: Overview of observations.

Table 5.15 presents an overview of observations from cell tests I- III. T_b refers to the time taken by water phase to reach the bottom of the cell. The visualisation of the process was graded on the scale: good, intermediate and poor.

Lenormand et al. (1984) studied imbibition in glass micromodels and made observations on the shape of the water front and imbibition type with varying capillary number. To correlate our observations with theoretical findings, the capillary number has to be calculated. A rough estimation of the capillary number from the data available in these tests is given below:

The injected fluid velocity is given by:

$$u = \frac{Q}{A}$$

where Q is the flow rate of the water phase, A is cross-sectional area of the cell and u is mean velocity of the water phase. In cell tests I, II and III we assume that Q was constant as the water phase was injected slowly on top of porous media and imbibition was gravity driven. However, cross-sectional area increased with the increase in cell thickness as:

$$A = width * thickness$$

With Q as a constant, an increase in A will lead to a decrease in velocity of water phase (u). Capillary number C_a is given by:

$$C_a = \frac{u * \mu_w}{\sigma_{ow}}$$

where μ_w is the viscosity of water phase and σ_{ow} is the interfacial tension between the water and oil phases. A decrease in u, will cause a decrease in C_a, since μ_w and σ_{ow} are constant for all cell tests. Following is a calculation process to prove that an increase in cell thickness leads to decrease in capillary number, given other parameters remain constant.

In cell test I-III, the flow of water was gravity driven, and porous media was a complex 3-D network opposed to etched glass networks of a known pore and throat size. These factors make it difficult to calculate the capillary number for the test. However, we can

get a rough estimate by calculating the velocity of the water phase in pores using distance covered over a given time.

For cell test II, the water front reached the bottom boundary of the cell in 5 minutes. The total height of porous media was half the height of the cell, i.e. 6.9 cm. Hence, the velocity of water in porous media can be roughly estimated as:

$$u = \frac{6.9}{5 * 60} cm/sec$$

μ_w at 20°C is 1 cP (10^{-3} Pa-s) and σ_{ow} between n-decane and water is 29 dynes/cm (1 dyne = 10^{-5} Newton). 1 Pa = 10^{-4} N/cm^2.

Using values of μ_w, σ_{ow} and u, C_a can be estimated as:

$$C_a = \frac{6.9 * 10^{-3} * 10^{-4}}{29 * 10^{-5} * 5 * 60}$$
$$C_a = 8 * 10^{-6}$$

Similarly, for cell test III:

Time taken to reach the bottom of the cell was 15 minutes. Hence, the velocity of water in porous media is given by:

$$u = \frac{6.9}{15 * 60} cm/sec$$

C_a can be estimated as:

$$C_a = \frac{6.9 * 10^{-3} * 10^{-4}}{29 * 10^{-5} * 15 * 60}$$
$$C_a = 2 * 10^{-6}$$

Given below are the conclusions drawn from cell tests I-III:

1. The shape of water front in the porous media was a function of capillary number. Estimates of the capillary number in cell test II and III showed that with a decrease in capillary number from $8 * 10^{-6}$ to $2 * 10^{-6}$ the shape of water front in porous media became more like a percolation process.
2. Results from the Lenormand's correlation of C_a and the shape of advancing water front are observed in complex 3-D porous media with variation in the distribution of pores and non-uniform packing (Lenormand & Zarcone, 1984). These results are:
   (a) For medium capillary number ($10^{-6} < C_a < 10^{-4}$): Lenormand proposed that the flow rate is too high for water front to advance as a pure percolation process. As a result, the shape of water front is a crossover between the frontal drive (piston type) and percolation process. This effect was observed in cell test II where the water front movement was a crossover between piston-like displacement at the beginning followed by movement along the side edges of the cell (percolation process). Cell test I showed limited crossover between piston-like and percolation type movement.

      As we have shown in the calculations above, an increase in the cell thickness leads to a decrease in the capillary number. Hence it can be inferred: capillary

number in cell test I was higher than the capillary number in cell test II. Lenormand's study also stated that a decrease in capillary number leads to an increase in the length of fingers. In our tests, this was seen in cell test II (fig.5.62b) where the length of fingers along the side edges of the cell was longer as compared to the length of fingers in cell test I (fig.5.62a).

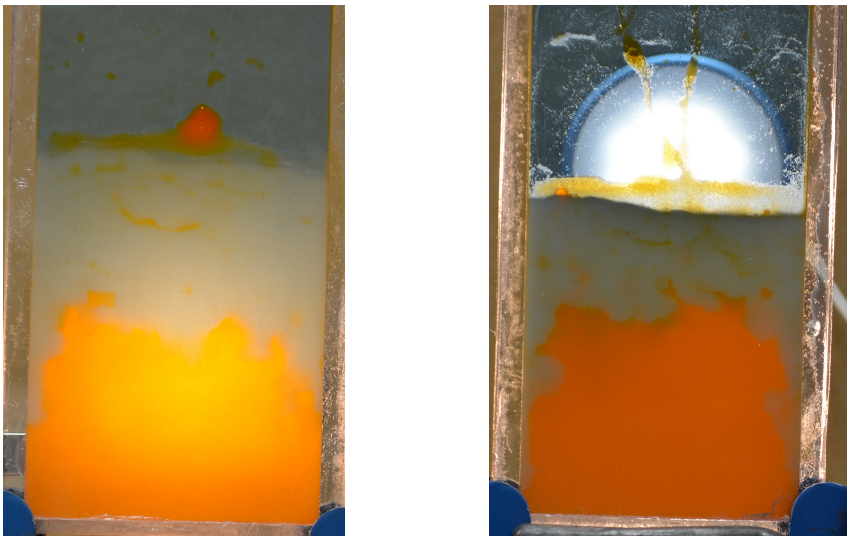

(a) Limited crossover between frontal drive and percolation process in cell test I

(b) Crossover between frontal drive and percolation process in cell test II

Figure 5.62: Cell test I and II showed the movement of the front as a crossover between piston-like process and the movement along the side edges of the cell.

(b) For low capillary number ($10^{-9} < C_a < 10^{-6}$): Lenormand's study stated that front advancement was more towards percolation process and less piston-like. As capillary number decreased in cell test III, the movement of water front became more percolation process along the side edges of the cell.

3. With an increase in the thickness of the cell, the ability of light to pass effectively through the porous media decreased. As a result, the visualisation of low pH water movement in porous media became poor as the thickness of the cell increased.

4. The movement of oil from porous media to the free oil phase on top of the cell was in the form of droplets along the cell walls or via a channel created during water injection in the cell. Polycarbonate being preferentially oil-wet allowed the oil to flow on the walls of the cell as opposed to droplets rising from the porous media (seen in tube tests).

5. The limitation in the calculation of capillary numbers was imposed by the fact that as the capillary number increases, the shape of water front becomes more piston-like and time taken to reach the bottom of the cell increases.

   In cell test I, more porous media was swept by piston-like displacement compared to cell test II and III where fewer porous media was invaded in the centre of the cell, but water front reached the bottom of the cell faster because of the movement along the side edges of the cell.

5.4.5 Cell test IV: Polycarbonate cell with 3 mm thickness and porous media type C

As the glass beads settled, a distinct interface between glass beads and free oil phase on top was seen (fig.5.63a). The invasion of the water phase in porous media was instantaneous (fig.5.63b). Oil mobilisation was observed as an oil droplet escaped the porous media and moved towards the free oil phase on top (fig.5.63d). The movement of water in porous media was in the form of clusters along the sides of the cell (marked by arrows in fig.5.63d).

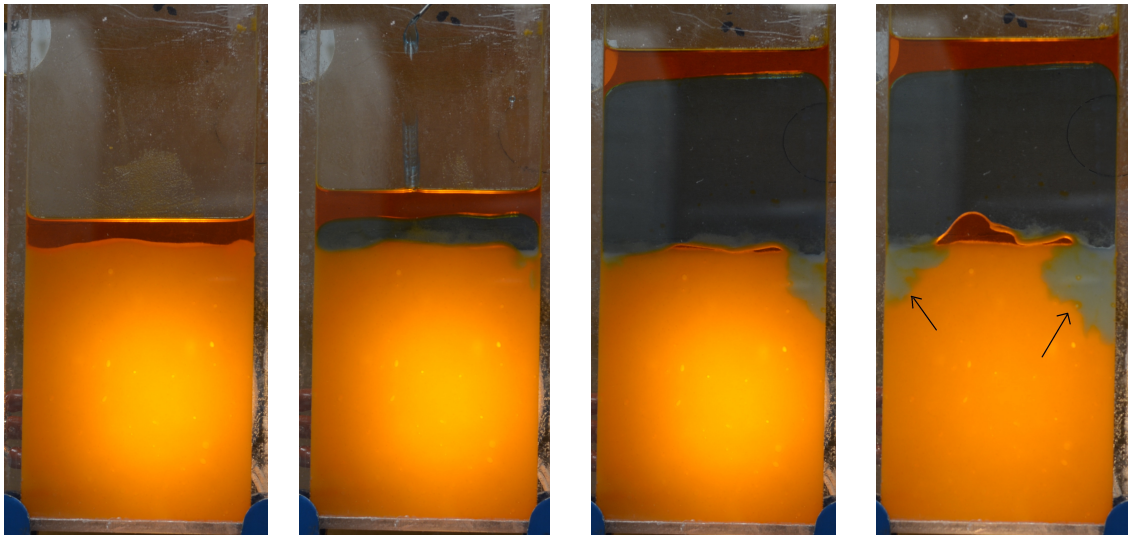

(a) Oil phase (b) t=0 (c) t=10 sec (d) t=1 min

Figure 5.63: Cell test IV: Water phase began invading the porous media instantaneously as it was added to the cell.

The movement of water phase in the porous media continued as clusters grew bigger and merged to form a common water front (fig.5.64). Oil droplets escaping the porous media were seen adhering to the walls because polycarbonate is preferentially oil-wet. The movement of the merged water front was piston-like as seen in cell test I (fig.5.47).

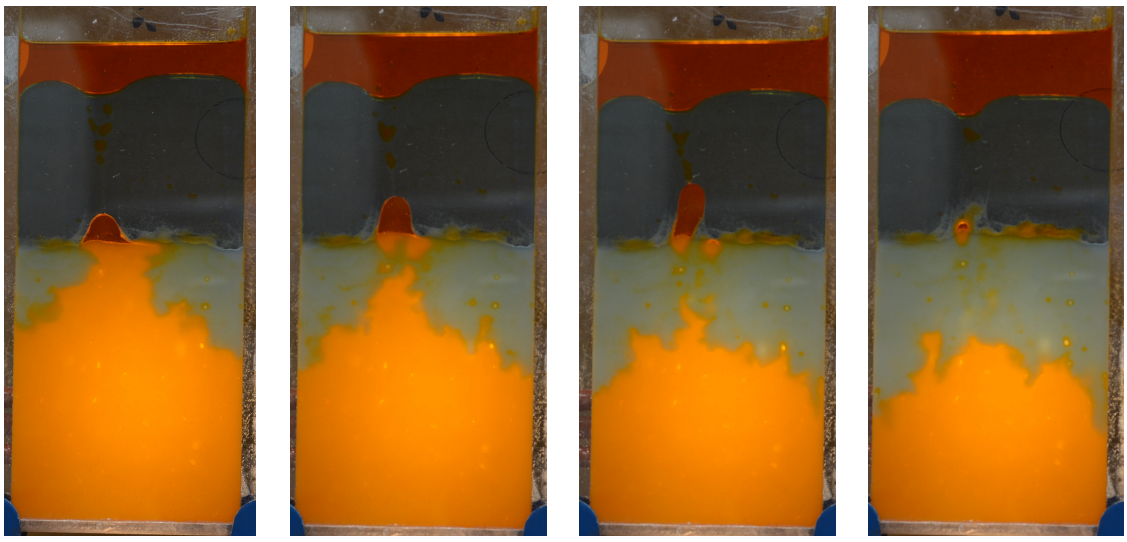

(a) t=1.5 min (b) t=2 min (c) t=3 min (d) t=5 min

Figure 5.64: Cell test IV: Water phase began invading the porous media in the form of clusters growing on side edges of the cell.

After 6 minutes, water phase on the side edges of the cell began advancing faster compared to the water phase moving in the center of the cell (marked by arrows in fig.5.65a), this was similar to observation in cell test I (fig.5.48a). The water front advancement on the side edges was faster and reached the bottom of the cell first. The time taken by water front to reach the bottom of the cell was 14 minutes, and upon reaching the bottom of the cell, the water phase began moving along the bottom boundary of the cell (marked by arrows in fig.5.65d).

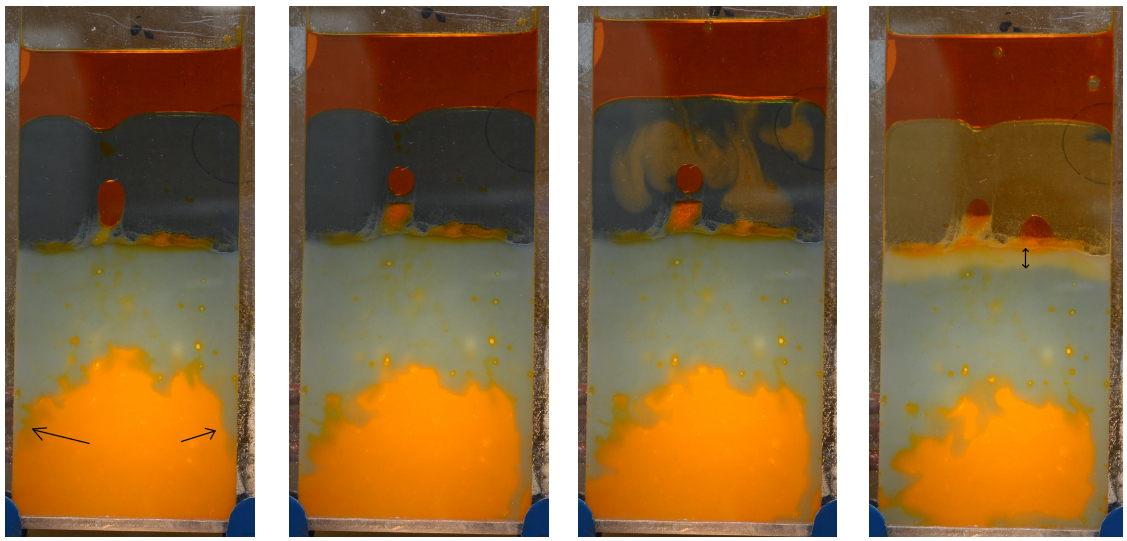

(a) t=6 min (b) t=9 min (c) t=14 min (d) t=15 min

Figure 5.65: Cell test IV: Water front reached the bottom of the cell and began moving along the bottom boundary of the cell.

HCl was added to the cell, and on reacting with the water phase, it changed the colour of water phase from blue to yellow indicating a drop in pH below 6. The movement of low pH water in pores was piston like (marked in fig.5.65d.

The water phase covered the bottom boundary of the cell and surrounded a part of oil-filled porous media from all sides (fig.5.66a). Oil from this section of the porous media was recovered slowly but consistently (seen as decreasing oil in porous media in fig.5.66a to fig.5.66d). The movement of low pH water in porous media was piston-like and was observed as a change in colour of porous media from blue to white (fig.5.66).

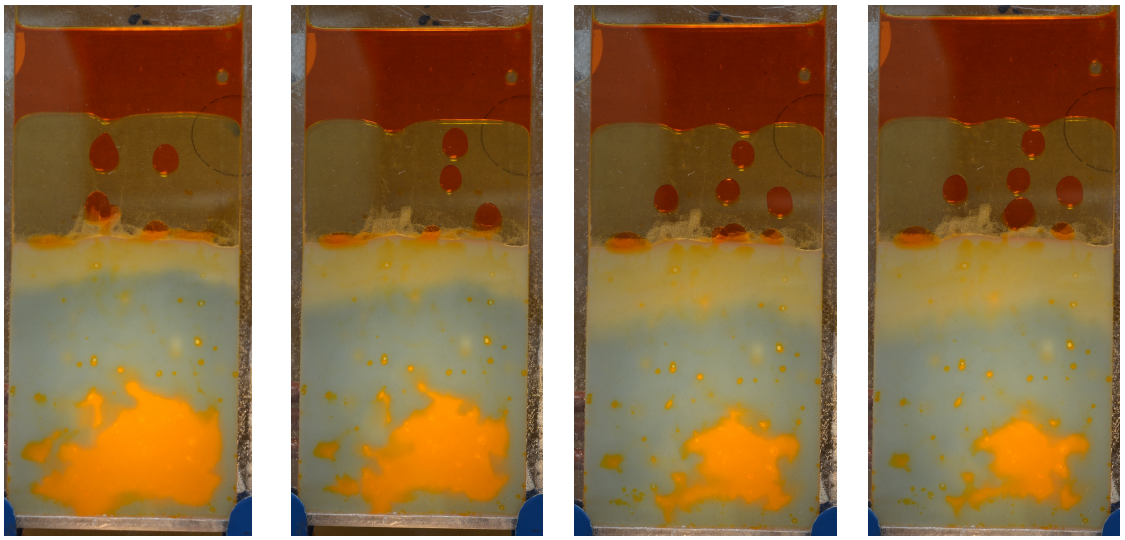

(a) t=17 min (b) t=21 min (c) t=27 min (d) t=29 min

Figure 5.66: Cell test IV: The movement of low pH water in porous media was piston-like and oil recovered was seen moving towards free oil phase on top of the cell.

Without the use of external force, like constant pressure CO_2 injection in the larger tube tests, the reaction of low pH water with high pH (blue) water was a slow process. As a result, oil mobilisation from the porous media slowed down at the end of the experiment. The oil trapped in porous media is seen marked by circles in fig.5.67d.

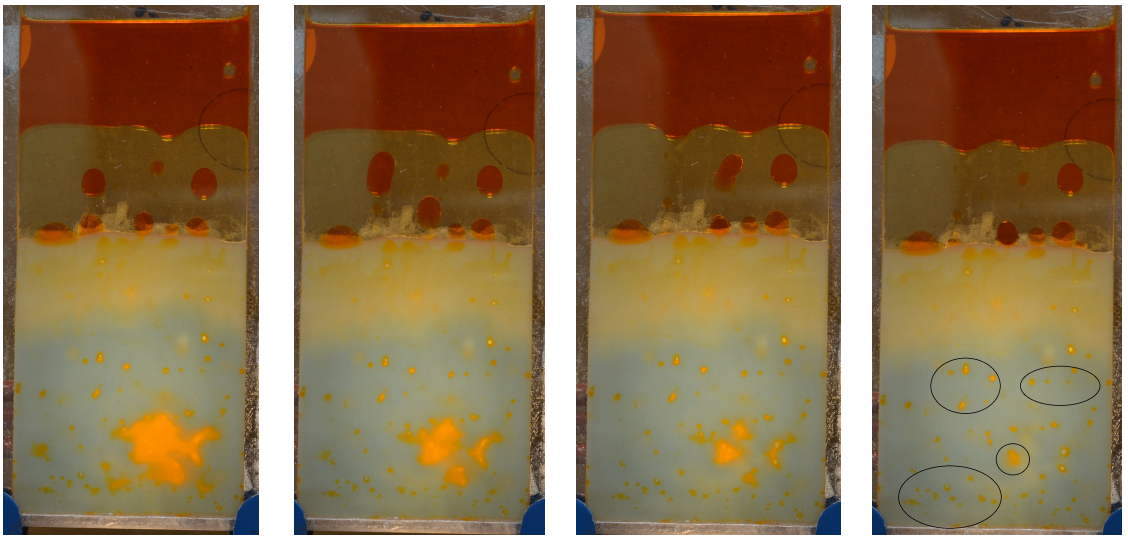

(a) t=31 min (b) t=35 min (c) t=38 min (d) t=41 min

Figure 5.67: Cell test IV: Oil trapped in the porous media at the end of the experiment.

5.4.6 Cell test V: Polycarbonate cell with 5 mm thickness and porous media type C

Fig.5.68a shows a clear interface observed between glass beads and the free oil phase. The water phase instantaneously began invading the porous media from the side edges of the cell (fig.5.68d) and oil mobilisation from porous media to free oil phase on top was via a channel created during water injection (marked by an arrow in fig.5.68d).

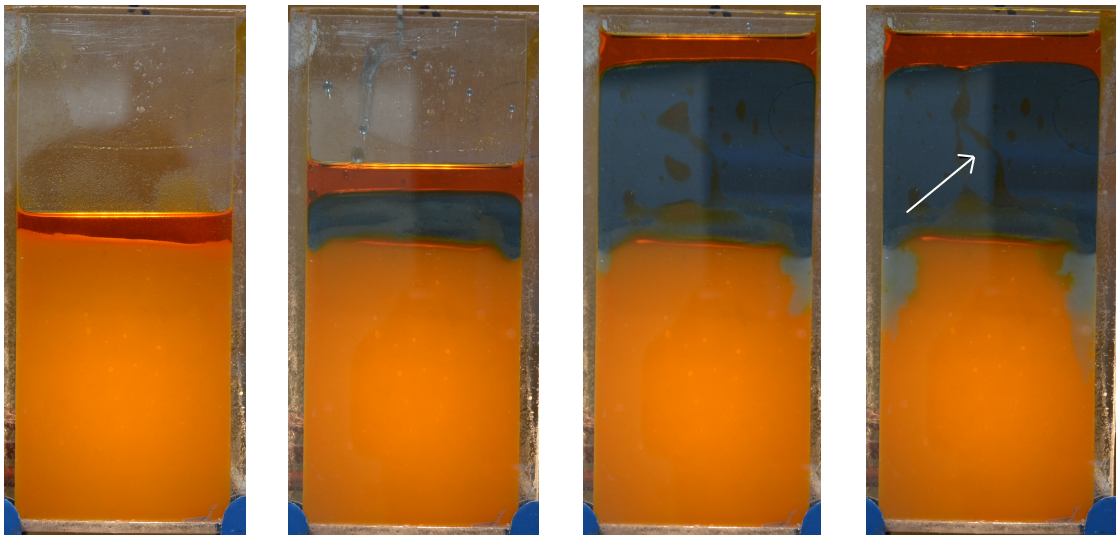

(a) Oil phase (b) t=0 (c) t=1 min (d) t=1.5 min

Figure 5.68: Cell test V: Water phase began to move along the side edges of the cell.

Cluster-like movement of the water phase close to water-glass beads interface was observed (fig.5.69b). These clusters swept the porous media horizontally and merged to form a common water front (fig.5.69c). The time taken by water phase to reach the bottom of the cell was 6 minutes. A change in colour of the water phase from blue to yellow indicated a drop in pH below 6 due to the addition of HCl (fig.5.69d).

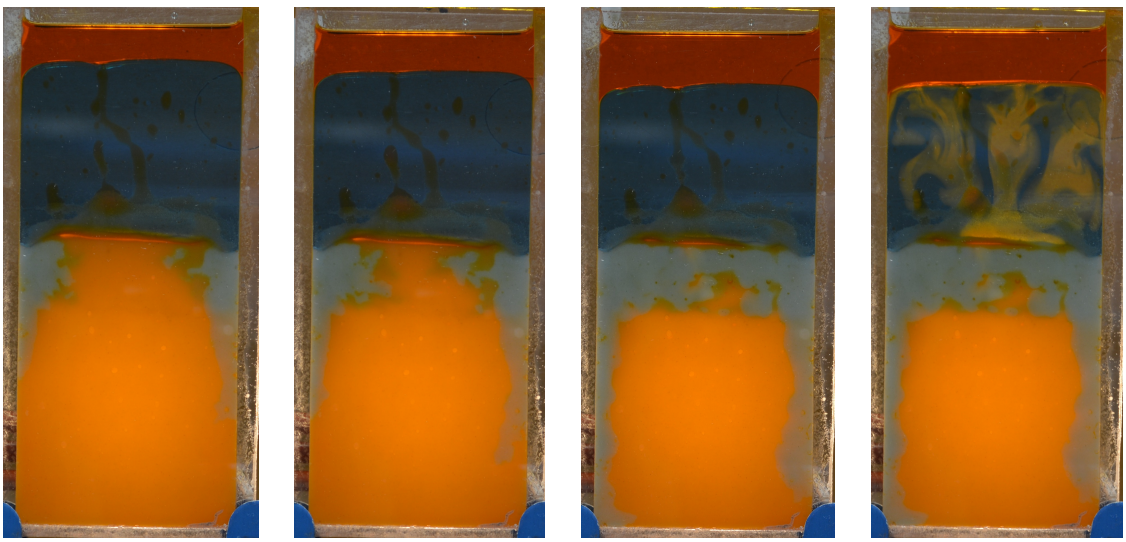

(a) t=2 min (b) t=3 min (c) t=7 min (d) t=8 min

Figure 5.69: Cell test V: Water phase moved along the side edges of the cell and reached the bottom of the cell in 6 minutes.

Once the water phase reached the bottom of the cell, it began moving along the bottom boundary of the cell (seen in fig.5.70a). Oil filled porous media was surrounded by the water phase (fig.5.70b) and from this point onwards oil recovery was a slow process. The movement of low pH water in porous media was piston-like in the beginning (fig.5.70b).

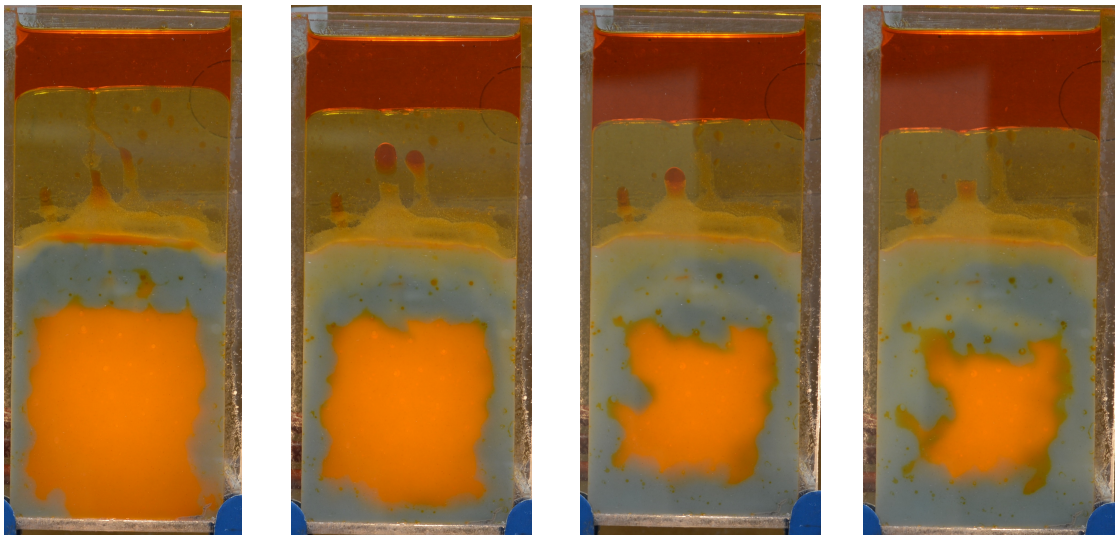

(a) t=11 min (b) t=31 min (c) t=64 min (d) t=90 min

Figure 5.70: Cell test V: Water phase surrounded oil-filled porous media and oil mobilisation was a slow process from this point.

Oil mobilisation was a slow process due to the higher quantity of oil trapped in the porous media when the water phase surrounded it. Oil trapped in porous media at the end of the test is seen marked by circles in fig.5.71d.

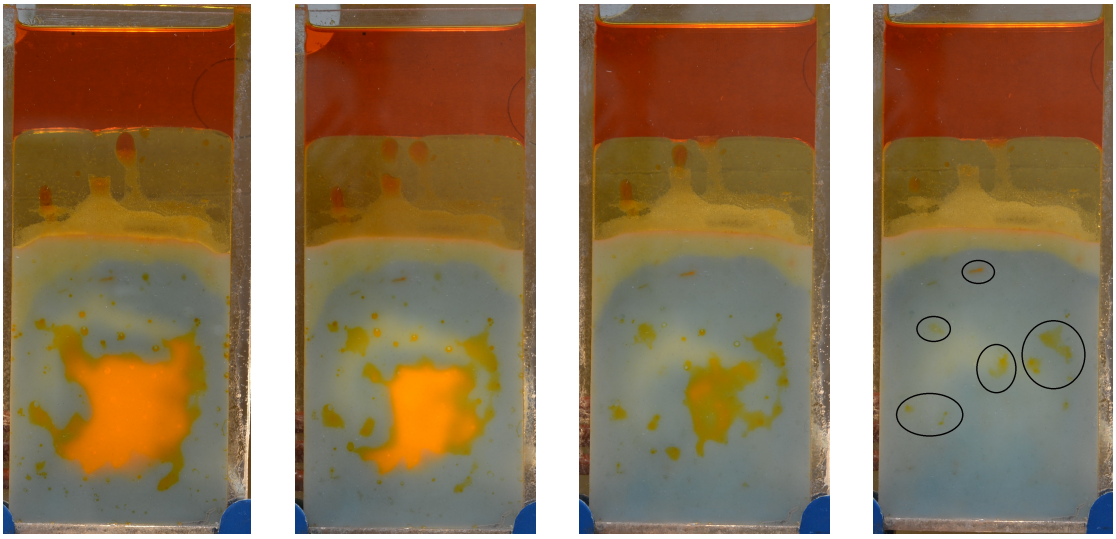

(a) t=102 min (b) t=136 min (c) t=198 min (d) t=256 min

Figure 5.71: Cell test V: Oil trapped in porous media at end of the test.

5.4.7 Cell test VI: Polycarbonate cell with 8 mm thickness and porous media type C

The use of an ultrasonic bath provided better packing of the porous media and oil-glass beads interface was clearly observed in fig. 5.72aThe water phase invasion in porous media was instantaneous, and the shape of the front was piston-like (fig. 5.72c), opposed to percolation type observed in cell test III (fig. 5.58b on page 103). Oil recovery from porous media was via a flow channel created during water injection process (marked by an arrow in fig. 5.72d).

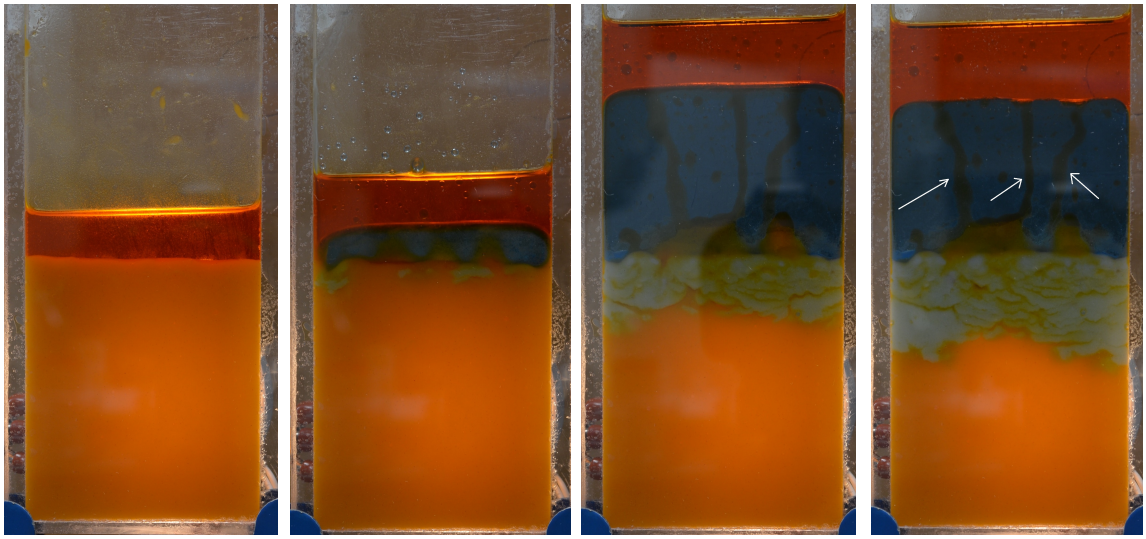

(a) Oil phase (b) t=0 (c) t=10 sec (d) t=1 min

Figure 5.72: Cell test VI: Shape of water front in porous media was piston-like.

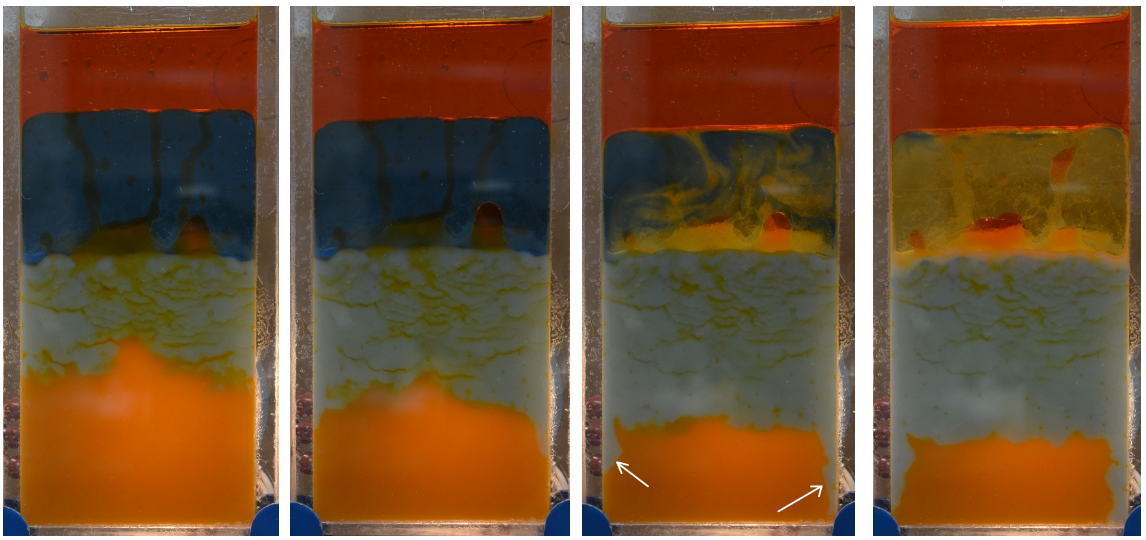

(a) t=2 min (b) t=3 min (c) t=6 min (d) t=9 min

Figure 5.73: Cell test VI: Movement of the water phase in porous media was a fast piston-like process in the beginning and switched to movement along the side edges of the cell after 6 minutes.

After 6 minutes, the water phase began moving along the side edges of the cell (marked by arrows in fig.5.73c) and reached the bottom of the cell in 7 minutes. On adding HCl,

the colour of the water phase changed from blue to yellow (fig.5.73d). The movement on low pH water in porous media was slow process (fig.5.74c).

Water phase began moving along the bottom of the cell surrounding a portion of oil-filled porous media (fig.5.74b). Oil in the porous media surrounded by water phase was slowly recovered, and a limited visualisation of oil trapped in porous media was possible the end of the experiment.

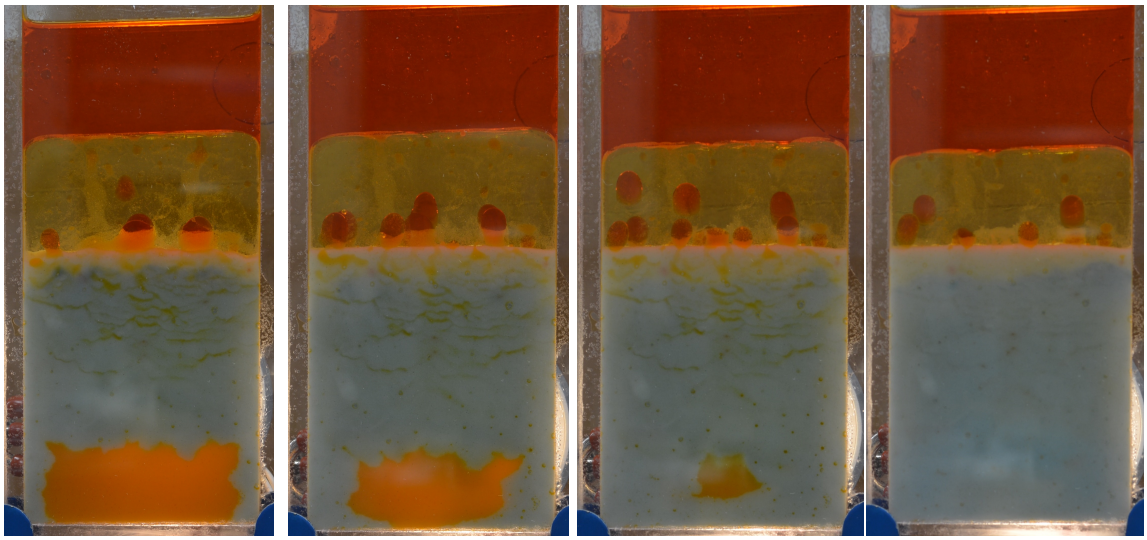

(a) t=14 min (b) t=28 min (c) t=45 min (d) t=105 min

Figure 5.74: Cell test VI: Oil mobilisation from porous media surrounded by water phase was a slow process.

5.4.8 Conclusions: Cell tests with varying thickness in porous media type C

Aim of this test was to study the effect of small change in grain size on imbibition process. Conclusions from these tests are given below:

Parameter	Cell test I (3 mm)	Cell test IV (3 mm)
Porous media type	Type B	Type C
Time to reach bottom of the cell	16 min	14 min
Shape of water front	Piston like + limited movement on cell edges	Piston-like + movement on cell edges
Visualisation / operational ease	Good visualisation / poor operational ease	Good visualisation / poor operational ease

Table 5.16: Comparison between results from cell test I and IV.

Note: Quality of visualisation and operational ease was graded on the scale: good, intermediate and poor.

1. Table 5.16 compares observations made in cell test I and IV. The shape of water front in porous media was of similar nature in both the tests. One possible reason for a cluster like front seen in cell test IV was the resistance offered by oil escaping from the porous media and moving towards free oil phase on top of the cell. Time taken by the water phase to reach the bottom of the cell was in close range for both tests. The filling and cleaning of the porous media in the cell was challenging.

Parameter	Cell test II (5 mm)	Cell test V (5 mm)
Porous media type	Type B	Type C
Time to reach bottom of the cell	5 min	6 min
Shape of water front	Piston like + flow along the cell edges	Piston-like + flow along the cell edges
Visualisation / operational ease	Good visualisation / good operational ease	Good visualisation / good operational ease

Table 5.17: Comparison between results from cell test II and V.

2. Table 5.17 compares observations from cell test II and V. A change in grain size of glass beads did not visually affect the shape of the water front in porous media. In cell test V, the water front showed a formation of clusters near the entrance of porous media. The cluster like formation is believed to be due to the resistance offered by oil rising from porous media at the center of the cell. Both the cells provided good quality visualisation of the processes and were easy to fill and clean the porous media.
3. The length of fingers along the side edges of the cell was longer in cell test V compared to those in cell test IV (seen in fig.5.75). As explained in subsection 5.4.4, an increase in the thickness of the cell leads to decrease in capillary number and as a result, the water front advances more like a percolation process and less piston-like.

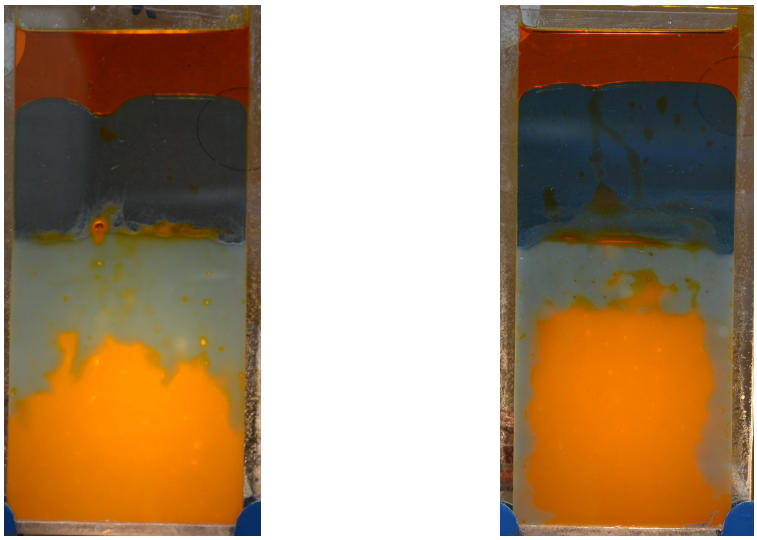

(a) Crossover between frontal drive and percolation process in cell test IV

(b) Crossover between frontal drive and percolation process in cell test V

Figure 5.75: Length of fingers along the side edges of the cell increased as capillary number in cell test V was lower than capillary number in cell test IV.

Parameter	Cell test III (8 mm)	Cell test VI (8 mm)
Porous media type	Type B	Type C
Time to reach bottom of the cell	15 min	7 min
Shape of water front	Percolation type on the cell edges	Fast piston-like
Visualisation / operational ease	poor visualisation / good operational ease	poor visualisation / good operational ease

Table 5.18: Comparison between results from cell test III and VI.

4. Comparison between observations made in cell test III and VI are presented in table 5.18. A change in grain size of glass beads changed the shape of the water front in porous media. Piston-like displacement noticed in cell test VI was opposite of percolation type movement observed in cell test III. Possible reasons for the piston-like pattern are:

   (a) A difference in grain size of porous media used: As a result, the size of pores was smaller in cell test VI compared to cell test III. Studies in the literature show that in small pores, the flow of the water phase is piston-like in the bulk of ducts and also along the corners of the pores (Lenormand & Zarcone, 1984).

   (b) The difference in diameter of grains in cell test VI was 40 μm and in cell test III was 60 μm. As a result, the porous media in cell test VI was densely packed due to less variation in the grain size.

Parameter	Tube test XIII	Cell test IV	Tube test XII	Cell test V	Tube test XI	Cell test VI
Diameter / Thickness	3.75 mm	3 mm	5.55 mm	5 mm	7.85 mm	8 mm
Shape of water front	Piston-like	Crossover	Crossover	Crossover	Piston-like	Piston-like
Visualisation / operational ease	Good / Poor	Good /Poor	Good/Good	Good/Good	Intermediate/Good	Poor/Good

Table 5.19: Comparison of observations made in tube test of varying diameter and cell tests IV-VI.

Note: Quality of visualisation and operational ease was graded on the scale: good, intermediate and poor. Porous media of type C was used in all the tests in the table 5.19.

5. Table 5.19 compares observations made in tube tests with varying diameter and cell tests IV-VI. Filling and cleaning of the porous media were easier as the diameter/ thickness increased. However, an increase in the thickness caused the quality of visualisation to decline.

6. The shape of water front in the porous media was comparable in tests of similar thicknesses (e.g. crossover between piston-like and movement on side edges seen in cell test V and tube test XII).

5.5 Tests in POM cell with CO_2 injection at 10 bar

POM cell tests were conducted to visualise the movement of CO_2 in the water phase and to study the oil-water system under CO_2 injection at 10 bar. Porous media of type C was used in these experiments.

5.5.1 POM cell test I: CO_2 injection with water phase in the cell

The water solution was injected into the cell at a low flow rate till water level in the cell reached approximately half the height of the cell. CO_2 injection at a constant pressure of 10 bar was started. On opening the inlet valve to the cell, the level of the water phase in the cell reduced (seen in fig.5.76c).

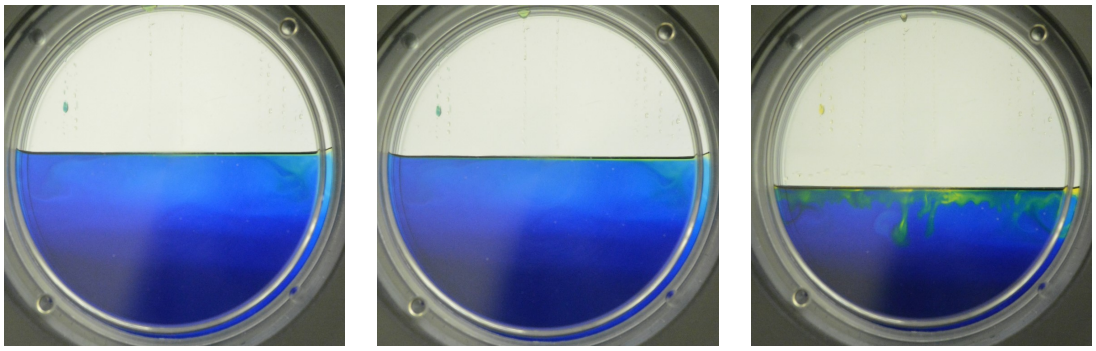

(a) Water phase (b) t=0 (c) t=1 min

Figure 5.76: POM cell test I: A drop in the level of water phase was observed upon initiating CO_2 injection into the cell.

CO_2 reacted with the water phase to form carbonated water and a change in colour of water phase from blue to yellow was seen. CO_2 movement in the water phase was in the form of fingers (fig.5.77) due to the difference in viscosity of CO_2 and water phase. Due to the circular design of the cell, CO_2 reached the boundary much faster on the left and right sides of the cell and began to move along the boundary of the cell (marked by arrows in fig.5.77c).

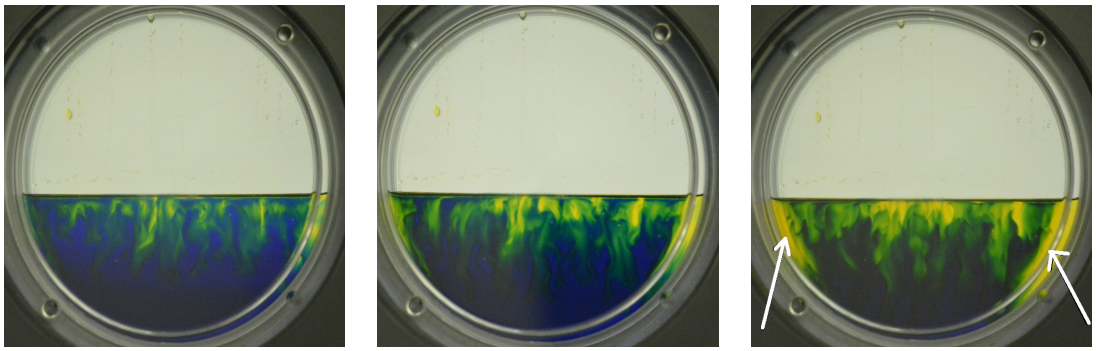

(a) t=2 min (b) t=2.5 min (c) t=3 min

Figure 5.77: POM cell test I: CO_2 moved along the side boundaries of the cell.

After 4 minutes, the CO_2 front on both left and right sides reached the bottom of the cell (fig.5.78a) and unreacted high pH water (blue) mixed with CO_2. The time required for complete dissolution of CO_2 in the water phase was 6.5 minutes. Because of the difference in density of water phase and the carbonated water, downwards movement of carbonated water was observed. This effect was more pronounced in this test due to a higher surface area available for CO_2 to react with water phase compared to CO_2 injection in larger tube test I (Sub-subsection 5.3.1 on page 77).

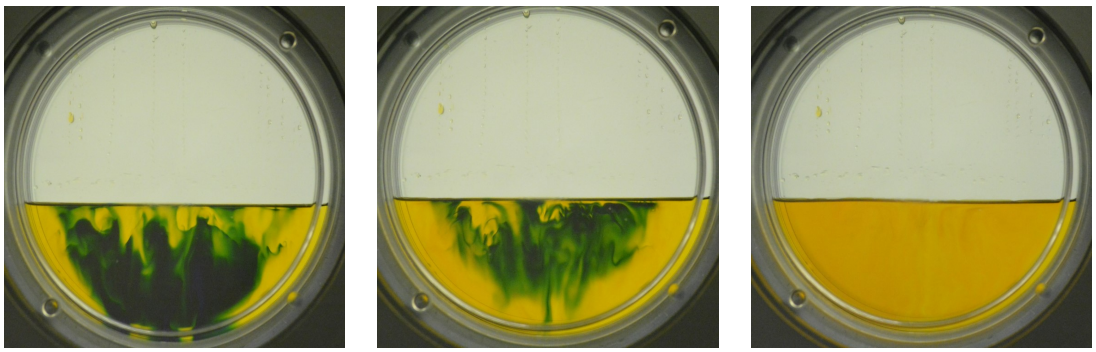

(a) t=4 min (b) t=5 min (c) t=6.5 min

Figure 5.78: POM cell test I: CO_2 front from both sides reached the bottom of the cell and mixed with unreacted water phase to form carbonated water.

5.5.2 POM cell test II: CO_2 injection with oil on top of water phase in the cell

Upon completion of water injection, the oil phase was injected into the cell to leave a small layer on top of the water phase. As CO_2 injection into the cell began, a small yellow line at the water-oil interface (fig.5.79b) was observed due to the instantaneous reaction of CO_2 and water phase present in the injection line and on the walls of the cell. A drop in the level of fluids was observed as the cell was pressurised to 10 bar (fig.5.79c).

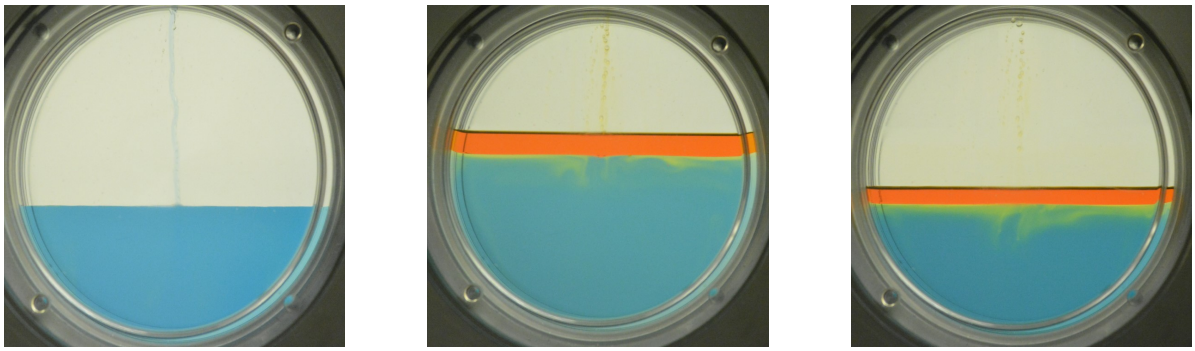

(a) Water phase injection (b) t=0 (c) t=10 sec

Figure 5.79: POM cell test II: CO_2 injection commenced and a drop in the level of fluids was observed.

Due to the presence of an oil layer on top, CO_2 had to pass through the oil phase first to reach the water. As a result, the movement of CO_2 in the water phase was slower compared to POM cell test I. A similar effect was observed in larger tube test II (Subsection 5.3.2 on page 79). Development of fingers was observed due to a difference in viscosity of water phase and CO_2 (fig.5.80).

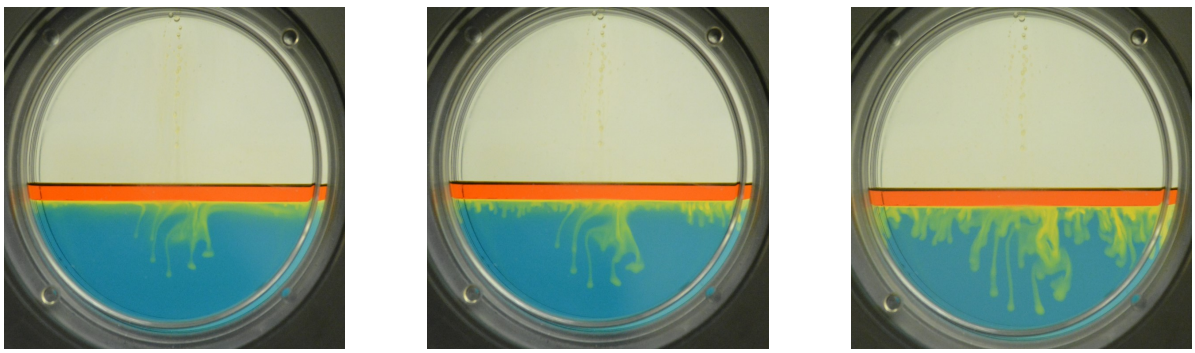

(a) t=0.5 min (b) t=1.5 min (c) t=2 min

Figure 5.80: POM cell test II: Development of fingers in the water phase was observed.

The movement of CO_2 along the walls of the cell was not as pronounced as POM cell test I (marked by arrows in fig.5.81c). This was noticed as the fingers at the center reached the bottom of the cell before fingers from the sides (comparing fig.5.81b and fig.5.78a). A reason for this was, the delayed CO_2 injection into the water phase due to the presence of an oil layer. This delay allowed better mixing of CO_2 already present in the water phase.

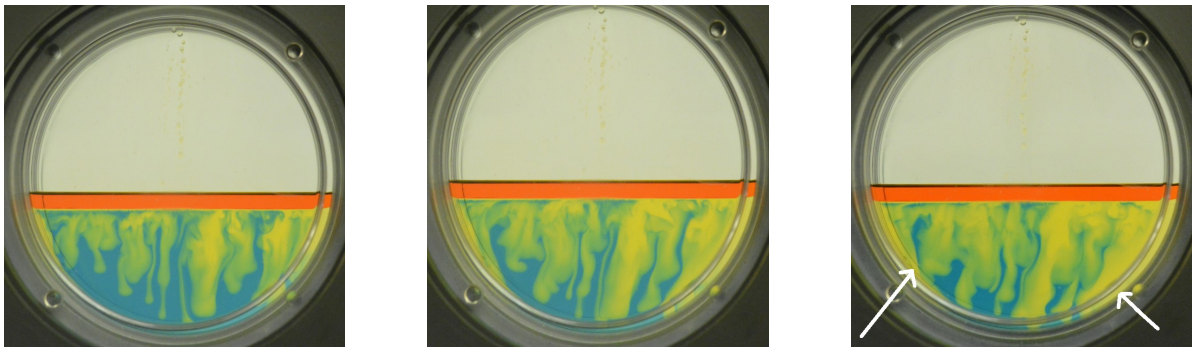

(a) t=3 min (b) t=4 min (c) t=5 min

Figure 5.81: POM cell test II: The movement of CO_2 along the center of the cell was faster than the movement along the side walls of the cell.

As the CO_2 front reached the bottom of the cell, unreacted water (blue) mixed with CO_2 causing the pH of the water phase to drop below 6. Similar to the observation in the larger tube test II (Subsection 5.3.2 on page 79), the amount of unreacted water (blue) behind the CO_2 front was lower in tests with the water-oil system compared to tests with only the water phase in the cell or tube. The time taken for complete dissolution of CO_2 into the water phase was 12 minutes, approximately twice the amount of time it took in POM cell test I. This effect was similar to observations made in the larger tube test I and II.

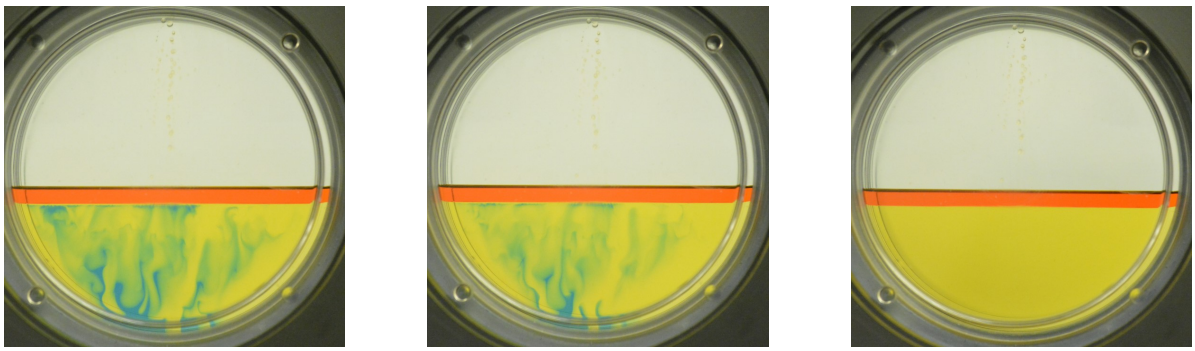

(a) t=6 min (b) t=8 min (c) t=12 min

Figure 5.82: POM cell test II: Total time for complete dissolution of CO_2 in the water phase was higher compared to POM cell test I.

5.5.3 POM cell test III: CO_2 injection with oil-water system in porous media

A total of 35 mL oil phase was injected into the cell. After adding the porous media to the cell, it was allowed to settle for 30 minutes since there was no other option to ensure proper packing (e.g. use of an ultrasonic bath). The water phase injection was carried on for 1 minute before switching to CO_2 injection at 10 bar (fig.5.83b).

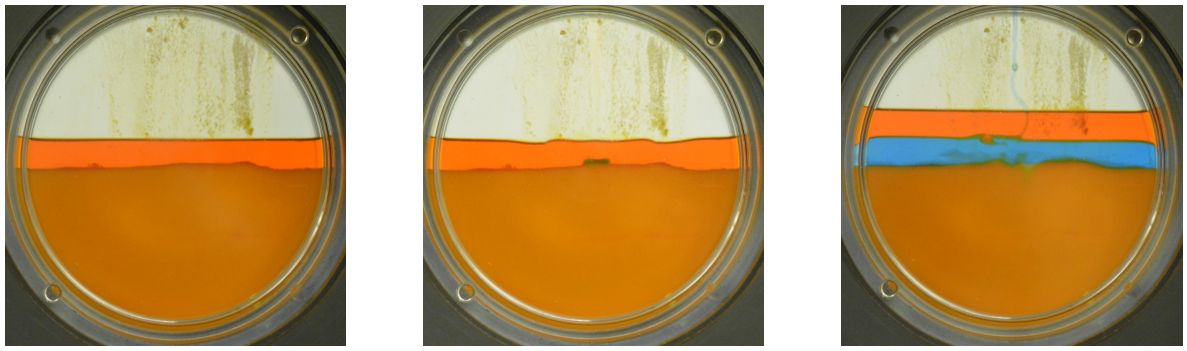

(a) Oil phase (b) t= 0 (c) t=0.25 min

Figure 5.83: POM cell test III: Filling of the porous media and the water phase in the cell.

Before the CO_2 injection commenced, the high pH water phase (blue) invaded the porous media. The movement of water in the porous media was non-uniform. A reason for this can be improper packing of porous media as ultrasonic bath could not be used in this case. A finger-like pattern emerged near glass beads-water interface (as marked by arrows in fig.5.84b).

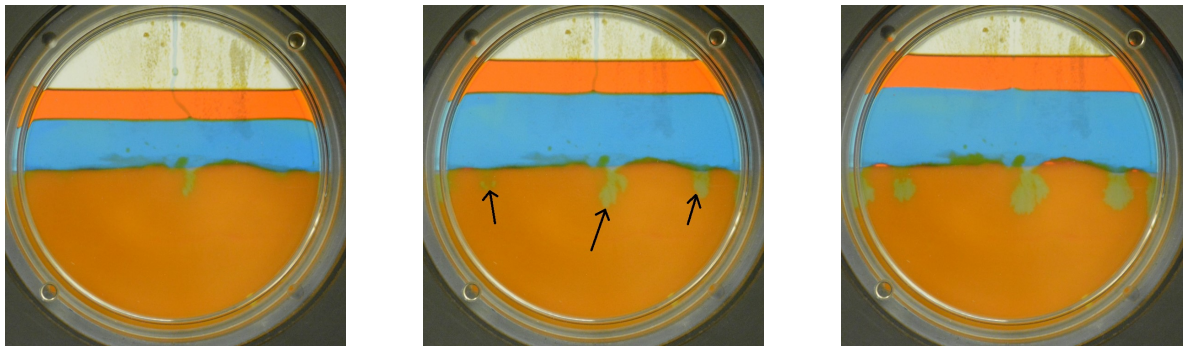

(a) t=0.5 min (b) t=0.75 min (c) t=1 min

Figure 5.84: POM cell test III: Water phase began invading the porous media and finger like pattern formed at glass beads-water interface.

After 2 minutes, CO_2 injection was initiated, and the level of fluids and porous media dropped (comparing fig.5.85b and fig.5.85c). Meanwhile, the fingers invading pores had grown in the form of clusters and oil was recovered due to the difference in density of water and oil phases. Oil trapped in porous media swept by the water phase was observed (marked by circles in fig.5.85c). Another reason for the movement of water front in the form of clusters could be the resistance offered by oil rising from porous media(seen in fig.5.85b).

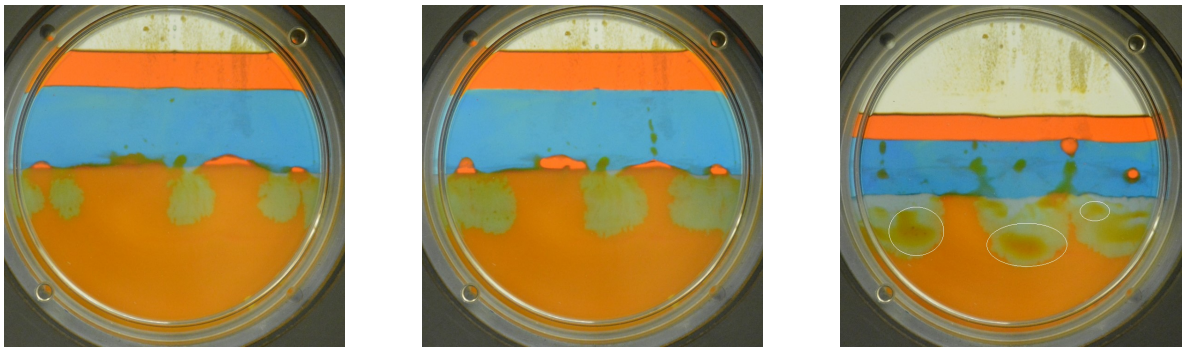

(a) t=1.5 min (b) t=2 min (c) t=2.5 min

Figure 5.85: POM cell test III: Oil trapped in porous media behind the advancing water front was observed.

As CO_2 began to dissolve in the water phase, the pH of water phase dropped below 6 and the colour changed to yellow (fig.5.86c). The water phase invading in the form of clusters merged to form a single front which showed piston-like movement in porous media (fig. 5.86c shows clusters joining to form a single front). The dissolution of CO_2 in the water phase was a fast process compared to POM cell test II, due to improved mixing provided by oil escaping the porous media and rising to the top of the cell towards the free oil phase. Another reason was also the decreased quantity of water phase left for CO_2 to react with, as a significant quantity of water phase had invaded the porous media before CO_2 injection began.

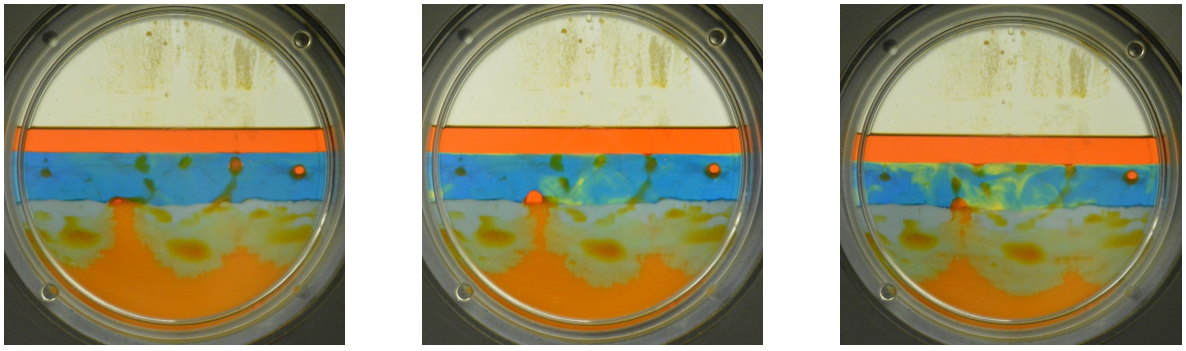

(a) t=3 min (b) t=3.5 min (c) t=4 min

Figure 5.86: POM cell test III: The dissolution of CO_2 in water phase caused the pH to drop, and colour of water phase changed to yellow.

Complete dissolution of CO_2 into the water phase took 4 minutes. The advancement of water in porous media switched from cluster movement to piston-like (fig.5.87a and fig.5.87b). The movement of low pH water phase in porous media and was observed as a change in colour from blue to white (marked by arrows in fig.5.87c).

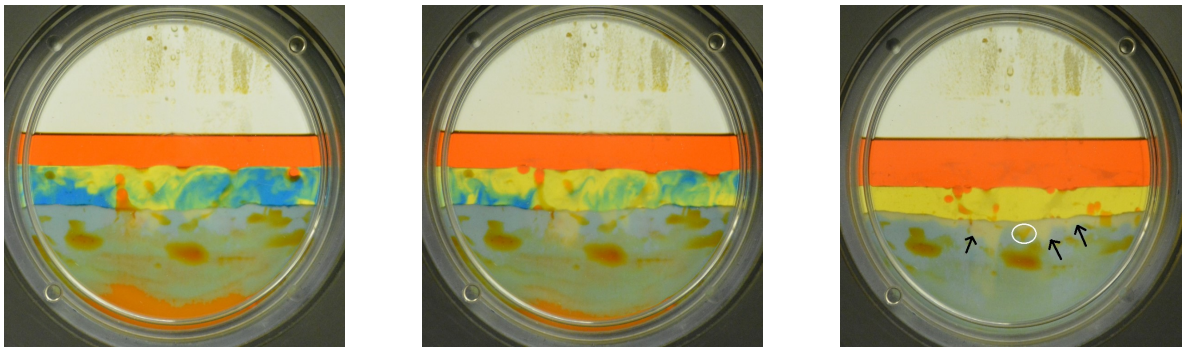

(a) t=4.5 min (b) t=5 min (c) t=7 min

Figure 5.87: POM cell test III: Complete dissolution of CO_2 in water phase took 4 minutes and movement of low pH CO_2 rich water phase began in porous media.

Invading high pH water front reached the bottom of the cell in 8 minutes. The movement of carbonated water in porous media was piston-like and a slow process. As carbonated water entered the porous media, it recovered a part of the trapped oil left behind by high pH (blue) water (marked by circles in fig.5.87c and fig.5.88a).

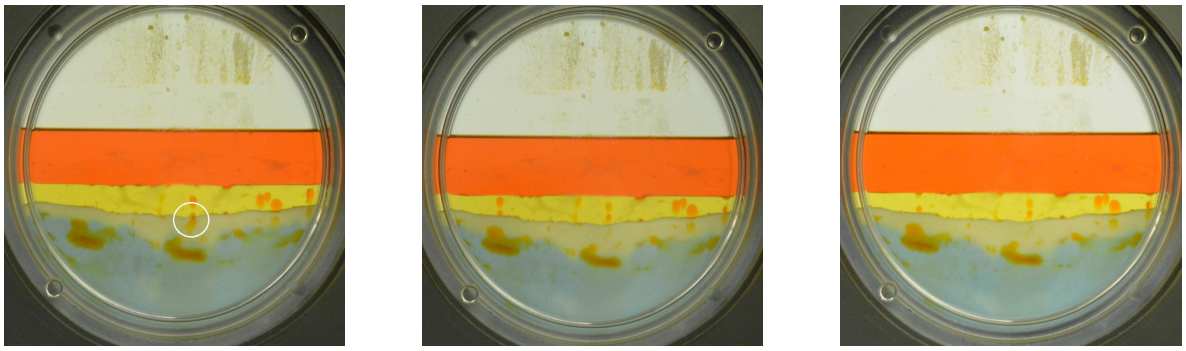

(a) t=23 min (b) t=25 min (c) t=38 min

Figure 5.88: POM cell test III: Carbonated water recovered part of trapped oil left behind by high pH water phase.

Carbonated water invaded the porous media and reacted with the high pH water. The experiment was stopped after 1300 minutes since the advancement of the carbonated water front was a slow process after 1000 minutes. The oil recovery was estimated to be 66% (Accuracy:± 5% , recovery estimation explained in appendix B).

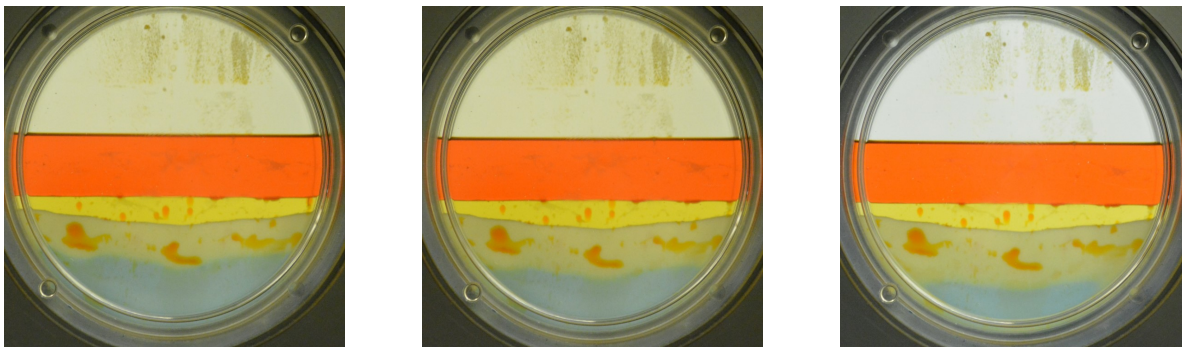

(a) t=440 min (b) t=714 min (c) t=1300 min

Figure 5.89: POM cell test III: Experiment was stopped after 1300 minutes as the advancement of carbonated water front was a very slow process.

5.5.4 Conclusions: Tests in POM cell

Label	pH of water phase	Dissolution time for CO_2	Movement of CO_2 in water	Movement of water phase in pores
PCT I	8.1	6.5 min	Faster on the side walls of the cell	–
PCT II	7.85	12 min	Faster on the center of the cell	–
PCT III	7.83	4 min	Turbulent	Clusters to piston-like

Table 5.20: POM cell tests (PCT): Overview of observations

Experiments were conducted in POM cell to study the effectiveness of dyes and indicators to aid visualisation and to conduct experiments under CO_2 injection at 10 bar which helped develop operational procedure in the cell and formed baseline results for further experiments in the cell. The conclusions drawn from these tests are given below:

1. As mentioned in table 5.20, the pH of the water phase dropped from 8.1 in test I to 7.85 in test II. The drop in pH was a result of overnight storage of the water phase in the piston cell and the reaction of the water phase and air present in injection lines. This drop in pH was noticed by a lighter colour of the water phase in PCT II compared to PCT I.

2. The level of fluids dropped upon initiating CO_2 injection in the cell. This was due to the compression of air trapped in the glass filter installed in the filter module at the bottom of the cell. As a result, when CO_2 injection began the glass filter incorporated fluids from the cell and the level of fluids dropped. A procedure to avoid air entrapment in glass filter has to be included in experiments conducted in the future.

3. Similar to observations made in the larger tube test I and II, the presence of an oil layer on top slowed the movement CO_2 in water phase compared to POM cell test I. This was observed as more time taken by CO_2 to completely dissolve in the water phase (see table 5.20).

4. Slower movement of CO_2 into the water phase led to a better mixing of CO_2 and water. As a result, the movement of CO_2 along the boundaries of the cell was less pronounced in PCT II.

5. In PCT III, the water phase invasion in porous media began before CO_2 injection started. The mixing of CO_2 and the water phase was accelerated by oil rising from the porous media. This is observed as low dissolution time for CO_2 in table 5.20.

6. The movement of the water phase was in the form of clusters at the entrance of porous media, which merged later to form a common water front. The oil trapped in porous media after high pH water flooding was partially recovered when carbonated water invaded the porous media.

7. Visualisation technique used in this test demonstrated the ability of carbonated water to mobilise oil trapped in pores after waterflooding, and laid insight into the movement pattern of CO_2 in water phase with and without porous media.

Chapter 6

Summary and Proposed Future Work

In this chapter, overall summary of this study is presented and recommendations for future work are proposed.

6.1 Summary

1. The fluid system was studied using indicator testing, tube tests and larger tube tests. Principal conclusions from studying the fluid system are:
    - Bromothymol blue can be used as aqueous phase pH indicator in visualisation tests, both with and without porous media. The movement of CO_2 is well represented by a change in colour of the water phase to yellow.
    - The pH of water solution decreased over time due to a reaction with CO_2 in the air. It is recommended that a stock solution of 0.04 wt% bromothymol blue be prepared, which can be diluted for use before each test.
    - Sudan II showed good contrast with a dyed aqueous phase in the porous media and did not lose colour with the change in pH during CO_2 injection. The movement of CO_2 in oil phase was not visualised, and further research needs to be conducted to identify a dye which can help visualise the dissolution of CO_2 in the oil phase.
    - 0.1 M HCl can be used as an analog fluid to represent the change in pH due to the dissolution of CO_2 in the water phase.
    - Dyes and indicator solutions aided the visualisation of various phenomena occurring during imbibition like the formation of an oil bank in porous media as a result of the snap-off mechanism.
    - A low concentration of CO_2 is required to cause a drop in pH of the water phase and form carbonated water.
    - Use of bromothymol blue in a crude oil system led to a loss in the colour of the water phase over time.
2. The porous media was studied during tube tests and tests in the larger tube. Given below are the conclusion drawn from studying the porous media:
    - The addition of glass beads to the water phase caused the pH to rise from 7.65 to more than 9.65. Acid treatment of the glass beads limits this rise in the

pH. This phenomenon has not been addressed widely in the studies done in the literature.
- Tests conducted using acid-washed porous media showed lower oil recovery compared to non-acid-washed porous media. A reaction between acid and glass beads is believed to cause a change in the surface properties of glass beads (e.g. roughness) or making the glass beads preferentially adsorb oil phase. More study needs to be done to understand this phenomenon further.
- The hydrophobicity of the glass beads prevents the water phase from entering the porous media and is the primary reason for lower oil recovery observed when using porous media as a mix of hydrophobic and hydrophilic glass beads.
- The packing of the porous media is an influential factor in determining the fluid movement and the resulting shape of the water front. Using an ultrasonic bath provides better packing of the porous media.
- Using glass beads as porous media helped visualisation of the processes due to the transparent nature of the glass beads.

3. The effect of cell dimensions on the shape of water front in the porous media, quality of the visualisation, and operational ease was studied in tube tests (with varying the diameter of the tube) and cell tests. The conclusions drawn from studying the effect of cell dimension are:

    - The shape of invading water front changed with a variation in thickness/diameter of the cell/tube. Limited data available during the experiments were used to estimate the capillary number in cell tests. The relation between capillary number and the shape of the water front studied in the literature showed a good match with the observations in the test.
    - The ability to visualise a process improved as the thickness of the cell decreased. However, a decrease in thickness made filling and cleaning of the cell more challenging.
    - The thickness of the cell selected is a balance between visualisation quality and the operational ease. The lower the thickness of the cell, the closer it is to a 2-D system.

4. Using the results obtained in the tests above a choice of fluid system and porous media was made to conduct tests in POM cell with CO_2 injection at 10 bar. Main conclusions from tests in POM cell are:

    - An ultrasonic bath could not be used to pack the porous media due to the large size of the POM cell. An alternate method to ensure proper packing is wet-packing, in which the glass beads and oil or water are mixed and filled as a slurry type mixture in the cell. Challenges faced during wet-packing include wetting the walls of the cell during porous media filling, smaller diameter glass beads may remain in suspension and the estimation of porosity or initial oil saturation for recovery calculations.
    - The presence of an oil layer on top of water phase delayed the movement of CO_2 in water. As a result of this delayed movement, a better mixing of CO_2 and water phase was visualised.
    - The ability of carbonated water to recover oil trapped in the porous media after waterflooding was visually demonstrated.

6.2 Recommendations for future work

The work done in this thesis has touched upon various factors which play a role in the visualisation of CO_2 in the porous media. Staring from visualisation of CO_2 dissolution in water to demonstrating the recovery of trapped oil from porous media swept during waterflooding. The thesis has also touched upon various factors which play a role in the visualisation of CO_2 in the porous media. Recommendations given below for future work can enhance our knowledge and experience in the visualisation techniques:

1. The ability of bromothymol blue to represent the water phase in ion-rich brine system needs to be studied. The effects of oil composition on the stability of pH indicator should also be studied to further understand the loss of colour in the presence of crude oil. This will aid in conducting visualisation experiments in crude oil-brine systems.
2. Future experiments conducted in the high-pressure cell will provide the ability to study various phenomena such as swelling of oil due to CO_2 dissolution, visualisation of supercritical CO_2 injection in the oil-water system and the ability of dyes to represent water and oil phases.
3. A limitation faced while using glass beads, is the consistent and limited mineral composition of glass beads which does not represent the complex heterogeneity of reservoir. Part of this limitation was mitigated by mixing hydrophobic and hydrophilic glass beads, but complex mineral reactions and ion-exchange encountered during CO_2 injection need to be studied further.
4. The rise in pH of water phase due to the addition of glass beads needs to be studied further. The studies conducted in the literature on the use of sudan II as oil phase dye indicate no effect of the dye on the wettability, but the majority of these studies are limited to glass etched micromodels and not glass beads. The effect of dyes on the wettability of glass beads can be studied further.
5. These experiments proved the ability of pH indicator to demonstrate a drop in pH of the water phase by dissolution of CO_2 at low concentration. Similar studies can be helpful in studying the ocean acidification.

References

Agartan, E., Trevisan, L., Cihan, A., Birkholzer, J., Zhou, Q., & Illangasekare, T. H. (2015). Experimental study on effects of geologic heterogeneity in enhancing dissolution trapping of supercritical co2. *Water Resources Research*, *51*(3), 1635–1648.

Akervoll, I., & Bergmo, P. E. (2010). CO2 eor from representative north sea oil reservoirs. In *SPE International Conference on CO2 Capture, Storage, and Utilization.* New Orleans, Louisiana, USA. (Paper SPE 139765)

Backhaus, S., Turitsyn, K., & Ecke, R. (2011). Convective instability and mass transport of diffusion layers in a hele-shaw geometry. *Physical review letters*, *106*(10), 104501.

Bathurst, R. G. (1972). *Carbonate sediments and their diagenesis* (Vol. 12). Elsevier.

Carroll, J. J., Slupsky, J. D., & Mather, A. E. (1991). The solubility of carbon dioxide in water at low pressure. *Journal of Physical and Chemical Reference Data*, *20*(6), 1201–1209.

Castor, T., Somerton, W., & Kelly, J. (1981). Recovery mechanisms of alkaline flooding. In *Surface Phenomena in Enhanced Oil Recovery* (pp. 249–291). Boston, MA: Springer.

Chatenever, A., & Calhoun Jr, J. C. (1952). Visual examination of fluid behaviour in porous media. *AIME Jour. Petrol. Tech.(June)*, 149–156.

Chatzis, I., & Dullien, F. (1983). Dynamic immiscible displacement mechanisms in pore doublets: theory versus experiment. *Journal of Colloid and Interface Science*, *91*(1), 199–222.

Conybeare, C. (1967). Influence of compaction on stratigraphic analyses. *Bulletin of Canadian Petroleum Geology*, *15*(3), 331–345.

Darcy, H. (1856). *Les fontaines publiques de la ville de dijon: exposition et application...* Paris: Victor Dalmont.

Dastyari, A., Bashukooh, B., Shariatpanahi, S. F., Haghighi, M., & Sahimi, M. (2005). Visualization of gravity drainage in a fractured system during gas injection using glass micromodel. In *SPE Middle East Oil and Gas Show and Conference.*

Dong, Y., Dindoruk, B., Ishizawa, C., & Lewis, E. J. (2011). An experimental investigation of carbonated water flooding. In *SPE Annual Technical Conference and Exhibition.* Denver, Colorado, USA. (Paper SPE 145380)

Emami-Meybodi, H., Hassanzadeh, H., Green, C. P., & Ennis-King, J. (2015). Convective dissolution of co2 in saline aquifers: Progress in modeling and experiments. *International Journal of Greenhouse Gas Control*, *40*, 238–266.

Espie, A. (2005, nov). A new dawn for co2 eor. In *International Petroleum Technology Conference (IPTC).* Doha, Qatar.

Faisal, T. F., Chevalier, S., & Sassi, M. (2013). Experimental and numerical studies of density driven natural convection in saturated porous media with application to co2 geological storage. *Energy Procedia*, *37*, 5323–5330.

GCCSI. (2016). *Sleipner co2 storage* (Project database). Global CCS Institute. (https://www.globalccsinstitute.com/projects/sleipner%C2%A0co2-storage-project)

GCCSI. (2018, feb). *The properties of co2.* Retrieved from https://hub.globalccsinstitute.com/publications/hazard-analysis-offshore-carbon-capture-platforms-and-offshore-pipelines/21-properties-co2 (Accessed : 2018-02-20)

Geistlinger, H., & Mohammadian, S. (2015). Capillary trapping mechanism in strongly water wet systems: comparison between experiment and percolation theory. *Advances in water resources*, *79*, 35–50.

Global CCS Institute, I. E. A. I., Carbon Sequestration Leadership Forum (CSLF). (2010, jun). *Iea/cslf report to the muskoka 2010 g8 summit. carbon capture and storage: progress and next steps.* Retrieved from http://www.globalccsinstitute.com/publications/ieacslf-report-muskoka-2010-g8-summit (Accessed Feb. 2018)

Gozalpour, F., Ren, S., & Tohidi, B. (2005). Co2 eor and storage in oil reservoir. *Oil & Gas Science and Technology*, *60*(3), 537–546.

Green, D. W., & Willhite, G. P. (1998). *Enhanced Oil Recovery* (Vol. 6). Henry L. Doherty Memorial Fund of AIME, Society of Petroleum Engineers Richardson, TX.

Grigg, R. B., & Schechter, D. S. (1997, oct). State of the industry in co2 floods. In *Spe Annual Technical Conference and Exhibition.* San Antonio, TX. (Paper SPE 38849)

Grubb, A. (2009.). *Energy bulletin.* Retrieved from http://www.energybulletin.net/primer.php

Guo, X., Ma, J., Li, J., Hao, Y., & Wang, H. (2012). Effect of reservoir temperature and pressure on relative permeability. In *SPETT 2012 Energy Conference and Exhibition.* Port-of-Spain, Trinidad.

Hatiboglu, C., & Babadagli, T. (2005, jun). Visualization studies on matrix-fracture transfer due to diffusion. In *Canadian International Petroleum Conference.* Alberta,Canada.

Hebach, A., Oberhof, A., & Dahmen, N. (2004). Density of water+ carbon dioxide at elevated pressures: measurements and correlation. *Journal of Chemical & Engineering Data*, *49*(4), 950–953.

Hickok, C., & Ramsay Jr, H. (1962). Case histories of carbonated waterfloods in dewey-bartlesville field. In *Spe Secondary Recovery Symposium.*

Holm, L. (1963). CO2 requirements in CO2 slug and carbonated water recovery processes. *Producer Monthly. September*.

Holm, L., & Josendal, V. (1974, dec). Mechanisms of oil displacement by carbon dioxide. *Journal of Petroleum Technology*, *26*(12), 1–427.

IEA. (2017). *International energy agency- world energy outlook 2017.* Retrieved from https://www.iea.org/weo2017/#section-2

IPCC. (2007). *Working group iii report climate change 2007: Mitigation of climate change.* (Vol. 10; Fourth Assessment Report No. 5.4). Intergovernmental Panel on Climate Change.

Johnson, W., Macfarlane, R., Breston, J., & Neil, D. (1952, nov). Laboratory experiments with carbonated water and liquid carbon dioxide as oil recovery agents. *Prod. Monthly*, *17*.

Kapelke, M., & Caballero, E. (1984). Prevention of calcium carbonate precipitation from calcium chloride kill fluid in co2-laden formations. In *Spe California Regional Meeting.* (doi:10.2118/12752-MS)

Keelan, D. K. (1982). Core analysis for aid in reservoir description. *Journal of Petroleum Technology*, *34*(11), 2–483.

Khatib, A. K., Earlougher, R., & Kantar, K. (1981). CO2 injection as an immiscible application for enhanced recovery in heavy oil reservoirs. In *Spe California Regional Meeting.* Bakersfield. (SPE 9928)

Kimbler, O., & Caudle, B. (1957). New technique for study of fluid flow and phase distribution in porous media. *Oil & Gas Journal*, *55*(50), 85–88.

Kneafsey, T. J., & Pruess, K. (2010). Laboratory flow experiments for visualizing carbon dioxide-induced, density-driven brine convection. *Transport in porous media*, *82*(1), 123–139.

Kneafsey, T. J., & Pruess, K. (2011). Laboratory experiments and numerical simulation studies of convectively enhanced carbon dioxide dissolution. *Energy Procedia*, *4*, 5114–5121.

Lake, L., Carey, G., Pope, G., & Sepehrnoori, K. (1984). Isothermal, multiphase, multicomponent fluid flow in permeable media. *In Situ;(United States)*, *8*(1).

Lenormand, R., & Zarcone, C. (1984). Role of roughness and edges during imbibition in square capillaries. In *Spe annual technical conference and exhibition.*

Lenormand, R., Zarcone, C., & Sarr, A. (1983). Mechanisms of the displacement of one fluid by another in a network of capillary ducts. *Journal of Fluid Mechanics*, *135*, 337–353.

Lindeberg, E., & Holt, T. (1994). Eor by miscible co2 injection in the north sea. In *SPE/DOE Improved Oil Recovery Symposium.*

MacMinn, C. W., Neufeld, J. A., Hesse, M. A., & Huppert, H. E. (2012). Spreading and convective dissolution of carbon dioxide in vertically confined, horizontal aquifers. *Water Resources Research*, *48*(11).

Martin, D., & Taber, J. (1992). Carbon dioxide flooding. *Journal of Petroleum Technology*, *44*(04), 396–400.

Martin, J. (1951). Additional oil production through flooding with carbonated water. *Producers Monthly*, *15*(7), 18–22.

Mayer, E. H., Earlougher Sr, R., Spivak, A., & Costa, A. (1988, feb). Analysis of heavy-oil immiscible co2 tertiary coreflood data. *SPE Reservoir Engineering*, *3*(01), 69–75.

McKellar, M., & Wardlaw, N. (1982). A method of making two-dimensional glass micromodels of pore systems. *Journal of Canadian Petroleum Technology*, *21*(04), 39–41.

Miller, J. S., & Jones, R. A. (1981). A laboratory study to determine physical characteristics of heavy oil after co2 saturation. In *SPE/DOE Enhanced Oil Recovery Symposium.* Tulsa, OK.

National Energy Technology Laboratory, U. D. o. E. (2018, feb). *Rangely weber unit.* https://www.netl.doe.gov/publications/proceedings/04/carbon-seq/198.pdf. (Accessed : 2018-02-20)

NIST. (2013). *Nist chemistry webbook.* Retrieved from http://webbook.nist.gov/

Pettijohn, F. (1975). Sedimentary rocks. *New York - Harper and Row Publishers*(3).

Pham, V., & Halland, E. (2017). Perspective of co2 for storage and enhanced oil recovery (eor) in norwegian north sea. *Energy Procedia*, *114*, 7042–7046.

Preston, C., Monea, M., Jazrawi, W., Brown, K., Whittaker, S., White, D., ... Rostron, B. (2005). Iea ghg weyburn co2 monitoring and storage project. *Fuel Processing Technology*, *86*(14-15), 1547–1568.

Przybylinski, J. L. (1987). The role of bicarbonate ion in calcite scale formation. *SPE Production Engineering*, *2*(01), 63–67. (doi:10.2118/13547-PA)

Riazi, M., Sohrabi, M., Bernstone, C., Jamiolahmady, M., & Ireland, S. (2011). Visualisation of mechanisms involved in co2 injection and storage in hydrocarbon reservoirsand water-bearing aquifers. *Chemical Engineering Research and Design*, *89*(9), 1827–1840.

Ross, G. D., Todd, A. C., Tweedie, J. A., & Will, A. G. (1982). The dissolution effects of co2-brine systems on the permeability of uk and north sea calcareous sandstones. In *SPE Enhanced Oil Recovery Symposium.* (doi:10.2118/10685-MS)

Sajadian, V., & Tehrani, D. (1998, oct). Displacement visualization of gravity drainage by micromodel. In *Abu Dhabi International Petroleum Exhibition and Conference.* (SPE-49557)

Sayegh, S., Krause, F., Girard, M., & DeBree, C. (1990). Rock/fluid interactions of carbonated brines in a sandstone reservoir: Pembina cardium, alberta, canada. *SPE Formation Evaluation*, *5*(04), 399–405. (doi:10.2118/19392-PA)

Schlumberger. (2018a, feb). *Schlumberger oilfield glossary -effective porosity.* Retrieved from http://www.glossary.oilfield.slb.com/Terms/e/effective_porosity.aspx (Accessed Feb. 2018)

Schlumberger. (2018b, feb). *Schlumberger oilfield glossary -minimum miscibility pressure.* Retrieved from http://www.glossary.oilfield.slb.com/Terms/m/minimum_miscibility_pressure.aspx (Accessed : 2018-02-12)

Scott, J., & Forrester, C. (1965). Performance of domes unit carbonated waterflood-first stage. *Journal of petroleum technology*, *17*(12). (SPE-1126-PA)

Sehbi, B. S., Frailey, S. M., & Lawal, A. S. (2001, may). Analysis of factors affecting microscopic displacement efficiency in co2 floods. In *SPE Permian Basin Oil and Gas Recovery Conference.* (Paper SPE 70022)

Shi, R., & Kantzas, A. (2008, oct). Enhanced heavy oil recovery on depleted long core system by ch4 and co2. In *International Thermal Operations and Heavy Oil Symposium.* Calgary, Alberta. (Paper SPE 117610)

Sohrabi, M., Emadi, A., Farzaneh, S. A., & Ireland, S. (2015). A thorough investigation of mechanisms of enhanced oil recovery by carbonated water injection. In *SPE Annual Technical Conference and Exhibition.* Houston, TX.

Sohrabi, M., Kechut, N. I., Riazi, M., Jamiolahmady, M., Ireland, S., & Robertson, G. (2011). Safe storage of co2 together with improved oil recovery by co2-enriched water injection. *Chemical Engineering Research and Design*, *89*(9), 1865–1872. (https://doi.org/10.1016/j.cherd.2011.01.027)

Sohrabi, M., Riazi, M., Jamiolahmady, M., Ireland, S., & Brown, C. (2009). Mechanisms of oil recovery by carbonated water injection. In *SCA annual meeting.*

Soroush, M., Wessel-Berg, D., Torsaeter, O., Taheri, A., Kleppe, J., et al. (2012). Affecting parameters in density driven convection mixing in co2 storage in brine. In *Spe europec/eage annual conference.*

Stalkup, J., F.I. (1984). *Miscible displacement* (Vol. ISBN 0-89520-319-7). Dallas, Tex.,: Society of Petroleum Engineers of AIME. (204 P)

Stone, T., Boon, J., & Bird, G. (1986). Modelling silica transport in large-scale laboratory experiments. *Journal of Canadian Petroleum Technology*, *25*(01).

Tzimas, E., Georgakaki, A., Cortes, C. G., & Peteves, S. (2005). Enhanced oil recovery using carbon dioxide in the european energy system. *Report EUR*, *21895*(6), 118.

Van Poollen, H. (1980). Fundamentals of enhanced oil recovery.

Verma, M. K. (2015). *Fundamentals of carbon dioxide-enhanced oil recovery (co2-eor): A supporting document of the assessment methodology for hydrocarbon recovery using co2-eor associated with carbon sequestration.* http://dx.doi.org/10.3133/ofr20151071.: US Department of the Interior, US Geological Survey Washington, DC.

Yang, D., Tontiwachwuthikul, P., & Gu, Y. (2005). Interfacial tensions of the crude oil+ reservoir brine+ co2 systems at pressures up to 31 mpa and temperatures of 27 c and 58 c. *Journal of Chemical & Engineering Data*, *50*(4), 1242–1249.

Yellig, W., & Metcalfe, R. (1980). Determination and prediction of co2 minimum miscibility pressures. *Journal of Petroleum Technology*, *32*(01), 160–168.

zeroco2.no website. (2018, feb). *Salt creek project.* http://www.zeroco2.no/projects/salt-creek-eor. (Accessed : 2018-02-20)

Zolotukhin, A. B., & Ursin, J.-R. (2000). *Introduction to petroleum reservoir engineering.* Norwegien Academic Press.

Appendix A

Recovery and Pore Volume Calculations in Tube Tests

A.1 Calculations in tube tests I-X

This appendix explains recovery factor calculations in tube tests I-X in section 5.2 on page 55.

During the experimental procedure, the following data were noted and used to give an estimate of oil recovery during the test. For example case, we use TT5: tube test V (subsection 5.2.3.1 on page 65).

The first step of the procedure is to note the amount of oil phase taken in the tube at the beginning of the test. In this case, it is 3 mL.

After the addition of glass beads, some amount of oil is trapped in the porous media, and some exist as free oil above the glass beads-oil interface. The water phase is added to the test tube, and the oil mobilisation process starts. The amount of HCl added is 2-3 drops, and the increase in water level due to this is negligible.

1. Amount of oil taken in the tube before addition of the glass beads, initial oil = 3 mL
2. Upon settlement of glass beads, an interface exists between glass beads and free oil phase in the tube. Interface level = 4.1 mL
3. Level of free oil column on top of the glass beads, Final oil level = 5.4 mL
4. Amount of oil out of porous media = Level of free oil column - Initial oil taken in the tube = Oil volume out of pores = (5.4 - 3)= 1.3 mL
5. Pore volume = Oil trapped in pores (S_{oi}) = Initial oil taken in the tube - Oil volume out of pores = 3 - 1.3 = 1.7 mL
6. Upon addition of water to the tube, initial water level = 8 mL
7. Final water level at the end of the test = oil/water interface level at the end of the test = 6.8 mL
8. Amount of water invaded in porous media = Initial water level - Final water level = 8 - 6.8 = 1.2 mL

Experiment label	Initial oil(mL)	Interface level(mL)	Final oil level(mL)	Oil out of pores(mL)	Pore volume(mL)	Initial water leve(mL)	Final water level(mL)	Water invaded in pores(mL)	Final oil saturation(mL)	Recovery (%)
TT1	3	3	4.7	1.7	1.3	5.2	4.2	1	0.3	77
TT2	5	2.9	6.6	3.7	1.3	7.5	6.5	1	0.3	77
TT3	4.3	4.3	6.9	2.6	1.7	9.2	7.7	1.5	0.2	88
TT4	4	4.3	6.9	2.6	1.4	9.5	8.3	1.2	0.2	86
TT5	3	4.1	5.4	1.3	1.7	8	6.8	1.2	0.5	71
TT6	3	4.5	5.2	0.7	2.3	10	9.5	0.5	1.8	22
TT7	3	5.1	6.2	1.1	1.9	10	9.9	0.1	1.8	5
TT8	3	3.1	4.7	1.6	1.4	6	6	0	1.4	0
TT9	3	4	5.3	1.3	1.7	7	6.1	0.9	0.8	53
TT10	3	4.3	5.6	1.3	1.7	7.3	6.9	0.4	1.3	24

Table A.1: Recovery data for tube tests I-X. 'TT' refers to 'tube test'.

9. Here we assume that amount of water invaded in porous media is equal to the oil mobilised from pores. Hence, Oil recovered from pores = Amount of water invaded in the porous media = 1.2 mL

10. Amount of oil left in pores = Final oil saturation (S_{or}) = Pore volume - Oil recovered from pores = 1.7 - 1.2 = 0.5 mL

$$Recovery(fraction) = \frac{S_{oi} - S_{or}}{S_{oi}} \tag{A.1}$$

Recovery (%)= Recovery(fraction)*100 = 100*(1.7 - 0.5) / (1.7) = 71%.

Note: Accuracy in calculations: 10 % recovery $\approx$ 0.2 mL oil recovered. Similar calculations were done for tube tests I-X and the values are summarized in table A.1.

A.2 Calculation in tube tests of varying diameter

This appendix explains recovery factors calculations in tube tests XI-XIII in subsection 5.2.4.

During the experiment, the following data were noted and used to calculate porosity and the recovery factor. As an example case, we will use tube test in diameter 7.85 mm. The volume in the tube can be approximated by the volume in a cylinder. Since the radius of the tube remains constant, all calculations involving the ratio of volumes (like porosity or recovery factor) can be calculated using the ratio of heights.

$$Porosity, \phi = \frac{V_p}{V_b}$$

where, V_p and V_b are pore volume and bulk volume respectively.

Calculations for tube test XI can be made as given below:

1. Initial height of oil column (before glass beads addition) = 6 cm
2. After adding glass beads to the tube, the height of glass beads column = 11 cm
3. Amount of oil out of pores, measured as the height of free oil column above glass beads = 1.7 cm
4. Pore volume, I_p = Amount of oil in pores = Initial height of oil column - Amount of oil out of pores = 6 - 1.7 = 4.3 cm
5. Porosity,ϕ= Amount of oil in pores / height of glass beads column = $\frac{4.3}{11} * 100$ = 39.1 %
6. Amount of oil out of pores before water injection, I_o = 1.7 cm
7. Amount of oil of pores at the end of the experiment, I_f = 2.3 cm
8. Amount of oil in the oil bank due to snap-off, I_{so} = 0.5 cm
9. Oil recovery (%) = $\frac{I_f + I_{so} - I_o}{I_p} * 100 = 26\%$

Similar calculations were done tube tests in tube with diameter 5.55 mm and 3.75 mm. Results are summarised in table A.2.

Experiment label	Initial oil(cm)	Glass beads level(cm)	Free oil level(cm)	I_p(cm)	ϕ(%)	I_o (cm)	I_f (cm)	I_{so} (cm)	Recovery (%)
TT11 (7.85 mm)	6	11	1.7	4.3	39.09	1.7	2.3	0.5	26
TT12 (5.55 mm)	5	10	0.7	4.3	43.00	0.7	4.2	0	81
TT13 (3.75 mm)	8.5	8	5.2	3.3	41.25	5.2	5.5	0.3	18

Table A.2: Recovery data for tests in tube with varying diameter

Note: Accuracy in recovery calculations for tube tests XI and XII: 10% recovery = 4.3 mm height of oil column in the tube.

For tube test XIII, accuracy in recovery calculations: 10% recovery = 3.3 mm height of oil column in the tube.

A.3 Calculations in tests with CO_2 injection at 10 bar: larger tube tests V-X

This appendix explains recovery estimation in larger tube tests V-X in section 5.3.

Recovery calculations will be explained using one example, and rest of the data is summarized in table A.3.

Larger tube used in this experiment has gradings of length (cm). As seen in figure 4.3 on page 36, there is a ungraded zone of 2.5 cm on top and bottom of the tube. This has to accounted for during the calculations of pore volume and recovery.

As an example case we will use LT5: larger tube test V (subsection 5.3.5 on page 83).

1. Height of oil column before addition of glass beads = Initial oil = 8.2 + 2.5 (ungraded zone) = 10.7 cm
2. Level of glass beads-oil interface = Glass beads level = 16.2 + 2.5 = 18.7 cm
3. Level of free oil column after filling of glass beads = Free oil level = 20.1 + 2.5 = 22.6 cm. *Note*: This height is observed to be low in the fig. 5.41b on page 90 because some oil was taken out of the tube to leave only a small layer of free oil above porous media.
4. Amount of oil out of pores = Level of free oil - level of glass beads column = 22.6 - 18.7= 3.9 cm
5. Oil present in pores (calculated as the height of oil column) = Height of initial oil column - Amount of oil out of pores = 10.7 - 3.9= 6.8 cm
6. Since radius of the tube is constant, ratio of height's can be used to calculate ratio of volumes. Porosity (%)= (100* Oil present in pores)/(Bulk volume of tube) = (100*6.8)/18.7 = 36.36 %
7. Level of water column at the start of CO_2 injection = 29 + 2.5= 31.5 cm
8. Level of water column at the end of experiment = 27.2 + 2.5= 29.7 cm
9. Amount of water invaded in pores (as height of water column) = 31.5 - 29.5 = 1.8 cm
10. Height of oil column before CO_2 injection = 1.3 cm (Height of free oil column was 3.9 cm, but excess oil was taken out before water injection).
11. Height of oil column at the end of experiment = 2.8 cm
12. Height of oil column due to snap-off = Height of oil column in porous media= 1.6 cm
13. Recovery fraction= [Oil column at end of experiment + Oil column in pores due to snap-off - Oil column before CO_2 injection] / [Oil present in pores]

    = [2.8 + 1.6 - 1.3] / [6.8] = 0.456

    Recovery, % = 46 %

Note: Accuracy in recovery calculations: 10% recovery ≈ 7 mm height of oil column in the tube

Experiment label	Initial oil(cm)	Glass beads level(cm)	Free oil level(cm)	Oil out of pores(cm)	Oil in pores(cm)	Porosity(%)	Oil column before injection (cm)	Oil column at the end of experiment (cm)	Oil column due to snap-off (cm)	Recovery (%)
LT5	10.7	18.7	22.6	3.9	6.8	36.3	1.3	2.8	1.6	46
LT6	8.5	19.3	20.6	1.3	7.2	37.3	1.3	3.3	0	28
LT7	9.5	19.6	22.1	2.5	7	35.7	2.5	3	0	7
LT8	8.5	19.8	21.5	1.7	6.8	34.3	1.7	1.7	0	0
LT9	10.5	18.4	22.2	3.8	6.7	36.4	1.3	2.5	0	18
LT10	10.9	18.5	22.3	3.8	7.1	38.4	1	1.2	0	3
Type C (No US)	10.5	18.4	20	1.6	8.9	48.4	-	-	-	-
A-W type C (No US)	8.5	18.4	19.1	0.7	7.8	42.39	-	-	-	-

Table A.3: Recovery data for larger tube tests V-X. 'LT' refers to 'larger tube'

Appendix B

Recovery estimation in POM cell

This appendix explains how to get an approximate recovery factor for POM cell test III in subsection 5.5.3 on page 123.

Amount of oil injected in the POM cell before addition of glass beads is known. In this case, Initial oil = 35 mL.

Next step is to add glass beads and allow them to settle. Upon settling a small column of oil is left above glass beads layer. We can estimate the oil in this section and oil recovery in the following way.

1. All images during the experiment were taken at the same distance from the cell. Hence, we can use a ruler to approximate the distance between two points on an image with the dimension of the cell. For example, the diameter of the cell was measured to be 10 cm on the image, while the actual diameter of the cell was 17 cm. Hence we can estimate using the fact that 1 cm on our ruler is 1.7 cm on the POM cell.

2. As shown in fig.B.2, a column of oil can be approximated as a trapezium and its area can be calculated based on the formula for the area of a trapezium. Once we have the area, the volume can be calculated as (area* cell thickness). Eq. B.1 gives the formula for the area of a trapezium.

$$Area = \frac{(a+b)*h}{2} \tag{B.1}$$

   Area calculated from above formula is multiplied by 1.7^2 to get area from measured dimensions (using a ruler) to cell dimensions.

3. Area of the oil column before water injection begins is measured and multiplied with the thickness of the cell (0.5 cm) to get the volume of oil outside porous media.

4. The volume of oil outside the porous media is subtracted from the initial oil (35 mL) to give pore volume. Pore volume = 35 - 11.38 = 23.61 cc.

5. At the end of the experiment, the area of oil column is measured and multiplied with the thickness of the cell to get total oil volume. Total oil volume at the end of displacement subtracted by the volume of oil outside the porous media at the beginning of the experiment gives the volume of oil recovered. Oil recovered at the end of experiment = 26.91 - 11.38 = 15.52 cc

6. The volume of oil recovered divided by pore volume gives recovery factor. Recovery factor = 15.52/ 23.61= 66%. Accuracy of estimation: ± 5%.

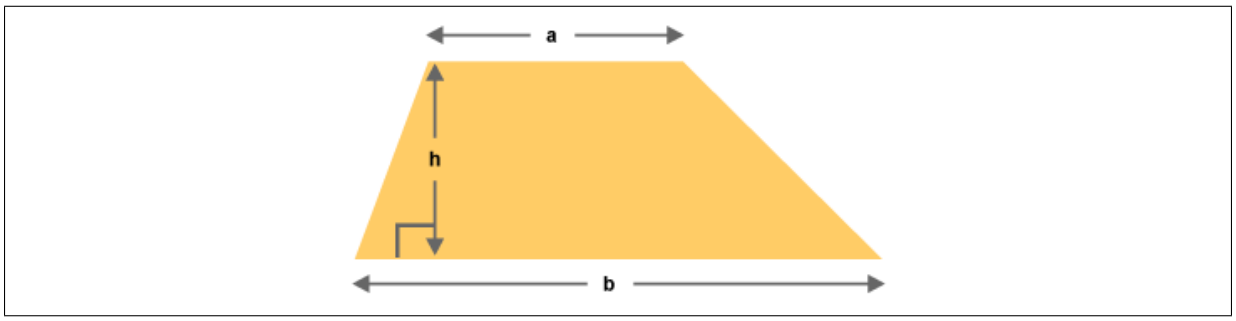

Figure B.1: Trapezium dimensions used to estimate area of oil column.

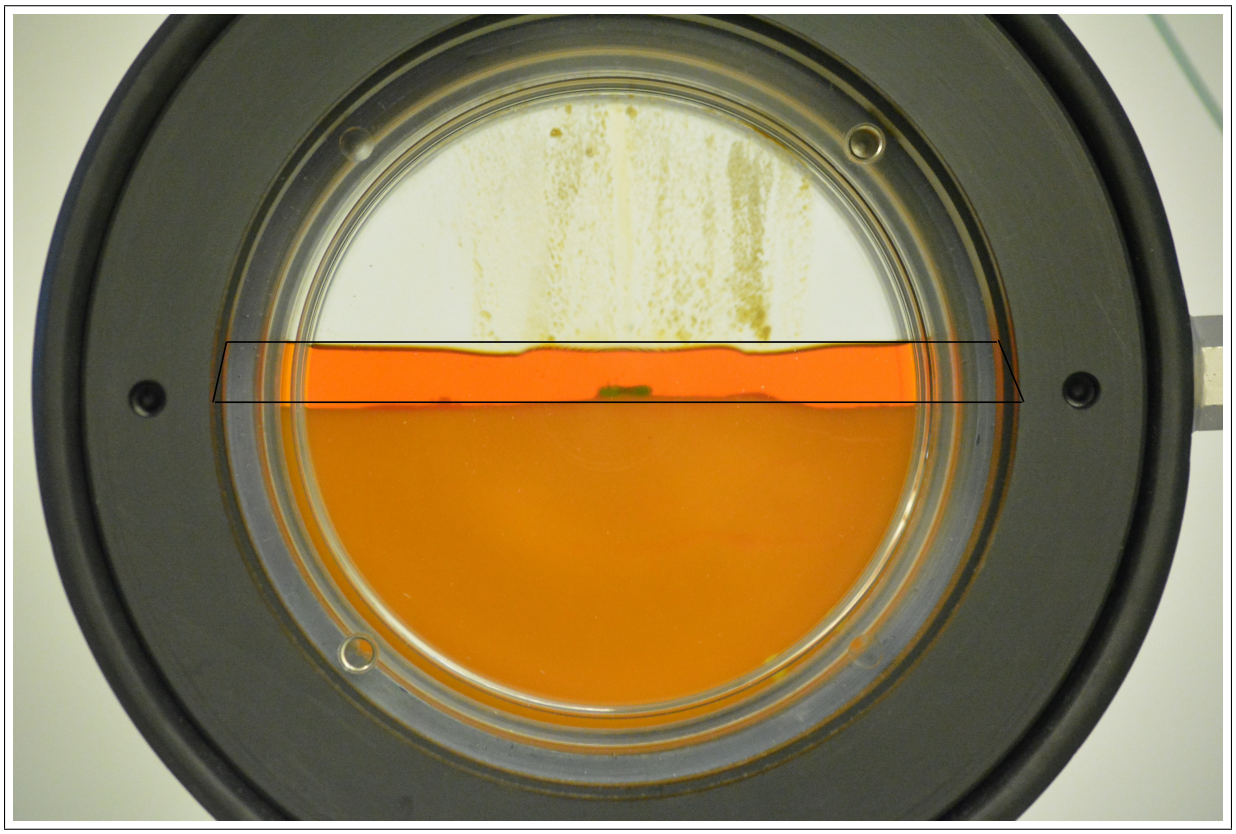

Figure B.2: Approximation of oil column as trapezium

Label	a(cm)	b(cm)	h(cm)	Area (converted into real cell dimensions,cm^2)	Volume (area*0.5, cc)
Oil out of porous media	10	9.7	0.8	22.77	11.38
End of experiment	9.9	9.7	1.9	53.81	26.91

Table B.1: Data for recovery calculation in POM cell

Appendix C

Size distribution of the glass beads

The size distribution of glass beads as given by the supplier:

Size (in μm)	Value (in %)
<50	0.57
50 - 60	0.65
60 - 70	3.06
70 - 80	9.95
80 - 90	18.22
90 - 100	21.06
100 - 110	17.74
110 - 120	10.97
120 - 130	5.09
>130	1.69

Table C.1: Size distribution of glass beads type C/D.

Size distribution of the glass beads is plotted in fig.C.1.

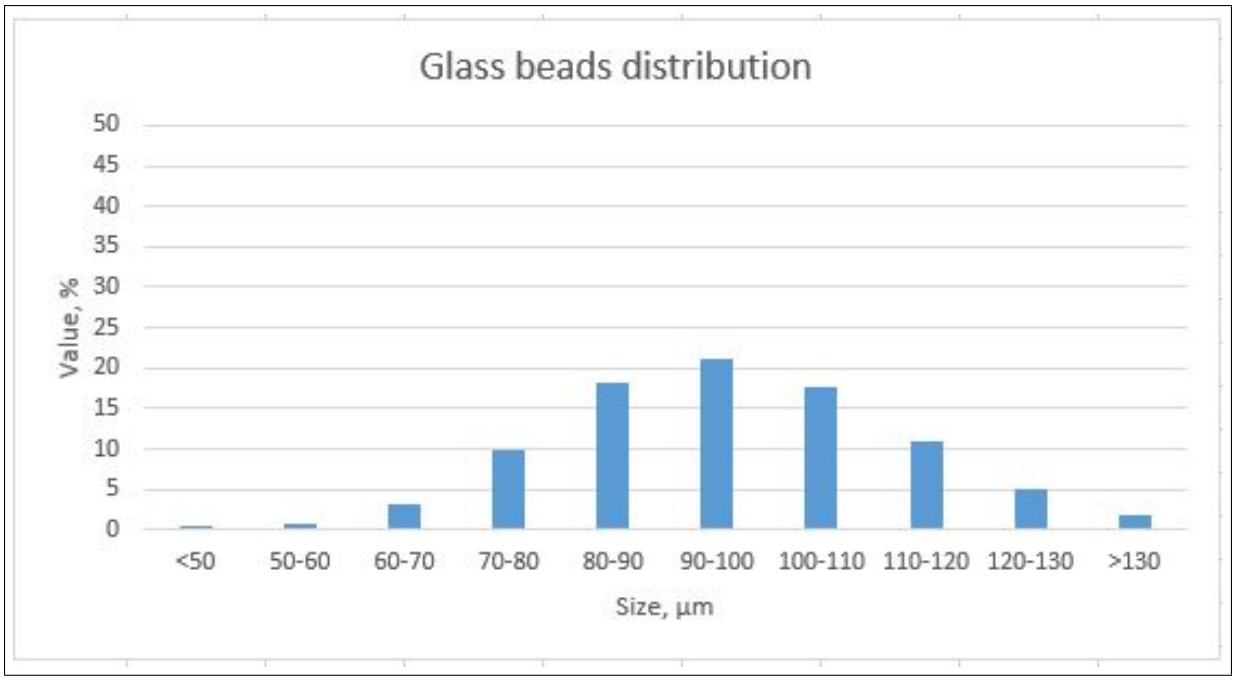

Figure C.1: Size distribution of glass beads type C/D.